Coordination and supramolecular chemistry of aromatic *N*-oxides

A Dissertation submitted to the
Indian Institute of Technology Guwahati as
partial fulfillment for the Degree of
Doctor of Philosophy in Chemistry

Submitted by

Rupam Sarma

Department of Chemistry

Indian Institute of Technology Guwahati

November 2010

Dedicated to My Family
&
Friends…

Statement

I hereby declare that this thesis entitled "**Coordination and supramolecular chemistry of aromatic *N*-oxides**" is the outcome of research work carried out by me under the supervision of Prof. Jubaraj B. Baruah, at the Department of Chemistry, Indian Institute of Technology Guwahati, India.

In keeping with the general practice of reporting scientific observations, due acknowledgement has been made whenever work described here has been based on the findings of other investigators.

IIT Guwahati
November, 2010

Rupam Sarma

Certificate

This is to certify that Rupam Sarma has been working under my supervision since January, 2007 as a regular registered Ph. D. student. I am forwarding his thesis entitled "**Coordination and supramolecular chemistry of aromatic *N*-oxides**" being submitted for the Ph. D. (Science) Degree of this Institute.

I certify that he has fulfilled all the requirements according to the rules of this institute regarding the investigations embodied in his thesis and this work has not been submitted elsewhere for a degree.

IIT Guwahati
November 15, 2010

Prof. Jubaraj B. Baruah

Acknowledgements

The enlightening experience of doing science under the guidance of Prof. Jubaraj B. Baruah can hardly be described in words. The numerous discussions and interactions I had with him expanded my horizons to hitherto unknown frontiers of science and knowledge. I am indebt to this wonderful person for all that he has given me and above all for motivating me towards scientific research.

I would like to acknowledge my sincere gratitude to all my doctoral committee members for their insightful advices and valuable suggestions. I am also grateful to the entire faculty and staff in the Department of Chemistry, Indian Institute of Technology Guwahati for providing a wonderful work atmosphere throughout this period.

I would like to thank my lab mates Dr. Anirban Karmakar, Babulal Das, W. Marjit Singh, Debendra, Dip, Bhaskar, Himangshu, Bigyan, Subham and Anvita whom I had an opportunity to work with. No words can express my thankfulness for giving me their time and companionship, which made the time spent in the laboratory and outside pleasant and memorable. I would like to give my special thanks to my friends Pranab and Moushumi for their timely help, support and for the wonderful time we shared during this period.

The financial support from Council of Scientific and Industrial Research (CSIR), New Delhi for the research fellowship is duly acknowledged.

Finally, my Ph. D. endeavor could not be completed without the endless love, unending support, tolerance and blessings from my family and my graduate teacher Dr. Diganta Choudhury. They are the main soul and inspiration for each and every step that I achieve in my life.

Preview

Aromatic *N*-oxides are a special class of heterocyclic aromatic compounds containing exo-cyclic *N*-oxo functionality. They are a class of useful ligand for the generation of coordination complexes as well as supramolecular architectures especially coordination polymers. Being an exo-dentate ligand *N*-oxide possesses a number of coordination and hydrogen bond modes. Depending on these possible modes, different supramolecular architectures are designed. Stability of these architectures is guided by supramolecular interactions like hydrogen bonding, π-π stacking or weak electrostatic interactions exhibited by the *N*-oxide ligands. This thesis deals with the studies on synthesis, characterization and structural aspects of a number of coordination polymers and molecular complexes of aromatic *N*-oxides. An important aspect of the study is the synthetic route of the coordination polymers. Generally the coordination polymers are synthesized using solvothermal methodologies. Such synthetic methodologies may lose informations regarding any intermediate products or kinetic products. The coordination polymers reported here are synthesized under mild solution state reaction conditions. In a couple of instances intermediate species formed during coordination polymerization are isolated and characterized which is not possible in solvothermal process. Electronic spectral properties and magnetic behavior of some of the coordination polymers are studied. Moreover, suitable conditions to synthesize metal containing molecular complexes of aromatic *N*-oxides are explored and presented. The content of the thesis is divided into six chapters as described below.

Chapter 1: Introduction

In this chapter, a general introduction to the aromatic *N*-oxide is brought forward with their structural features and spectroscopic properties. A brief account on the coordination complexes of aromatic *N*-oxide as ligand is compiled based on the existing literature. Moreover, the *state of the art* report on various aspects related to the synthesis, structure and properties of coordination polymers/ molecular complexes of aromatic *N*-oxide ligands are presented. This chapter also features discussion on

several possible coordination modes of both mono and di-*N*-oxides which are employed to design new open framework structures. The gas separation, magnetic, and catalytic properties of coordination polymers having *N*-oxide ligands are discussed.

Chapter 2: Synthesis, characterization and properties of *N*-oxide complexes of manganese(II), copper(II) and zinc(II)

Chapter 2 discusses the studies on synthesis, characterization and properties of *N*-oxide based coordination polymers of manganese(II), copper(II) and zinc(II). A number of coordination polymers of manganese(II) *N*-oxide are synthesized and studied (Scheme 1). One pot reaction of manganese(II) acetate tetrahydrate, aromatic carboxylic acid and pyridine *N*-oxide (PNO) in methanol:toluene mixed solvent led to formation of one dimensional coordination polymers with the general composition $[Mn(ArCOO)_2(PNO)]_n$. All these coordination polymers are characterized by X-ray diffraction technique along with other spectroscopic methods. To understand magnetic properties of the synthesized coordination polymers temperature dependent magnetic susceptibility is studied and found them to show antiferromagnetic behavior.

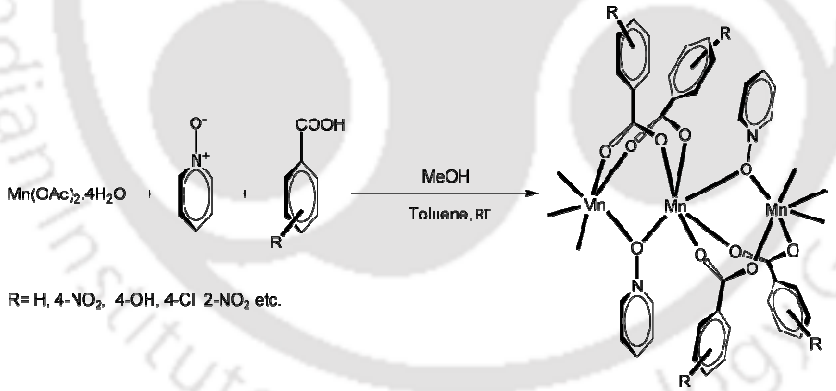

Scheme 1

A number of *N*-oxide based copper(II) coordination polymers are synthesized and characterized. In general copper(II) carboxylate prefers paddle wheel geometry and in such complexes axial positions are occupied by solvents or by ancillary ligands. Thus, by use of bidentate spacer ligands to connect these paddle wheel units the distance of separation between the paddle wheel cores may be controlled. As shown in scheme 2 such distance will be different for different ligands used (d1 > d2),

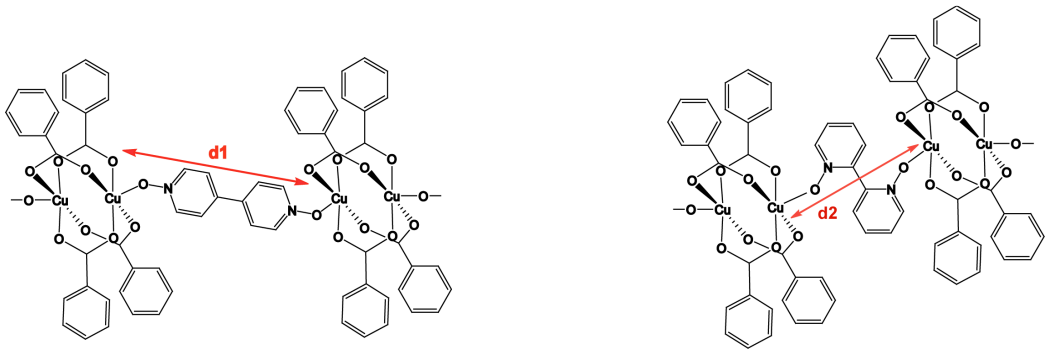

Scheme 2

which in turn may have significant effects on their magnetic exchange properties. We have studied complexes of *N*-oxide ligands such as pyridine *N*-oxide, 2,2'-bipyridyl-*N,N'*-dioxide and 4,4'-bipyridyl-*N,N'*-dioxide to compare the structural as well as magnetic features of the different complexes formed. Furthermore, a number of aromatic *N*-oxide based zinc(II) coordination polymers are also synthesized and characterized to understand their structural aspects and supramolecular behaviour and are discussed in this chapter.

Chapter 3: Synthesis, characterization and structural aspects of *N*-oxide complexes of cadmium(II), mercury(II) and lead(II)

Owing to the large ionic radii, metal ions such as cadmium(II), mercury(II) and lead(II) can adopt a range of coordination numbers varying from two up to twelve. Based on the versatile coordination possibility, various coordination polymers of cadmium(II) are prepared and reported from time to time although report on mercury(II) complex is scarce. Comparatively, lead(II) complexes are extensively studied. Although solvothermal reactions are widely used for the preparation of these coordination polymers, control over isolation of an intermediate species formed during a reaction is not possible. Solution chemistry is found to be advantageous in this respect, as transient complexes formed during the reaction can sometimes be isolated. Thus, understanding of possible inter-conversion or transformation among polymeric species is of importance. The solution phase synthesis, characterization and structural features of different aromatic *N*-oxide based coordination polymers of cadmium(II), mercury(II) and lead(II) as elucidated by spectroscopic and X-ray crystallographic data are the subject of this chapter.

Chapter 4: Synthesis, characterization and structural aspects of *N*-oxide complexes of lanthanide(III)

The tendency of lanthanides to adopt high coordination numbers makes the *f*-block metal ions attractive for designing of coordination polymers with new and unusual network topologies. Moreover, coordination polymers of lanthanides have enormous interest due to their important magnetic, catalytic as well as luminescent properties. A number of reports on coordination networks of lanthanides with aromatic *N*-oxide-based ligands have appeared. This chapter elaborates the synthesis and characterization of a number of coordination polymers of Ln(III) benzoate (Ln=La, Ce, Eu, Gd, Tb) with 4,4'-bipyridyl-*N,N'*-dioxide obtained from one pot multi-component reactions to understand the role of the central metal ions and stoichiometry of reactants in the reaction conditions. We have observed that, in general, varying the metal to ligand ratio, results in varying dimensionality of the coordination polymers:

Ln(III): 4,4'-BPNO =1:0.5 one dimensional coordination polymer

Ln(III): 4,4'-BPNO =1:1 three dimensional coordination polymer

A schematic presentation for the synthesis of the coordination polymers of Tb(III) is shown in scheme 3.

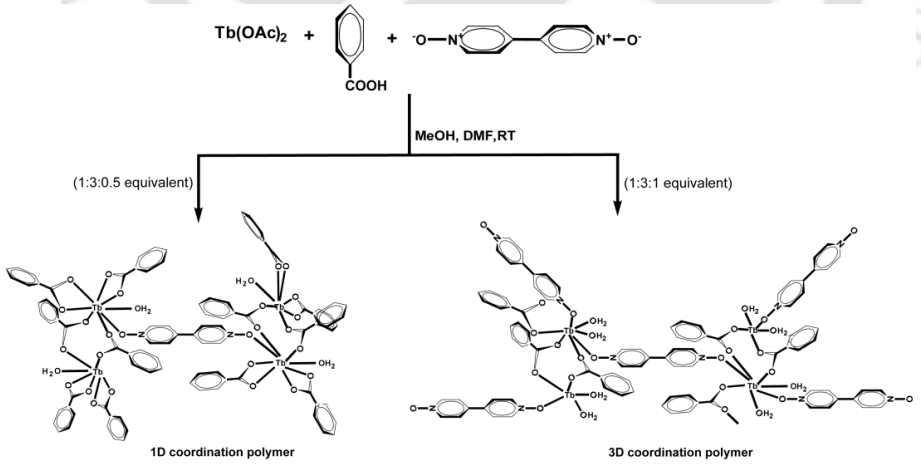

Scheme 3

The afforded new crystalline coordination polymers were characterized by conventional spectroscopic techniques as well as by both single crystal and powder X-ray diffraction techniques. The thermogravimetric, luminescence, and the magnetic properties of the complexes are studied and discussed in this chapter.

Chapter 5: Supramolecular aspects of multi-component molecular complexes containing aromatic *N*-oxides: syntheses and characterizations

In the earlier chapters, we have observed that aromatic *N*-oxides form metal complexes easily on reaction with metal carboxylate. However, aromatic *N*-oxides along with carboxylic acids are rarely studied as molecular complexes with metal ions. Such multi-component molecular crystals are expected to throw light on the nucleation process during formation of metallo organic hybrid complexes as well as on the role of intermolecular hydrogen bonding interactions in the synthesis of coordination polymers. With this objective, we have studied formation of multi-component molecular complex between hexa aquo metal ions, aromatic *N*-oxides and aromatic carboxylate ions. This chapter describes the synthesis, characterization, and supramolecular aspects of a number of such molecular complexes.

In chapter 2 we have discussed about the reaction between 4-nitrobenzoic acid, pyridine *N*-oxide and manganese(II) acetate tetrahydrate in methanol leading to the formation of one dimensional coordination polymer with μ^2 bridging pyridine *N*-oxide. The same reaction when carried out in aqueous methanol resulted in the formation of the molecular complex of pyridine *N*-oxide co-crystallizing with hexa aquo manganese(II) ion and 4-nitrobenzoate ion (Scheme 4). This reaction is highly substrate dependent and we could get such multi-component molecular complexes only from 4-nitrobenzoic acid out of several aromatic carboxylic acids such as benzoic acid, methylbenzoic acids (all three isomers), 2-nitrobenzoic acid etc.

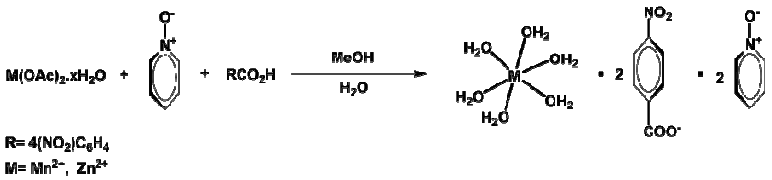

Scheme 4

The reaction between 4-nitrobenzoic acid, quinoline *N*-oxide and manganese(II) acetate tetrahydrate in aqueous methanol resulted in the formation of the molecular complex of quinoline *N*-oxide co-crystallizing with hexa aquo manganese(II) ion, 4-nitrobenzoate ion and a water of crystallization (Scheme 5).

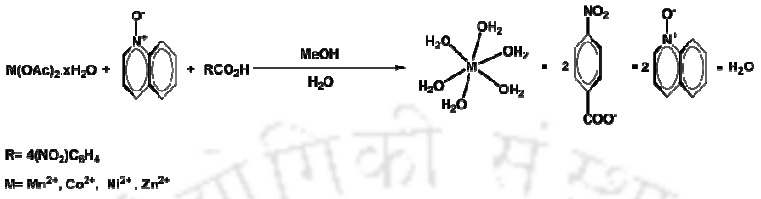

Scheme 5

The molecular complexes are stabilized by extensive short-range interactions existing between the aqua, *N*-oxo and the carboxylato groups. Moreover, the aromatic rings of the carboxylic acid and the aromatic *N*-oxide are held together by strong π-stacking interactions. These short-range interactions make the molecular complexes stable enough and prevent the formation of the coordination polymer through coordination of the *N*-oxide to the metal ions.

Chapter 6: Supramolecular aspects of molecular complexes of aromatic *N*-oxides with phenyl boronic acid: syntheses, characterizations and DFT calculations

Phenylboronic acid bears similarity with aromatic carboxylic acids towards formation of supramolecular assemblies. A few works are reported based on these similarities. Heteromeric assemblies of boronic acids with aromatic amines are also studied. However, supramolecular assemblies of phenylboronic acids with *N*-oxides were not studied. The chapter 6 describes structural features of a few supramolecular assemblies of 1,4-benzenediboronic acid with aromatic *N*-oxides viz. pyridine *N*-oxide (**6.1**), quinoline *N*-oxide (**6.2**), isoquinoline *N*-oxide (**6.3**), and 4,4'-bipyridyl-*N,N'*-dioxide (**6.4**) as shown in scheme 6.

The molecular complexes of 1,4-benzenediboronic acid with different aromatic *N*-oxides namely pyridine *N*-oxide (PNO), quinoline *N*-oxide (QNO), isoquinoline *N*-oxide (IQNO), and 4,4'-bipyridyl-*N,N'*-dioxide (BPNO) are easily

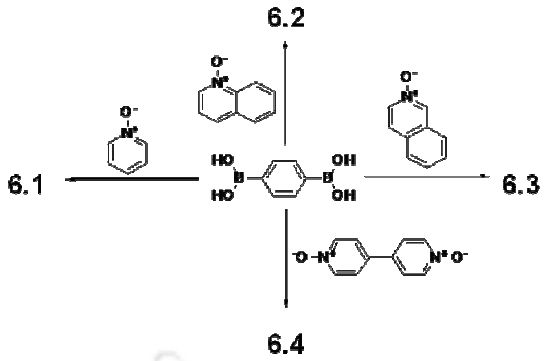

Scheme 6

prepared by mixing respective solution of the corresponding *N*-oxide with the *p*-phenylenediboronic acid. The structures of each of them are determined by means of crystallography and their packing patterns are analyzed and described in this chapter. Besides other weak interactions, each of these adducts exhibits the O-H···O hydrogen bond as the primary interaction to form network structures. The common point in each of these structures is the strong hydrogen bonding interactions between the *N*-oxo groups of aromatic *N*-oxides with the B–OH groups of the *p*-phenylenediboronic acid molecules. Role of relatively less conventional weak interactions such as the B···π aromatic interactions in the formation of network structure are discussed. The experimentally observed weak interactions are correlated with theoretical ones by carrying out DFT calculations on different model assemblies of the molecular complexes.

Contents

Chapter 1

Introduction

1.1 General features of aromatic *N*-oxides

Aromatic *N*-oxides are a special class of heterocyclic aromatic compounds containing exocylic *N*-oxo functionality and are characterized by the presence of a coordinate-covalent bond between the nitrogen and oxygen atom.[1] The bond between nitrogen and oxygen is formed by the overlap of a non-bonding pair of electrons on nitrogen with an empty orbital on oxygen atom. This N-O functionality of heteroaromatic *N*-oxide possesses dual nature, being able to act both as π-electron donor and π-electron acceptor.[2] Moreover, the presence of oxygen atom increases the aromaticity and delocalization of the aromatic ring in heteroaromatic *N*-oxides and a number of canonical forms can be drawn for them. As an illustrative example, the canonical forms for pyridine *N*-oxide are shown in figure 1.1.

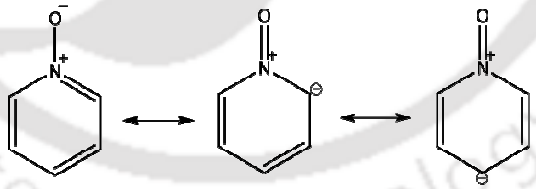

Figure 1.1: Canonical forms of pyridine *N*-oxide

There are number of reports on theoretical calculations to find out correlation of electronic properties with spectroscopic properties of heteroaromatic *N*-oxide molecules.[3] Among these, pyridine *N*-oxide (PNO) is extensively studied and the photo electron spectrum of pyridine *N*-oxide shows the presence of the first band at a relatively lower potential (8.38 eV) than pyridine. This band corresponds to a π-orbital mainly centered on the oxygen atom. Such a structure of the HOMO is a

common feature for aromatic *N*-oxide. However, the ionization potential decreases with increase in conjugation; also, the localization of the HOMO on the oxygen atom decreases. The second band appears at 9.22 eV and corresponds to a σ-orbital centered on the oxygen atom. However, in case of pyridine the highest energy π-orbital has very close energy with the σ-orbital and is stabilized as compared to pyridine *N*-oxide. The energy levels corresponding to highest energy molecular orbitals for pyridine and pyridine *N*–oxide are shown in figure 1.2.

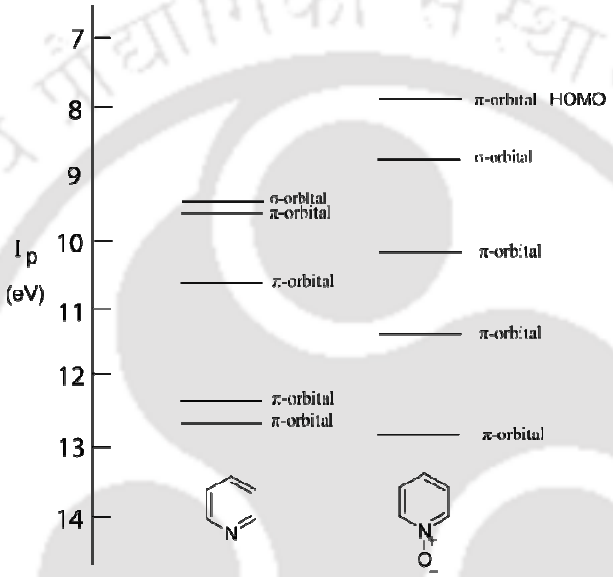

Figure 1.2: Energy levels corresponding to highest energy molecular orbitals of pyridine and pyridine *N*–oxide

Being prototype of heteroaromatic *N*-oxides, the properties of pyridine *N*-oxide have been extensively studied.[2] For the ring hydrogen atom of an isolated molecule of pyridine *N*-oxide, the IR spectrum shows a band at 3052 cm^{-1} due to =C-H stretch. The strongest band in the IR spectrum is observed at around 1231 cm^{-1} together with adjacent absorptions at 1238 and 1250 cm^{-1}; these are assigned to the N-O stretch, because this vibration is accompanied by a large change in dipole moment and polarizability.

The electronic structures and spectra of heteroaromatic *N*-oxides have been extensively studied. In case of pyridine *N*-oxide, a strong band is observed near 280 nm, in aprotic solvents, however in protic solvent it undergoes a blue shift up to 263

nm.[4] This band is assigned to π-π* transition with a strong internal charge transfer character. This internal charge transfer takes place from the π–orbital localized on the oxygen atom to one π–orbital delocalized on the aromatic ring. On going from pyridine *N*-oxide to 2,6-dimethylpyridine *N*-oxide this band shows a blue shift to 274 nm. Substitution by halogen at the 3-position of 2,6-dimethylpyridine *N*-oxide has shown that apart from the strong 272-278 nm band, there exist two or three more bands in the regions 220-240 nm and 310-330 nm. The third, weak band is observed at 363 nm which is expected to originate from n-π* transition,[2] i.e. excitation from HOMO to either the LUMO or higher MO. In case of 2,2'-bipyridyl-*N,N*'-dioxide (2,2'-BPNO) the maximum absorption appears around 273 nm.[4] 4,4'-bipyridyl-*N,N*'-dioxide (4,4'-BPNO) absorbs at two different wavelengths viz. 223 and 330 nm,[3] in protic solvent, like in the case of 3-halo-2,6-dimethylpyridine *N*-oxides.

1.2 Synthesis and reactivity of aromatic *N*-oxides

Generally, the heteroaromatic *N*-oxides are synthesized by oxidation of their amine analogues.[1] The oxidizing agent used in those oxidation reactions is either hydrogen peroxide or percarboxylic acid. When the oxidizing agent used is hydrogen peroxide, a carboxylic acid usually acetic acid is used as a mixture so that the oxidizing agent present in equilibrium is the per acid. In a typical oxidation of heteroaromatic amine to aromatic *N*-oxide, a mixture of glacial acetic acid and hydrogen peroxide (30-40%) has been extensively used and the reaction is carried out at 60-80 ^{o}C. Usually excess amount of hydrogen peroxide is used and peroxide is often added in portions. Once the reaction is completed the excess peroxide is decomposed. Such decomposition can be caused by adding manganese dioxide also. Pyridine *N*-oxide, isoquinoline *N*-oxide, 4-dimethylamino pyridine *N*-oxide etc. are reported to be prepared through this synthetic procedure with over 80% yield. Alternatively, 3-choloroperbenzoic acid (MCPBA) is used extensively as oxidizing agent. The advantage of using MCPBA is that after the reaction 3-cholorobenzoic acid is formed and precipitates out which can be filtered off. This makes the work up easier.

Various catalytic pathways are also employed for synthesis of aromatic *N*-oxides. Variety of pyridine derivatives were converted into their corresponding *N*-

oxides in good yields in the presence of hydrogen peroxide as oxygen donor, catalytic amount of manganese tetrakis(2,6-dichlorophenyl) porphyrin [Mn(TDCPP)Cl] and ammonium acetate as co-catalyst in acetonitrile/chloroform.[5]

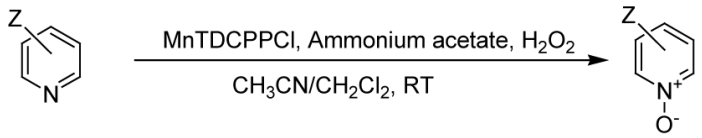

Z = H, 2-CH_3, 4-CH_3, 2-Cl

Pyridine is oxidized in high yield to pyridine *N*-oxide by using 30% aqueous H_2O_2 in the presence of catalytic amount of methyltrioxorhenium. Some substituted pyridines are also reported to be oxidized by the same procedure.[6]

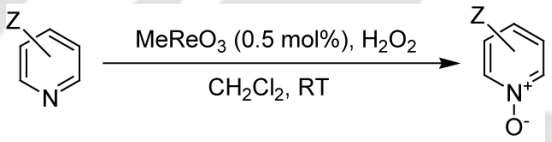

Z = H, 2-CN, 4-CN, 4-CH_3CO, 2F

The high molecular weight aromatic *N*-oxides such as 2,2'-bipyridyl-*N,N'*-dioxide and 4,4'-bipyridyl-*N,N'*-dioxide are usually prepared by using mixture of glacial acetic acid and hydrogen peroxide as the oxidizing agent.[7,8]

Substitution reactions on pyridine ring are difficult but conventional. In case of pyridine substitution at 3- and 5- position takes place only when drastic conditions are employed. This behaviour is due to the influence exerted by the pyridine ring nitrogen. Compared to this, in the case of pyridine *N*-oxide the overall concentration of electrons is different from that exists in pyridine. The effect of the presence of the *N*-oxo functionality is an increased concentration of electrons at the 2- and 4-positions, thereby making these positions quite receptive to substitution by electrophilic reagents. Thus, pyridine *N*-oxide undergoes electrophilic substitution reactions relatively easily and nitration of pyridine *N*-oxide can be achieved readily by dissolving it in a mixture of sulphuric acid and nitric acid. The product is 4-nitropyridine *N*-oxide in high yield. In contrast, the *N*-oxide of 4-picoline, 2,4-lutidine *N*-oxide and 2,4,6-collidine *N*-oxide do not undergo nitration easily.[9]

Apart from the direct substitution reactions, various metallation followed by electrophilic substitution reactions of pyridine *N*-oxide are also studied. The reaction of butyl lithium with 3,4-dimethoxypyridine *N*-oxide results in metallation at C-2 position and leads to lithiated species as an intermediate. This species on reaction with various electrophiles afford the corresponding 2-, 6- or 2, 6- functionalized products.

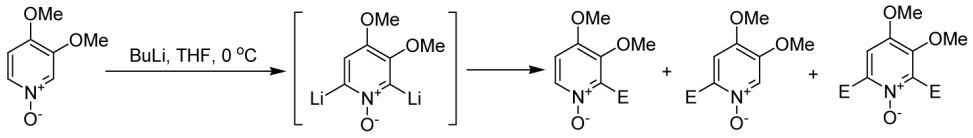

It has been reported recently that direct arylation of pyridine *N*-oxides can be achieved with a wide range of aryl bromides by catalytic cross coupling reactions. Palladium acetate in combination with tri-*tert*-butylphosphine is used as a catalyst for these reactions.[10]

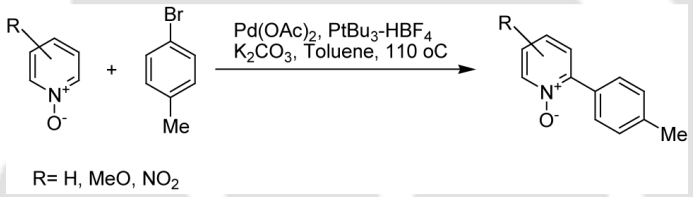

Hiyama has recently reported a few such C-H activation reactions.[11]They have reported that aromatic *N*-oxide undergoes addition reactions across alkynes in the presence of a catalyst generated from [Ni-$(cod)_2$] (cod=cyclooctadiene) and tricyclopentylphosphine in toluene. The reaction is successful with a number of substituted pyridine *N*-oxides and with isoquinoline *N*-oxide. Apart from these, activation of C-H bond of pyridine *N*-oxide to result in organometallic complexes of actinides is also reported. It has been demonstrated that U(IV) and Th(IV) bis(alkyl) complexes readily activate both sp^2 and sp^3 hybridized C-H bonds in pyridine *N*-oxides. The addition of one equivalent of pyridine *N*-oxide to a toluene solution of the U(IV) bis(alkyl) complexes $[(C_5Me_5)_2An(R)_2]$ (R=CH_3, CH_2Ph; An= U, Th) results in activation of an sp^2 hybridized C-H bond, with loss of alkane and formation of the novel cyclometalated pyridine *N*-oxide complexes $[(C_5Me_5)_2An(R)(\eta^2$-(O,C)-

$ONC_5H_4)$].[12] This is in contrast to the known oxygen atom transfer reactivity patterns of pyridine *N*-oxides with oxophilic metal complexes.

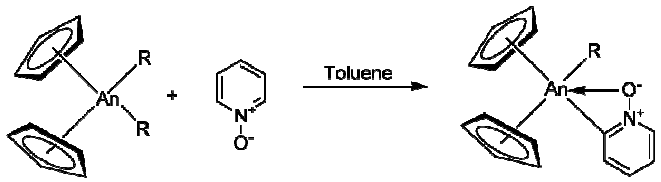

Another important feature of the reactivity of aromatic *N*-oxides is their de-oxygenation reactions. For example, treatment of a number of 4-substituted pyridine *N*-oxides with dimethylthiocarbamoyl chloride (DMTCC) results in the de-oxygenation of the *N*-oxide yielding the parent pyridine.[13]

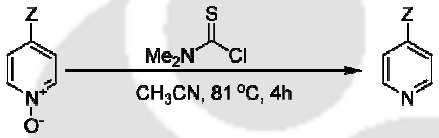

Deoxygenation reactions of pyridine *N*-oxide derivatives catalyzed by *N*-fused porphyrin rhenium(VII) trioxo complex are also reported. These reactions afford the corresponding pyridine derivatives in quantitative yields with excellent turnover numbers.[14] Deoxygenation of pyridine *N*-oxide derivatives are also carried out by Cu(I) reagents such as CuI and CuCl.[15]

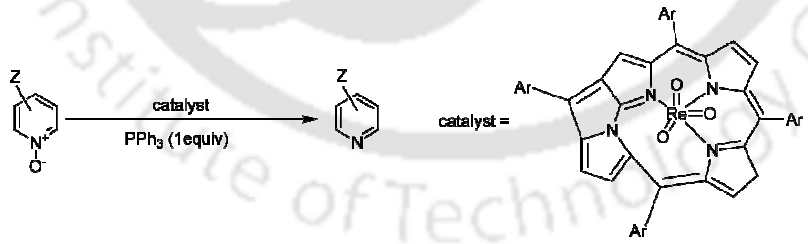

1.3 Coordination complexes of aromatic *N*-oxides

The coordination chemistry of aromatic *N*-oxide ligands was initiated by D. D. Perrin around 50 years ago with a report on metal complexes of adenine *1N*-oxide and adenosine *1N*-oxide with the divalent metal ions Cu(II), Mn(II), Co(II), Ni(II) and Zn(II).[16] Prior to this, investigations involving donation by amine oxides were limited

to studies on the reaction of trimethylamine oxide with several Lewis acids (BF_3, $SiCl_4$ etc.).[17] D. D. Perrin in his paper reported the formation of 1:1 complexes of the two ligands, namely, adenine *1N*-oxide and adenosine *1N*-oxide at appropriate *p*H in the presence of base. They had determined the stability constants for all the complexes and also predicted the structures of the complexes as shown in figure1.3. They concluded the adenine *1N*-oxide complex to be of lower stability than the corresponding adenine complexes.

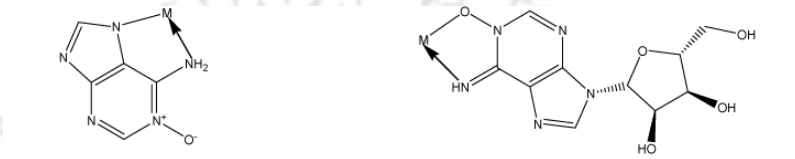

Figure 1.3: Complex formation by adenine *1N*-oxide and adenosine *1N*-oxide

After these initial investigations by Perrin on the coordination properties of aromatic *N*-oxide, R. L. Carlin in the year 1961 reported complexation behaviour of pyridine *N*-oxide towards transition metal ions.[18] Carlin's investigation was based on the affinity of pyridine *N*-oxide for protons and donor properties of covalent molecular oxides such as triphenylphosphine oxide and dimethylsulphoxide. Carlin in this paper has reported nine different complexes of pyridine *N*-oxide with transition metal perchlorates, the metals being Cr(III), Mn(II), Fe(III), Co(II), Ni(II), Cu(II), Zn(II) and Hg(II). He noted that in all these complexes the metal tends to attain the highest possible coordination number towards pyridine *N*-oxide as a ligand. Thus, all but Cu(II) yielded complexes with the general composition $[M(PNO)_6]^{n+}(ClO_4)_n$; where M is the metal centre, PNO is pyridine *N*-oxide. With $Cu(ClO_4)_2$, pyridine *N*-oxide gave two products: four coordinated $[Cu(PNO)_4]$ $(ClO_4)_2$ and six coordinated $[Cu(PNO)_6]$ $(ClO_4)_2$. The Mn(II) and Ni(II) complexes showed unusual colouration with a yellow cast which was accounted for charge transfer transition.

Contemporarily, a number of literature appeared concerning the coordination complexes of pyridine *N*-oxide and substituted pyridine *N*-oxide during the 60's decade. Most of them described the coordination complexes of transition metal ions and a few reporting complexes with lanthanides. Among the transition metal *N*-oxide complexes copper(II) complexes were largely explored due to their interesting

magnetic properties along with a few reports on cobalt(II) and nickel(II) complexes. The copper(II) complexes were of special interest due to their unusually low magnetic moment. Understanding of such isolated magnetic interactions needs structural information and various workers in this area reported a bi- or polynuclear structure of copper(II) halide-PNO complexes on the basis of the low magnetic moment at room temperature and, later, in view of the temperature dependence of the magnetic susceptibility. The 1:1 complex between $CuCl_2$ and PNO was studied extensively. Harris, *et al.*[19] had confirmed the abnormally low magnetic moment reported by Quagliano, *et al.*[20] for the complex $CuCl_2$(PNO) through a study of the temperature dependence of the magnetic susceptibility. Later on the magnetic susceptibility data for a series of 4-substituted pyridine *N*-oxide complexes of copper(II) chloride suggested that the spin-spin coupling in these compounds occurred by a super-exchange mechanism operating through the orbitals of the bridging oxygen atoms.[21]

Although a few PXRD data of pyridine *N*-oxide complexes were available for structural comparison, two or three dimensional structures were not determined until 1965, when, Schafer *et al.* had determined the crystal structure of $[(C_6H_5NO)CuCl_2]_2$ by two dimensional single-crystal X-ray diffraction technique and indicated an oxygen bridged dimer (Figure 1.4).[22] A complete three dimensional X-ray examination of single crystals of the same molecule was then carried out by Sager *et al.* which revealed that the dimeric molecule consisted of two distorted tetrahedra sharing an edge with the oxygen atoms from the pyridine *N*-oxide ligands acting as the bridging units.[23]

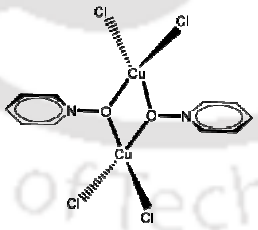

Figure 1.4: Dimeric structure of $[(C_6H_5NO)CuCl_2]_2$

Subsequently a number of 1:1 and 2**:**1 complexes of pyridine *N*-oxide and copper(II) halides was prepared and characterized. Structure determination of the 2:1 complex indicated that the $[Cu(PNO)_2C1_2]_2$ and $[Cu(PNO)_2Br_2]_2$ are dinuclear (Figure 1.5) with one pyridine *N*-oxide ligand acting as a bridging and the other as a

monodentate ligand.[24, 25] In $[Cu(PNO)_2C1_2]_2$ the coordination at the copper atom is distorted tetragonal pyramidal with the terminal pyridine *N*-oxide ligand in the apical position; in $[Cu(PNO)_2Br_2]_2$ the coordination at the copper atom is distorted trigonal bipyramidal with the terminal pyridine *N*-oxide ligand in an equatorial position. Also, the crystal structure of dimeric dibromobis(pyridine *N*-oxide)copper(II) consists of two crystallographically non-equivalent centro-symmetric dimeric molecules of $[(C_5H_5NO)_2CuBr_2]_2$.[26]

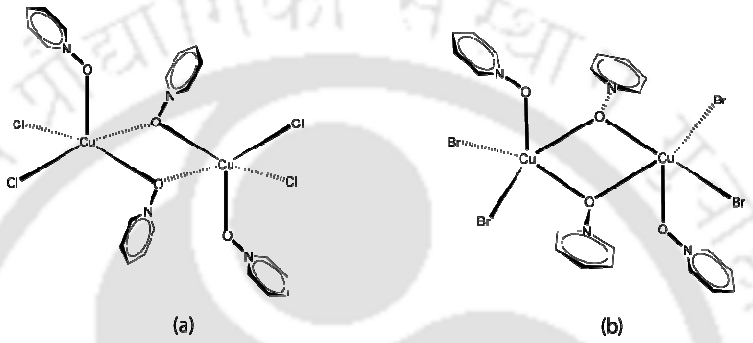

Figure 1.5: Structure of the dinuclear complexes (a) $[Cu(PNO)_2C1_2]_2$ and (b) $[Cu(PNO)_2Br_2]_2$

Following these in 1968, diverting from the extensively studied copper(II) halide complexes, Horrocks *et al*. had reported an acetylacetonato (AA) complex of Ni(II) having PNO as the ancillary ligand. The crystal is composed of discrete molecules of $[Ni(AA)_2(C_5H_5NO)_2]$ (Figure 1.6) in which the six oxygens are coordinated to the nickel in a very nearly regular octahedral array. The two pyridine *N*-oxide molecules occupy positions *cis* to one another in the coordination sphere of the nickel.[27]

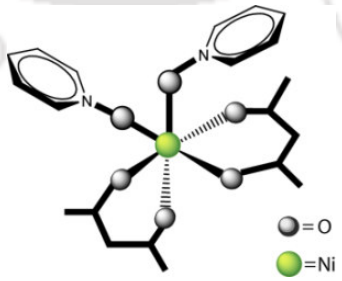

Figure 1.6: Structure of the mononuclear complex $[Ni(AA)_2(C_5H_5NO)_2]$

N. M. Karayannis *et al*. in 1969 reported the first binuclear chlorine-bridged complexes of manganese(II) and nickel(II) chlorides with pyridine *N*-oxides. They had pointed out that the electronic spectra and magnetic moments of the Mn(II) and Ni(II) binuclear complexes are suggestive of the presence of tetracoordinated metal(II) ions with a geometry intermediate between distorted tetrahedral and square planar. Moreover, the magnetic moments of the Mn(II) complexes are suggestive of possible spin-spin interaction. Similarities in their X-ray powder diffraction patterns indicated that the Mn(II) and Ni(II) dinuclear complexes are of nearly the same structure.[28]

J. A. Bertrand and D. L. Plymale in 1964 reported the structural study on tris(pyridine *N*-oxide)cobalt(II) halide complexes.[29] However, only a few cobalt(III) amine *N*-oxide complexes had been reported, in sharp contrast to the large number of complexes known with other transition metals. Nathan *et al.* in 1979 described the synthesis of three Co(III) complexes with bidentate ligands containing at least one amine *N*-oxide function and offered several reasons for the dearth of other examples.[30] Among these were the weak donor properties of the *N*-oxide function and the difficulty of nonaqueous oxidation of cobalt(II) precursors. In 1988 W.L Purcell reported the synthesis of pentaammine(pyridine *N*-oxide)cobalt(III) and complexes with substituted pyridine *N*-oxide ligands. They had also studied the reactivity of these complexes through aquation kinetic and electron transfer by chromium(II) reduction. Rate constants for the reduction of pentaammine(pyridine *N*-oxide)cobalt(III) by hexaaquachromium(II) were higher than those found in most outer-sphere Cr(II)/Co(III) redox reactions. Based on this and on certain properties of the *N*-oxide ligand they had assigned the electron transfer process to be an inner-sphere process.[31]

Based on the studies on substituted pyridine *N*-oxides it was shown that the complexes of substituted pyridine *N*-oxides exhibited a regular trend between the magnitude of the metal-metal interaction and the basicity of the pyridine *N*-oxide. The magnitude of this interaction increases as the basicity of the ligand decreases. This was attributed to the π-back bonding. Quinoline *N*-oxides (QNO) and isoquinoline *N*-oxides (IQNO) are known to be better π-back bonding ligand than the analogous pyridine *N*-oxides. Attributing interest towards the upcoming importance of QNO complexes, various literature had appeared during 60's and 70's. In 1966 William E.

Hatfield *et al.* had reported the study on magnetic properties of a number of complexes of substituted quinoline *N*-oxides with copper(II) chloride and copper(II) bromide. The *N*-oxide ligands they had considered were quinoline *N*-oxide, 4-methylquinoline *N*-oxide, 6-methylquinoline *N*-oxide, 4-chloroquinoline *N*-oxide, 6-methyl-3-nitroquinoline *N*-oxide, 6-methyl-4-nitroquinoline *N*-oxide and 4-nitroquinoline *N*-oxide. Based on the pKa values of the ligands they had concluded that the substituted *N*-oxides with high pKa values tend to form oxygen bridged species. Thus, 4-methylquinoline *N*-oxide having a pKa value of 1.44 forms oxo bridged complex $[CuCl_2(4\text{-methylquinoline } N\text{-oxide})]_2$. The magnetic moment value of the complex was found to be 0.62 BM at 299 ^oC. For *N*-oxides with extremely low pKa values only halogen bridged compounds were formed *eg.* 4-nitroquinoline *N*-oxide, with a pKa of -1.39, falls in this category and consequently the high magnetic moment (2.93 BM at 299 ^oC) of the complex $[CuCl_2(4\text{-nitroquinoline } N\text{-oxide})]_2$ were explained in terms of halogen bridging.[32]

Contemporarily, R. W. Kluiber and W. D. Horrocks reported the complexes $Ni(AA)_2.L$ and $Co(AA)_2.L$ (where L is pyridine *N*-oxide, quinoline *N*-oxide, or isoquinoline *N*-oxide and AA is acetylacetonate). They had shown that more electron spin density is delocalized onto the π-system of quinoline *N*-oxide and isoquinoline *N*-oxide than onto pyridine *N*-oxide.[33]

Following this in 1968 Nelson *et al.* reported the coordinating properties of a series of 4-substituted quinoline *N*-oxides toward nickel(II) and cobalt(II) perchlorates. The compounds were assigned octahedral structures with the general formula $M(4\text{-Z-}C_9H_6NO)_6(C1O_4)_2$ (where Z = H, CH_3O, CH_3, Cl and NO_2) on the basis of analytical data and the magnetic moments. The magnetic moments were found to be in the range 3.33-3.61 BM and 4.91-5.25 BM for nickel(II) and cobalt(II), respectively. The electronic spectra were also studied and ligand field parameters were determined. Considerable evidence for dπ-pπ back-bonding (synergic bonding) was also discussed, back-bonding interaction is much more important in quinoline *N*-oxides and isoquinoline *N*-oxide than in pyridine *N*-oxides. It is clear that the addition of the aromatic ring in the quinoline ring system helps to delocalize electrons and lowers the π* molecular orbitals in these systems significantly, thereby creating more effective π overlap with the metal ion.[34] Later on in 1976 MacDougall *et al.* reported a series of 4-substituted quinoline *N*-oxide and isoquinoline *N*-oxide complexes with

copper(II) acetate. The compounds were of the general formula $[Cu(CH_3COO)_2(4\text{-}Z\text{-}C_9H_6NO)]_2.xH_2O$ (where Z = H, CH_3O, CH_3 and Cl). The electronic spectra and the magnetic moments were reported and compared with those obtained for a similar series of substituted pyridine *N*-oxide ligands. On the basis of these data they had concluded that even though the basicity of the two series of ligands differ somewhat, their donor abilities toward copper(II) acetate were similar. So, it was inferred that since the steric effect is greater in the quinoline *N*-oxide series than in the pyridine *N*-oxide series, there is a greater amount of π-back bonding in the quinoline *N*-oxide complexes than in the pyridine *N*-oxide complexes. Consequently, π-back bonding seemed to be more important in determining the magnitude of the metal-metal interaction than steric effects. By π-back donation into the *N*-oxide antibonding orbitals, electron density is being removed from orbitals which are essentially copper-copper antibonding in character. These data were all consistent with the δ-bonding model for the metal-metal interaction and suggested that the strength of this interaction increases as the electron density at copper decreases.[35]

Compared to the aromatic mono *N*-oxides, *N,N′*-dioxide were relatively less explored. 1,10-phenanthroline *N,N′*-dioxide and 2,2'-bipyridyl-*N,N*'-dioxide were among the earliest known ones. The difference between the two ligands arises from the presence of the third aromatic ring in 1,10-phenanthroline *N,N′*-dioxide which makes it more rigid and acts as a chelating ligand. However, 2,2'-bipyridyl-*N,N*'-dioxide is comparatively flexible and can act either as a chelating or as a bridging ligand.

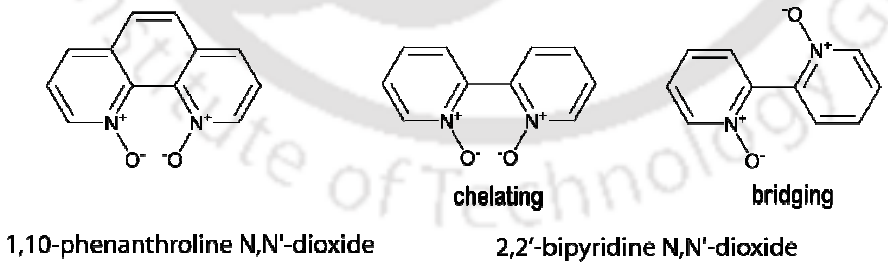

Figure 1.7: *N,N′*-dioxide ligands with their possible binding modes

The donor properties of 2,2'-bipyridyl-*N,N*'-dioxide were first studied by P. G. Simpson *et al.* in 1963.[36] They prepared a number of coordination compounds of 2,2'-bipyridyl-*N,N*'-dioxide (2,2'-BPNO) with metal salts and determined their structures by elemental analysis, conductivity, and magnetic susceptibility measurements. The

compounds were found to be electrolytes, containing tris-chelate cations $[M(2,2'\text{-}BPNO)_3]^{2+}$ of the metal ions from Mn(II) to Zn(II) and Cd(II) and the anions ClO_4^- and $[PtCl_4]^{2-}$. Most of the complexes were hydrated ones. Exceptionally, Cu(II) does not form a tris-chelate complex when the anion is $[PtCl_4]^{2-}$; rather it forms a complex with the composition $[Cu(2,2'\text{-}BPNO)_2][PtCl_4].4H_2O$. The values of the magnetic moments showed that the complex cations have the same number of unpaired electrons as the free metal ions, therefore considered to have an octahedral structure utilizing sp^3d^2 hybridization.

The preparation and characterization of number of compounds containing the tris-chelate complex cations, $[M(2,2'\text{-}BPNO)_3]^{n+}$, where ($M = Al^{3+}$, Cr^{3+}, Fe^{3+}, Co^{2+}, Ni^{2+}, Zn^{2+}, Cd^{2+}, and Hg^{2+}) are reported.[37] In all of these complexes, 2,2'-bipyridyl-*N,N*'-dioxide forms seven-membered rings and the two aromatic rings adopt a staggered conformation. The compounds were characterized by their electrical conductance and electronic spectra, magnetic moments, and infrared spectra. Apart from these, the compounds $Co(2,2'\text{-}BPNO)_2Cl_2$, $Cu(2,2'\text{-}BPNO)Cl_2$, $[Ag(2,2'\text{-}BPNO)_2]ClO_4{\cdot}3H_2O$, $Pb(2,2'\text{-}BPNO)_2(ClO_4)_2$, $[ZrO(2,2'\text{-}BPNO)_3](ClO_4)_2{\cdot}2H_2O$, $[Th(2,2'\text{-}BPNO)_4](ClO_4)_4$, $[VO(2,2'\text{-}BPNO)_2](ClO_4)_2$, $[UO_2(2,2'\text{-}BPNO)_2](ClO_4)_2$, $Mo_2O_4Cl_2(2,2'\text{-}BPNO)_2]{\cdot}2H_2O$ and $[Mo_2O_3Cl_4(2,2'\text{-}BPNO)_2]{\cdot}2H_2O$ are also reported.[37]

A number of halocarbonyl complexes of rhenium(I) having 2,2'-bipyridyl-*N,N*'-dioxide ligand were reported by Sartorally *et al*. They had prepared the complexes $Re(CO)_3(2,2'\text{-}BPNO)X$ (where X is Cl, Br or I) by substitution of two carbonyl groups of halopentacarbonylrhenium(I) by 2,2'-BPNO ligand. Based on the infrared spectrum and the dipole moments of the compounds they suggested the structure of the compounds to be like shown in figure 1.8.[38]

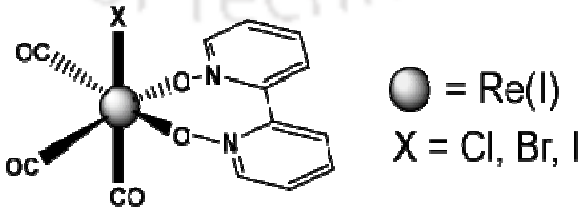

Figure 1.8: Structure of the complex $Re(CO)_3(2,2'\text{-}BPNO)X$

Apart from the extensively studied transition metal chemistry of 2,2'-BPNO the synthesis and physical properties of a series of lanthanide compounds of 2,2'-BPNO was also reported. In contrast to the tris-chelate complexes of transition metal ions, the lanthanide complexes were reported to have the general formula $[Ln(2,2'\text{-}BPNO)_4](ClO_4)_3$ (where Ln = La, Pr, Nd, Sm, Gd, Dy, Ho, Er, Yb, Y). Based on the infrared spectra as well as conductance measurements it was concluded that the M-O bond is weaker in the lanthanide complexes than in the similar transition metal complexes.[39] The crystalline compounds $[Eu(2,2'\text{-}BPNO)_4](ClO_4)_3$ and $[Tb(2,2'\text{-}BPNO)_4](ClO_4)_3$ were characterized by infrared spectra and conductance measurements. Both these complexes were observed to exhibit fluorescence in both solid and solution state.[40]

Although number of reports on coordination complexes of 2,2'-bipyridyl-*N,N'*-dioxide were available during the early sixties only a few of them carried any structural aspect of the complexes. The structural characterization of the $[La(2,2'\text{-}BPNO)_4](ClO_4)_3$ by Karaghouli *et al.* showed it to have a cubic coordination geometry. This is the first example of cubic eight-coordination for a lanthanide complex.[41]

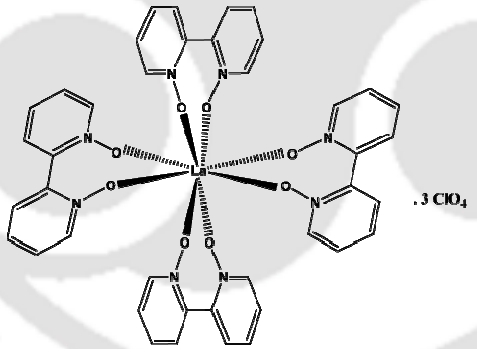

Figure 1.9: Structure of the eight-coordinated $[La(2,2'\text{-}BPNO)_4](ClO_4)_3$ complex

After these initial studies on various aromatic *N*-oxide complexes numbers of reports have appeared in the literature with various new features especially under the banner of *supramolecular chemistry*. Besides the mono or dinuclear complexes various coordination polymers are being reported from time to time. The one dimensional, two dimensional or three dimensional coordination polymers are shown to be of importance as magnetic materials, catalyst or even towards gas separation

technique. Due to such wide diversity of the coordination polymers containing aromatic *N*-oxides, a brief discussion on them is presented in the following sections.

1.4 Coordination modes of aromatic *N*-oxides

Binding of heteroaromatic *N*-oxide ligands occurs through the oxygen which is obvious as the HOMO preferentially reside over the oxygen atom. The binding modes of the different heteroaromatic *N*-oxide ligands vary with the number of *N*-oxo functionality available in the molecule. Pyridine *N*-oxide binds to metal ions either through a monodentate binding mode or through a μ^2 bridging mode. Similar is the case for quinoline *N*-oxide ligand. However, bipyridine *N,N'*-dioxide ligand shows versatility in their binding modes owing to the presence of two *N*-oxo functionality. Bipyridine *N,N'*-dioxide binds to metal ions in both monodentate and bidentate coordination modes and both of these coordination modes can be accompanied by the μ^2 bridging mode of the *N*-oxo functionality. The 2,2'-bipyridyl-*N,N'*-dioxide is an interesting ligand and act either as a chelating or as bridging ligand. This is possible because of the free rotation around the C^{ipso}-C^{ipso} single bond between the two aromatic rings of 2,2'-bipyridyl-*N,N'*-dioxide. In other words it can be said that 2,2'-bipyridyl-*N,N'*-dioxide can coordinate to metal centres either in a *cis* or a *trans* configuration as shown in figure 1.10. However, simultaneous μ^2 bridging by both the *N*-oxo groups is not common in this ligand, may be due to steric factor.

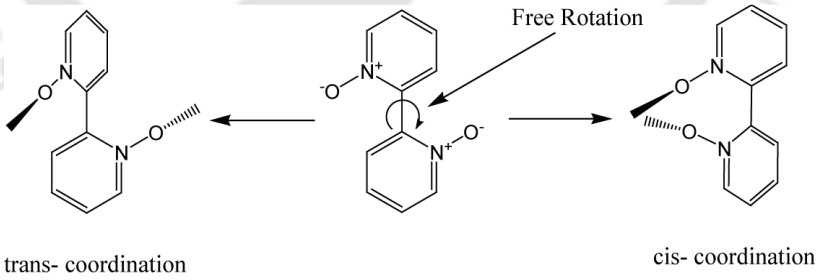

Figure 1.10: Two conformations of 2,2'-bipyridyl-*N,N'*-dioxide towards coordination

4,4'-bipyridyl-*N,N'*-dioxide is comparatively much more flexible as a ligand since it exhibits a number of coordination mode on binding to metal centres (Figure 1.11). In general, 4,4'-BPNO coordinates to metal ion as a bridging ligand although

the monodentate binding (C) is also common. Interestingly, two different μ^2 bridging is possible for this ligand: one is the monodentate μ^2 bridging (D) and the other is the bidentate μ^2 bridging (E, F). Owing to the orientation of the lone pair on the *N*-oxo oxygen atom the bidentate μ^2 bridging can be of *trans* (E) or *cis* (F) conformation. Apart from these, various peculiar yet possible coordination modes of 4,4'-BPNO are possible such as bidentate μ^3 bridging and bidentate μ^4

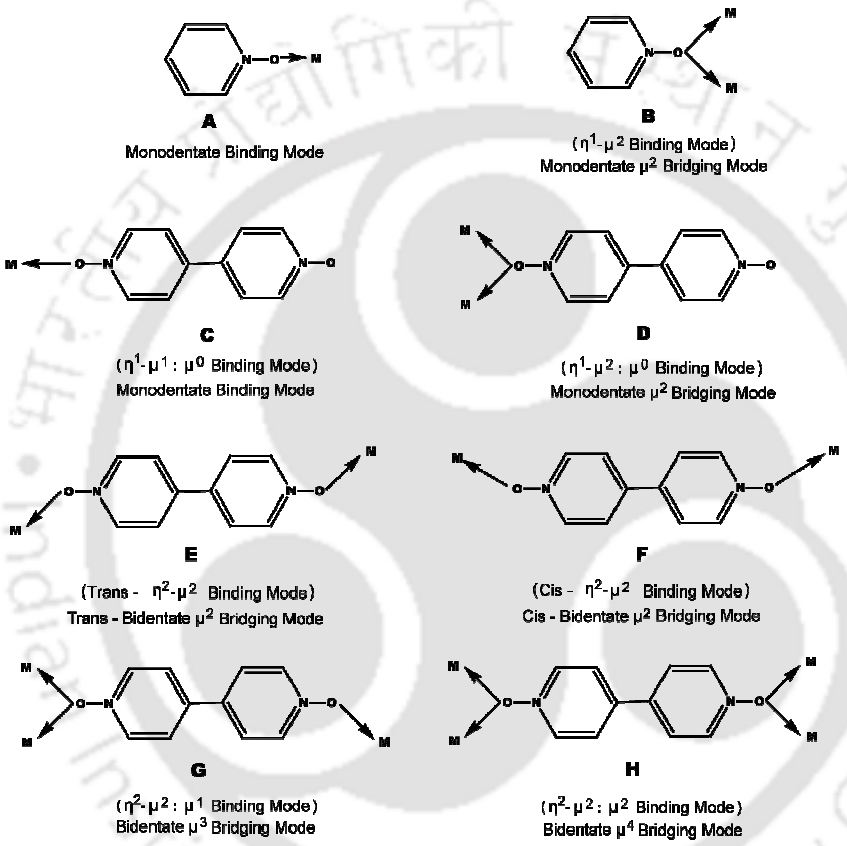

Figure 1.11.: Different possible binding modes of pyridine *N*-oxide and 4,4'-bipyridyl-*N,N'*-dioxide ligands

bridging mode. These two coordination modes are very rare and appear in only one or two examples. To simplify distinguishing these coordination modes from each other, a simple terminology based on the bridging pattern (μ) and denticity (η) of the ligand is proposed and will be used throughout the text in the next sections. According to this terminology the monodentate μ^2 bridging can be abbreviated as η^1-μ^2:μ^0 binding mode as it involves only one *N*-oxo group to bridge between two metal centres. Similarly the bidentate μ^2 bridging mode is abbreviated as η^2-μ^2 binding mode and the

bidentate μ^3 bridging mode is abbreviated as η^2- μ^2: μ^1 binding mode; μ^1 refers to mono coordination by the *N*-oxo group and μ^2 refers to di-coordination (bridging) to metal centres.

1.5 Aromatic *N*-oxides based coordination polymers

Coordination polymers are integral constituent of inorganic *crystal engineering* and thereby of *supramolecular chemistry*. The term coordination polymer encompasses any extended structure based on metal ions linked into an infinite chain, a two dimensional sheet or a three dimensional architecture by bridging ligands.[42] The inspiration behind the design of such polymeric macromolecules, held together by coordination interactions, comes from the well known zeolite chemistry. Once formed the coordination polymers can have different architectures such as zigzag chain, ladder, diamondoid net etc. Some of such architectures are shown in figure 1.12. A more particular class of these coordination polymers is metal organic framework (MOF). Those crystalline solids which have an ordered three dimensional structure and which are both robust and porous are known as MOF.[42] The diamondoid net and the octahedral nets shown in figure 1.12 are examples of MOF.

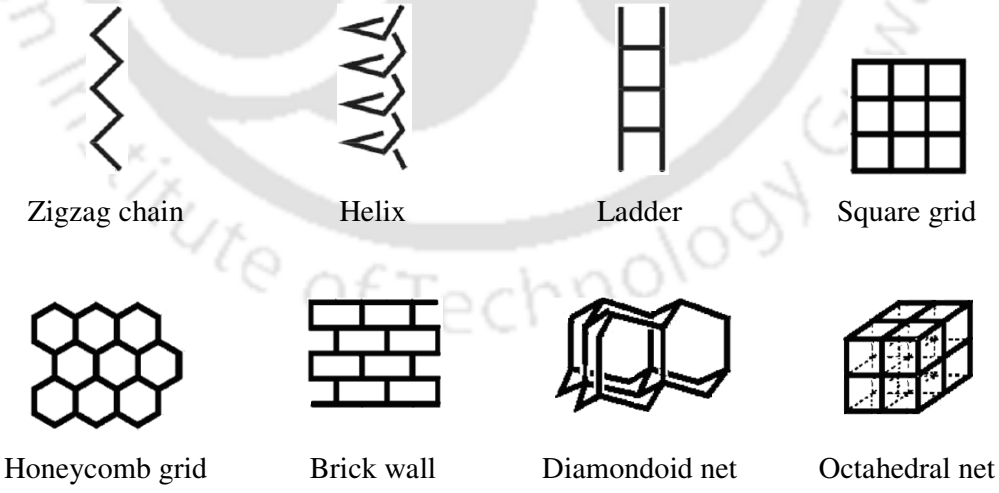

Figure 1.12: Different architectures adopted by coordination polymers

The common way to classify coordination polymers are by their dimensionalities. The coordination polymers can have different dimensionalities beginning from one dimension through three dimension. To illustrate the wide diversity of coordination polymers of aromatic *N*-oxide some examples are presented in the following sub-sections.

1.5.1 One dimensional coordination polymers

The structural variety of the coordination polymers constructed from *N*-oxide ligands depends upon a number of factors such as the coordination modes of the ligand, the number of ligating sites in the ligand as well as the number of ligands involved in the coordination sphere of the metal ions. Depending upon all these factors, coordination polymers may adopt different architectures. Being a neutral ligand, only criteria for complex formation with aromatic *N*-oxides is the presence of an anionic counterpart that can compensate for the cationic charge on the metal center. For the synthesis of coordination polymers, anionic ligands such as carboxylate, nitrate, sulphate etc. are preferred due to their strong binding affinity to the metal centers compared to bulkier ligands such as perchlorate, tetrafluoroborate or hexafluorophosphate etc.

Pyridine *N*-oxide or other mono *N*-oxides often form zero dimensional complexes either due to monodentate non-bridging coordination mode of the ligand or due to blockade of coordination sites by other ligands. For instance, the complex $\{(4\text{-MPyO})_2(CuCl_2)_2(H_2O)(C_2H_5OH)\}$ [where 4-MPyO is the 4-(4-methoxystyryl)pyridine *N*-oxide], is obtained by mixing solutions of 4-(4-methoxystyryl)pyridine *N*-oxide and $CuCl_2 \cdot 2H_2O$ in ethanol.[43] The geometry around both of the copper(II) ions can be described as a tetragonal pyramid with a trapezoidal base, at the corners of which are two oxygen atoms of *N*-oxide and two chlorine atoms (Figure 1.13). The oxygen atoms of either water or ethanol are at the apex of the pyramid. Two molecules of the adduct form a hydrogen bonded dimer in which they are connected to each other through O-H···Cl hydrogen bonds. The copper(II) atoms are antiferromagnetically coupled within a dimeric unit.

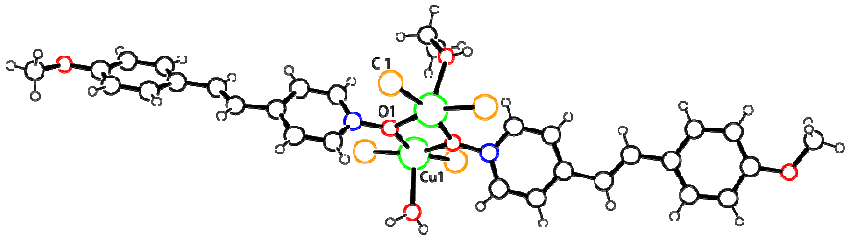

Figure 1.13: Structure of the complex $\{(4\text{-MPyO})_2(CuCl_2)_2(H_2O)(C_2H_5OH)\}$

Some other such examples of low dimensional *N*-oxide complexes come from the report of 2-Iminopyridine *N*-oxide (PymNox) complexes with nickel(II) and palladium(II). A series of nickel(II) PymNox bromide complexes and palladium(II) PymNox chloride complex are prepared that are basically mononuclear complex with *N*-oxo coordination (Figure 1.14). The nickel(II) PymNox complexes with different substitution patterns in the ligand have been shown to be active as ethylene polymerization catalysts. [44]

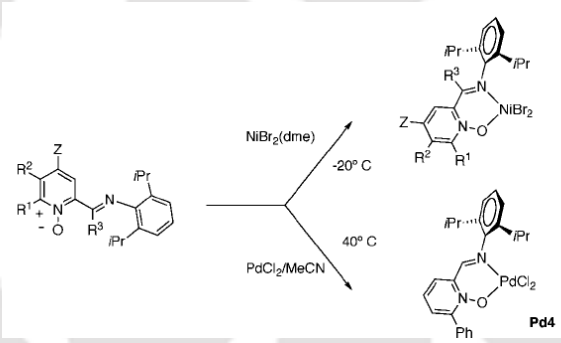

	R¹	R²	R³	Z
Ni1	H	H	Me	H
Ni2	H	H	H	H
Ni3	benzo		H	H
Ni4	Ph	H	H	H
Ni5	H	H	H	NO_2
Ni6	H	H	H	OMe

Figure 1.14: Synthesis of a series of nickel(II) PymNox bromide complexes and palladium(II) PymNox chloride complex

In contrast to these observations on association with suitable anionic ligands, mono *N*-oxides can lead to high dimensional coordination polymers also. For example, structural characterization of the *bis*-pyridine *N*-oxide cobalt(II) *bis*-dicyanamide complex, $[Co(PNO)_2(dca)_2]_n$ (where PNO, pyridine *N*-oxide and dca, dicyanamide), reveals it to be an one dimensional coordination polymer where dca acts as bridging ligand and the *N*-oxo group is attached to Co(II) in a monodentate fashion. Each octahedral Co(II) in the 1D coordination chain is attached with four 1,5-dicyanamide and two pendant pyridine *N*-oxide ligands (Figure 1.15). The one-dimensional chains are connected to each other through non-covalent π-π interactions, giving rise to a two dimensional infinite sheet-like structure. The variable temperature

magnetic measurement shows that the metal centers in the one dimensional chains are weakly anti-ferromagnetically coupled.[45]

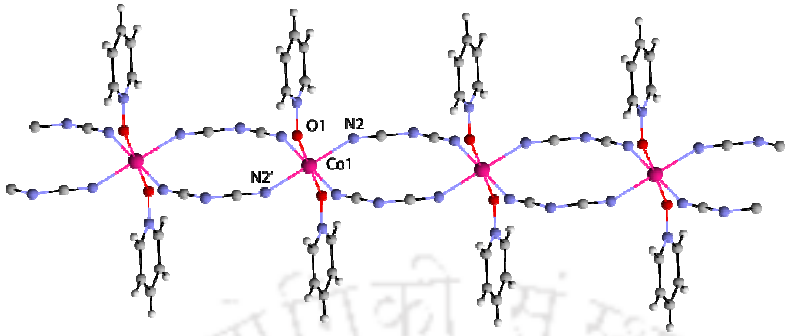

Figure 1.15: one dimensional chains of $[Co(PNO)_2(dca)_2]_n$

Hydrothermal reaction of $Zn(NO_3)_2.6H_2O$ with pyridine-2,6-dicarboxylic acid *N*-oxide (PDCO) yields a one dimensional helical coordination polymer $[Zn(PDCO)(H_2O)_2]_n$.[46] The coordination geometry around zinc(II) center is a slightly distorted octahedron, the equatorial plane of which comprises of four oxygen atoms from the carboxylate groups and *N*-oxide moieties of two different PDCO anions. Two coordinated water molecules occupy the remaining apical coordination sites. The *N*-oxo group here acts as a μ^2 bridging ligand and connects the nearby metal centers (Figure 1.16).

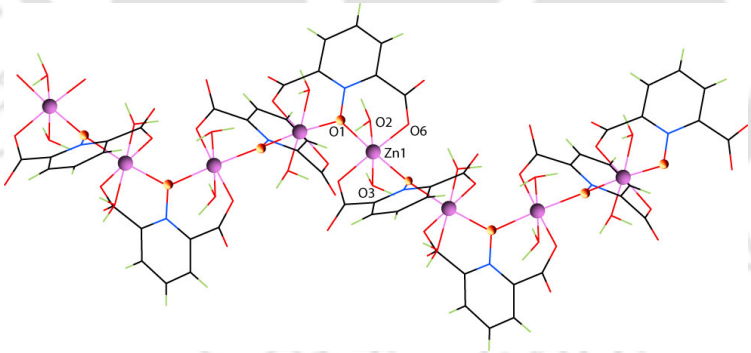

Figure 1.16: The one dimensional helical coordination polymer $[Zn(PDCO)(H_2O)_2]_n$

Compared to the mono *N*-oxide, supramolecular chemistry of di *N*-oxides such as pyrazine-*N,N'*-dioxide, 1,2-bis(pyridin-4-yl)ethane-*N,N'*-dioxide etc. is more explored, especially of 4,4'-bipyridyl-*N,N'*-dioxide (4,4'-BPNO). Also, these are much better ligand due to their possibility of versatile coordination modes. Treatment of $[M(hfac)_2(H_2O)_2]$ (where, M=Co or Cu, hfac= hexafluoroacetylacetonato) with 4,4'-

bipyridyl-*N,N'*-dioxide in 1:1 molar ratio gives $[Co(hfac)_2(4,4'\text{-BPNO})]_n$ and $[Cu(hfac)_2(4,4'\text{-BPNO})]_n$ respectively, which form isostructural linear chains. The linear one dimensional chains consist of $[M(hfac)_2]$ acting as the node connecting with each other through the spacer ligand 4,4'-BPNO that coordinates the metal centres with a *trans* η^2-μ^2 binding mode (Figure 1.17).[47]

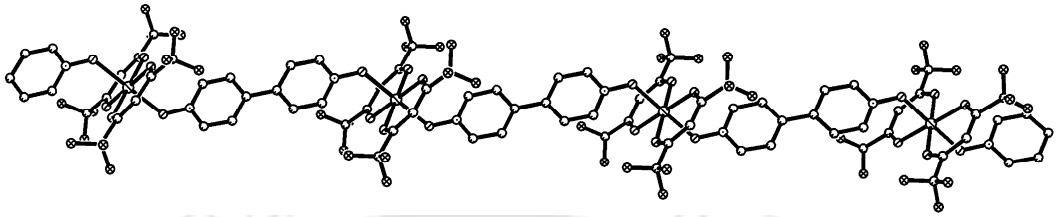

Figure 1.17: The linear one dimensional chain of $[Co(hfac)_2(4,4'\text{-BPNO})]_n$

A series of one dimensional coordination polymers of 4,4'-BPNO containing tetraaquo metal(II) cation have been synthesized by simple solution state methodology and characterized.[48] They have the general composition $\{[M(H_2O)_4(4,4'\text{-BPNO})][ClO4]_2.\ 2(4,4'\text{-BPNO})\ \}_n$ (M = Co, Ni, Cu or Zn). The coordination polymers are isomorphous, crystallizing in the triclinic space group *P-1*. 4,4'-BPNO ligands are coordinated to the metal centers through the *trans* η^2-μ^2 binding mode and bridge the metal centers to form a one dimensional chain. Two molecules of 4,4'-BPNO remain as solvate and are involved in hydrogen bonding with the aquo hydrogen atoms. This in turn results in the formation of three dimensional open frameworks that include ClO_4^- anions within the channels through weak C-H···O interactions.

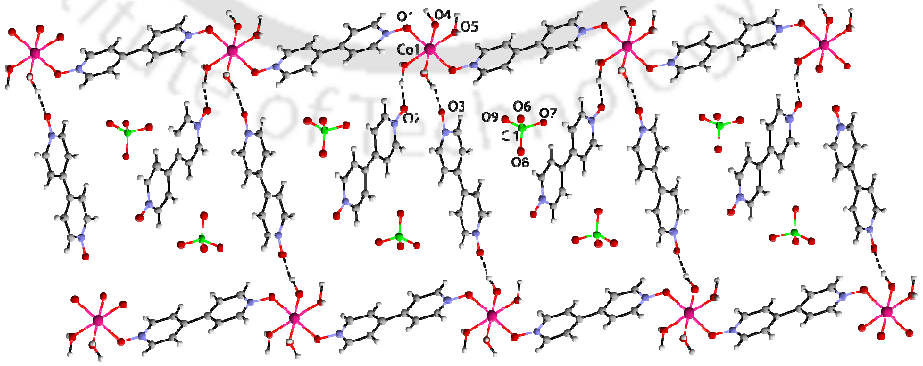

Figure 1.18: Three dimensional open framework of $\{[M(H_2O)_4(4,4'\text{-BPNO})][ClO4]_2.\ 2(4,4'\text{-BPNO})\ \}_n$ that includes ClO_4^- anions within the channels

Two isomorphous heteropolynuclear complexes with the general composition $[\{(H2O)_5(4,4'\text{-BPNO})Pr\text{-}NC\text{-}M(CN)_5\}(\mu\text{-}L)]\cdot 0.5(4,4'\text{-BPNO})\cdot 4H_2O$ were obtained from the reaction of $Pr(NO_3)_3\cdot 6H_2O$ with 4,4'-bipyridyl-*N,N'*-dioxide and $K_3[M(CN)_6]$ [M=Fe(III), Co(III)]. The complexes contain two different types of 4,4'-BPNO ligands, one acting as terminal and other as bridging ligand. The structure can be described as being formed by the neutral binuclear entities $\{(H_2O)_5(4,4'\text{-BPNO})Pr\text{-}NC\text{-}M(CN)_5\}$ that are bridged by 4,4'-bipyridyl-*N,N'*-dioxide, resulting in infinite *zig-zag* chain (Figure 1.19).[49]

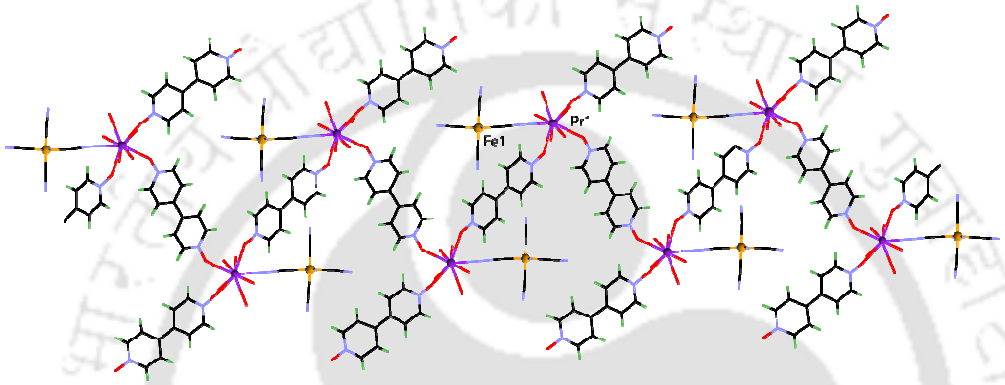

Figure 1.19: One dimensional *zig-zag* chain of the heteropolynuclear complex of Pr(III) and Fe(III)

Solvent diffusion method yields the one dimensional coordination polymer of 4,4'-BPNO with terbium(III) nitrate with the composition $[Tb(4,4'\text{-}BPNO)(CH_3OH)(NO_3)_3]_n$. Structure determination shows it to be an one dimensional *zig-zag* chain (Figure 1.20). The terbium(III) centres in the coordination polymer adopt a nona-coordinated TbO_9 environment with one oxygen atom from each of two different 4,4'-BPNO molecules, one from a coordinated methanol, and six others from three bidentate nitrate anions. Like in the other cases here also the two 4,4'-BPNO ligands coordinate the metal centres with the *trans* $\eta^2\text{-}\mu^2$ binding mode. Neighbouring terbium centres in the chain are separated by 4,4'-BPNO with a distance of about 13.2 Å. The coordinated MeOH and nitrate groups on adjacent chains are involved in strong hydrogen bonding interactions. With the aid of these contacts the *zig-zag* network forms a three dimensional (3D) structure of 6^6 topology.[50]

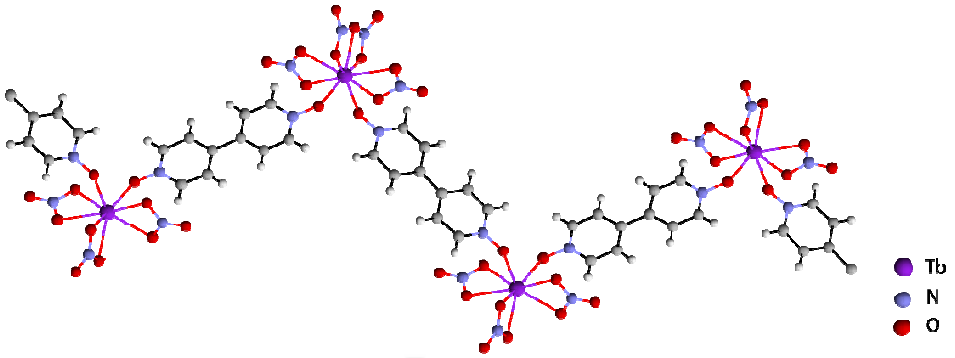

Figure 1.20: One dimensional coordination polymer [Tb(4,4'-BPNO)(CH_3OH)(NO_3)$_3$]$_n$

Hydrothermal reaction of $GdCl_3.6H_2O$, $MnCO_3$, $MnSO_4.H_2O$ and picolinic acid *N*-oxide (picoNO) produces the one dimensional coordination polymer $[Gd(picoNO)(H_2O)_2(SO_4)]_n$. The $MnCO_3$ plays a role to deprotonate picolinic acid *N*-oxide ligand and $MnSO_4.H_2O$ provides the sulfate ion. The complex is a one dimensional chainlike polymer. Each Gd(III) ion is in a triply capped trigonal prismatic geometry, chelated by one picoNO and two SO_4^{2-} ligands, and further coordinated by one SO_4^{2-} ligand and two water molecules. As expected the picoNO ligand acts as a chelating ligand and chelates one Gd(III) ion via its *N*-oxide oxygen atom and one of the carboxylate oxygen atoms. The dimensionality of the chain is provided solely by the sulphate anions bridging three Gd(III) centres through μ^2-O bridging coordination mode (Figure 1.21).[51]

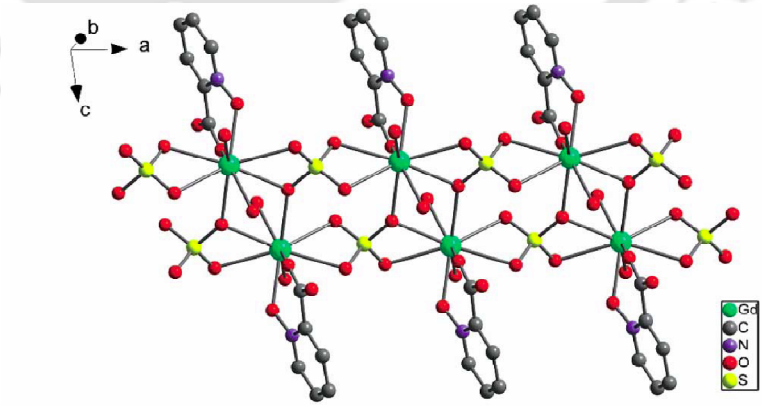

Figure 1.21: The one dimensional coordination polymer $[Gd(picoNO)(H_2O)_2(SO_4)]_n$

1.5.2 Two dimensional coordination polymers

In the previous subsection we have described various one dimensional coordination polymers that are reported in literature. Besides that different types of two dimensional coordination polymers having a variety of architecture are also reported. In this subsection synthesis and structural properties of different types of two dimensional coordination polymers are discussed.

Hydrothermal reaction of $GdCl_3.6H_2O$, $MnCO_3$, $MnSO_4.H_2O$ and nicotinic acid *N*-oxide (nicoNO) produced a 2D wavelike coordination sheet with composition $[Gd(nicoNO)(H_2O)_2(SO_4)]_n$.[51] In the structure of the coordination polymer the Gd(III) ion exhibits a square anti-prism coordination environment formed by two *N*-oxide groups and two carboxylate oxygen atoms from nicoNO, two oxygen atoms from two SO_4^{2-} ligands and two coordinated water molecules. Two Gd(III) ions bridged by a pair of SO_4^{2-} ions in a bidentate bridging mode forms a discrete dimer. The neighbouring dimers are connected by two nicoNO ligands with their *N*-oxide groups acting as μ^2 bridging ligand to give an infinite chain running along the *b* axis. The chains, running along *b* axis are further linked along *a* axis through carboxylate coordination of nicoNO ligands to result in the two dimensional sheet (Figure 1.22).

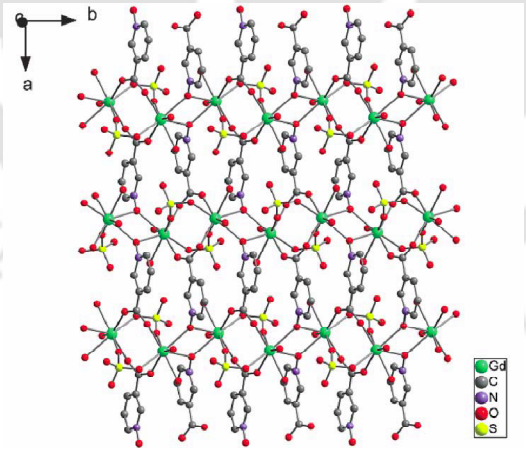

Figure 1.22: 2D coordination sheet of $[Gd(nicoNO)(H_2O)_2(SO_4)]_n$

One of the most common architecture in two dimensional polymers is the layered sheet network. Such a 2D layered structure is displayed by the complex $[Mn(ox)(4,4'\text{-BPNO})]_n$, where ox is oxalate anion, prepared through solution state

mixing of 4,4'-BPNO, $MnCl_2.4H_2O$ and disodium oxalate.[52] The structure exhibits a (4,4) topology where the manganese ions occupy the 4-connecting nodes while the chelating oxalate and 4,4'-BPNO ligands form the rhomboid grid. The oxalate bridging provides a metal-metal separation of 5.657(2) Å while the 4,4'-BPNO linkers separates the metal ions by 12.537 Å. The coordination sphere around each manganese(II) center comprises of *trans*-located 4,4'-BPNO oxygen atoms and four oxalate donors in the equatorial plane (Figure 1.23).

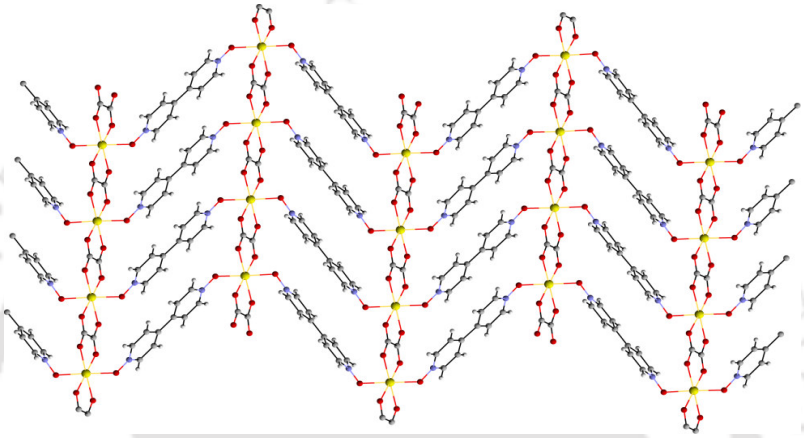

Figure 1.23: 2D layered structure of the complex $[Mn(ox)(4,4'\text{-BPNO})]_n$

Solvent layering of an ethanolic or methanolic solution of 4,4'-BPNO on top of a layer of zinc(II) bromide solution in chloroform yields a binuclear complex with composition $[Zn_2Br_4(4,4'\text{-BPNO})_2]_n$.[53] Crystal structure analysis reveals the complex to be a 2D coordination polymer. The Zn(II) metal centres are coordinated to two

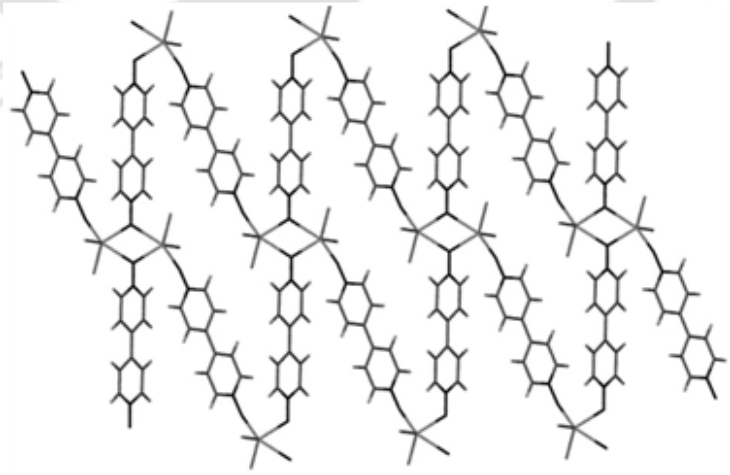

Figure 1.24: Two dimensional polymeric chain of $[Zn_2Br_4(4,4'\text{-BPNO})_2]_n$

bromide ions and three 4,4'-BPNO ligands thereby adopting a distorted trigonal bipyramidal coordination geometry with oxygen atoms in the equatorial plane and bromide ions in the axial positions. The complex forms a planar layer with metal centres bridged by the 4,4'-BPNO ligands via terminal oxygen atoms forming double stranded polymeric chains (Figure 1.24).

Hydrothermal reaction of $Mn(CH_3COO)_2{\cdot}4H_2O$, 4,5-imidazoledicarboxylic acid (H_3IMDC), 4,4'-BPNO in deionized water leads to a 2D coordination polymer having composition $[Mn(HIMDC)(4,4'\text{-}BPNO)_{0.5}(H_2O)]_n$. The asymmetric unit consists of one Mn atom, one HIMDC ligand, half a 4,4'-BPNO and one coordinated water molecule. The Mn(II) centre adopts a distorted octahedral coordination environment. During the formation of the coordination polymer each HIMDC group bonds to two Mn atoms to form a 1D helical chainlike structure. These left-handed and right-handed helical chains are then linked by 4,4'-BPNO ligand through a *trans* coordination mode to generate an infinite 2D herringbone architecture (Figure 1.25).[54]

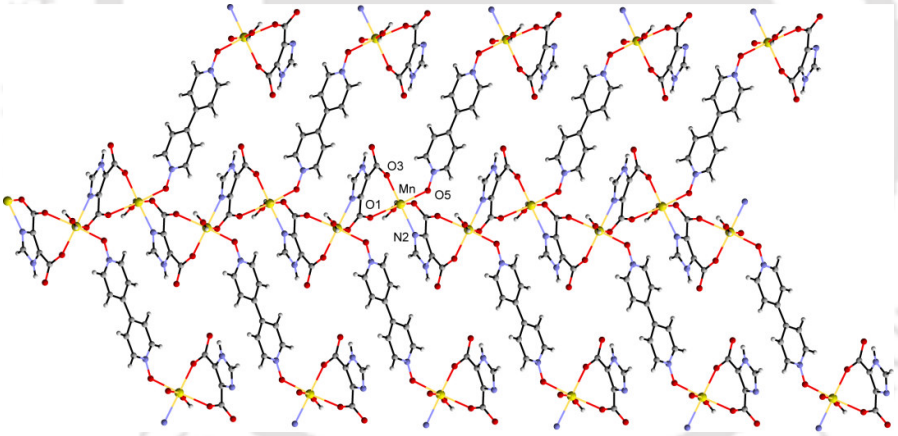

Figure 1.25: 2D herringbone architecture formed by $[Mn(HIMDC)(4,4'\text{-}BPNO)_{0.5}(H_2O)]_n$

Another such two dimensional coordination polymer of indium(III) with composition $\{[In_2(pdc)_2(4,4'\text{-}BPNO)(H_2O)2Cl_2]{\cdot}2H_2O\}_n$ (where pdc is 2,5-pyridine-dicarboxylic acid) is reported recently.[55] The coordination to each of the indium ions in the complex is provided by two oxygen atoms from two pdc ligands, one nitrogen atom from a pyridine ring, one oxygen atom from one 4,4'-BPNO ligand, one water molecule and one chloride ion. The pdc ligand connects the metal ions to generate a

1D chain. The 4,4'-BPNO adopt a *trans* connection mode and join the chains through the coordinated oxygen atoms in the *ac* plane to form a 2D wave-like architecture (Figure 1.26). The photoluminescent spectra of the compound, recorded in the solid state at room temperature, show a broad peak with a maximum at 497 nm. This emission band was assigned to ligand-to-metal charge transfer (LMCT) transition.

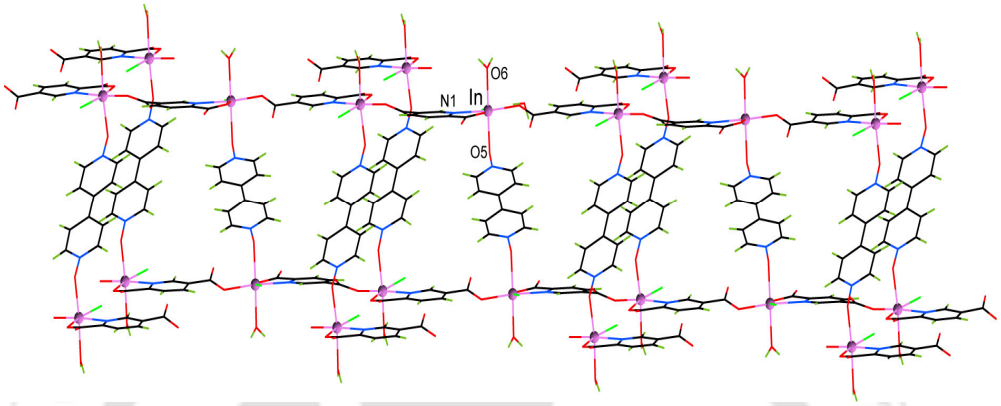

Figure 1.26: Two dimensional coordination polymer of indium(III) with 4,4'-BPNO

Number of lanthanide based two dimensional coordination polymers derived from 3,5-bis(3-pyridyl-*N*-oxide)-4-amino-1,2,4-triazole (**L**) have been reported recently. The compounds are synthesized by the solution state reactions of **L** with various perchlorate salt of Ln(III) viz.(La, Pr, Nd, Sm, Eu, Gd). The 1,2,4-triazole-bridged *N,N'*-dioxide ligand is synthesized by the oxidation of 3,5-bis(3-pyridyl)-4-amino-1,2,4-triazole with H_2O_2 in the presence of AcOH at ambient temperature. All the complexes are isostructural where the ligand acts as a bidentate ligand to bind the

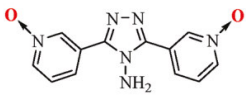

=L

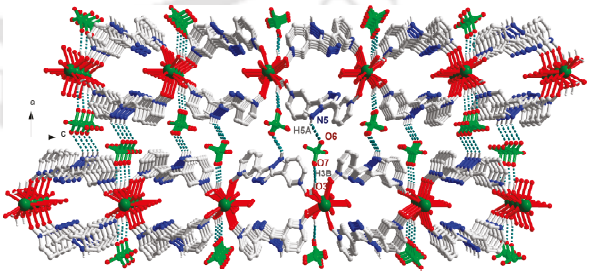

Figure 1.27: Perchlorate anions embedded within the pores of the hydrogen bonded three dimensional networks formed by a 2D coordination polymer of Ln(III)

Ln(III) cations resulting into a non-interpenetrating two dimensional network structure. The ligands bridge to create one dimensional chains of cations connected by terminal *N*-oxide moieties. These one dimensional chains are double-stranded and extend along the crystallographic *b* axis and further crosslinked through the Ln(III) nodes into a two dimensional net. The perchlorate anions remain embedded within the pores of the hydrogen bonded three dimensional networks formed by the 2D coordination polymers (Figure 1.27).[56]

1.5.3 Three dimensional coordination polymers

Three dimensional coordination polymers of mono *N*-oxide are relatively scarce. Recently, a number of three dimensional coordination polymers of Mn(II) using pyridine *N*-oxide and its derivatives viz. 4-methyl-pyridine *N*-oxide and 3,5-dimethyl-pyridine *N*-oxide acting as neutral μ^2 bridging ligands are reported.[57] The anionic ligand used is the dianion of 1,4-benzenedicarboxylic acid (H_2BDC). All these coordination polymers were prepared under solvothermal conditions using $Mn(NO_3)_2$ aqueous solution, H_2BDC, and corresponding pyridine *N*-oxide ligand as precursors in DMF at 120 °C. The coordination polymer derived from pyridine *N*-oxide is shown in figure 1.28 and can be formulated as $[Mn(BDC)PNO]_n$. During formation of the coordination polymer the pyridine *N*-oxide ligands extend the polymeric chain along one direction through the *N*-oxo bridging which are then extended to three dimensions by the BDC ligand.

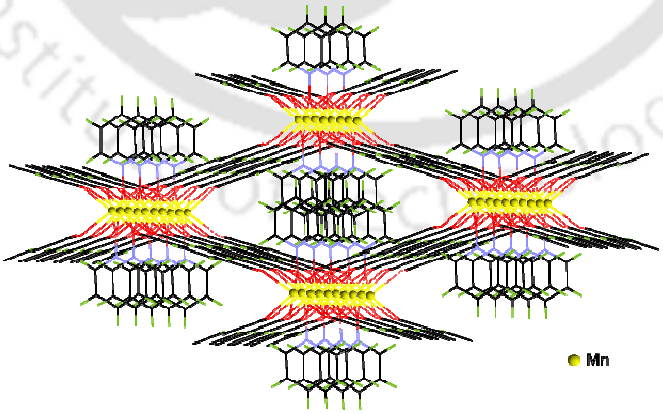

Figure 1.28: Three dimensional coordination polymer of Mn(II) with pyridine *N*-oxide

Hydrothermal reaction between $GdCl_3.6H_2O$, $MnCO_3$, $MnSO_4.H_2O$ and isonicotinic acid *N*-oxide resulted in a 3D coordination framework with the composition $[Gd(INO)(H_2O)(SO_4)]_n$ (INO=isonicotinate *N*-oxide).[51] This framework can be described as a two-fold interpenetrated 3D herringbone structure. Each Gd(III) ion in the molecule adopts a triply capped trigonal prism coordination polyhedron with three sites occupied by the oxygen atom of the *N*-oxide group of one INO and the chelating carboxylate group of another INO, five sites by oxygen atoms from three SO_4^{2-} ligands, and one site by a water. Each of the sulphate anions bridges three Gd(III) centres through μ^2-O bridging coordination mode and thereby results in a one dimensional chain. These one dimensional chains are then connected to each other by the INO ligands which then radiate from it in different directions to generate a 3D structure. The INO ligand coordinates the Gd(III) ion with one of its two binding sites viz. the monodentate *N*-oxide group or the chelating carboxylate group and thus increases the dimensionality (Figure 1.29).

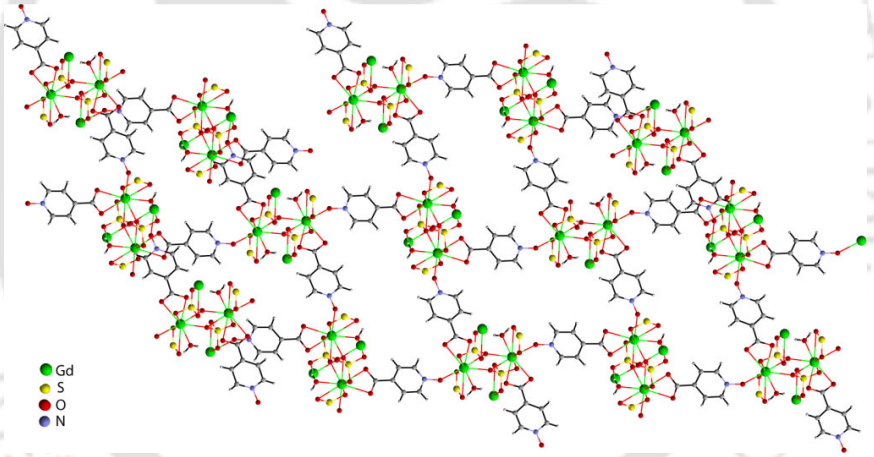

Figure 1.29: 3D herringbone framework formed by $[Gd(INO)(H_2O)(SO_4)]_n$

Solvothermal reaction between $Mn(NO_3)_2$ aqueous solution, H_2BDC, and 4,4′-bipyridine-*N*,*N*′-dioxide as precursors in DMF at 120 °C yields a novel three dimensional coordination polymer $[Mn_2(BDC)_2(4,4'\text{-}BPNO)_4\cdot(DMF)_2]_n$.[57] In this compound both the BDC ligand and the 4,4′-bipyridine-*N*,*N*′-dioxide coordinate through η^2-μ^2:μ^2 binding mode. It appears as if the manganese oxide chains are further interconnected by 4,4′-BPNO units besides BDC to result in the 3D coordination motif having one dimensional channels with sizes 13.24 Å and 17.71 Å in two

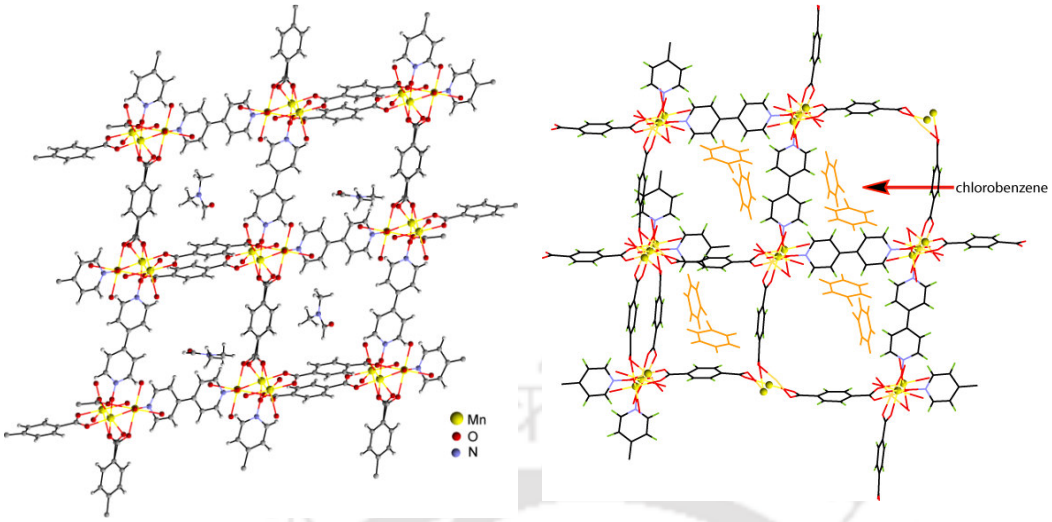

(a) (b)

Figure 1.30: (a) Three dimensional coordination polymer $[Mn_2(BDC)_2(4,4'\text{-}BPNO)_4{\cdot}(DMF)_2]_n$ (b) intercalation of chlorobenzene molecules in the channels

different directions. The open 1D channels are occupied by DMF molecules (Figure1.30a). Because of the possibility of porous channels the adsorption and separation of C6-C8 aromatics viz. benzene, toluene, ethylbenzene etc. are investigated using evacuated porous form of this coordination framework. Upon immersing the evacuated coordination framework into liquids including benzene, toluene, xylenes, ethylbenzene, and chlorobenzene, only C6-C7 molecules could be intercalated. Furthermore, when it was immersed into a mixture of benzene and toluene with 1:1 volume ratio, only benzene could be selectively adsorbed. The intercalation of chlorobenzene molecules in the channels is shown in figure 1.30b.

The coordination polymer $\{[La(\mu\text{-}L)_2L(H_2O)_2](CF_3SO_3)_3\}_n$ has been prepared by mixing aqueous solution of $La(CF_3SO_3)_3.9H_2O$ with solution of anhydrous bis(4-pyridyl)ethane-*N,N*□-dioxide (L).[58] The crystal structure of the coordination polymer consists of a three-dimensional (3D) cationic coordination framework $\{[La(\mu\text{-}L)_2L(H_2O)_2]^{3+}$ and uncoordinated $(CF_3SO_3)^{3-}$ counter anions. Each La(III) centre remains coordinated to eight oxygen donors from six adjacent L ligands and two water molecules in a square antiprismatic coordination environment. In the coordination polymer the ligand L displays different coordination modes: (a) monodendate, (b) bidendate (η^2-μ^2) and (c) tridendate (η^2-μ^2:μ^1) bridging mode. The centrosymmetric dimeric La_2O_2 motifs linked by the L ligand are extended into a 3D

architecture by the L ligands exhibiting bridging fashions (b) and (c). The channels of the resultant framework are occupied by the monodendate L ligands and the uncoordinated $(CF_3SO_3)^{3-}$ anions (Figure 1.31).

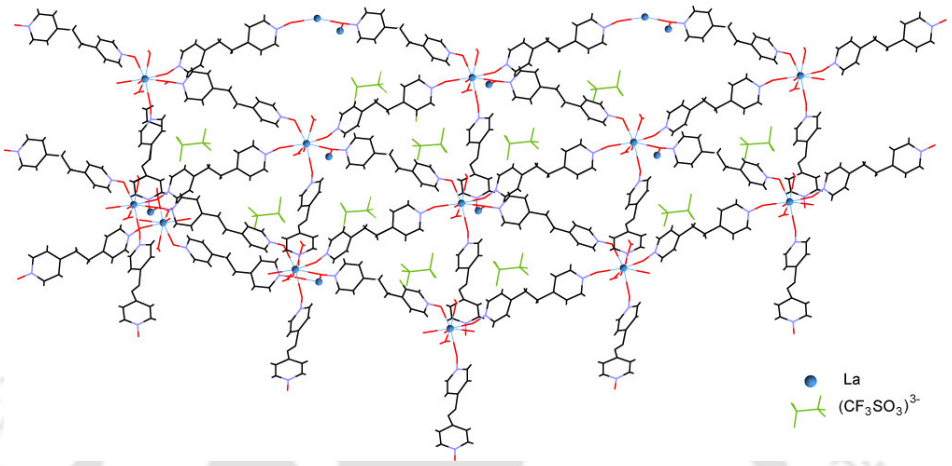

Figure 1.31: Crystal structure of the coordination polymer $\{[La(\mu\text{-}L)_2L(H_2O)_2](CF_3SO_3)_3\}_n$

A three-dimensional coordination polymer from a predesigned bis(triester)hexavanadate derivative $[V_6O_{13}\{(OCH_2)_3C(NHCH_2C_6H_4\text{-}4\text{-}CO_2)\}_2]^{4-}$, 4,4'-bipyridyl-*N,N'*-dioxide, and Tb(III) ions has been prepared by slow diffusion technique.[59] Two dimensional layers comprising Tb(III) centers and 4,4'-BPNO units are linked by the hexavanadate derivative into the three dimensional coordination network (Figure 1.32). In the largest channel, the longest and shortest dimensions are 8.0 and 5.2 Å, respectively. The solvent-accessible internal volume of the coordination polymer is 50.5% of the crystal volume. In the open framework structure, the channels are largely blocked by solvent molecules viz. dimethylformamide. This is a rare example of a heterogeneous aerobic oxidation catalyst that catalyzes oxidation of organic reactants by t-butyl hydroperoxide (TBHP) but more importantly catalyzes O_2-based oxidations and does so under very mild conditions.

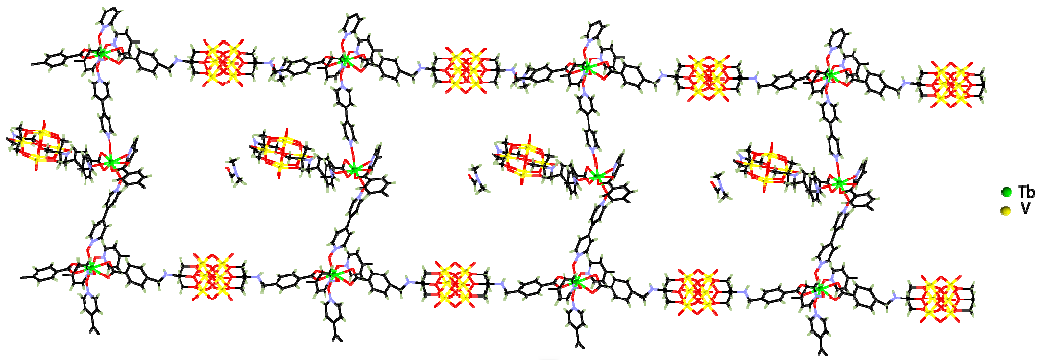

Figure 1.32: A three dimensional coordination network of Tb(III) encapsulating DMF molecules

Polyoxometalates (POMs) represent a large class of inorganic oxo clusters that contain early transition metals. Recently a polyoxometalate-based lanthanide-organic framework was reported that exhibits heterogeneous catalytic behaviour for phosphodiester bond cleavage in aqueous solution.[60] The compound $\{[Ho_4(4,4'\text{-}BPNO)_8(H_2O)_{16}BW_{12}O_{40}].2H_2O\}(BW_{12}\text{-}O_{40})_2.(H_{1.5}pz)_2.(H_2O)_{11}$ was synthesized through a hydrothermal method using $HoCl_3.6H_2O$, 4,4'-bipyridyl-*N,N*'-dioxide (4,4'-BPNO), $HoH_2BW_{12}O_{40}.nH_2O$, and hexahydropyrazine (pz) as the reaction origins. Four Ho^{3+} ions connected by four bridged 4,4'-BPNO ligands, alternatively, consolidate the main skeleton of the nanocage $\{[Ho_4(4,4'\text{-}BPNO)_8(H_2O)_{16}].2H_2O\}^{12+}$. Adjacent cages are linked together through coordination bonds by bridging 4,4'-BPNO ligands generating a one dimensional ribbon composed of the nanocages. Adjacent ribbons are linked together through intermolecular hydrogen bonds and π···π stacking interactions in the crystal. Free $(BW_{12}O_{40})^{5-}$ anions and solvent water molecules fill the pores of the crystals. This compound is an example of heterogeneous catalyst towards phosphodiester bond cleavage reactions in bis(4-nitrophenyl) phosphate generating 4-nitrophenoxide anions in aqueous medium.

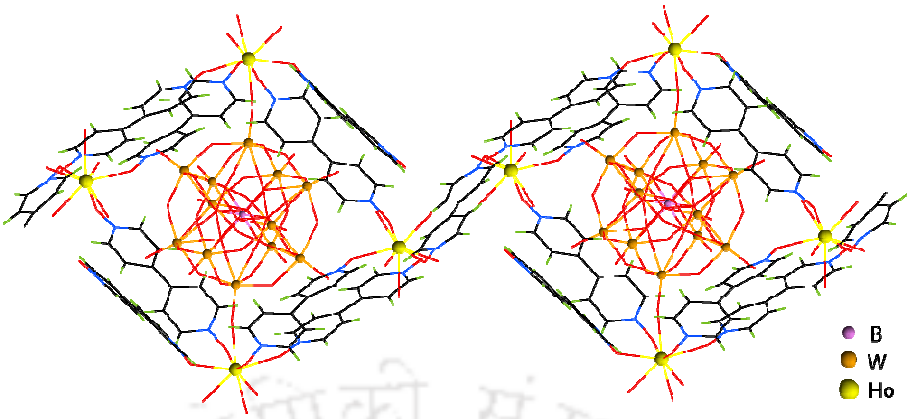

Figure 1.33: Polyoxometalate based lanthanide-organic framework of Ho(III)

1.6 Molecular complexes of aromatic *N*-oxides

The formation of molecular complexes is governed by hydrogen bonds and other allied interactions and these short-range interactions are of general interest in chemistry and biology.[61] Apart from the rich coordination chemistry, molecular complexes of aromatic *N*-oxides have attracted significant interest towards material designing. Numbers of molecular complexes of aromatic N-oxides both of organic and inorganic origin are reported.

Hexaaquo cobalt(II) salts of different anions (Cl^-, Br^-) co-crystallizes with 4,4'-bipyridyl-*N,N'*-dioxide.[62] The hydrogen bonding and packing motifs in these complexes are almost identical. In the molecular complexes, two adjacent $[Co(H_2O)_6]^{2+}$ cations are bridged by two 4,4'-BPNO molecules, which are held in place by hydrogen bonds between the *N*-Oxo···H-O-Co. Four of the coordinated aquo

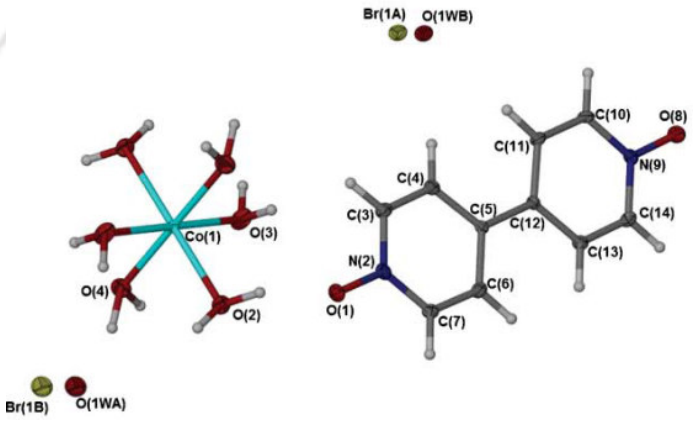

Figure 1.34: The molecular complex $[Co(H_2O)_6](Br)_2.\ 2H_2O$. 4,4'-BPNO

ligands are involved in these hydrogen bonds to 4,4'-BPNO. The remaining two water molecules are engaged in hydrogen bond to a guest water molecule which in turn hydrogen bonds to the halide ion. Adjacent 4,4'-BPNO molecules stack with the aid of π···π interactions. These short-range interactions impart the molecule a complicated three dimensional hydrogen bonded architecture (Figure 1.34).

A similar hexaaquo cobalt(II) based molecular complex of 4,4'-BPNO has been reported.[63] In this complex 1,2,4,5-benzenetetracarboxylic acid (H_4bta) was used as the source of anionic counterpart. The structure is built of $[Co(H_2O)_6]^{2+}$ cations, H_2bta^{2-} anions, free 4,4'-BPNO and water molecules of crystallization (Figure 1.35) which are linked by electrostatic forces, hydrogen bonds and van der Waals interactions. Layers of isolated $[Co(H_2O)_6]^{2+}$ units are separated by anionic layers of $H_2bta^{2-}$and 4,4'-BPNO molecules placed alternatively, and four water molecules of crystallization. An extensive network of hydrogen bonds and π···π interactions contribute to the stabilization of the supramolecular 3D structure.

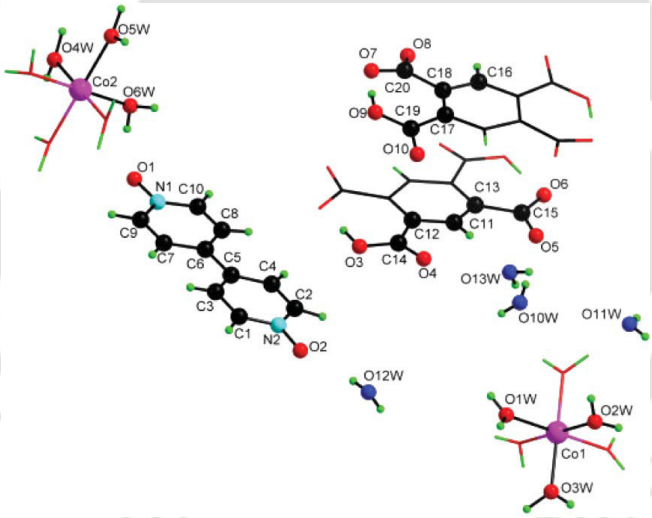

Figure 1.35: The molecular complex between $[Co(H_2O)_6]^{2+}$, H_2bta^{2-} and 4,4'-BPNO

There are examples of molecular complexes of organic origin, such as the molecular complex of urea with picoline *N*-oxide.[64] The crystal structure comprises of four independent urea molecules forming host channels in which the picoline *N*-oxide molecules are embedded. The 1D hydrogen-bonded arrays are extended explicitly through N-H···O=C interactions. This results in the formation of a strongly folded 2D hydrogen-bond arrangement of the host lattice. The two independent picoline *N*-oxide

molecules are stacked in the host channels of urea through N-H···O-N interactions and densely fill the empty space (Figure 1.36).

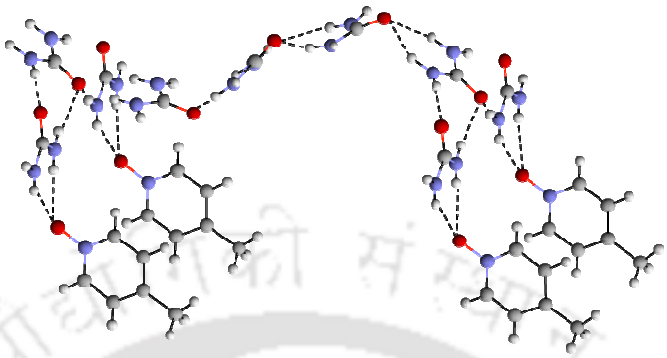

Figure 1.36: The molecular complex of urea with picoline *N*-oxide

A few self-assemblies bearing carboxamide-pyridine *N*-oxide synthon are also reported.[65] The aromatic *N*-oxide systems considered are isonicotinamide *N*-oxide, nicotinamide *N*-oxide and picolinamide *N*-oxide. All these assemblies are sustained via N-H···O hydrogen bonding and C-H···O interactions. Isonicotinamide *N*-oxide is shown to assemble in a triple helix architecture. Nicotinamide *N*-oxide has linear tapes of amide *N*-oxide connected via *anti* N-H···O to produce inversion-related helices. Because of intramolecular *anti* N-H···O bonds in picolinamide *N*-oxide *syn* NH groups aggregate via the amide dimer. The same heterosynthon is exploited to synthesize co-crystals of barbiturate drugs with 4,4'-bipyridyl-*N,N'*-dioxide (Figure 1.37b).

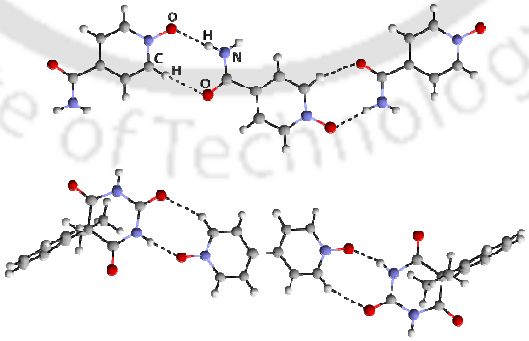

(a) (b)

Figure 1.37: Co-crystals of (a) isonicotinamide *N*-oxide bearing carboxamide-pyridine *N*-oxide synthon and (b) barbiturate drugs with 4,4'-bipyridyl-*N,N'*-dioxide

1.7 Scope of the present work

The foregoing subsections clearly depicted the different types of coordination frameworks as well as molecular complexes of aromatic *N*-oxide ligands. The utility of such materials towards selective separations of aromatic compounds, as well as in catalysis are coming up and needs further attention. Metallo organic frameworks are considered as new generation materials. In recent years, the crystal engineering of these multidimensional networks has achieved considerable progress. They are also used as storage material,[66] sensor,[67] in molecular recognition,[68] molecular magnetic material,[69] and also have prospective applications in catalysis.[70]

For the synthesis of supramolecular multimetallic assemblies two or more components are necessary: the metal ion and ligand(s) capable of connecting the metal centres. It is the different coordination ability of the ligand and the coordination geometry of the metal ion which dictate the self-assembly processes. Of course, the solvent molecules and the counter ions influence the final supramolecular architecture. Exo-bidentate (divergent) ligands such as pyrazine or 4,4□-bipyridine are widely used as building blocks in designing coordination polymers.[71,72] In progressing years these works are being extended to much promising ligands such as aromatic *N*-oxides and comparisons are made between these two types of ligands.[73] Aromatic *N*-oxides having the exo-dentate *N*-oxo functionality show versatile coordination modes and are thus better ligands compared to analogous pyridine ligands. However, the utilization of these ligands to obtain interesting structures is unexploited until recently.

Majority of the polymeric and polynuclear species are synthesised under hydrothermal or solvothermal conditions at high temperature and pressure. There is every possibility to lose information of intermediate species formed during such reactions and such intermediate if at all formed are often not isolated. Alternatively, solution chemistry can still be very useful for synthesis of coordination polymers, since, transient complexes formed during the reaction can sometimes be isolated. Thus there is scope to study the ligand exchange reactions to make various complexes in solution state chemistry.

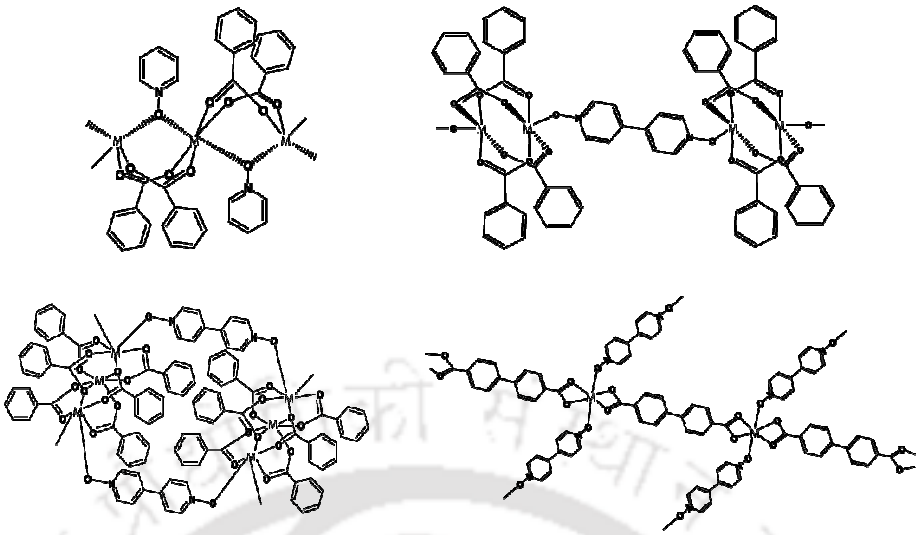

Figure 1.38: Potential supramolecular assemblies of aromatic *N*-oxide ligands

Looking at the potential of the aromatic *N*-oxide ligands as linkers and spacers, to obtain interesting supramolecular assemblies (as shown in figure 1.38) the synthesis, characterisation and properties of metal complexes/ coordination polymers of a few aromatic *N*-oxides are studied in this present work. Such systems could exhibit interesting magnetic, optical or catalytic properties. Supramolecular aspects of a number of molecular complexes of aromatic *N*-oxides are also studied. The designed synthesis can be done only when low nuclearity complexes are studied in details. Such studies would provide their self-assembling and other supramolecular features. Further to these, the selectivity and the rigidity are two independent issues which becomes a major factor in deciding the macromoecular synthesis. The effect of reaction conditions such as role of solvent and ligands as well as variations of functional groups in ligands matters a lot in deciding the fate of formation and stability of framework structure. Thus the syntheses that are carried out in the solution state and in a few cases solvothermal conditions needs comparison to arrive at the kinetic and thermodynamic control on synthesis. Furthermore the transformation of the complexes formed as intermediate product needs clear attention to modify and dictate the course of reactions. With this background the coordination chemistry of aromatic *N*-oxides with carboxylate as anionic ligand are being investigated.

Chapter 2

Synthesis, characterization and properties of *N*-oxide complexes of manganese(II), copper(II) and zinc(II)

As discussed earlier, *N*-oxides can act as monodentate or bridging ligand and they can lead to polymeric complexes through their versatile coordination modes. Interest in heterocyclic aromatic *N*-oxides has flourished because of their practical impact as magnetic materials.[51, 63, 74-78] They can lead to polymeric complexes even with simple mono carboxylic acids as well as with dicarboxylic acids. [57, 79] It has been shown that in the case of pyridine *N*-oxide bridged coordination polymers, the metal-metal separations lie in the 3.6-3.7 Å range and they exhibit antiferromagnetic exchange interactions.[80-83] On the other hand, the weak interactions are essential for supramolecular assembly which in turn control certain molecular property.[42, 72] In order to understand the supramolecular aspects and magnetic behaviours of *N*-oxide complexes, a systematic structural study is required. This chapter deals with the synthesis and characterization of a series of manganese(II) and copper(II) *N*-oxide complexes synthesized through solution state synthetic route and studies on their temperature dependent magnetic properties. Furthermore, a number of aromatic *N*-oxide based zinc(II) coordination polymers are also synthesized and characterized to understand their supramolecular behaviour and are discussed in this chapter.

2.1 Synthesis, characterisation and magnetic properties of manganese(II) *N*-oxide complexes

The reaction of pyridine *N*-oxide and aromatic carboxylic acid with manganese(II) acetate tetrahydrate under ambient condition leads to *N*-oxo bridged co-ordination polymers as illustrated in scheme 2.1.1. The reaction proceeds smoothly

with a number of aromatic carboxylic acids such as benzoic acid, 4-nitrobenzoic acid, 4-hydroxybenzoic acid, 4-chlorobenzoic acid etc (Table 2.1).

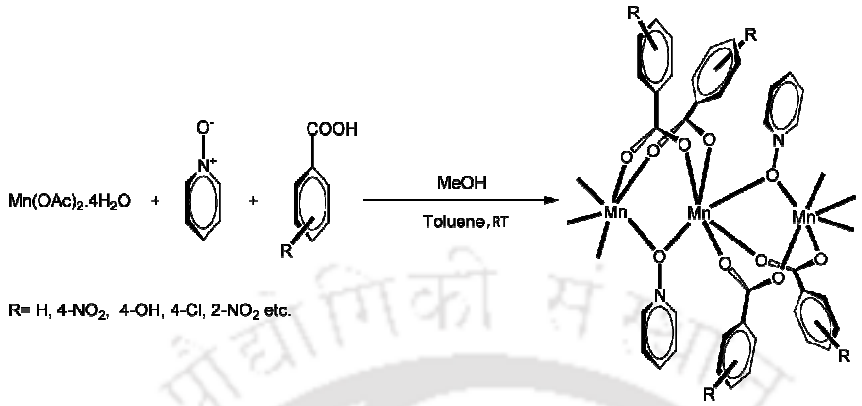

Scheme 2.1.1

Table 2.1: Different complexes prepared and their IR stretching frequencies

Complex	IR stretching Frequency (KBr, cm^{-1})	μ_{eff} (BM, RT)	Molar Conductance (MeOH, Scm^2mol^{-1})
$[Mn(C_6H_5COO)_2(PNO)]_n$ **2.1**	1593 ($\nu_{as}CO_2^-$), 1397 ($\nu_sCO_2^-$), 1219 (N-O_{str}), 549 (Mn-O_{str})	5.38	55.0
$[Mn(4\text{-}NO_2C_6H_4COO)_2(PNO)]_n$ **2.2**	1580 ($\nu_{as}CO_2^-$), 1343 ($\nu_sCO_2^-$), 1208 (N-O_{str}), 543 (Mn-O_{str})	5.62	52.31
$[Mn(4\text{-}OHC_6H_4COO)_2(PNO)]_n$ **2.3**	3299 (O-H_{str}) 1552 ($\nu_{as}CO_2^-$), 1391 ($\nu_sCO_2^-$), 1205 (N-O_{str}), 546 (Mn-O_{str})	5.43	55.96
$[Mn(4\text{-}ClC_6H_4COO)_2(PNO)]_n$ **2.4**	1597 ($\nu_{as}CO_2^-$), 1399 ($\nu_sCO_2^-$), 1218 (N-O_{str}), 529 (Mn-O_{str})	5.57	48.40

The molar conductances of the coordination polymers are found to lie in the ranges of 40-60 Scm^2mol^{-1} in methanol, this suggests them to be non-ionic in nature. The μ_{eff} values are lower than predicted for a d^5 system signifying interplay of magnetic interactions between the Mn(II) centers.

The linear coordination polymer **2.1** with the composition $[Mn(C_6H_5COO)_2(PNO)]_n$ has characteristic IR stretching frequencies at 1593 cm^{-1} and 1397 cm^{-1} due to the asymmetric and symmetric carboxylate stretching

respectively. The *N*-oxo stretching of the coordinated pyridine *N*-oxide appears at 1227 cm^{-1}. The single-crystal X-ray analysis reveals that the polymer **2.1** crystallizes in the orthorhombic *Pbcn* space group. In the coordination polymer, each manganese ion (Mn1) is situated on an inversion center and adopts a near octahedral geometry with four of the coordination sites occupied by the oxygens O1, O2, O1* and O2* from two different benzoate ligands. The rest of the coordination sites are occupied by the *N*-oxo, O3, of the pyridine *N*-oxide ligand. All the Mn-O bonds are in the range 2.11 to 2.22 Å. The benzoate ligands are in bidentate bridging mode (η^2-μ^2) and the pyridine *N*-oxide acts as a μ^2 bridging ligand that connects the nearest manganese(II) centers. The distance of separation between the nearest manganese centers is 3.78 Å. These bridgings extend the molecule along the *c* crystallographic axis thereby resulting in a one dimensional coordination polymer.

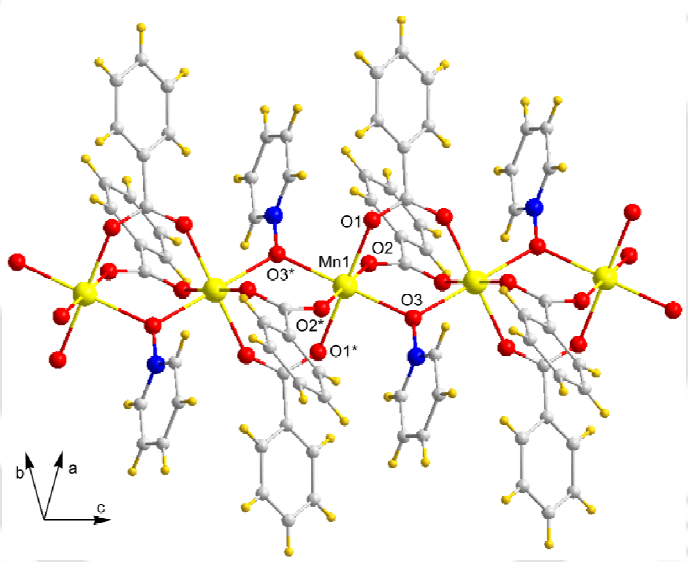

Figure 2.1.1: One dimensional chain of the coordination polymer **2.1** [* =1-x, 1-y, -z]

Similar reactions between manganese(II) acetate tetrahydrate, pyridine *N*-oxide (PNO), 4-nitrobenzoic acid or 4-hydroxybenzoic acid in methanol:toluene mixed solvent lead to formation of the one dimensional coordination polymers **2.2** and **2.3** with the compositions $[Mn(4\text{-}NO_2C_6H_4COO)_2(PNO)]_n$ and $[Mn(4\text{-}OHC_6H_4COO)_2(PNO)]_n$ respectively. The coordination polymer **2.2** crystallizes in the monoclinic *C2/c* space group while **2.3** crystallizes in the orthorhombic *Pbcn* space group. Both these coordination polymers have a similar structure as **2.1**. Here also, the substituted benzoate ligands are in bidentate bridging mode and the pyridine *N*-oxide

acts as a μ^2 bridging ligand. The only structural difference between the three coordination polymers arises due to relative orientation of the benzoate ligands; while in **2.1** and **2.3** they are in a *cis* orientation, in **2.2** the 4-nitrobenzoate ligands stay apart from each other adopting a *trans* orientation. Moreover, the presence of the hydroxyl group impart the coordination polymer **2.3** some more supramolecular features. There exist a strong hydrogen bonding interaction between the 4-hydroxy group and carboxylato oxygen through O2-H2···O1 interaction ($d_{D\text{-}H\cdots A}$ (Å), O2-H2···O1, 2.03; and ∠D-H···A (º), ∠O2-H2···O1, 151) that holds the nearby 1D chains together. This results into an infinite two dimensional hydrogen bonded architecture in the coordination polymer **2.3**. The one dimensional chain of **2.2** is shown in figure 2.1.2a and the hydrogen bonding in **2.3** is shown in figure 2.1.2b.

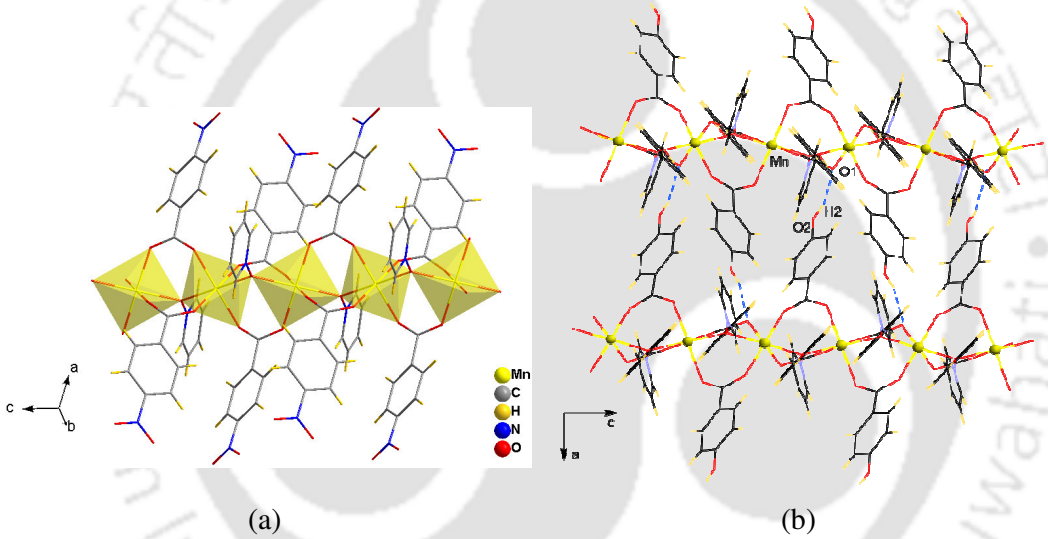

(a) (b)

Figure 2.1.2: (a) One dimensional chain of the coordination polymer **2.2** and (b) Hydrogen bond interactions among the one dimensional chains of the coordination polymer **2.3**

The coordination polymer **2.4** prepared from the reaction of 4-chlorobenzoic acid with manganese(II) acetate tetra hydrate and pyridine *N*-oxide could not be crystallised from methanol but it could be crystallised from pyridine. A mono-nuclear complex namely aqua-*bis*-pyridine *bis*-4-chlorobenzoate manganese(II) crystallizes out initially which on re-dissolution in the residual solution in which the original reaction was carried out gives the coordination polymer **2.4**. Thus, it can be suggested that the coordination polymer **2.4** when dissolved in pyridine solvent gives

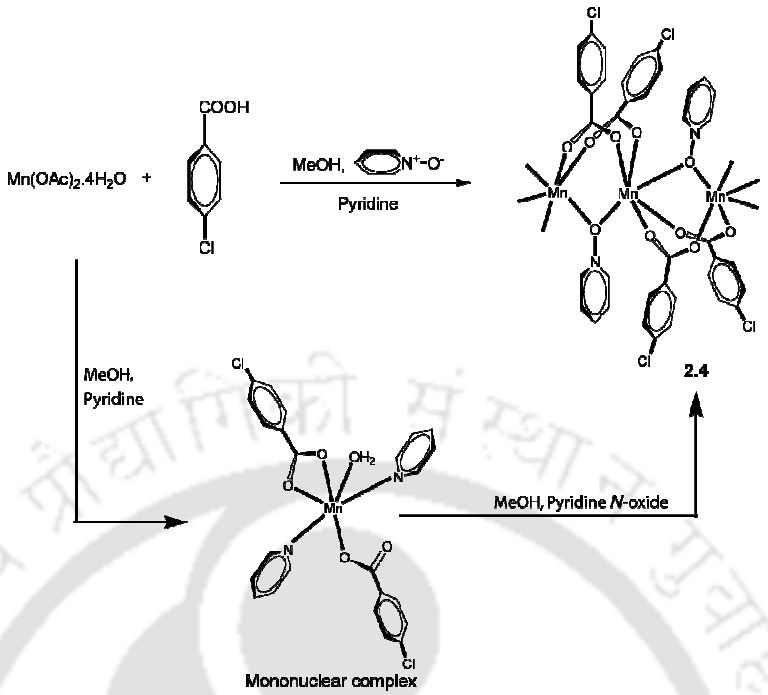

Scheme 2.1.2

a mononuclear complex initially, which further reacts with pyridine *N*-oxide to give the coordination polymer. The reaction is shown in scheme 2.1.2. The complex *bis*-pyridine *bis*-4-chlorobenzoate manganese(II) can also be prepared in high yield by alternative route i.e. by reacting manganese(II) acetate tetrahydrate with 4-chlorobenzoic acid and pyridine. The characteristic N-O stretching frequency at 1217cm^{-1} is observed in the FT-IR spectrum of the coordination polymer **2.4** and is absent in the pyridine complex. The coordination polymer **2.4** crystallizes in the orthorhombic space group *Cmcm*. The manganese centres are nearly octahedral with four equivalent Mn1-O1 bond from the bridging carboxylates and two Mn1-O2 bonds from bridging pyridine *N*-oxide ligands. Overall the structure of the coordination polymer **2.4** is similar to that of **2.1** and the bridging takes place with the aid of both carboxylate and pyridine *N*-oxide ligands.The polymeric chain grows uniformly along the crystallographic *c* axis as shown in figure 2.1.3. The Mn-O bond distances in **2.4** lie in the range of 2.146- 2.204 Å and the Mn···Mn bond distances are 3.74 Å, similar to be found in the dinuclear aqua and carboxylate bridged complexes.

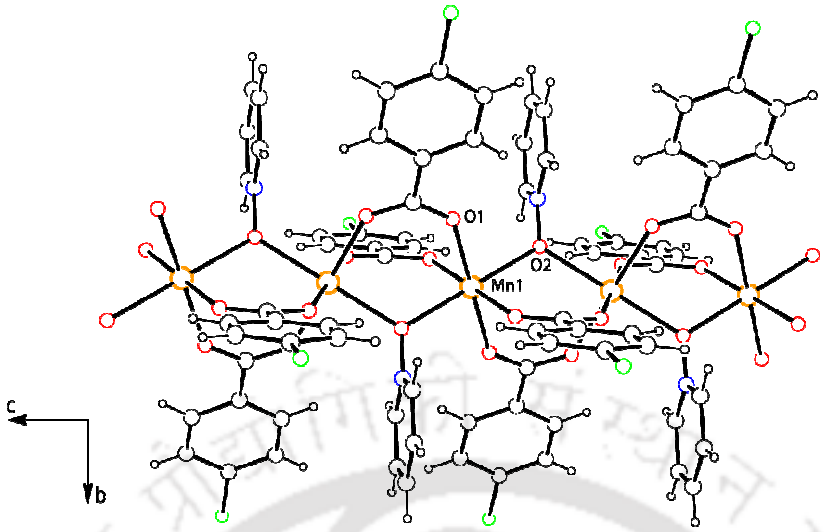

Figure 2.1.3: One dimensional chain of the coordination polymer **2.4**

The reaction of benzoic acid, manganese(II) acetate tetrahydrate and 4,4'-bipyridyl-*N,N'*-dioxide (4,4'-BPNO) in methanol (MeOH) leads to the formation of the coordination polymer **2.5** with the composition $[\{Mn_3(C_6H_5COO)_6(4,4'\text{-}BPNO)_2(MeOH)_2\}(MeOH)_2]_n$ as shown in scheme 2.1.3. In the FT-IR spectra of **2.5** the N-O stretching of the *N*-oxide appears at 1219 cm^{-1}. The asymmetric and symmetric stretching of carboxylate groups appears at 1603 cm^{-1} and 1398 cm^{-1} respectively. The methanol O-H stretching appears at 3421 cm^{-1}. The room temperature magnetic moment (μ_{eff}) for the coordination polymer **2.5** is found to be 5.39 BM corresponding to the spin only value of Mn(II).

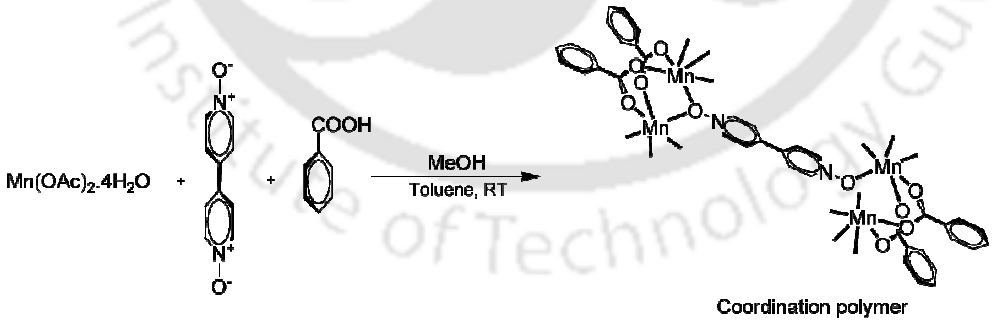

Scheme 2.1.3

The coordination polymer **2.5** crystallizes in the monoclinic space group *P2(1)/c*. A close look at the structure shows that all the three manganese centres in a trinuclear unit adopt a near octahedral geometry, however, the coordination environments around the three are not same. The middle one (Mn1) is coordinated by

four benzoate ligands and two *N*-oxide ligands thereby fulfilling the hexa coordination around the metal center. Both the terminal manganese(II) centres (Mn2) are equivalent and each of them is coordinated to two bridging benzoate groups and one monodentate benzoate group. The remaining coordination sites of Mn2 are occupied by two *N*-oxide groups and one methanol ligand. The Mn1 centre is connected to the terminal manganese(II) centres (Mn2) through four bridging benzoate ligand coordinating through the η^2-μ^2 bridging mode and two 4,4'-bipyridyl-*N,N'*-dioxide ligands. Two different binding modes of the 4,4'-BPNO ligand are observed in the structure; one end of the *N*-oxide binds to the metal centre in the bridging bidentate mode and the other end is bound in monodentate mode for every 4,4'-BPNO ligand. Overall the binding mode of the *N*-oxide ligand can be assigned as η^2-μ^2: μ^1 binding mode connecting a total of three manganese(II) centers. The bridging bidentate mode of 4,4'-BPNO along with the carboxylate bridging holds the trinuclear units. Each of these trinuclear units is then connected to a nearby one through the 4,4'-BPNO ligand thereby extending the coordination polymer along the *a* crystallographic axis.The structure of the coordination polymer **2.5** is shown in the figure 2.1.4.

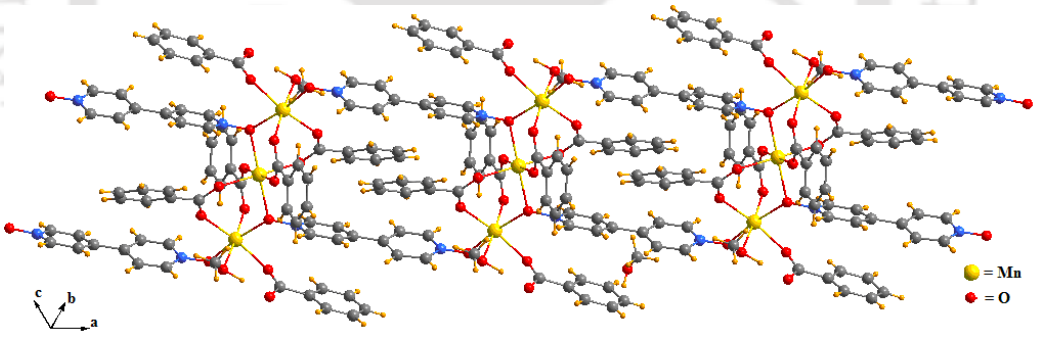

Figure 2.1.4: The one dimensional chain of the coordination polymer **2.5**

Magnetic properties

From the structural discussions of the complexes **2.1**-**2.4** it is seen that they have identical one dimensional structure. Their variable temperature magnetic susceptibility data were collected at 300 K to 4 K and found to show similar behaviour. As an illustrative example, the temperature dependence of magnetic susceptibility (χ_M) for the compound **2.1**, investigated in the range 4–300 K with an applied field of 1000 Oe, is shown in figure 2.1.5. Upon cooling the sample, the χ_M

value increases reaching a maximum of 0.15 cm^3 mol^{-1} K at 4 K, and then decreases on further cooling. At room temperature, the $\chi_M T$ value (Figure 2.1.5) remains basically at 4.12 cm^3 mol^{-1} K, which is close to the expected value (4.37 cm^3 mol^{-1} K) for one non-interacting Mn(II) center with S = 5/2. Then on cooling, the $\chi_M T$ value gradually drops attaining a value 0.55 cm^3 mol^{-1} K at 4 K, indicating the occurrence of an antiferromagnetic interaction between the magnetic transition metal ions.

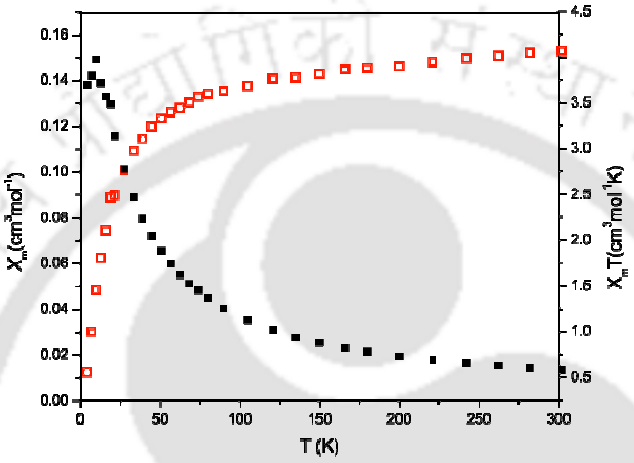

Figure 2.1.5: χ_M vs T and $\chi_M T$ vs T experimental data for the complex **2.1**

Thermogravimetric analysis

Thermal stability of the complexes **2.1-2.5** is studied. Having similar composition and structure the coordination polymers **2.1-2.4** shows similar thermal stability. The coordination polymers are thermally stable up to around 200-250 ^oC. Then after, degradation takes place initially for the loss of one carboxylic acid molecule, followed by the loss of pyridine *N*-oxide molecule. Finally, the other carboxylic acid molecule gets lost. The thermogram of the coordination polymer **2.5** shows weight loss in two steps. In the first step, weight loss occurs at 60-295 °C, which corresponds to 34.7 % of the total weight. This loss of weight is accounted for loss of four methanol and two 4,4'-BPNO molecules. The second loss occurs in the range 295-460 °C that corresponds to weight loss of 79.6% of the residue due to loss of the six benzoic acid molecules.

2.2 Synthesis, characterisation and magnetic properties of copper(II) *N*-oxide complexes

In general, copper(II) carboxylates prefer paddle wheel geometry and in such complexes axial positions are occupied by solvents or by ancillary ligands. By use of bidentate spacer ligands to connect these paddle wheel units the distance of separation between the paddle wheel cores may be controlled. As shown in scheme 2.2.1, such distance will be different for different ligands used (d1 > d2), which in turn may have significant effects on their magnetic exchange properties. However, in the

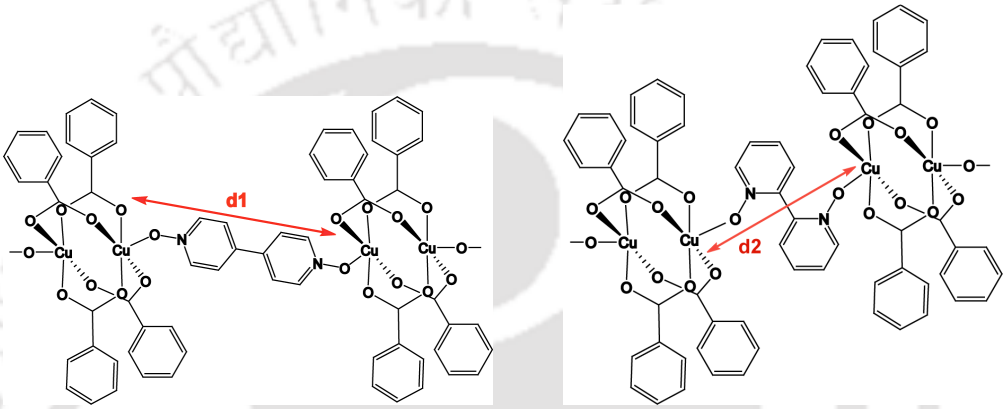

Scheme 2.2.1

case of 2,2'-bipyridyl-*N,N'*-dioxide ligand there is another possibility such as chelation, which needs to be overcome so that polymeric structures are preferred. With the intention of studying magneto-structural correlations of some copper(II) complexes we have synthesized a number of coordination complexes/polymers of copper(II) aromatic *N*-oxides having carboxylate as the anionic ligand and studied their magnetic properties as a function of temperature.

The reaction of pyridine *N*-oxide (PNO) along with benzoic acid with copper(II) acetate monohydrate leads to the formation of the co-crystal (**2.6**) of two paddle wheel copper(II) complexes, one having pyridine *N*-oxide and the other having methanol (MeOH) as the ancillary ligand. This copper(II) *N*-oxide complex **2.6** crystallizing in the triclinic space group *P-1* has the composition $[Cu_2(C_6H_5COO)_4(PNO)_2]$ $[Cu_2(C_6H_5COO)_4(MeOH)_2]$. The two Cu-Cu distance of separation in the two neutral paddle wheel units are 2.61 Å and 2.62 Å which are comparable to copper(II) carboxylate complexes with aromatic carboxylato groups.[84] A number of such co-crystals, that can arise from self-assembling of two or more

neutral inorganic complexes, have been reported recently.[85] They are generally held in the lattices by weak interactions such as O-H···O, C-H···O and C-H···π interactions. The two components in **2.6** are also held together in the lattice by O3-H3A···O7 ($d_{D-H\cdots A}$ (Å), 2.61 Å and ∠D-H···A (º), 166) interactions. The crystal structure of the compound is shown in figure 2.2.1. It shows magnetic moment value of 1.93 BM at room temperature. The compound has a broad absorption in visible spectra at 713 nm which is attributed to E-T_2 transition.

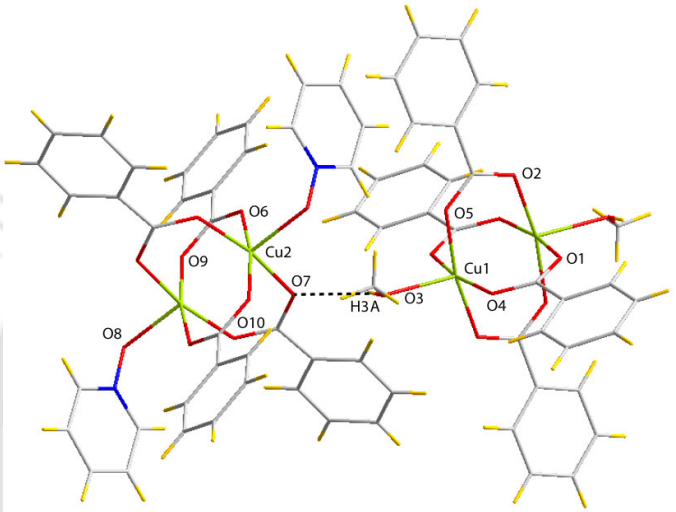

Figure 2.2.1: Crystal structure of the co-crystal **2.6**

Copper(II) acetate reacts with 2-nitrobenzoic acid and pyridine *N*-oxide resulting in the formation of the complex **2.7** having composition $[Cu_2(2\text{-}NO_2C_6H_4COO)_4(PNO)_2]$. It has a dinuclear paddle wheel structure with two terminal pyridine *N*-oxide coordinations. The complex exhibits characteristic IR stretching frequencies at 1614 cm^{-1} and 1410 cm^{-1} due to the carboxylate stretching, the *N*-oxo stretching appears at 1227 cm^{-1}. The single-crystal X-ray analysis reveals that **2.7** crystallizes in the monoclinic $P2_1/c$ space group. The asymmetric unit of **2.7** consists of two *o*-nitrobenzoate ligands and one pyridine *N*-oxide ligand coordinated to a copper(II) centre. In the dinuclear molecule (Figure 2.2.2) each of the copper centres (Cu1) adopts a square pyramidal geometry with the four oxygen atoms O1, O2, O5 and O9 from four different carboxylate ligands residing at the corners of the basal plane. The apical position is occupied by the *N*-oxo, O8, of the pyridine *N*-oxide ligand. The basal atoms are almost coplanar and the Cu1 is positioned 0.224 Å above

the basal plane. The bond lengths for the basal bonds (Cu-O1, Cu-O2, Cu-O5, Cu-O9) lie in the range 1.963 to 1.993 Å, while that of the axial bond (Cu1-O8) is 2.116 Å and the Cu-Cu separation is 2.686 Å which is normal for other copper complexes reported. [74]

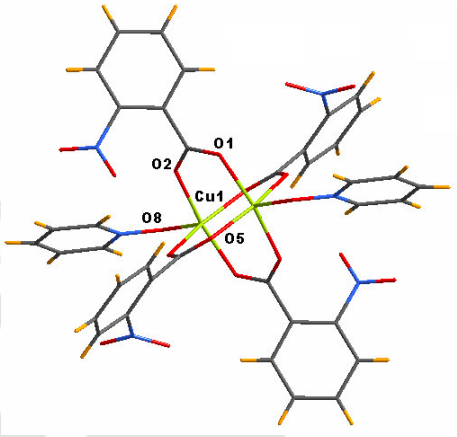

Figure 2.2.2: Dinuclear paddle wheel unit of **2.7**

With the intention of linking together the dinuclear paddle wheel units as formed in case of **2.6** we have reacted copper(II) acetate, benzoic acid with the 'spacer' ligand 2,2'-bipyridyl-*N,N'*-dioxide. This ligand being a bidentate ligand resulted in the formation of the 1D coordination polymer **2.8** with the composition $[Cu_2(C_6H_5COO)_4(2,2'\text{-BPNO})]_n$. The 2,2'-bipyridyl-*N,N'*-dioxide ligand can act either as a chelating or as bridging ligand. This is possible because of the free rotation around the C-C single bond between the two rings of 2,2'-bipyridyl-*N,N'*-dioxide. In other words it can be said that 2,2'-bipyridyl-*N,N*'-dioxide can coordinate to metal centres either in a *cis* or a *trans* configuration as shown in scheme 2.2.2.

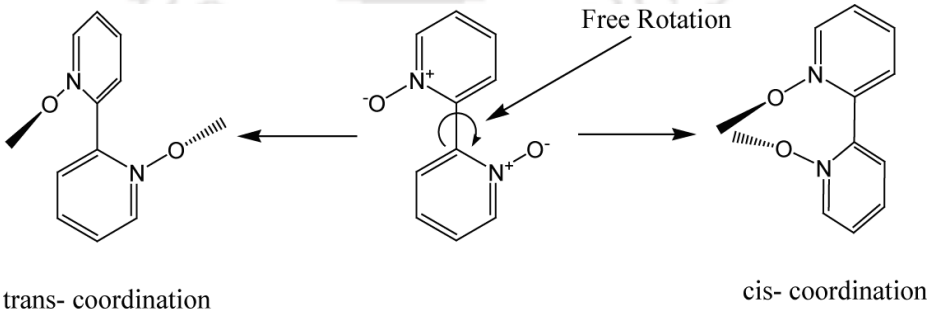

Scheme 2.2.2

There are a few reports available on the chelating coordination mode of 2,2'-bipyridyl-*N,N'*-dioxide.[86-89] However, in case of the coordination polymer **2.8** the 2,2'-bipyridyl-*N,N'*-dioxide coordinates in the *trans*-fashion to bridge two paddle wheel units of copper(II) benzoate. The crystal structure of **2.8** is shown in figure 2.2.3. It crystallizes in the monoclinic space group *C*2/c and each asymmetric unit of **2.8** consists of one copper(II) atom, two benzoate ligands and half a 2,2'-bipyridyl-*N,N'*-dioxide molecule. Like in **2.7**, here also each of the copper(II) centres adopts a square pyramidal geometry, with the *N*-oxo of 2,2'-bipyridyl-*N,N'*-dioxide apically coordinated. Four of the carboxylate oxygens O1, O2, O3 and O4 occupy the corners of the basal plane, with bond lengths spanning the 1.957-1.983 Å range. The apical oxygen O5 is residing at a distance 2.171 Å from the copper(II) centre and the copper(II) centre is at a distance of 0.202 Å from the basal plane. The Cu-Cu distance in the paddle wheel unit is 2.639 Å, while the smallest Cu···Cu distance between two paddle wheel units is 8.035 Å. Moreover the two planes of the two aromatic rings of 2,2'-bipyridyl-*N,N'*-dioxide form an angle of 67.12° which differs significantly from those reported for the *cis*-coordination geometries.

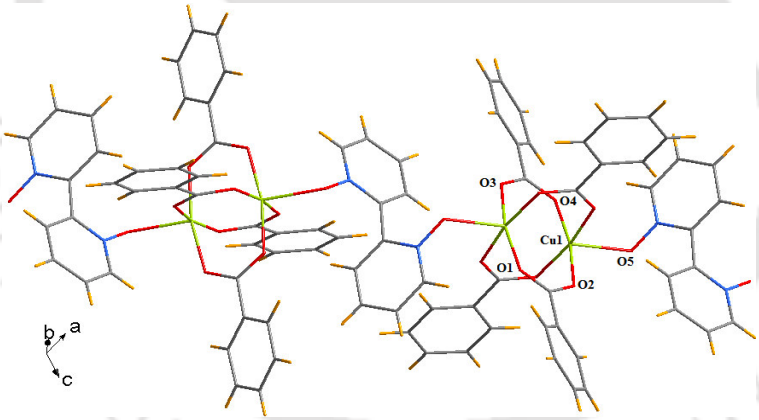

Figure 2.2.3: 1D chain of the coordination polymer **2.8**

A similar reaction of copper(II) acetate monohydrate and benzoic acid with 4,4'-bipyridyl-*N,N'*-dioxide led to an one dimensional coordination polymer **2.9** of composition $[Cu_2(C_6H_5COO)_4(4,4'\text{-BPNO})]_n$ with the paddle wheel building blocks of copper(II) benzoate bridged through the spacer *N*-oxide ligand. The complex belongs to the triclinic space group *P*-1 and the structure of the coordination polymer is as shown in figure 2.2.4. In the coordination polymer **2.9** also, the copper(II) adopts the expected tetragonal pyramidal geometry. However, the difference comes in the

orientation of the 4,4'-bipyridyl-*N,N'*-dioxide ligand which gets distorted may be due to the geometry forced by the copper(II) ions. The two aromatic rings of the ligand are inclined at an angle 23.96° to each other. The separation between two nearest paddlewheel units is 12.57 Å.

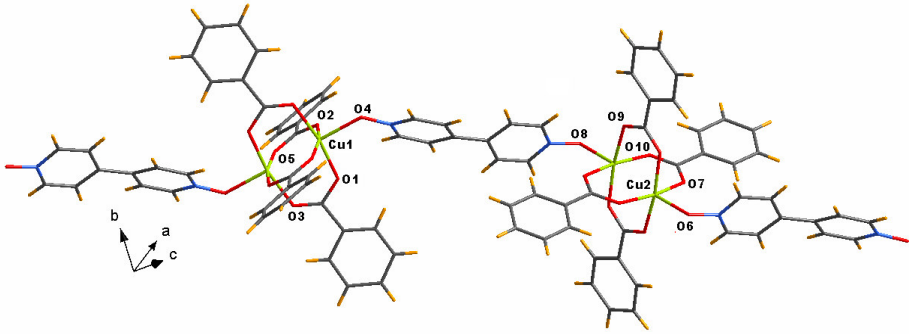

Figure 2.2.4: 1D chain of the coordination polymer **2.9**

The reaction between copper(II) acetate monohydrate, *p*-hydroxybenzoic acid and 4,4'-bipyridyl-*N,N'*-dioxide leads to the formation of another 1D coordination polymer **2.10** with composition $[Cu(4\text{-}OHC_6H_4COO)_2(4,4'\text{-}BPNO)_2.H_2O]_n$. It differs significantly from the earlier two polymers in that unlike **2.8** and **2.9**, **2.10** does not possess paddle wheel units, rather it forms mononuclear copper(II) units bridged

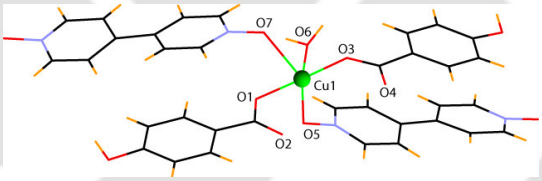

(a)

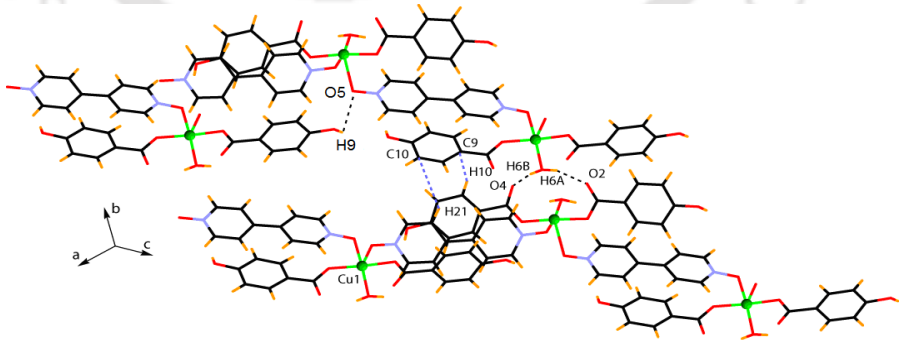

(b)

Figure 2.2.5: (a) Coordination environment around Cu in **2.10**, (b) Self assembly of **2.10** showing various short range interactions

through the spacer ligand. The structure of **2.10** is shown in figure 2.2.5a which shows a square pyramidal geometry around the copper(II) centre. Two of the coordinations come from two benzoate ligands, two from the 4,4'-bipyridyl-*N,N'*-dioxide and the rest from the aquo ligand. The oxygen O7 from 4,4'-bipyridyl-*N,N'*-dioxide occupies the apical position with a Cu-O bond distance of 2.527 Å. Here, the distance between two nearest copper(II) centres bridged by 4,4'-bipyridyl-*N,N'*-dioxide is 12.007 Å. The one dimensional chains interact through the hydrogen bonds O6-H6A···O2 and O6-H6B···O4 between aquo groups and the carboxylate oxygen and O8-H8···O7, between the hydroxy group on the aromatic carboxylate ring and one of the *N*-oxo groups. The hydrogen bonded self assembly is shown in the figure 2.2.5(b).

Magnetic properties

Magnetic susceptibility data for complexes **2.7**-**2.9** are shown in figure 2.2.6. For all three complexes, the $\chi_M T$ product at 300 K is 0.44-0.45 cm^3 mol^{-1} K, significantly lower than the values predicted for two non-interacting S = 1/2 spins (0.82 cm^3 mol^{-1} K, g = 2.1), suggesting the interplay of antiferromagnetic interactions. This conclusion is corroborated by the decrease of the $\chi_M T$ products of all three complexes upon cooling. These are stabilized below ~50 K, forming plateaus of different values. This indicates the presence of paramagnetic impurities, of different fractions for each complex.

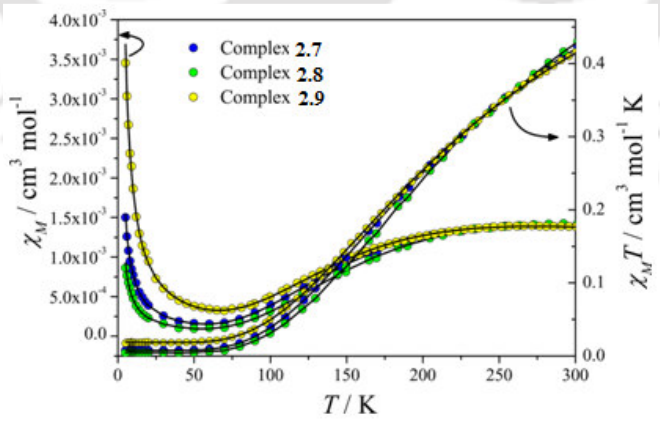

Figure 2.2.6: χ_M vs T and $\chi_M T$ vs T experimental data for complexes **2.7**-**2.9** and calculated curves according to the model described in the text

For the analysis of the magnetic data a simple isotropic exchange model was employed, according to the Hamiltonian:

$$H = -2J\hat{\mathbf{S}}_i\hat{\mathbf{S}}_j$$

In this model we also took into account a fraction ρ of S = 1/2 paramagnetic impurity following the Curie law.

Fits to these data using this model were of good quality, yielding best-fit parameters J = -159 cm^{-1}, g = 2.07, ρ = 2.0%, R = 2.0×10^{-4} (complex **2.7**), J = -168 cm^{-1}, g = 2.13, ρ = 1.2%, R = 1.2×10^{-3} (complex **2.8**) and J = -157 cm^{-1}, g = 2.04, ρ = 4.9%, R = 2.2×10^{-4} (complex **2.9**). These values fall in the range of values previously determined for paddle wheel dicopper(II) carboxylate complexes.[74, 80, 90-92]

The quality of the fits does not allow us the incorporation of additional parameters, namely a mean-field correction for the determination of eventual interactions between dinuclear units in **2.8** and **2.9**, without overparametrizing the problem. Therefore we conclude that such interactions, if indeed operative, must be very weak. This is in agreement with the fact that such interactions would have to be transmitted through a superexchange pathway involving the apical coordination position of the square-pyramidal copper(II) ions; since this position occupies a non-magnetic orbital (of d_{z^2} character), this interaction is expected to be very weak. Moreover, the size and shape of the bridging ligands is probably not favourable for the transmission of significant magnetic exchange.

Thermogravimetric analysis

The **t**hermogram of the complex **2.7** reveals weight loss in the range 225-275 °C which corresponds to 67.2% (calc. 67.6%) of the total weight and is accounted for loss of four 2-nitrobenzoic acid. Then the weight loss due to the two pyridine *N*-oxide molecules takes place. For the coordination polymer **2.8**, weight loss occurs in two steps: the first step within the range 195-250 °C corresponds to weight loss of 59.5% (calc. 58.3%) due to loss of the two benzoic acid molecules and the second step, 350-525 °C, is due to the loss of half a 2,2'-bipyridyl-*N,N*'-dioxide molecule (experimental 57.4 % from the first step; calc. 59.1%). The coordination polymer **2.9** also shows a similar thermal behaviour as **2.8** and the coordination polymer **2.10** shows a continuous thermal degradation in the range 200-525 °C.

2.3 Synthesis, characterisation and supramolecular aspects of zinc(II) *N*-oxide complexes

The reaction of zinc(II) acetate, benzoic acid and pyridine *N*-oxide leads to formation of an one dimensional coordination polymer **2.11** with a composition $[Zn(C_6H_5COO)_2(PNO)]_n$. This coordination polymer has characteristic IR stretching frequencies at 1591 cm^{-1} and 1399 cm^{-1} due to the carboxylate stretching; the *N*-oxide stretching appears at 1221 cm^{-1}.

The single-crystal X-ray analysis reveals that **2.11** crystallizes in the orthorhombic *Pbcn* space group and is found to be isomorphous to the manganese(II) analog **2.1** discussed earlier. The asymmetric unit of **2.11** consists of one benzoate ligand and half a pyridine *N*-oxide ligand coordinated to half a zinc(II) centre. Each of the zinc(II) ion in the coordination polymer is situated on an inversion center and adopts a near octahedral geometry with four coordination sites occupied by the oxygens O1, O2, O1' and O2' from two different benzoate ligands. The other two coordination sites are occupied by the *N*-oxo of the pyridine *N*-oxide ligand. The Zn-O bonds span the 2.04-2.14 Å range. The benzoate ligands are in bidentate bridging mode (η^2-μ^2) and the pyridine *N*-oxide acts as a μ^2 bridging ligand that connects the nearest zinc(II) centers. The distance between the nearest zinc(II) centers is 3.69 Å which is well within the limit for complexes of zinc(II).[93] These bridgings extend the molecule along the *bc* crystallographic plane resulting in an one dimensional coordination polymer. The crystal structure of the coordination polymer is shown in figure 2.3.1.

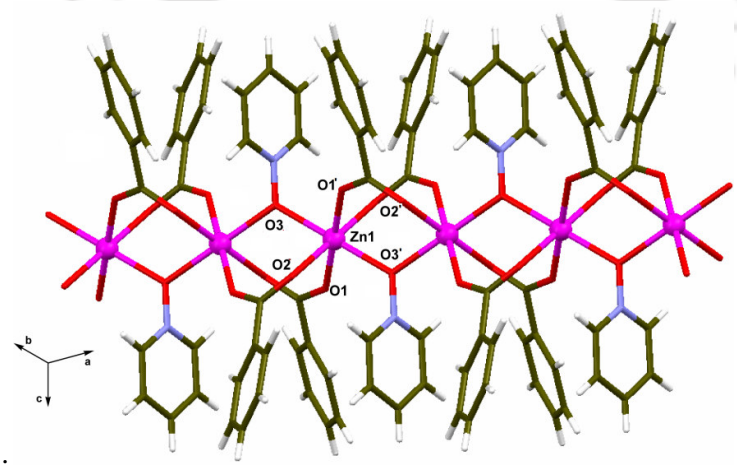

Figure 2.3.1: One dimensional chain of the coordination polymer **2.11** [' =1-x, 1-y, -z]

Coordination polymer **2.12** crystallizes in the triclinic space group *P-1*. The asymmetric unit of **2.12** consist of two symmetrically equivalent zinc(II) centers (Zn1 and Zn2) coordinated to four benzoate and a 4,4'-BPNO ligand. Here each of the zinc(II) centers adopts a square pyramidal geometry with the *N*-oxo of 4,4'-bipyridyl-*N,N'*-dioxide apically coordinated. Four of the carboxylate oxygen atoms O1, O2, O3 and O4 coordinating to Zn1 occupy the corners of the basal plane. The bond lengths of these Zn-O bonds span the range 2.007-2.066 Å. The apical oxygen O5 has a Zn-O distance 1.986 Å and the Zn1 centre is positioned at a distance of 0.355 Å above the basal plane. Zn2 is also coordinated to four carboxylate oxygen atoms O7, O8, O9 and O10 which occupy the corners of the basal plane of the square pyramidal geometry. The metal-metal (Zn1···Zn1, Zn2···Zn2) distance within the paddle wheel unit is 2.95 Å, while the smallest Zn···Zn distance between two paddle wheel units is 12.35 Å. Repeating unit of the polymeric structure are composed of paddle wheel zinc(II) benzoate core bridged by 4,4'-bipyridyl-*N,N'*-dioxide ligands. Thus the one dimensional polymer is extended along the *ab* diagonal plane with the spacer 4,4'-BPNO ligand connecting the nearest paddle wheel units through a *trans* bidentate μ^2 binding mode (*trans* η^2-μ^2 coordination). It is interesting to note here that the two aromatic rings of the ligand 4,4'-BPNO are puckered and are inclined at an angle 26.84^o to each other. The crystal structure of the coordination polymer is shown in figure 2.3.2.

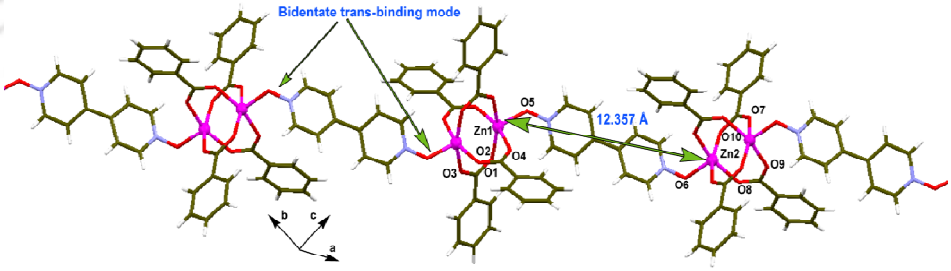

Figure 2.3.2: One dimensional chain of the coordination polymer **2.12**

Photoluminescence property of the coordination polymer **2.12** is studied in the solution state. The UV absorption spectra shows that the methanolic solution of the compound **2.12** (10^{-4} M) has two absorption bands at 220 nm and 330 nm which are much closer to those observed for the free ligand (at 224 nm and 326 nm) and believed to arise due to π-π* transition of the ligand. Upon excitation at 310 nm,

compound **2.12** emits at 380 nm. A comparison with the emission spectra of the free ligand (10^{-4} M in methanol) shows that the free ligand emits at two different wavelengths at 385 nm and at 490 nm. As the MLCT or LMCT transitions can be ignored in case of a d^{10}- electronic configuration, the emission observed in the compound is only because of the π-π* transition of the ligand. However due to coordination to the metal ion its position in the wavelength scale gets shifted slightly. The emission spectra for the compound as well as for the ligand are shown in figure 2.3.3.

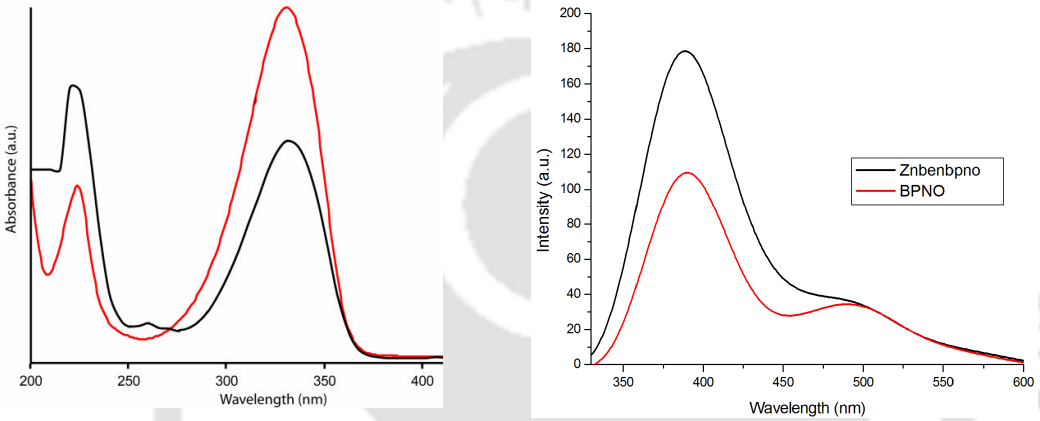

(a) (b)

Figure 2.3.3: (a) UV absorption and (b) fluorescence emission spectra for the compound **2.12** and 4,4'-BPNO ligand

The reaction of zinc(II) acetate dihydrate, terephthalic acid and 4,4'-BPNO yields a two dimensional coordination polymer **2.13** with the composition $[Zn_4(C_6H_4C_2O_4)_4(4,4'\text{-}BPNO)_2(H_2O)_5]_n.nH_2O$. It crystallizes in the monoclinic space group *C2/c*. The coordination polymer **2.13** has three symmetrically equivalent zinc(II) centers with different coordination environments. Among the three different zinc(II) centers Zn1 has a near octahedral geometry and the other two (Zn2 and Zn3) have distorted square pyramidal geometries. In Zn1 four of the coordination sites are occupied by four aquo ligands while carboxylate oxygens fulfill the rest of the coordination sites, the Zn1-O bond lengths remaining in the range 2.03-2.15 Å. The Zn2 centre is coordinated by two carboxylate oxygen, two *N*-oxo from 4,4'-BPNO and one aquo ligands. The oxygen atoms O6, O6′, O7 and O7′ form the basal plane with O12 coordinating epically to the metal center. All the Zn2-O bond distances

remain in the range 1.97- 2.10 Å. Zn3 center also adopts a distorted square pyramidal geometry with the oxygen atoms O3, O4, O5 and O13 occupying the distorted basal plane. O14 provides the apical coordination to the metal center and the metal center resides 0.53 Å above the basal plane with the Zn3-O bond distances spanning the 1.96-2.15 Å range. Among the three zinc(II) centers Zn1 is not coordinated by any 4,4'-BPNO ligand. The Zn1 centers are connected to the Zn3 centers through the terephthalate ligands while the Zn2 centers are connected to the Zn3 centers through bridging via both terephthalate as well as 4,4'-BPNO ligands. The terephthalate ligands are coordinated to the metal centers in three different coordination modes. It binds to Zn1 and Zn2 in monodentate coordination mode only; whereas Zn3 centre is coordinated through two different types of carboxylates: one in bidentate chelating mode and another in μ^2 bidentate bridging mode. This μ^2 bidentate bridging mode, in fact, connects two nearby Zn3 centers which in turn is connected to a nearby Zn1 centre via monodentate terephthalate connectivity. Moreover the Zn3 and Zn2 are bridged by a 4,4'-BPNO ligand coordinated through monodentate *cis* coordination

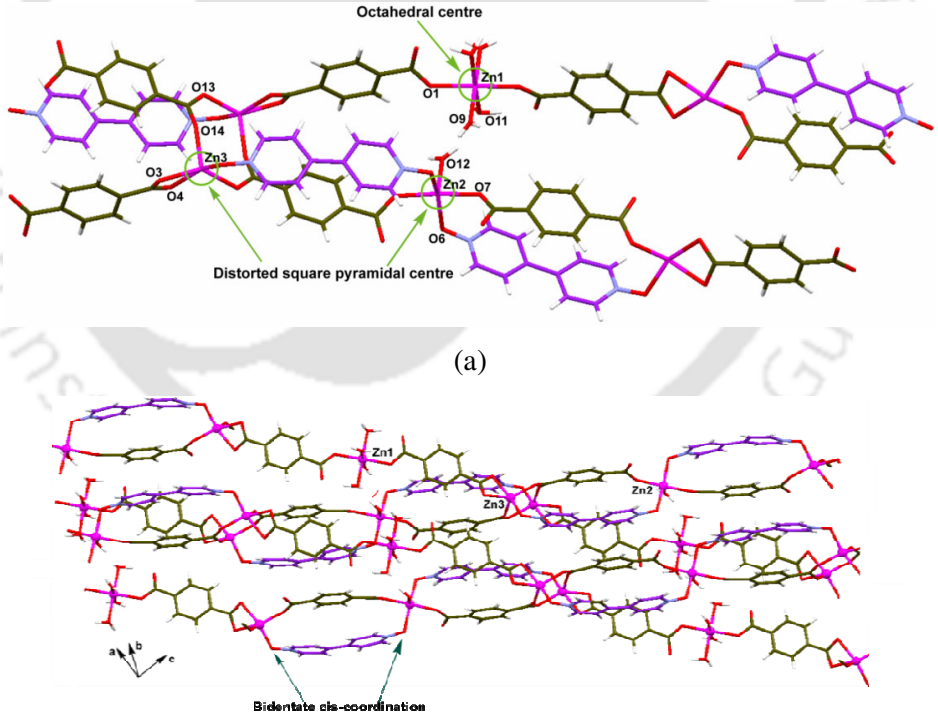

Figure 2.3.4: (a) Different types of zinc(II) centers and connectivity of the ligands in **2.13** (water of crystallization is omitted for clarity), (b) 2D structure of the coordination polymer **2.13**

mode (*cis* η^2-μ^2 coordination). The μ^2 bidentate bridging mode of terephthalate operating between two Zn3 centers extend the polymer along the *bc* crystallographic plane whereas the terephthalate cum 4,4'-BPNO combo-bridging extend it in the *ac* crystallographic plane thereby leading to the 2D network architecture. The structure of the two dimensional coordination polymer is shown in figure 2.3.4b with the different types of zinc centers and connectivity of the ligands in figure 2.3.4a.

PXRD analysis of the bulk samples of the coordination polymers **2.11**-**2.13** are carried out and found to match well with the simulated patterns. This depicts the pure phase of the synthesized compounds.

Thermogravimetric analysis

Thermal stability of the complexes **2.11**-**2.13** is studied and the thermograms show that all the coordination polymers are thermally stable up to ~200 ^{o}C. Thermogram of the complex **2.11** reveals that the weight loss occurs in two steps. In first step, weight loss occurs in the range 185-330 °C, which corresponds to 23.5 % of the total weight. This loss of weight is accounted for the loss of the pyridine *N*-oxide molecule (theoretical weight loss 23.6 %). The second loss occurs in the range 335-578 °C corresponding to weight loss of 78.8% of the residue from the first step (calc. 79.4 %) due to loss of two benzoic acid molecules. For the coordination polymer **2.12**, weight loss occurs in two steps: the first step within the range 185-425 °C corresponds to weight loss of 62.4 % (calc. 60.7%) due to loss of the four benzoic acid molecules and the second step, 425-660 °C, is due to the loss of a 4,4'-bipyridyl-*N,N*'-dioxide molecule (experimental 53.9 % of the residue from the first step; calc. 59.6%). Coordination polymer **2.13** also loses weight in two steps: the first step in the range 30-100 °C corresponds to weight loss of 10.6% (calc. 7.7 %) due to loss of the six water molecules and the second step, 275-495 °C is due to the loss of four terephthalic acid and two 4,4'-bipyridyl-*N,N*'-dioxide molecules (experimental 78.3% of the residue of the first step; calc. 80.3%).

2.4 Conclusion

In conclusion, we have synthesized and characterized a number of coordination polymers having aromatic *N*-oxide as ancillary ligands. Depending on the anionic and ancillary ligands used one dimensional and two dimensional

coordination polymers are found to be formed. Structure of each of such coordination polymers is guided by the nature of the metal ions and the spatial orientation of the ancillary ligands. Moreover, different architectures of the coordination polymers with repeated mononuclear, dinuclear or trinuclear M(II) (M=Mn, Cu, Zn) units are observed. Pyridine *N*-oxide interconnects metal nodes by acting as μ^2 bridging ligand. It appears that 4,4'-bipyridyl-*N,N'*-dioxide favors η^2-μ^2 coordination mode either *cis* or *trans* rather than η^2-μ^2:μ^0 coordination mode. However, the μ^2 bridging is generally favored by pyridine *N*-oxide. We have obtained preferential *trans* bidentate bridging binding mode of 2,2'-bipyridyl-*N,N*'-dioxide to form copper(II) coordination polymer rather than chelating mode, which is frequently come across. In the case of copper(II) and zinc(II) coordination polymers the paddle-wheel benzoate units act as secondary building units that are connected by 4,4'-bipyridyl-*N,N'*-dioxide which acts as a bidentate spacer ligand adopting a *trans* η^2-μ^2 coordination mode.The paddle wheel structures of copper(II) separated by different *N*-oxide spacers controls their structural features. The manganese(II) *N*-oxide coordination polymers **2.1**-**2.4** exhibit weak antiferromagnetic interactions between the nearest Mn(II) centers. Interactions between metal centers within the paddlewheel moieties of **2.7**-**2.9** were found to be strongly antiferromagnetic, with values typical of copper(II) carboxylates. However, inter-dinuclear interactions between these moieties were too weak to be detected, or non-existent.

2.5 Experimental section

Detailed synthetic methodologies are given below. Analytical data as well as spectroscopic data are also listed along with each of the complex. The instrumental details are given in Appendix.

Complex 2.1: $[Mn(C_6H_5COO)_2(PNO)]_n$

To a solution of benzoic acid (2 mmole, 0.242 g) in methanol (20 mL) $Mn(OAc)_2.4H_2O$ (1 mmol, 0.245 g) was added and stirred for 10 minutes. To this reaction mixture pyridine *N*-oxide (2 mmole, 0.190 g) was added with constant stirring at room temperature. The colour of the solution changes to yellow. A small amount (≈ 5 mL) of toluene was added to dissolve the precipitate that appeared after

addition of pyridine *N*-Oxide. Yellow coloured crystals were collected after five days and dried in air. Yield of the pure crystalline complex was found to be 27% (crude yield >70%).

IR (KBr, cm^{-1}): 1593 (m), 1557 (s), 1477 (w), 1397 (s), 1219 (m), 731 (m).

Molar Conductance: 55.0 S cm^2 mol^{-1} in methanol.

Magnetic moment μ_{eff} (RT): 5.38 B.M.

Complex 2.2: $[Mn(4\text{-}NO_2C_6H_4COO)_2(PNO)]_n$

Complex **2.2** was synthesized through a similar method as for **2.1**; only difference being the use of 4-nitrobenzoic acid in place of benzoic acid.

IR (KBr, cm^{-1}): 1580 (s), 1518 (m), 1471 (w), 1398 (s), 1343 (s), 1208 (m), 1102 (w), 1020 (m), 820 (m), 727 (m).

Molar Conductance: 52.31 S cm^2 mol^{-1} in methanol.

Magnetic moment μ_{eff} (RT): 5.62 B.M.

Complex 2.3: $[Mn(4\text{-}OHC_6H_4COO)_2(PNO)]_n$

Complex **2.3** was synthesized through a similar method as for **2.1**; only difference being the use of 4-hydroxybenzoic acid in place of benzoic acid.

IR (KBr, cm^{-1}): 3299 (b), 1608 (m), 1591 (m), 1552 (s), 1478 (m), 1391 (s) 1341 (m), 1205 (m), 793 (m).

Molar Conductance: 55.96 S cm^2 mol^{-1} in methanol.

Magnetic moment μ_{eff} (RT): 5.43 B.M.

Complex 2.4: $[Mn(4\text{-}ClC_6H_4COO)_2(PNO)]_n$

To a solution of 4-chlorobenzoic acid (2 mmol, 0.312 g) in methanol (15 mL) manganese acetate tetrahydrate (1 mmol, 0.245 g) was added and stirred for 10 minutes. To this solution, pyridine *N*-oxide (2 mmol, 0.190 g) was added with constant stirring at room temperature. The colour of the solution changes to yellow. Precipitation took place and a small amount (≈ 3 mL) of pyridine was added to dissolve the precipitate that appeared after addition of pyridine *N*-Oxide. The clear solution thus obtained on keeping for a week gave the yellow crystals of the coordination polymer **2.4** (yield 70%).

IR (KBr, cm^{-1}): 1597 (s), 1555 (s), 1474 (m), 1399 (s), 1218 (m), 771 (s).

Molar Conductance: 48.40 S cm^2 mol^{-1} in methanol.

Magnetic moment μ_{eff} (RT): 5.57 B.M.

Complex 2.5: $[\{Mn_3(C_6H_5COO)_6(BPNO)_2(MeOH)_2\}(MeOH)_2]_n$

To a solution of benzoic acid (2 mmol, 0.244g) in methanol (15 mL) manganese(II) acetate tetrahydrate (1 mmol, 0.245g) was added and stirred for 15 minutes to obtain a homogeneous solution. To this reaction mixture 4,4′-bipyridyl-*NN*′-dioxide (2 mmol, 0.376 g) was added with constant stirring at room temperature. The solution turns red. The mixture was kept for crystallization and red coloured crystals of **2.5** were obtained after three days. Yield, 55%.

IR(KBr, cm^{-1}): 3421(b), 2927(m), 1603(s), 1555(m), 1470(m), 1398(s), 1219(m), 1179(m), 1028(m), 725(m).

Magnetic moment μ_{eff} (RT): 5.39 B.M.

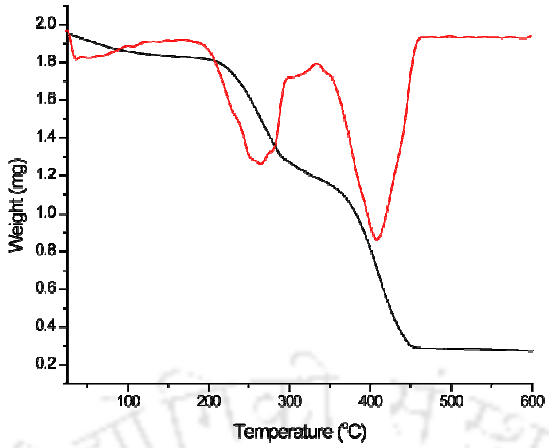

Figure 2.5.1: Thermogram of the coordination polymer **2.5**

Complex 2.6: $[Cu_2(C_6H_5COO)_4(PNO)_2].[Cu_2(C_6H_5COO)_4(MeOH)_2]$

To a solution of benzoic acid (2 mmol, 0.242 g) in methanol (15 mL) copper(II) actetate monohydrate (1 mmol, 0.199 g) was added and stirred for 10 minutes. To this reaction mixture pyridine *N*-oxide (2 mmol, 0.190 g) was added with constant stirring at room temperature. A small amount (≈ 5 mL) of toluene was then added to dissolve the precipitate that appeared after addition of pyridine *N*-Oxide. After about 4 days diffraction quality crystals were collected and dried in air.

IR (KBr, cm^{-1}): 3453 (bm), 3067 (m), 1627 (s), 1572 (s), 1470 (w), 1405 (s) 1224 (m) 1020 (m), 1176 (s), 719 (m).

Magnetic moment, μ_{eff} (RT): 1.93 B.M.

UV-vis λ_{max} (methanol): 713 nm; $\varepsilon = 350\ M^{-1}\ cm^{-1}$.

Complex 2.7: $[Cu_2(2\text{-}NO_2C_6H_4COO)_4(PNO)_2]$

To a solution of 2-nitrobenzoic acid (1 mmol, 0.167 g) in methanol (15 mL) copper(II) actetate monohydrate (0.5 mmol, 0.100 g) was added and stirred for 10 minutes. To this reaction mixture pyridine *N*-oxide (1 mmol, 0.095 g) was added with constant stirring at room temperature. A small amount (≈ 5 mL) of toluene was then added to dissolve the precipitate that appeared after addition of pyridine *N*-Oxide.

Diffraction quality crystals were collected after 7 days and dried in air. Yield of the pure crystalline complex was found to be >70%.

IR (KBr, cm^{-1}): 3421 (bw), 3084 (w), 1643 (s), 1614 (s), 1575 (m), 1529 (s), 1467 (m), 1410 (s), 1369 (m), 1351 (m), 1227 (m), 839 (m), 702 (m).

UV-vis λ_{max} (methanol): 733 nm; $\varepsilon = 108\ M^{-1}\ cm^{-1}$.

Complex 2.8: $[Cu_2(C_6H_5COO)_4(2,2'\text{-BPNO})]_n$

Complex **2.8** was prepared with a similar procedure and crystalline pure products with 55% yield were obtained.

IR (KBr, cm^{-1}): 3445 (bw), 3085 (w), 1618 (s), 1597 (m), 1572 (s), 1410 (s), 1228 (s), 719 (m).

UV-vis λ_{max} (methanol): 715 nm; $\varepsilon = 99\ M^{-1}\ cm^{-1}$.

Complex 2.9: $[Cu_2(C_6H_5COO)_4(4,4'\text{-BPNO})]_n$

Single crystals of **2.9** were grown by layering a solution of 4,4'- bipyridyl-*N,N*'-dioxide (0.25 mmol, 0.045 g) in water (3 mL) over a reaction mixture containing copper(II) acetate monohydrate (0.25 mmol, 0.050 g) and benzoic acid (0.5 mmol, 0.061 g) in toluene: methanol (3:1, 10 mL).

IR (KBr, cm^{-1}): 3421 (bw), 3110 (m), 1633 (s), 1614 (s), 1572 (m), 1462 (m), 1403 (s), 1230 (s), 1175 (w), 840 (m), 716 (m).

UV-vis λ_{max} (methanol): 711 nm; $\varepsilon = 246\ M^{-1}\ cm^{-1}$.

Complex 2.10: $[Cu(4\text{-}OHC_6H_4COO)_2(4,4'\text{-BPNO})_2.H_2O]_n$

To a solution of 4-hydroxybenzoic acid (1 mmol, 0.138 g) in methanol (15 mL) copper(II) acetate monohydrate (0.5 mmol, 0.100 g) was added and stirred for 10 minutes. To this reaction mixture 4,4'-bipyridyl-*N,N*'-dioxide (0.5 mmol, 0.095 g) was added with constant stirring at room temperature. A small amount (≈ 5 mL) of dimethylformamide was then added to dissolve the precipitate that appeared after

addition of 4,4'- bipyridyl-*N,N*'-dioxide. Diffraction quality crystals were collected after 12 days. Yield of the pure crystalline complex was found to be ≈ 40%.

IR (KBr, cm^{-1}): 3116 (bm), 1614 (s), 1598 (s), 1574 (s), 1475 (m), 1372 (s), 1225 (s), 1029 (m), 838 (m), 785 (m).

UV-vis λ_{max} (methanol): 703 nm; $\varepsilon = 117\ M^{-1}\ cm^{-1}$.

Complex 2.11: $[Zn(C_6H_5COO)_2(PNO)]_n$

To a solution of benzoic acid (1 mmol, 0.121 g) in methanol (15 mL), zinc(II) acetate dihydrate (0.5 mmol, 0.110 g) was added and stirred for 10 minutes. To this reaction mixture pyridine *N*-oxide (1 mmol, 0.095 g) was added with constant stirring at room temperature. A small amount of toluene (5 mL) was added to this reaction mixture and kept for crystallization. Diffraction quality crystals were collected a week after. Yield of the pure crystalline complex > 80%.

IR (KBr, cm^{-1}): 3445 (bw), 1591 (s), 1559 (s), 1477 (w), 1399 (s), 1221 (m), 731 (m).

^{1}H-NMR (DMSO-d^6, ppm): 8.2 (s, 2H), 7.9 (s, 4H), 7.4 (m, 9H).

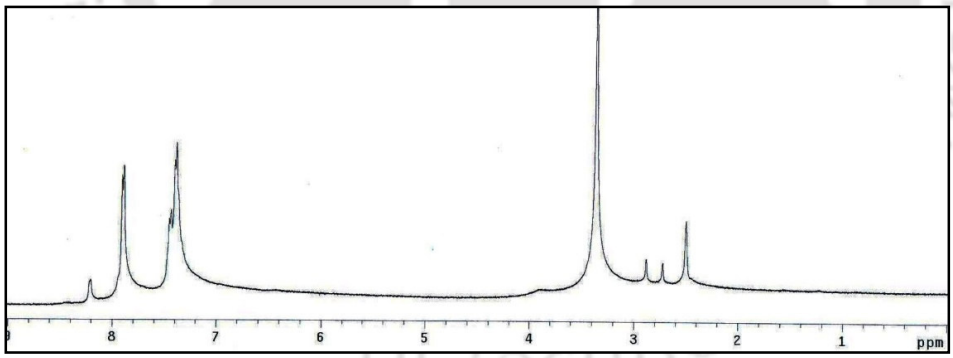

Figure 2.5.2: ^{1}H-NMR spectrum of the complex **2.11**

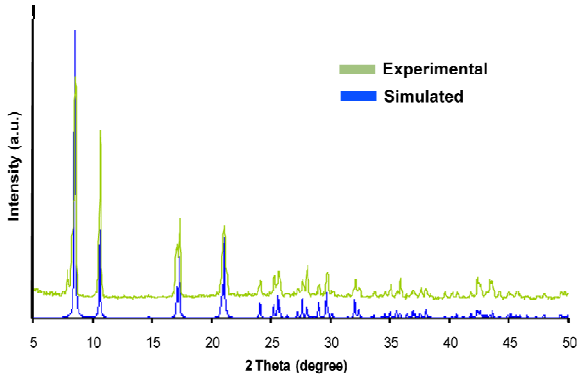

Figure 2.5.3: PXRD pattern of the complex **2.11**

Complex 2.12: $[Zn_2(C_6H_5COO)_4(4,4'\text{-BPNO})]_n$

Single crystals of **2.12** were obtained from a reaction mixture containing 4,4'-bipyridyl-*N,N'*-dioxide (0.25 mmol, 0.045 g), zinc(II) acetate dihydrate (0.25 mmol, 0.055 g) and benzoic acid (0.5 mmol, 0.061 g) in toluene : methanol (3:1, 20 mL). Yield 46 %.

IR (KBr, cm^{-1}): 3434 (bw), 3110 (w), 1639 (s), 1573 (m), 1469 (m), 1403 (s), 1221 (s), 1180 (w), 839 (m), 717 (m).

^{1}H-NMR (CD_3OD, ppm): 8.4 (d, 4H, J=8 Hz), 8.0 (d, 8H, J=8 Hz), 7.9 (d, 4H, J=8 Hz), 7.6 (m, 4H), 7.4 (m, 8H).

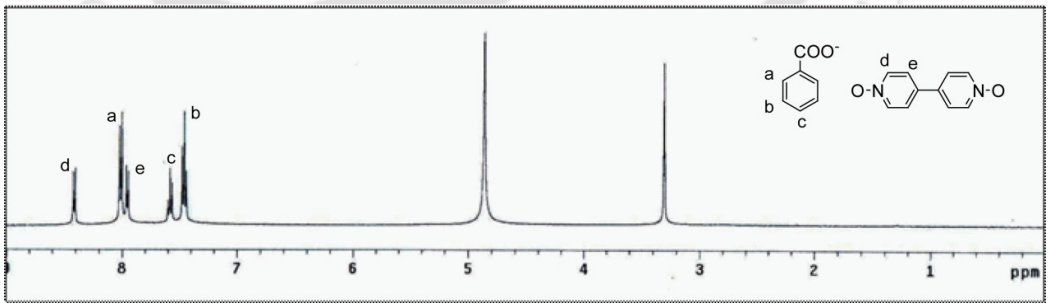

Figure 2.5.4: ^{1}H-NMR spectrum of the complex **2.12**

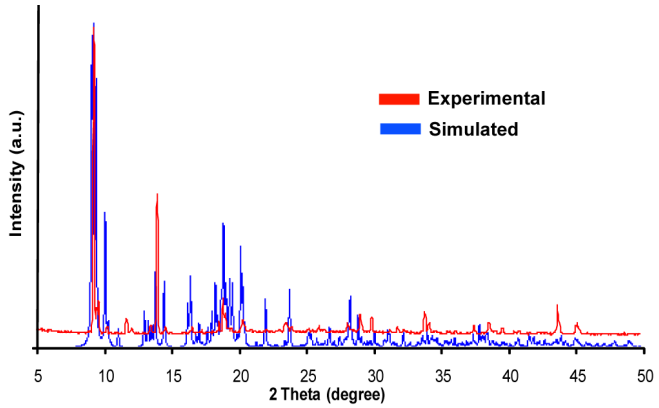

Figure 2.5.5: PXRD pattern of the complex **2.12**

Complex 2.13: $[Zn_4(C_6H_4C_2O_4)_4(4,4'\text{-}BPNO)_2(H_2O)_5]_n.nH_2O$

To a solution of terephthalic acid (0.5 mmol, 0.166 g) in methanol (15 mL), zinc(II) acetate dihydrate (0.5 mmol, 0.110 g) was added and stirred for 20 minutes. The precipitate formed during reaction was dissolved by adding water (5 mL). To this solution 4,4'-bipyridyl-*N,N'*-dioxide (0.5 mmol, 0.095 g) was added with constant stirring. Dimethylsulfoxide (10 mL) was then added to dissolve the precipitate that appeared after addition of 4,4'-bipyridyl-*N,N'*-dioxide. Slow evaporation of solvent gave single crystals of **2.12**. Yield 40%.

IR (KBr, cm^{-1}): 3390 (bm), 1592 (s), 1551 (s), 1469 (m), 1384 (s), 1212 (s), 1031 (m), 833 (m), 752 (m).

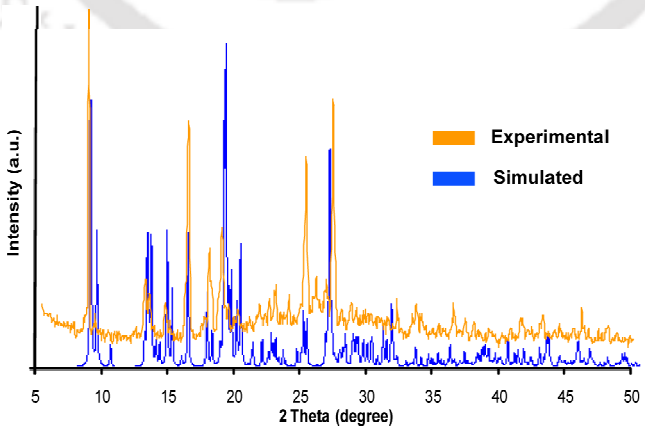

Figure 2.5.6: PXRD pattern of the complex **2.13**

Chapter 3

Synthesis, characterization and structural aspects of *N*-oxide complexes of cadmium(II), mercury(II) and lead(II)

In chapter 2 we have demonstrated the supramolecular aspects and magnetic behaviours of a series of manganese(II) and copper(II) *N*-oxide complexes. Furthermore, structural aspects of a few aromatic *N*-oxide based zinc(II) coordination polymers were also discussed. General strategy during syntheses of such polymers involves reaction of one or more ligands with appropriate coordination modes, and a metal ion that can act as a multidimensional hub to get a thermodynamically stable polymer. Owing to the large ionic radii, metal ions such as cadmium(II), mercury(II) and lead(II) can adopt a range of coordination numbers varying from two up to twelve.[95] Based on the versatile coordination possibility, various coordination polymers of cadmium(II) are prepared and reported from time to time although reports on mercury(II) complexes are scarce.[96-102] Comparatively, lead(II) complexes are extensively studied.[103-107] Although solvothermal reactions are widely used for the preparation of coordination polymers, control over isolation of an intermediate species formed during a reaction is not possible.[109, 110] Solution chemistry is found to be advantageous in this respect, as transient complexes formed during the reaction can sometimes be isolated.[111,112] Thus, understanding of possible inter-conversion or transformation among polymeric species is of importance. The solution phase synthesis, characterization and structural features of different aromatic *N*-oxide based coordination polymers of cadmium(II), mercury(II) and lead(II) as elucidated by spectroscopic and X-ray crystallographic data are the subject of this chapter. Apart from the various structural features of the coordination polymers synthesized, the solution state transformation of a couple of mixed anionic coordination polymers of lead(II) to homo anionic coordination polymers in solution phase is also discussed.

3.1 Synthesis, characterisation and structural aspects of cadmium(II) *N*-oxide complexes

Cadmium(II) acetate dihydrate reacts with pyridine *N*-oxide and benzoic acid to form coordination polymer having composition $[Cd(C_6H_5COO)_2(PNO)]_n$ (**3.1**) in which both pyridine *N*-oxide and the benzoate ligands act as μ^2 bridging ligand to connect the metal ions. The crystal structure of **3.1** shows that the coordination polymer crystallizes in the monoclinic space group *C2/c*. Each of the Cd1 centers in **3.1** is in distorted octahedral geometry with four carboxylate coordinations and two *N*-oxo coordinations satisfying the hexa coordination around the metal centres. All the Cd-O bond lengths are in the range 2.30-2.34 Å which are similar to the reported ones.[96-102; 113-115] The crystal structure of **3.1** is similar to the structure of the coordination polymer **2.1**. Here also, the benzoate ligands are in bidentate bridging mode and the pyridine *N*-oxide acts as a μ^2 bridging ligand that connects the nearest Cd(II) centers with a distance of separation 3.85 Å (Figure 3.1.1). The bridging executed by the benzoate as well as the pyridine *N*-oxide ligands extends the coordination polymer along the *c* crystallographic axis.

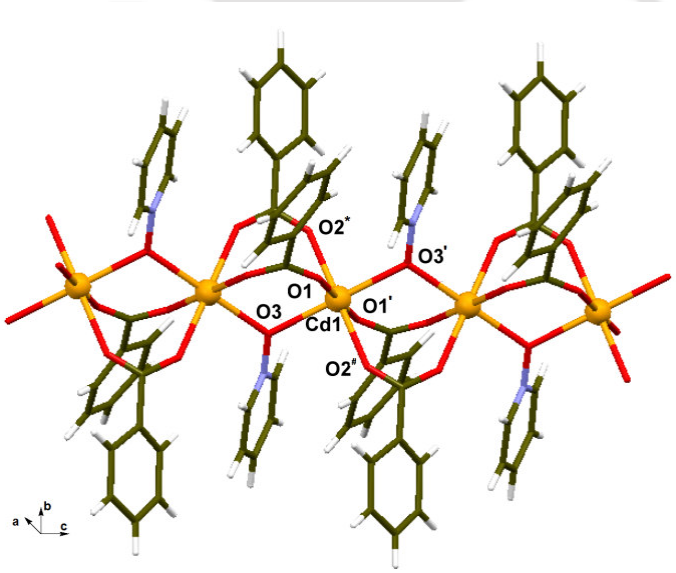

Figure 3.1.1: One dimensional chain of the coordination polymer **3.1** [' = -x, 1-y, 1-z; * = -x, y, ½-z; # = x, 1-y, ½+z]

The reaction of cadmium(II) acetate dihydrate, benzoic acid, and 4,4'-bipyridyl-*N,N*'-dioxide in methanol leads to the formation of a trinuclear Cd(II) coordination polymer (**3.2**) with a composition $[Cd_3(C_6H_5COO)_6(4,4'\text{-}BPNO)_2]_n.2nH_2O$. In the FT-IR spectra of **3.2**, the asymmetric and symmetric stretching of carboxylate groups appear at 1598 cm^{-1} and 1400 cm^{-1} respectively. The aqua O-H stretching appears at 3431 cm^{-1}. The N-O band which appears at around 1240 cm^{-1} in the IR spectrum of free 4,4'-BPNO, appeared at 1222 cm^{-1} in the complex **3.2**. The observed shift of 18 cm^{-1} to a lower frequency reflects the influence of the fact that the oxygen atom of 4,4'-BPNO is involved in the formation metal-oxygen bond.

The coordination polymer **3.2** crystallizes in the monoclinic space group *P2(1)/c*. The crystal structure shows the presence of a trinuclear unit of cadmium(II) benzoate that are bridged though the 4,4'-BPNO ligand to form a sheet like structure. All the three cadmium(II) centers of the trinuclear unit are not in identical coordination environment. The Cd1 (middle one) is connected to the terminal cadmium(II) centers (Cd2) through four benzoate ligands with bidentate bridging (η^2-μ^2) mode. Both the terminal cadmium(II) centers are coordinated to two bidentate bridging benzoate groups and one bidentate chelate bridging (η^3-μ^2) benzoate group. The remaining coordination sites of Cd2 are occupied by two *N*-oxo of 4,4'-bipyridyl-*N,N*'-dioxide ligands. The 4,4'-BPNO ligands coordinate the metal through *cis* bidentate μ^2 bridging mode (*cis* η^2-μ^2). Thus the bridging among the cadmium(II) centers within the trinuclear unit is provided by the benzoate group thereby extending the polymer in one direction. The 4,4'-BPNO ligands act as the linker between the nearest trinuclear units thereby extending the polymer along the *c* crystallographic axis. Moreover, the molecule contains two water molecules of crystallization hydrogen bonded to the *N*-oxo group as well as with the carboxylate oxygens via O9-H9A···O7, O9-H9B···O1 ($d_{D\text{-}H\cdots A}$ (Å), O9-H9A···O7, 2.69; O9-H9B···O1, 2.17 and <D-H···A (º), <O9-H9A···O7, 97; <O9-H9B···O1, 154) interactions. It appears that, this hydrogen bonding, blocks the extension of the coordination polymer along the *ab* crystallographic plane and consequently the width of the sheet is not infinite but have the value of ~9 Å. Although large structural variations are observed in cadmium carboxylate complexes, discrete tricarboxylate units are generally formed in manganese(II) complexes with chelating auxillary ligands and only rarely found in the

case of cadmium carboxylates.[96-102] The structure of the coordination polymer **3.2** is shown in the figure 3.1.2.

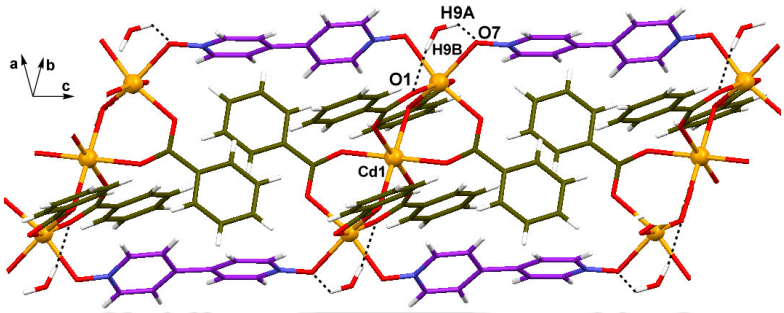

Figure 3.1.2: One dimensional coordination polymer **3.2** having trinuclear repeated units

The reaction of terephthalic acid with cadmium(II) acetate and 4,4'-BPNO yields a three dimensional coordination polymer having the composition $[Cd(C_6H_4C_2O_4)(4,4'\text{-BPNO})(H_2O)]_n$ (**3.3**). The compound crystallizes in the monoclinic space group *C2/c*. Each asymmetric unit of **3.3** contains half a cadmium(II) centre coordinated to half each of a terephthalate, 4,4'-bipyridyl-*N,N'*-dioxide and aqua ligand. The cadmium(II) centers in the structure are all hepta coordinated, four of them provided by the carboxylate groups and two by the *N*-oxo groups. The seventh coordination site is occupied by the aqua ligand. The carboxylate groups coordinate the metal centre through bidentate chelating mode and the Cd-O bond distances in **3.3** spans the 2.26-2.53 Å range. The dimensionality of the coordination polymer is provided by two different types of bridging units: the terephthalato ligands connect the nearby metal ions with a Cd-Cd separation of 11.25 Å resulting in the formation of 1D chains propagating along the *ac* diagonal plane as shown in figure 3.1.3a. These 1D chains are interconnected by the 4,4'-BPNO ligands through *trans* bidentate μ^2 bridging connectivity along the *a* crystallographic axis, thereby resulting in a complicated 3D network. It is interesting to note here that topological analysis of the coordination polymer **3.3** performed with *TOPOS-4.0* envisage that it is a 3-fold interpenetrated diamondoid network as shown in figure 3.1.3c in the simplified form. Figure 3.1.3b shows the 3-fold interpenetrated extension in **3.3**.

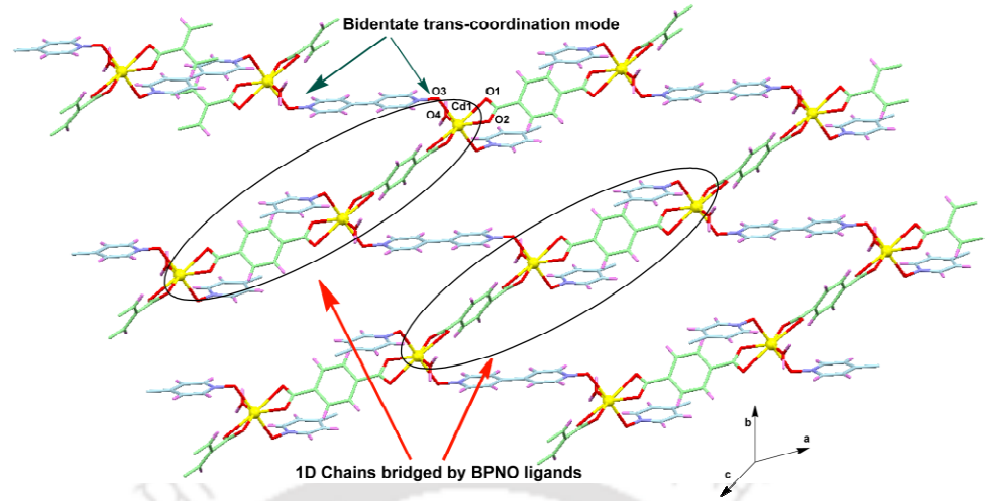

(a)

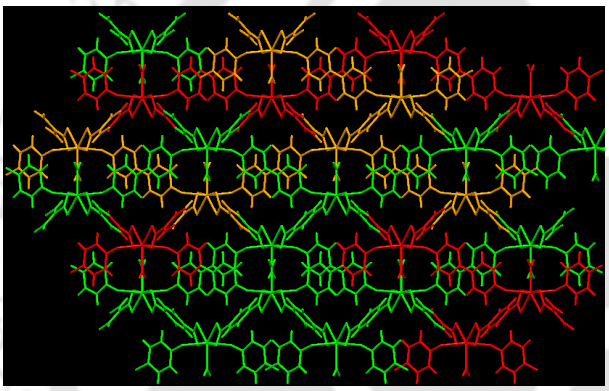

(b)

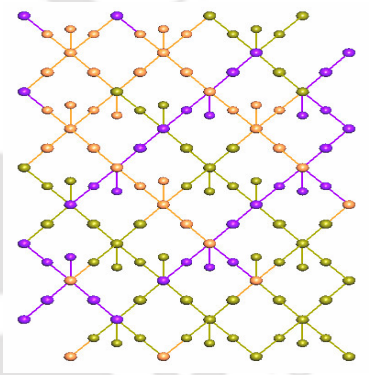

(c)

Figure 3.1.3: (a) Coordination environment and connectivity of the ligands in coordination polymer **3.3**, (b) 3-fold interpenetrated extensions in **3.3** and (c) simplified 3-fold interpenetrated nets.

PXRD and Thermogravimetric analysis

In order to check the purity of the bulk samples PXRD analysis of the coordination polymers **3.1**-**3.3** are carried out and found to match well with the simulated patterns. Thermal stability of the complexes **3.1**-**3.3** is studied. The coordination polymer **3.1** is thermally stable up to ~200 ^{o}C which undergoes continuous degradation in the range 200-290 °C corresponding to 72.2% (calc. 75.1%) of the total weight. This is accounted for loss of two benzoic acid and one pyridine *N*-oxide molecules. For the coordination polymer **3.2**, in the first step, weight loss occurs in the range 70-280 °C, which corresponds to 28.7% of the total weight. This loss of weight is accounted for two water molecules and two 4,4'-bipyridyl-*N,N*'-

dioxide molecules (theoretical weight loss 27.5%). Continuous degradation then takes place due to loss of the benzoic acid molecules. Coordination polymer **3.3** also loses weight in two steps: the first step in the range 70-130 °C corresponds to weight loss of 4.2% (calc. 3.7%) due to loss of the coordinated water molecule per formula and the second step, 295-590 °C is due to the loss of the terephthalic acid and 4,4'-bipyridyl-*N,N'*-dioxide molecules (experimental 77.4% of the residue of the first step; calc. 75.8%).

3.2 Synthesis, characterisation and structural aspects of mercury(II) *N*-oxide complexes

Mercury(II) acetate on reaction with benzoic acid followed by treatment with 2,2'-bipyridyl-*N,N'*-dioxide leads to a tetra coordinated mononuclear complex **3.4** with the composition $[Hg(C_6H_5COO)_2(2,2'\text{-BPNO})]$. The crystal structure of **3.4** is shown in figure 3.2.1a. It crystallizes in the monoclinic space group *C*2/c and each asymmetric unit of **3.4** consists of one mercury(II) atom, one benzoate ligand and half a 2,2'-bipyridyl-*N,N'*-dioxide molecule. The mercury(II) centre is of tetra coordinated geometry with the 2,2'-bipyridyl-*N,N'*-dioxide ligand acting as a bidentate chelating ligand. Two carboxylate groups coordinate through monodentate binding mode through the O1 oxygen atom.The Hg-O (benzoate) bond is much stronger than the Hg-O (*N*-oxo) bond as depicted by their bond lengths (Hg1-O1, 2.06 Å; Hg1-O3, 2.47 Å), however, both are well within the reported limits of Hg-O bond lengths.[116, 117] The other carboxylate oxygen, O2, interacts only weakly with the mercury atom (Hg1-O2, 2.81 Å). Apart from these there exist a number of strong C-H···O interactions ($d_{D\text{-}H\cdots A}$ (Å), C8-H8···O2, 2.71; C11-H11···O2, 2.44 and <D-H···A (°), C8-H8···O2, 127; C11-H11···O2, 152) between the carboxylate oxygen and the aromatic protons of the 2,2'-BPNO molecule. This interactions holds the nearby molecules of **3.4** connected to each other forming a two dimensional net like structure (Figure 3.2.1b).

Mercury(II) acetate on reaction with benzoic acid followed by treatment with 4,4'-bipyridyl-*N,N'*-dioxide leads to a mercury(II) benzoate coordination polymer **3.5** bridged by 4,4'-BPNO ligand as shown in figure 3.2.2. It exhibits characteristic IR stretching frequencies at 1595 cm^{-1} and 1387 cm^{-1} due to the carboxylate stretching; the *N*-oxo stretching appears at 1219 cm^{-1}.

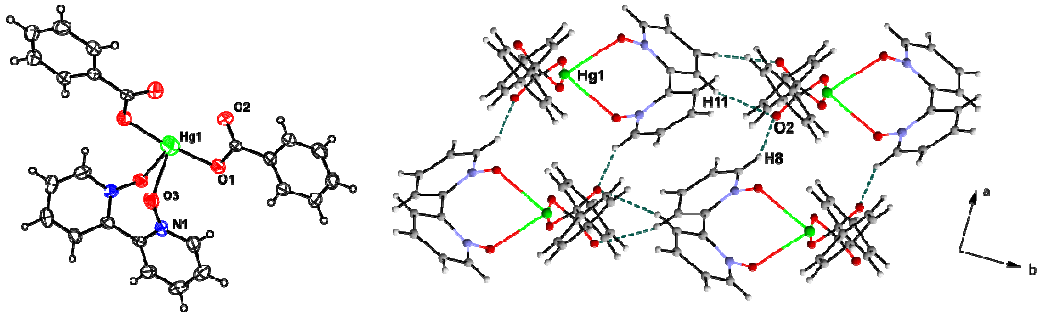

(a) (b)

Figure 3.2.1: (a) ORTEP of the mononuclear complex **3.4** (drawn with 30% probability ellipsoid) and (b) weak interactions in **3.4** leading to two dimensional net

The coordination polymer **3.5** crystallizes in the monoclinic space group *C2/c*. Each mercury(II) ion of the polymeric chain is associated with one chelating benzoate ligand and one monodentate benzoate ligand along with two bridging 4,4'-bipyridyl-*N,N'*-dioxide ligands. Thus, each mercury(II) ions in the coordination polymer **3.5** adopts a distorted square pyramidal geometry. All the Hg-O bond distances lie in the range 2.12-2.52 Å. The distance of separation between the Hg1 and O4 is 2.13 Å; the other carbxylate oxygen, O3, interacts weakly with the mercury atom (Hg1···O3 2.77 Å). This kind of asymmetric coordination of carboxylate groups to mercury(II) is also found in other mercury(II) complexes.[118, 119] These atoms form a square-pyramidal coordination which is not usual for Hg(II).[120] This is confirmed by the index of the degree of trigonality, τ of 0.11 (calculated as a difference between two largest angles divided by 60). This index is zero for a perfectly square-pyramidal and a unity for perfectly trigonal-bipyramidal geometry.[121] The metal centers are interconnected through the 4,4'-bipyridyl-*N,N'*-dioxide ligands coordinated through *cis* bidentate μ^2 bridging mode (*cis* $\eta^2:\mu^2$) which provides the dimensionality of the coordination polymer. Here, the coordination around the metal center forces the 4,4'-BPNO ligand to get twisted as the two aromatic rings of the ligand make an angle of 7.94° with respect to each other.

It is worth-mentioning that the one dimensional chains of the coordination polymer **3.5** take a spiral shape (Figure 3.2.2b). There exist numbers of short range interactions viz. C18-H18···O4, C19-H19···O6 ($d_{D-H\cdots A}$ (Å), C18-H18···O4, 2.64; C19-H19···O4, 2.70; C19-H19···O6, 2.45 and <D-H···A (°), <C18-H18···O4, 126; <C19-

H19···O4, 124; <C19-H19···O6, 164) along with π-π interactions (centroid-centroid distance 3.855 Å and 3.899 Å) between the aromatic rings of 4,4'-bipyridyl-*N,N'*-dioxide of two nearby one dimensional chains of the coordination polymer. These interactions impart stability to the helical structure of the polymer thereby leading to a one dimensional double helix as shown in figure 3.2.2c.

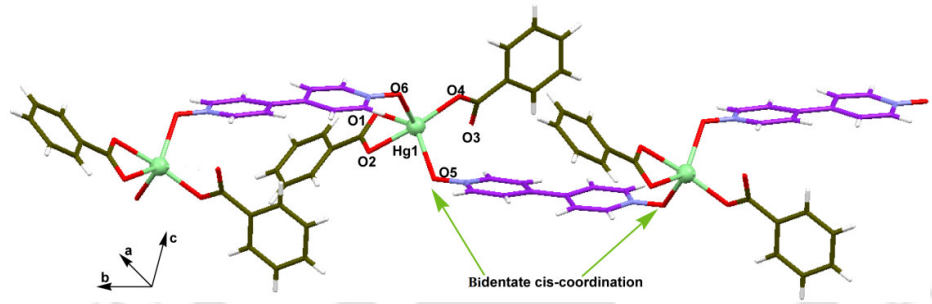

(a)

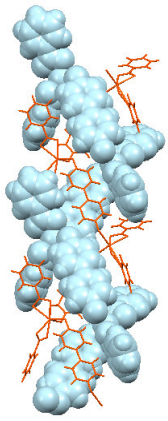

(b)

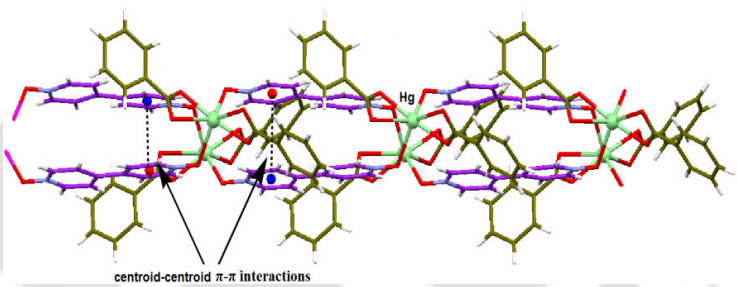

(c)

Figure 3.2.2: (a) The backbone of coordination polymer **3.5**, (b) the space-fill model of double helical polymer that holds another helical unit, (c) weak interactions between two helical chains

PXRD and Thermogravimetric analysis

PXRD analysis of the bulk samples of the complexes **3.4** and **3.5** are carried out and found to match well with the simulated patterns. This depicts the pure phase of the synthesized compounds. Thermal stability of the complexes **3.4** and **3.5** are studied and the thermogram shows weight loss in two subsequent steps for both of them. For the complex **3.4** initial loss of weight takes place in the range 95-270 °C

corresponding to loss of a 2,2'-bipyridyl-*N,N*'-dioxide and a benzoic acid molecules per formula (experimental 47.8%; calc. 48.7%). The other benzoic acid molecule is then lost in between 275-365 °C (experimental 35.8% of the residue; calc. 37.7%). For the complex **3.5** in the first step, weight loss occurs at 110-195 °C, which corresponds to 28.4% of the total weight. This loss of weight is accounted for loss of 4,4'-bipyridyl-*N,N*'-dioxide molecule per formula. The second loss occurs in the range 260-284 °C that corresponds to weight loss of 54.3% of the residue from the first step due to loss of the two benzoic acid molecules.

3.3 Synthesis, characterisation and structural aspects of lead(II) *N*-oxide complexes

Owing to the large ionic radii and the ability to adopt higher coordination number, lead(II) is considered to be a metal of choice for generation of coordination polymers.[103-108] We have prepared and characterized a number of coordination polymers of lead(II) with various aromatic *N*-oxide ligands such as pyridine *N*-oxide, quinoline *N*-oxide, 2,2'-bipyridyl-*N,N′*-dioxide and 4,4'-bipyridyl-*N,N′*-dioxide. While with pyridine *N*-oxide and quinoline *N*-oxide 1D coordination polymers are formed, with 4,4'-bipyridyl-*N,N′*-dioxide two or three dimensional coordination polymers are obtained depending upon the reaction condition. Use of 2,2'-bipyridyl-*N,N′*-dioxide yielded a mixed anionic one dimensional coordination polymer (scheme 3.3.1).

Solution state reaction of lead(II) nitrate, sodium benzoate and pyridine *N*-oxide led to the formation of a one dimensional coordination polymer **3.6** with the composition $[Pb_2(C_6H_5COO)_4(PNO)(H_2O)_2]_n$. The single crystal analysis of the coordination polymer **3.6** suggests the crystals are to be of monoclinic $P2_1/c$ space group. The asymmetric unit contains two coordinatively different lead(II) centers (Pb1 and Pb2) coordinated to four benzoate ligands, two aquo ligands and one pyridine *N*-oxide ligand. The pyridine *N*-oxide molecules coordinate the metal centers as a monodentate ligand and are coordinated to alternate Pb(II) centers. Pb1 center is coordinated to six carboxylate oxygens and an aquo oxygen thereby satisfying a seven coordinated geometry. The other lead(II) center (Pb2) is eight coordinated and the extra coordination is provided by a pyridine *N*-oxide molecule. One of the benzoate

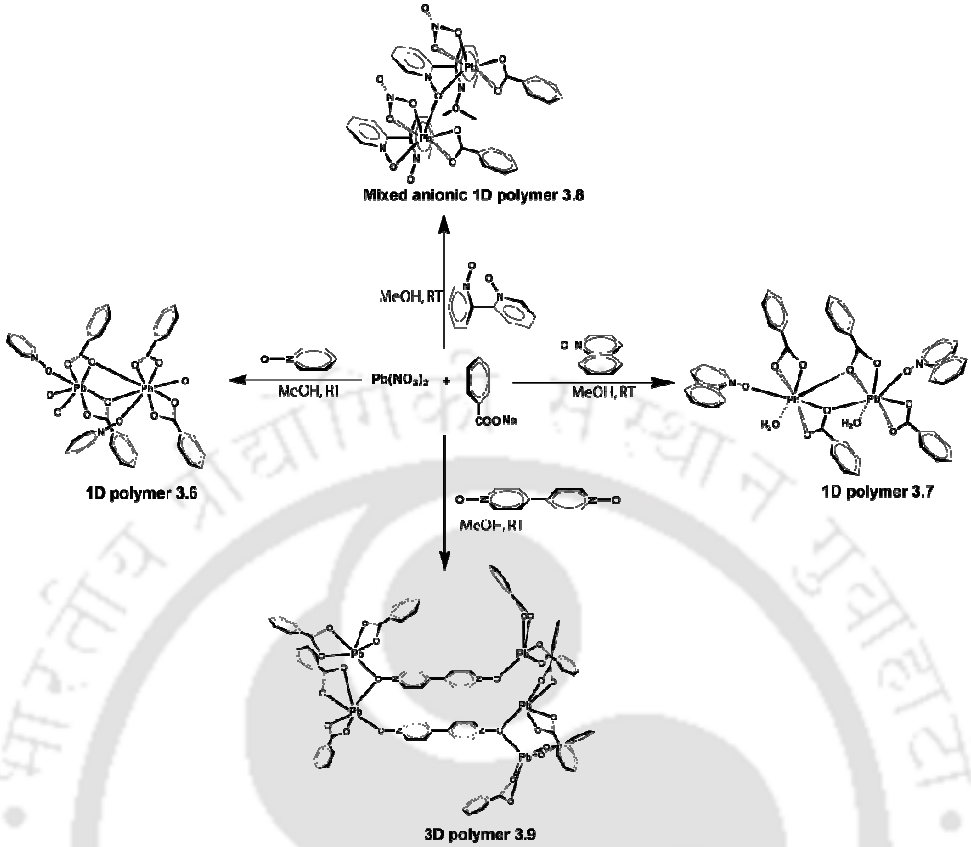

Scheme 3.3.1

groups coordinated to each lead(II) center is in chelating coordination mode while the other is in a μ^3 bridging mode. This carboxylate bridging connects the nearby Pb1 centers to the Pb2 centers and extends the coordination polymer along the crystallographic *b* axis to result in a one dimensional structure (Figure 3.3.1a). Use of quinoline *N*-oxide in place of pyridine *N*-oxide in a similar reaction resulted in the formation of a similar one dimensional coordination polymer **3.7** having the molecular composition $[Pb(C_6H_5COO)_2(QNO)(H_2O)]_n$ (where, QNO= quinoline *N*-oxide). Unlike in **3.6**, here all the Pb(II) centers are in an eight coordinated environment and are bridged to each other through μ^3 bridging mode of the benzoate ligands. Here also, the *N*-oxo group is coordinated to the metal center through monodentate binding mode. The Pb-O bond lengths in both of the coordination polymers lie in the range 2.38-2.81 Å which is normal for reported lead(II) coordination polymers.[103, 122-124] The geometry of the Pb1 center in the coordination polymer **3.6** is hemidirected, and there is clearly an identifiable gap in the Pb1

coordination sphere, suggesting that Pb1 contains a stereochemically active lone pair of electrons.[106, 124] However, the Pb2 center in **3.6** and Pb1 center in **3.7** are of hollow directed geometry.

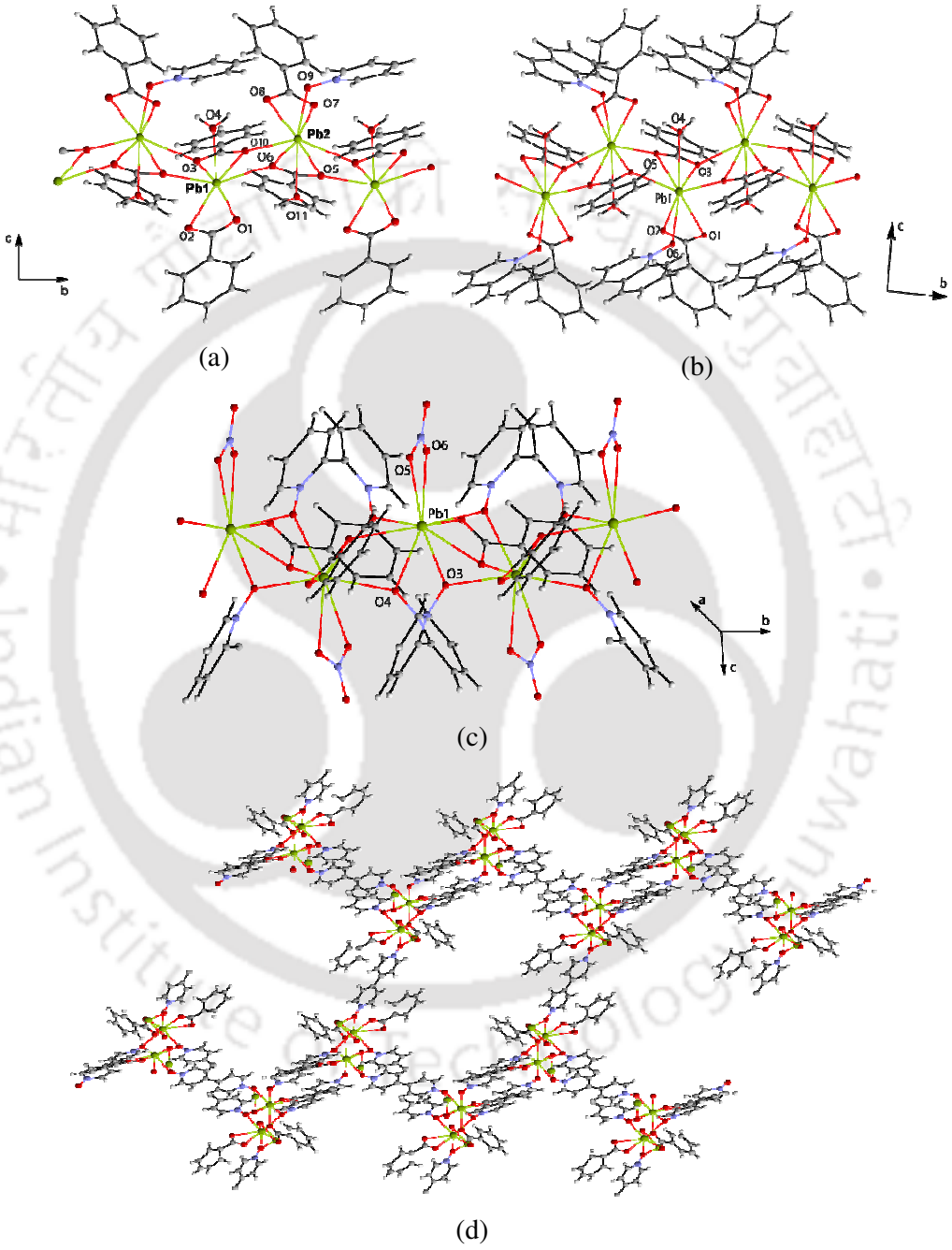

Figure 3.3.1: The one dimensional chains of the coordination polymer (a) **3.6**, (b) **3.7**; (c) the mixed anionic coordination polymer **3.8** and (d) the three dimensional coordination polymer **3.9**

Use of 2,2'-bipyridyl-*N,N'*-dioxide in a similar reaction yielded a mixed anionic one dimensional coordination polymer (**3.8**) where 2,2'-BPNO binds through a *trans* bridging mode. The coordination polymer crystallizes in the monoclinic space group $P2_1/c$. The structure of the coordination polymer is built upon the stacking of 1D chains that are made by the polymerization of asymmetric $[Pb(C_6H_5COO)(NO_3)(2,2'\text{-BPNO})]$ units. Each of the lead(II) centers in **3.8** is nine coordinated. Four of these coordinations are occupied by the bridging *N*-oxo oxygens, three by carboxylate oxygens and rest two are by a chelating nitrate ligand. Structure of the coordination polymer is shown in figure 3.3.1c. Pb-O bond distances fall in the range of 2.52-2.92 Å, similar to the reported Pb-O interactions.[121-124] The nearby lead(II) centers in **3.8** are connected through both carboxylate as well as *N*-oxo bridging. While the benzoate ligands are coordinated through the conventional bidentate chelate bridging mode, the 2,2'-bipyridyl-*N,N'*-dioxide binds through a relatively rare *trans* bidentate η^2-μ^2:μ^2 bridging mode. This bridging connects three nearby lead(II) centers per 2,2'-bipyridyl-*N,N'*-dioxide ligand and extends the molecule along the crystallographic *b* axis which results in a one dimensional structure.

The coordination polymer **3.9** has a three dimensional structure built by the aggregation of the asymmetric $[Pb_2(C_6H_5COO)_3(4,4'\text{-BPNO})_{2.5}]$ units. There are two coordinatively different Pb(II) centers in the molecule although both of them are eight coordinated. Pb1 is coordinated to three benzoate oxygen atoms and five *N*-oxo oxygens while Pb2 is coordinated to four benzoate oxygen atoms and four different *N*-oxo oxygens. The bridging between the nearby lead(II) centers are provided by both the benzoate as well as *N*-oxo ligands. The 4,4'-bipyridyl-*N,N'*-dioxide ligands connect the metal centers through two different binding modes (bidentate η^2-μ^2:μ^2 bridging and bidentate η^2-μ^2:μ^1 bridging) to bind together the one dimensional chains and generate a complicated three dimensional architecture. The structure of the three dimensional coordination polymer **3.9** is shown in figure 3.3.1d.

Apart from these a number of lead(II) *N*-oxide coordination polymers were synthesized using 4-nitrobenzoate ($4\text{-}NO_2C_6H_4COO^-$) as the anionic ligand. We have observed that the reaction of lead(II) nitrate with 4-nitrobenzoate and pyridine *N*-oxide in methanol initially gives a mixed anionic coordination polymer **3.10** having composition $[Pb(4\text{-}NO_2C_6H_4COO)(NO_3)(PNO)_2]_n$. This complex on keeping

dissolved in the mother liquor for about 24h gets converted to a mononuclear complex **3.11** having composition $[Pb(4\text{-}NO_2C_6H_4COO)_2(PNO)(H_2O)]$. Finally, the complex **3.11** slowly gets converted to a new coordination polymer **3.12** $[Pb(4\text{-}NO_2C_6H_4COO)_2(PNO)]_n$ on stirring in methanol solution. The reactions are presented in scheme 3.3.2.

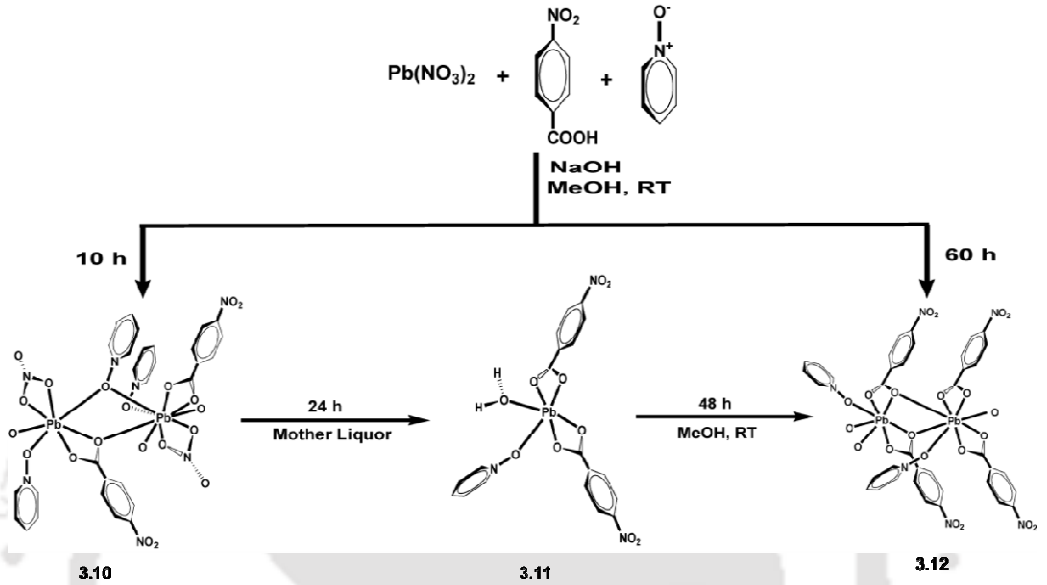

Scheme 3.3.2

The complex **3.10** has its characteristic IR absorptions at 1555 cm^{-1} due to the chelating nitrate group bound to metal ion and at 1216 cm^{-1} due to *N*-oxo stretching, the carboxyl frequency appears at 1573 cm^{-1} and 1387 cm^{-1}. In the ^{1}H-NMR spectra, the complex has the peaks arising from the protons of the 4-nitrobenzoate group at 8.1 and 8.3 ppm, in addition to the aromatic peaks of pyridine *N*-oxide.

The structure of the coordination polymer **3.10** is shown in figure 3.3.2. Each of the metal centers in **3.10** is octa coordinated in which 4-nitrobenzoate ligands satisfy three of the coordination sites and are in bidentate bridging mode. The nitrate groups in the polymer are chelating and each lead(II) center is associated with three different *N*-oxide oxygen atoms, two bridging and the rest being monodentate. The Pb-O distance for the bridging *N*-oxide is 2.74 Å whereas that for the monodentate *N*-oxide is 2.44 Å. The Pb-O distances for the nitrate ligand are Pb1-O1, 2.82 Å; Pb1-O2, 2.57 Å. A careful look on the coordination polymer shows that it comprises of mononuclear building blocks of composition $[Pb(4\text{-}NO_2C_6H_4COO)(NO_3)(PNO)_2]$ and

self assembling of these units through μ^2 *N*-oxo bridging results in the coordination polymer **3.10** with hollow directed lead(II) centers.

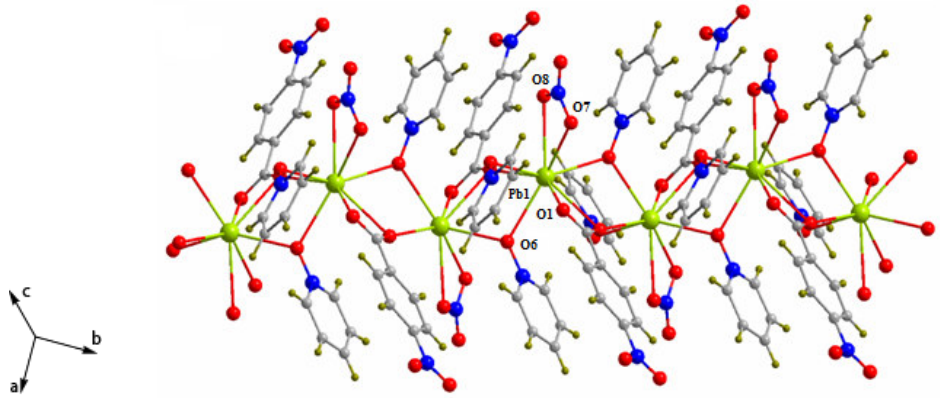

Figure 3.3.2: The mixed anionic one dimensional coordination polymer **3.10**

The coordination polymer **3.10** degrades in solution and gets converted to the mononuclear complex **3.11**. The degradation process involves replacement of the nitrate group by 4-nitrobenzoate group. The complex **3.11** has hexa coordinated hemi directed lead(II) centers coordinated by two bidentate carboxylates, one pyridine *N*-oxide and one aqua ligands. From the crystal structure of the complex it is observed that the Pb-O bonds in **3.11** (Pb1-O2, 2.37 Å; Pb1-O1, 2.78 Å; Pb1-O5, 2.38 Å; Pb1-O6, 2.77 Å) are much stronger than those in **3.10**. This may be one of the various factors responsible for the degradation of the coordination polymer **3.10** as it leads to formation of a complex (**3.11**) with much stronger metal-ligand bonds. The complex

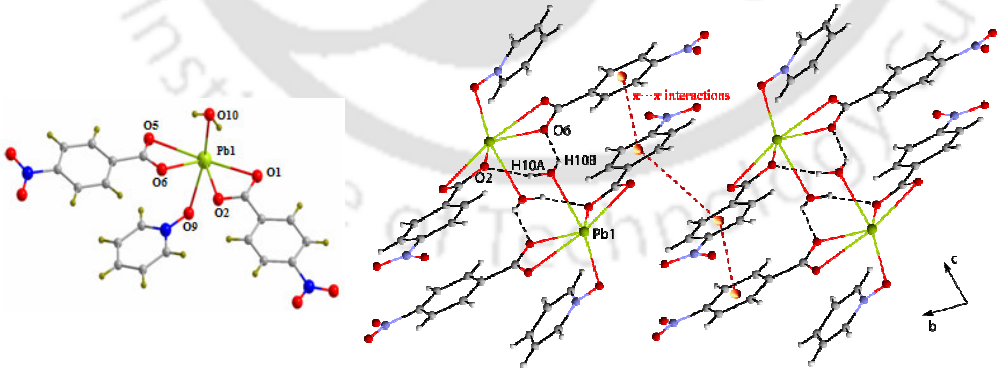

(a) (b)

Figure 3.3.3: (a) Structure of the mononuclear complex **3.11** (b) assembly of [Pb(4-$NO_2C_6H_4COO)_2(PNO)(H_2O)$] units through intermolecular hydrogen bonding and π···π stacking interactions in **3.11**

self assembles through weak O10-H10B···O2 ($d_{D\text{-}H\cdots A}$(Å), 1.993; <D-H···A (º), 162), O10-H10A···O6 ($d_{D\text{-}H\cdots A}$ (Å), 2.092; <D-H···A (º), 141) interactions and π···π interactions between the aromatic rings of 4-nitrobenzoate ligand (Figure 3.3.3b). The aromatic rings of the 4-nitrobenzoate groups are stacked parallel with the nitrobenzoate groups slightly off-set with a distance of separation 3.392 Å which is well within the limit for having π···π stacking interactions.[42, 72]

Complex **3.11** is unstable in solution and slowly gets converted to the homo anionic coordination polymer **3.12** by losing the aquo molecule. The complex **3.12** has IR absorptions at 1227 cm^{-1} due to *N*-oxo stretching; at 1621 cm^{-1} and 1384 cm^{-1} due to the carboxylate stretchings. The complex has a seven coordinated geometry around the lead(II) ions and remains as one dimensional coordination polymer. Six of

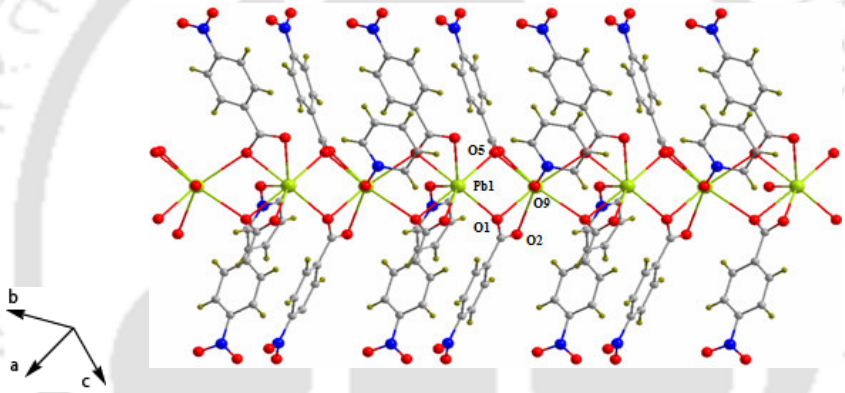

Figure 3.3.4: Building of the coordination polymer **3.12** through carboxylate bridges

these coordination sites are occupied by 4-nitrobenzoate groups while the seventh coordination is occupied by a pyridine *N*-oxide ligand. Pyridine *N*-oxide here acts as a monodentate ligand and the bridging between the nearest lead(II) centers takes place through carboxylate bridging. This carboxylate bridging solely provides the dimensionality to the molecule.

It is the tendency towards expansion of coordination number of the metal ion that acts as the driving force towards the elimination of the aqua ligand and results in the polymerization of **3.11** to give **3.12**. The Pb-O bond lengths in **3.12** are in the range of 2.40-2.83 Å, well within the reported limits. The structure of the complex is shown in figure 3.3.4. The ^{1}H-NMR spectra (Figure 3.3.5) of the three complexes

3.10-**3.12** recorded in DMSO-d^6 clearly indicates the presence of pyridine *N*-oxides and 4-nitrobenzoate groups.

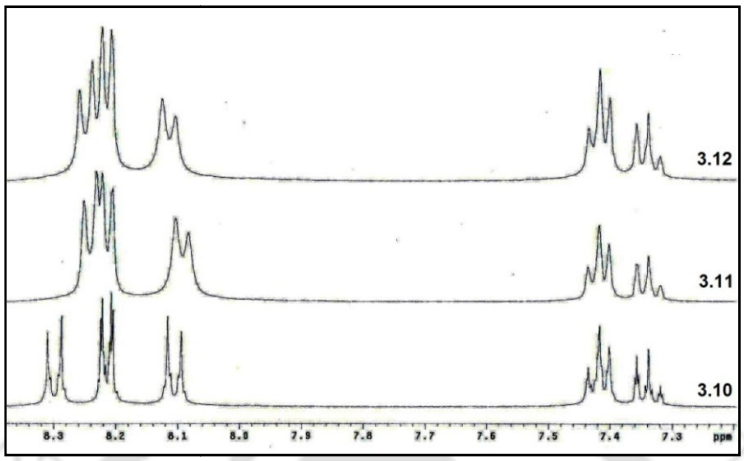

Figure 3.3.5: Overlay ^{1}H-NMR spectra for the complexes **3.10, 3.11** and **3.12**

Further support to these results comes from the fact that similar reactions of lead(II) nitrate, 4-nitrobenzoate with 4,4′-bipyridyl-*N*,*N*′-dioxide initially gives a mixed anionic two dimensional coordination polymer **3.13** which gets converted to another 2D coordination polymer **3.14** in the reaction mixture with time. This conversion is shown in scheme 3.3.3. Both the complexes are characterized by single crystal XRD and also by other conventional spectroscopic techniques.

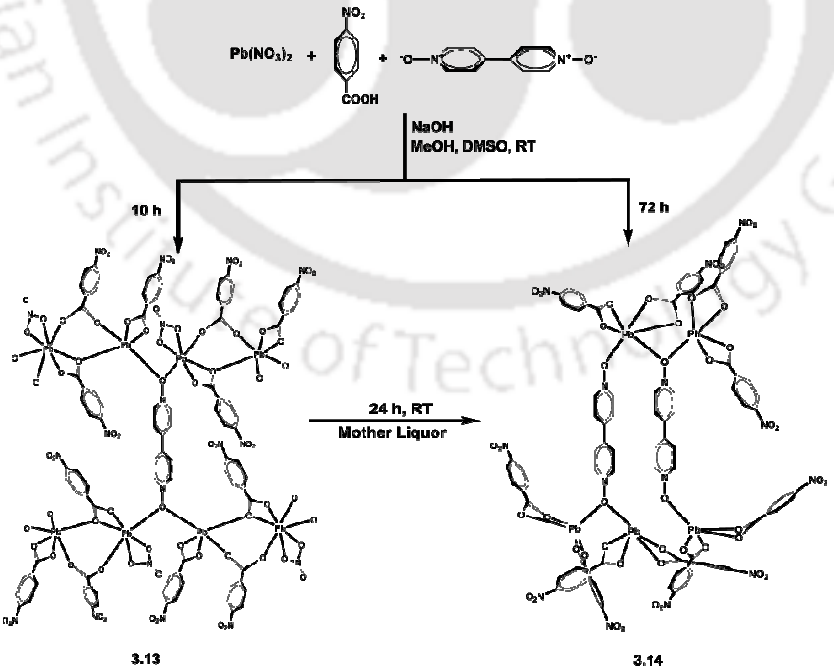

Scheme 3.3.3

The complex **3.13** has IR absorptions at 1519 cm^{-1} characteristic of the nitrate ligand. The bands at 1619 cm^{-1} and 1384 cm^{-1} are due to the carboxylate ligands and at 1214 cm^{-1} due to the N-O stretching of 4,4'-BPNO ligand. It has a two dimensional network structure growing along *b* and *c* crystallographic axes as shown in figure 3.3.6. The complex **3.13** has the composition $[Pb_2(NO_3)(4\text{-}NO_2C_6H_4COO)_3(4,4'\text{-}BPNO)_2]_n$ and is featured by two coordinatively distinct lead(II) centers. One of these lead(II) centers (Pb1) is octa coordinated (three coordinations from carboxylate oxygen, three from nitrate and rest are from 4,4'-BPNO ligands) with a hollow directed geometry. The other lead(II) center (Pb2) has hexa coordinated hemidirected geometry. Four of the hexa coordinations are from carboxylate oxygens and rest are from 4,4'-BPNO ligands. Pb1 is connected to another Pb1 through nitrate groups which in turn is connected to Pb2 via *N*-oxide oxygens as well as by carboxylate oxygens. The Pb-O bond lengths in **3.13** span the range 2.47-2.91 Å.

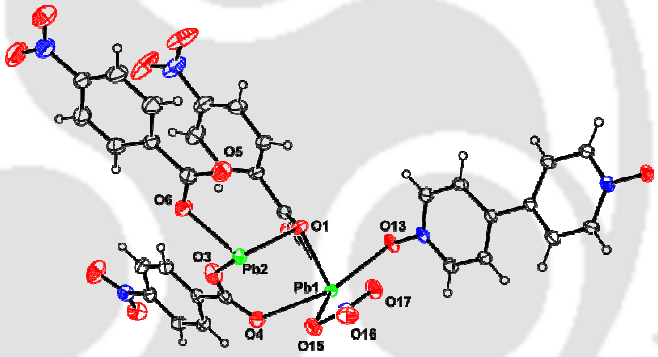

(a)

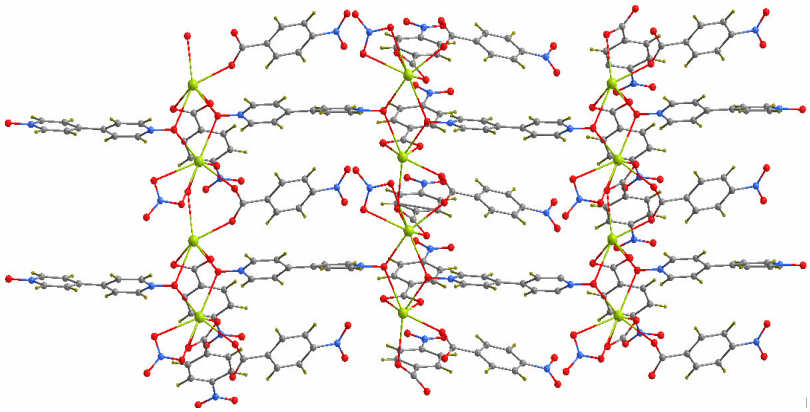

(b)

Figure 3.3.6: (a) The building block of coordination polymer **3.13** and (b) two dimensional polymeric structure of **3.13**

It has been observed that the complex **3.13** is unstable in the reaction mixture and on keeping dissolved in the mother liquor for 24h it gives a new two dimensional homo anionic coordination polymer, **3.14**, having composition $[Pb(4\text{-}NO_2C_6H_4COO)_2(4,4'\text{-BPNO})_2]_n$ with the removal of the weakly bound nitrate ligands. The ^{1}H-NMR spectra (Figure 3.3.7) of both these complexes **3.13** and **3.14** are recorded in DMSO-d^6 and shows the presence of 4-nitrobenzoate groups as well as the 4,4'-BPNO ligands. The complex **3.14** lacks IR absorptions around 1520 cm^{-1} which was present in **3.13** due to the nitrate ligands. The absorptions at 1619 cm^{-1} and 1380 cm^{-1} are due to the carboxylate ligand and at 1231 cm^{-1} due to the *N*-oxo stretching of the 4,4'-BPNO ligand. Each of the lead(II) centers in **3.14** has a hemidirected hepta coordinated geometry. Four of the coordinations are from two chelating carboxylate ligands and rest are from bridging as well as monodentate 4,4'-BPNO ligands. Here, the Pb-O bond lengths lie in the range 2.48-2.77 Å. In this case also, the formation of comparatively stronger Pb-O (carboxylate) forces the dissociation of the Pb-O (nitrate) bonds thereby forming the homo anionic coordination polymer from the mixed anionic one. This 2D coordination polymer extends along the *b* and *c* crystallographic axes as shown in figure 3.3.8b.

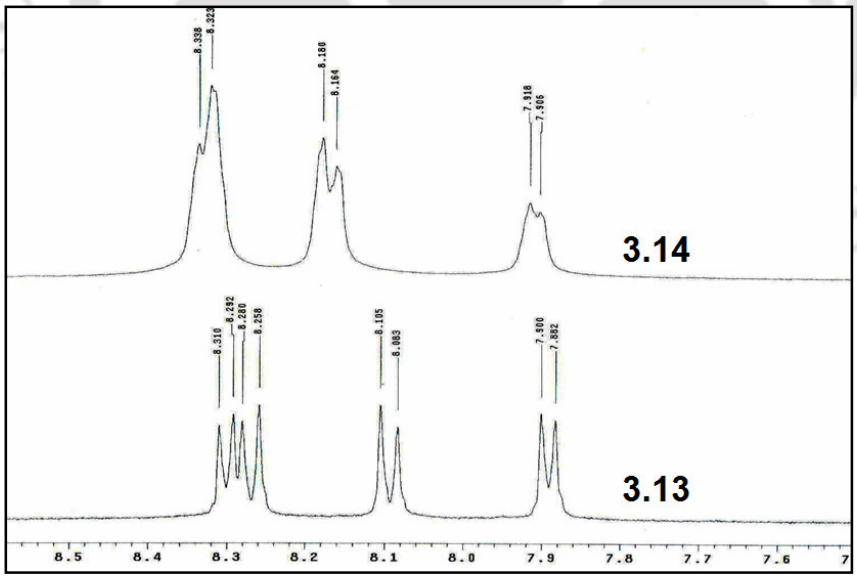

Figure 3.3.7: Overlay ^{1}H-NMR spectra for the complexes **3.13** and **3.14**

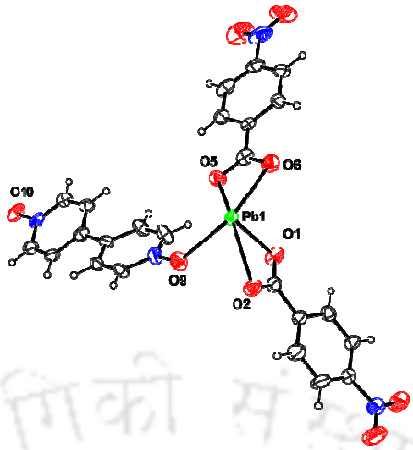

(a)

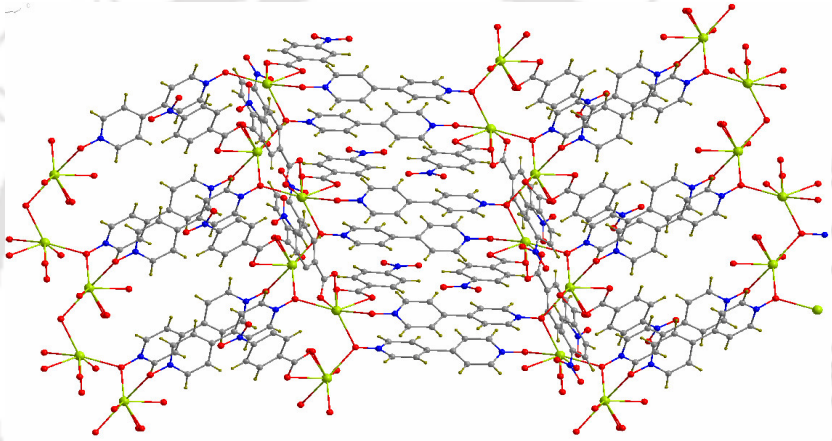

(b)

Figure 3.3.8: (a) The asymmetric unit and (b) the 2-D polymeric structure of the coordination polymer **3.14**

In both of these processes, it is observed that mixed anionic coordination polymer containing 4-nitrobenzoate as well as nitrate ligands is formed initially with the excess 4-nitrobenzoate remaining in the solution. However, these mixed anionic complexes are comparatively unstable in the mother liquor and get converted to polymeric species containing only 4-nitrobenzoate as anionic ligand through a process of ligand substitution of the nitrate ligand with 4-nitrobenzoate. As revealed by the reaction of PNO it is likely that the ligand substitution phenomenon takes place through a process of hydration followed by dehydration. However, we were unable to recover any hydrated species in case of the reaction with 4,4'-BPNO even if it is formed.

Thermogravimetric analysis

Thermal stability of the complexes **3.6**-**3.9** is studied and the thermograms show that all the coordination polymers are thermally stable up to ~200 ^{o}C. For thecoordination polymer **3.6**, weight loss occured in the first step within the range 140-310 °C corresponds to weight loss of 28.8% (calc. 27.2%) due to loss of the two benzoic acid molecules and two water moleculaes per formula. In the second step between the temperature range of 315-490 °C, loss of a pyridine *N*-oxide and a benzoic acid molecule takes place (experimental weight loss 27.1% of the residue from the first step; calc. 28.9%). Continuous degradation then takes place. Thermogram of the complex **3.7** reveals that the weight loss occurs in two steps. In the first step, weight loss occurs in the range 140-270 °C, which corresponds to 23.5% of the total weight. This loss of weight is accounted for the loss of the aquo ligand and the quinoline *N*-oxide molecule (theoretical weight loss 26.6%). The second loss occurs in the range 290-470 °C corresponding to weight loss of 52.8% of the residue from the first step (calc. 54.4%) due to loss of two benzoic acid molecules. Thermogram of the coordination polymer **3.8** reveals that it is thermally stable upto ~230 °C after which continuous degradation takes place within the range 230-455 °C due to loss of all the three ligands (experimental weight loss 65.6%; calc. 64.3%). Coordination polymer **3.9** loses weight in a multiple number of steps; weight loss in the temperature range of 70-240 °C corresponds to loss of half a 4,4'-bipyridyl-*N,N*'-dioxide molecule per formula (experimental weight loss 7.1%; calc. 7.6%). After this, weight loss of 19.3% takes place in between 245-325 °C that corresponds to loss of two benzoic acid molecules (experimental weight loss 21.1%). A third weight loss corresponding to 31.6% takes place in the temperature range 330-510 °C which is accounted for the loss of a benzoic acid and a 4,4'-bipyridyl-*N,N*'-dioxide molecules (experimental 33.8% of the residue).

3.4 Conclusion

In conclusion, we have demonstrated here the structural features of a number of coordination polymers of aromatic *N*-oxide with metal ions of relatively large ionic radius viz. Cd(II), Hg(II) and Pb(II). One dimensional through three dimensional coordination polymers are found to be formed. Formation of each of such motifs is guided by the nature of the metal ions as well as by the coordination behaviours of the

ligands. 4,4'-bipyridyl-*N,N'*-dioxide binds through the η^2-μ^2 coordination mode with both Cd(II) and Hg(II) metal ions while in case of Pb(II) coordination through either η^2-μ^2:μ^2 or η^2-μ^2:μ^1 mode is observed. Apart from the syntheses of coordination polymers with different architectures, isolation and characterization of a couple of mixed anionic coordination polymers of lead(II) formed as intermediate species are demonstrated. The linear polymer with trinuuclear block in the case of **3.2** which has breadth of around 9 Å, is a significant observation in making rod like polymeric structures. Moreover, interpenetrating structure and helical structure obtained in the case of coordination polymers **3.3** and **3.5** are of added value to the chemistry of coordination polymers as novel advanced materials.

3.5 Experimental section

Detailed synthetic methodologies for the synthesized complexes are given below. Analytical data as well as spectroscopic data are also listed along with each of the complexes. The instrumental details are given in Appendix.

Complex 3.1: $[Cd(C_6H_5COO)_2(PNO)]_n$

To a solution of benzoic acid (2 mmole, 0.242 g) in methanol (20 mL) $Cd(OAc)_2.2H_2O$ (1 mmol, 0.267 g) was added and stirred for 15 minutes. To this reaction mixture pyridine *N*-oxide (2 mmole, 0.190 g) was added with constant stirring at room temperature. The colour of the solution changes to yellow. A small amount (≈ 2 mL) of toluene was added to dissolve the precipitate that appeared after addition of pyridine *N*-Oxide. Colourless needle type crystals were collected after a week and dried in air. Yield of the pure crystalline complex was found to be >70%.

IR (KBr, cm^{-1}) : 3427 (bw), 3115 (w), 1593 (m), 1557 (s), 1473 (m), 1392 (s), 1221 (m), 728 (m).

^{1}H-NMR (DMSO-d^6, ppm): 8.2 (d, 4H, J=8 Hz), 7.9 (s, 2H, J=8 Hz), 7.4 (m, 8H).

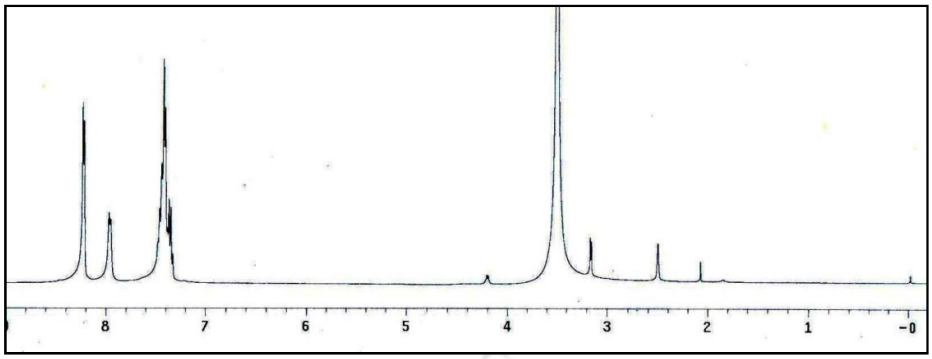

Figure 3.5.1: ^{1}H-NMR spectrum of the complex **3.1**

Complex 3.2: $[Cd_3(C_6H_5COO)_6(4,4'\text{-BPNO})_2]_n.2nH_2O$

Complex **3.2** was synthesized through a similar method as for **3.1**; only difference being the use of 4,4'-bipyridyl-*N,N'*-dioxide in place of pyridine *N*-oxide. Yield of the crystalline complex > 80%.

IR (KBr, cm^{-1}): 3403 (bm), 3431 (b), 1598 (s), 1557 (s), 1472 (m), 1400 (s), 1222 (m), 836 (m), 719 (m).

^{1}H-NMR (DMSO-d^6, ppm): 8.3 (d, 8H, J = 8 Hz), 8.0 (d, 12H, J = 8 Hz), 7.9 (d, 8H, J = 8 Hz), 7.5 (m, 18H).

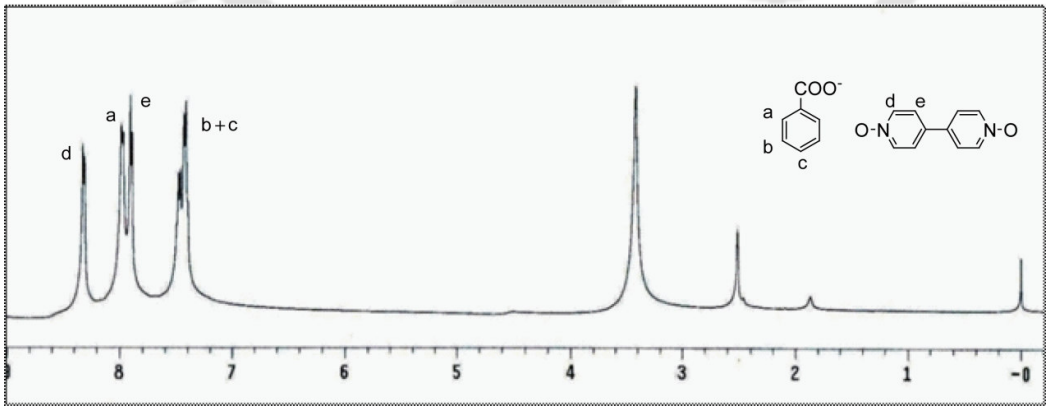

Figure 3.5.2: ^{1}H-NMR spectrum of the complex **3.2**

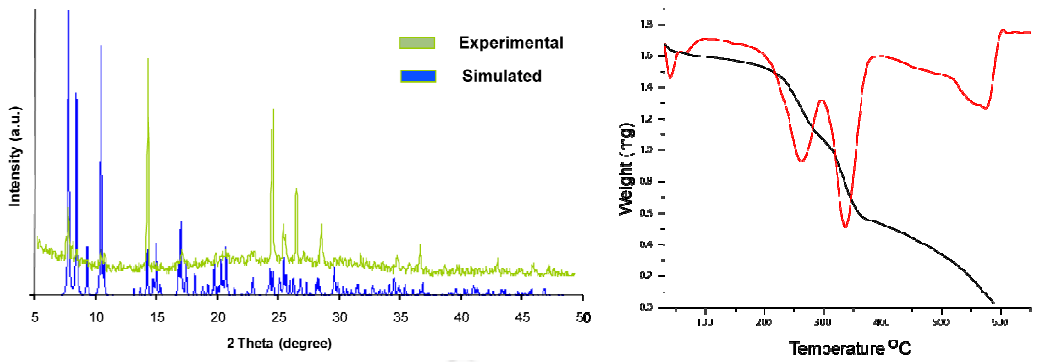

(a) (b)

Figure 3.5.3: (a) PXRD pattern and (b) TGA plot of the complex **3.2**

Complex 3.3: $[Cd(C_6H_4C_2O_4)(4,4'\text{-BPNO})(H_2O)]_n$

To a solution of terephthalic acid (0.5 mmol, 0.166 g) in dimethylformamide (15 mL) cadmium(II) acetate dihydrate (0.5 mmol, 0.133 g) was added and stirred for 20 minutes. To this reaction mixture 4,4'-bipyridyl-*N,N'*-dioxide (0.5 mmol, 0.095 g) was added and refluxed the reaction mixture for 3h at 100°C to dissolve the precipitate that appeared after addition of 4,4'-bipyridyl-*N,N'*-dioxide. Yield of the complex ~30%.

IR (KBr, cm^{-1}): 3422 (bm), 3103 (m), 1682 (s), 1574 (m), 1509 (m), 1424 (m), 1285 (s), 1225 (m), 733 (m).

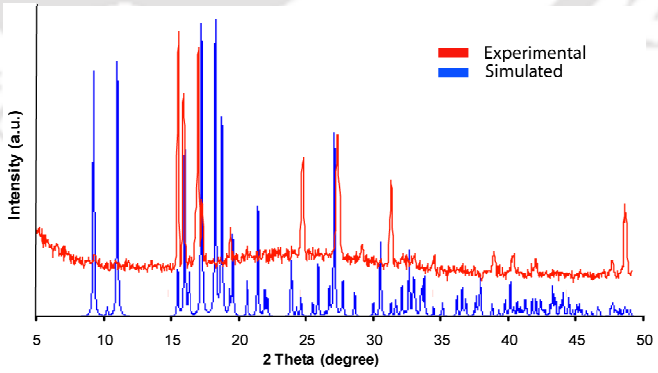

Figure 3.5.4: PXRD pattern of the complex **3.3**

Complex 3.4: [Hg(C_6H_5COO)$_2$(2,2'-BPNO)]

Complex **3.4** was prepared in a similar procedure that of **3.1** by reacting mercury(II) acetate with benzoic acid and 2,2'-bipyridyl-*N,N'*-dioxide. Yield > 60%.

IR (KBr, cm^{-1}): 3436 (b, m), 1598 (m), 1547 (s), 1465 (s), 1387 (s), 1223 (m), 737 (m).

Complex 3.5: [Hg(C_6H_5COO)$_2$(4,4'-BPNO)]$_n$

Complex **3.5** was prepared in a similar procedure that of **3.1** by reacting mercury(II) acetate with benzoic acid and 4,4'-bipyridyl-*N,N'*-dioxide. Yield > 90%.

IR (KBr, cm^{-1}): 3446 (bm), 3066 (m), 1595 (m), 1553 (s), 1470 (s), 1477 (w), 1387 (s), 1219 (m), 731 (m).

^{1}H-NMR (DMSO-d^6, ppm): 8.3 (d, 4H, J = 4 Hz), 8.0 (d, 4H, J = 8Hz), 7.9 (d, 4H, J = 4 Hz), 7.5 (m, 2H), 7.4 (m, 4H).

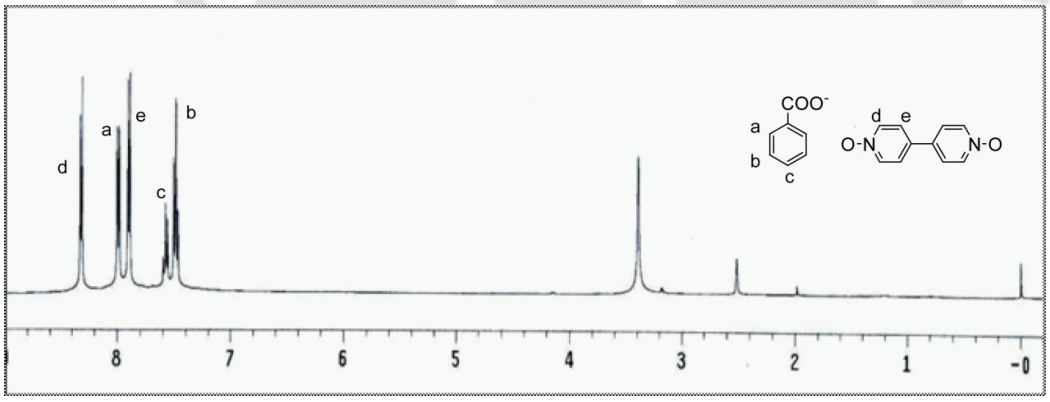

Figure 3.5.5: ^{1}H-NMR spectrum of the complex **3.5**

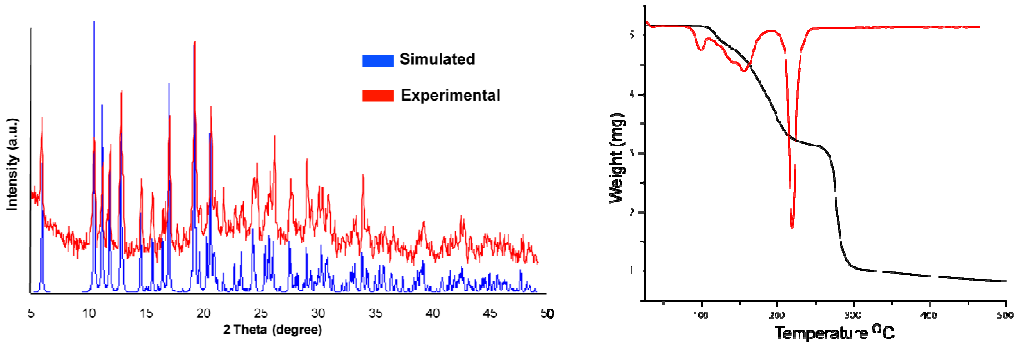

(a) (b)

Figure 3.5.6: (a) PXRD pattern and (b) TGA plot of the complex **3.5**

Complex 3.6: $[Pb_2(C_6H_5COO)_4(PNO)(H_2O)_2]_n$

To a solution of sodium benzoate (0.288 g, 2 mmol) in methanol (10 mL), $Pb(NO_3)_2$ (1 mmol, 0.331 g) was added and stirred for 30 min. To this solution, pyridine *N*-oxide (0.095 g, 1 mmol) was added at room temperature and stirred. 5 mL of toluene was added to the resulting colorless solution and then kept for crystallization. Colorless crystals of **3.6** were obtained after a week. Isolated yield, ~ 65%.

IR (KBr, cm^{-1}): 3435(b, m), 1592 (m), 1528 (m), 1469 (m), 1393 (s), 1221 (m), 714 (m).

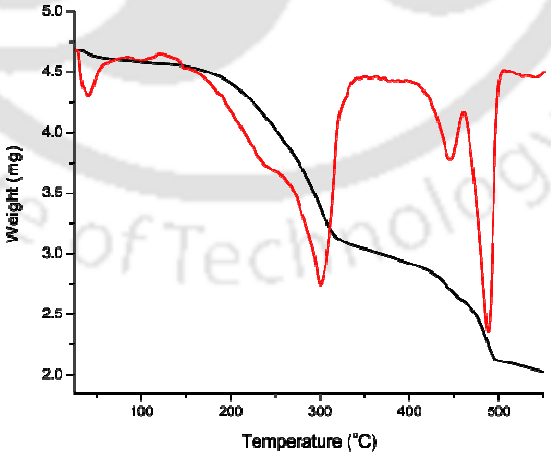

Figure 3.5.7: TGA plot of the complex **3.6**

Complex 3.7: $[Pb(C_6H_5COO)_2(QNO)(H_2O)]_n$

Complex **3.7** was synthesized through a similar method as for **3.6**; only difference being the use of quinoline *N*-oxide in place of pyridine *N*-oxide. Yield of the crystalline complex ~ 70%.

IR (KBr, cm^{-1}): 3465 (b, m), 1590 (m), 1530 (s), 1395 (s), 1223 (m), 849 (m), 713 (m).

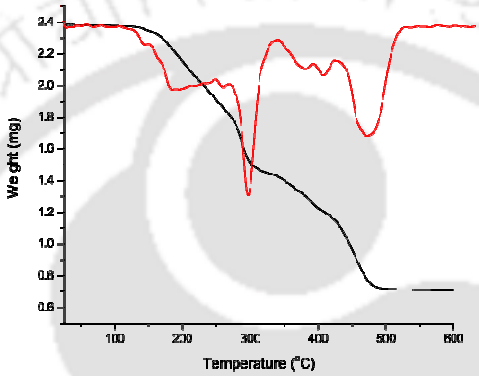

Figure 3.5.8: TGA plot of the complex **3.7**

Complex 3.8: $[Pb(C_6H_5COO)(NO_3)(2,2'\text{-}BPNO)]_n$

Complex **3.8** was synthesized through a similar method as for **3.6** using 2,2'-bipyridyl-*N,N'*-dioxide in place of pyridine *N*-oxide. Yield of the crystalline complex ~ 70%.

IR (KBr, cm^{-1}): 3435 (b, m), 1593 (s), 1537 (m), 1477 (m), 1384 (s), 1210 (m), 847 (m), 717 (m).

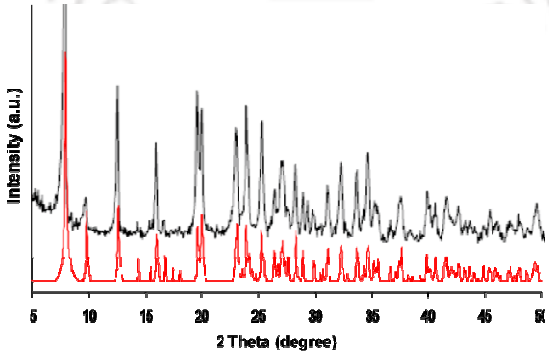

Figure 3.5.9: PXRD pattern of the complex **3.8**

Complex 3.9: $[Pb_2(C_6H_5COO)_3(4,4'\text{-BPNO})_{2.5}]_n$

To a solution of sodium benzoate (0.288 g, 2 mmol) in methanol (10 mL), $Pb(NO_3)_2$ (1 mmol, 0.331 g) was added and stirred for 30 min. To this solution, 4,4'-bipyridyl-*N,N'*-dioxide (0.095 g, 1 mmol) was added at room temperature and stirred. The resulting colorless solution and then kept for crystallization. Yellow coloured crystals of **3.9** were obtained after an hour which was dried in air. Isolated yield, ~ 35%.

IR (KBr, cm^{-1}): 3435 (b), 1599 (w), 1549 (m), 1474 (m), 1384 (s), 1221 (m), 837 (m).

^{1}H-NMR (DMSO-d^6, ppm): 8.2 (d, 10H, J = 7.2 Hz), 8.0 (d, 6H, J = 6.8 Hz), 7.7 (d, 10H, J = 7.2 Hz), 7.5 (t, 3H, J= 7.6 Hz) , 7.4 (t, 6H, J= 7.6 Hz).

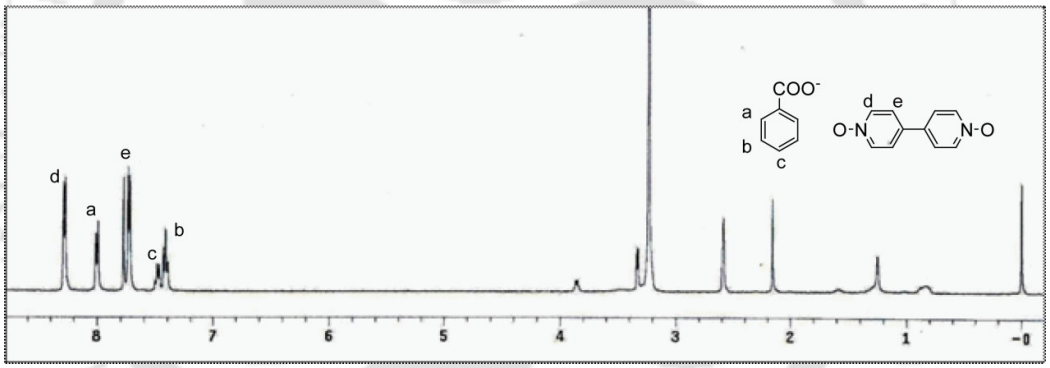

Figure 3.5.10: ^{1}H-NMR spectrum of the complex **3.9**

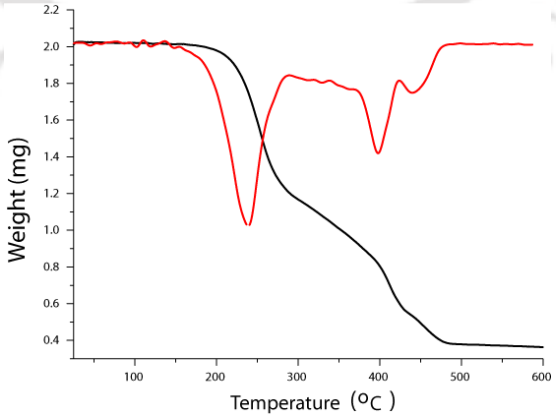

Figure 3.5.11: TGA plot of the complex **3.9**

Complex 3.10: $[Pb(4\text{-}NO_2C_6H_4COO)(NO_3)(PNO)_2]_n$

To a solution of 4-nitrobenzoic acid (2 mmol, 0.334 g) in methanol (20 mL) methanolic solution of NaOH (2 mmol, 0.080 g, 5 mL) was added. After stirring this reaction mixture for about 30 min $Pb(NO_3)_2$ (1 mmol, 0.331 g) was added and stirred for another 30 min and then pyridine *N*-oxide (1 mmol, 0.095 g) was added. A small amount of toluene was added. The clear solution was then kept for crystallization and good quality colorless crystals of **3.10** were obtained after about 12 h.

IR (KBr, cm^{-1}): 1573 (m), 1555 (m), 1470 (s), 1385 (s), 1350 (s), 1216 (m), 832 (m).

^{1}H-NMR (DMSO-d^6, ppm): 8.29 (d, 2H, J = 8.8 Hz), 8.21 (d, 2H, J = 7.2 Hz), 8.11 (d, 2H, J = 8.8 Hz), 7.41 (m, 2H,), 7.34 (t, 1H, J = 7.6 Hz).

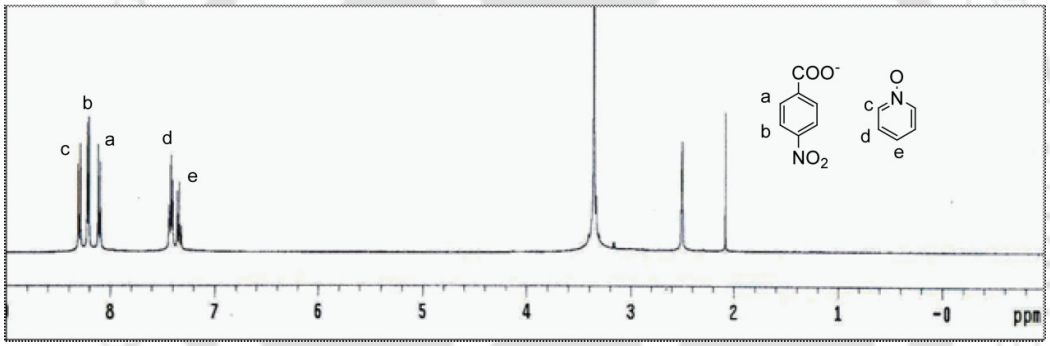

Figure 3.5.12: ^{1}H-NMR spectrum of the complex **3.10**

Complex 3.11: $[Pb(4\text{-}NO_2C_6H_4COO)_2(PNO)(H_2O)]$

The complex **3.10** was kept dissolved in the mother liquor at room temperature and from this solution crystals of **3.11** were obtained a day after.

IR (KBr, cm^{-1}): 1615 (m), 1578 (s), 1509 (m), 1384 (s), 1351 (s), 1220 (m), 831 (m).

^{1}H-NMR (DMSO-d^6, ppm): 8.22 (m, 4H), 8.09 (d, 2H, J = 8.4 Hz), 7.41 (m, 2H), 7.33 (t, 1H, J = 7.6 Hz).

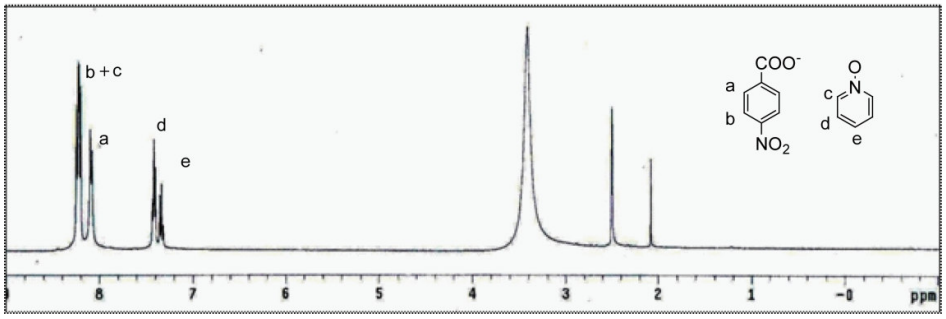

Figure 3.5.13: ^{1}H-NMR spectrum of the complex **3.11**

Complex 3.12: $[Pb(4\text{-}NO_2C_6H_4COO)_2(PNO)]_n$

Crystals of the complex **3.12** were obtained by further dissolving **3.11** in methanol and recrystallization.

IR (KBr, cm^{-1}): 1621 (m), 1583 (s), 1510 (m), 1474 (m), 1384 (s), 1350 (s), 1227 (m), 832 (m).

^{1}H-NMR (DMSO-d^6, ppm): 8.22 (m, 4H), 8.11 (d, 2H, J = 8.4 Hz), 7.41 (m, 2H), 7.33 (t, 1H, J = 7.6 Hz).

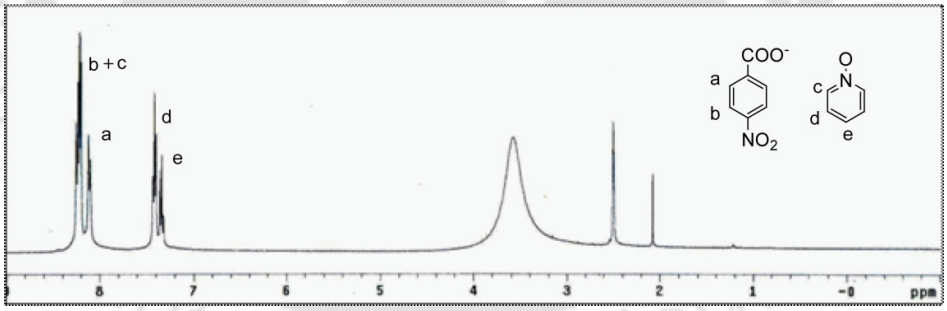

Figure 3.5.14: ^{1}H-NMR spectrum of the complex **3.12**

Complex 3.13: $[Pb_2(NO_3)(4\text{-}NO_2C_6H_4COO)_3(4,4'\text{-}BPNO)_2]_n$

For the synthesis of the complex **3.13**, 4-nitrobenzoic acid (2 mmol, 0.334 g) and sodium hydroxide (2 mmol, 0.080 g, 5 mL) was dissolved in methanol (20 mL). After stirring this reaction mixture for about 30 min lead nitrate (1 mmol, 0.331 g) and 4,4'-bipyridyl-*N,N'*-dioxide (0.188 g, 1 mmol) was added and stirred for another 30 min. Yellow colored precipitate appeared which was dissolved in DMSO. The

clear solution was then kept for crystallization and good quality colorless crystals of **3.13** were obtained after about 8h.

IR (KBr, cm^{-1}): 1619 (m), 1563 (s), 1519 (m), 1470 (m), 1384 (s), 1342 (s), 1214 (m), 833 (m).

^{1}H-NMR (DMSO-d^6, ppm): 8.31 (m, 4H), 8.10 (d, 2H, J = 8.4 Hz), 7.91 (d, 2H, J = 8.4 Hz).

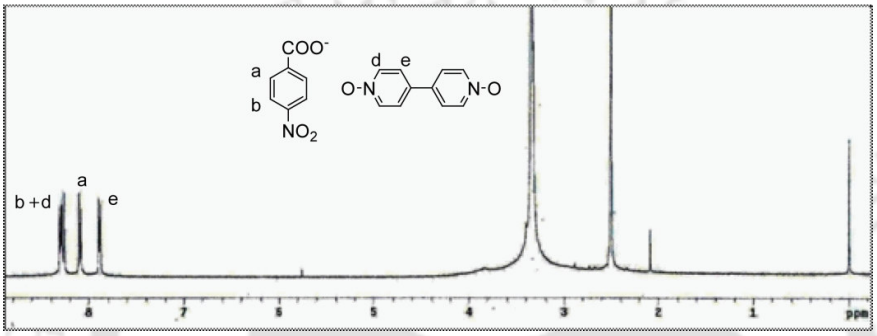

Figure 3.5.15: ^{1}H-NMR spectrum of the complex **3.13**

Complex 3.14: $[Pb(4\text{-}NO_2C_6H_4COO)_2(4,4'\text{-}BPNO)_2]_n$

The complex **3.13** was kept dissolved in the mother liquor and from this colourless crystals of **3.14** were obtained after 24 h.

IR (KBr, cm^{-1}): 1619 (m), 1580 (s), 1473 (m), 1389 (m), 1348 (s), 1231 (m), 840 (m).

^{1}H-NMR (DMSO-d^6, ppm): 8.33 (b, 4H), 8.11 (b, 2H), 7.91 (b, 2H).

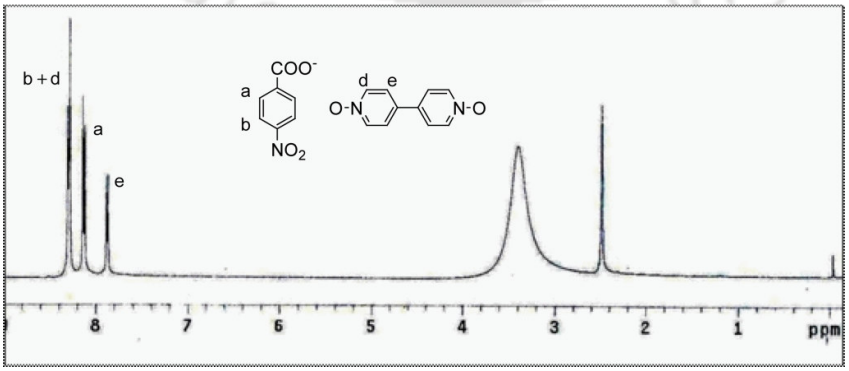

Figure 3.5.16: ^{1}H-NMR spectrum of the complex **3.14**

Chapter 4

Synthesis, characterization and structural aspects of *N*-oxide complexes of lanthanide(III)

Coordination polymers with transition metal ions are frequently studied, but less frequently with post-transition metals.[125-128] Though a few reports on coordination complexes of aromatic *N*-oxide with lanthanide were available during the early sixties, yet structural studies were scarce.[39, 40] Lanthanides can expand their coordination numbers as high as ten or twelve and are expected to lead to unusual and unprecedented structures due to such coordination flexibilities.[129-134] Coordination complexes of lanthanide(III) with seven, eight or nine coordination around the metal centers are well established.[129-138] These complexes can adopt different geometries; for example, seven coordinated complex can have either a capped octahedral geometry or a pentagonal bipyramidal geometry; on the other hand eight coordinated complex can adopt square antiprismatic, triangular dodecahedral geometry or bicapped trigonal prismatic type of structures.[139-142] Thus, coordination polymers arising from any of such geometries would have size and shape that is dependent not only on the inter-connecting units between the repeated motifs but also on the coordination environments. The report on the complex $[La(2,2'\text{-}BPNO)_4](ClO_4)_3$ by Karaghouli *et al.* was the first example of structural characterization for a lanthanide complex.[41] Recently, a few examples of lanthanide-based coordination polymers employing multidentate ligands have appeared in the literature.[143-148] The tendency of lanthanides to adopt high coordination numbers makes the *f*-block metal ions attractive for designing of coordination polymers with new and unusual network topologies.[149,150] Moreover, coordination polymers of lanthanides have enormous interest due to their important magnetic, catalytic as well as luminescent properties.[131-161] A number of reports on coordination networks of lanthanides with

aromatic *N*-oxide-based ligands have appeared.[49-51, 56, 58, 59, 152] This chapter elaborates the synthesis and characterization of a number of coordination polymers (**4.1**-**4.7**) of Ln(III) benzoate (Ln=La, Ce, Eu, Gd, Tb) with 4,4'-bipyridyl-*N,N'*-dioxide obtained from one pot multi-component reactions to understand the role of the central metal ions and stoichiometry of reactants in the reaction conditions. We have observed that, in general, varying the metal to ligand ratio, results in varying dimensionality of the coordination polymers. The afforded new crystalline products **4.1**-**4.7** were characterized by conventional spectroscopic techniques as well as by both single crystal and powder X-ray diffraction techniques. The thermogravimetric, luminescence and the magnetic properties of the complexes are studied.

4.1 Synthesis and characterisation of the lanthanide(III) *N*-oxide coordination polymers

Seven new coordination polymers (**4.1**-**4.7**) of lanthanide(III) ions with 4,4'-bipyridyl-*N,N'*-dioxide as ancillary ligand and benzoate as anionic ligand has been prepared and characterized. The structures represent the coordination polymerization of hybrid benzoate/4,4'-BPNO-Ln(III) arrays of different dimensionality. Three of them are of one-dimensional architecture and other four are three-dimensional wherein the metal nodes are bridged by atleast one or both of the organic tectones. All these coordination polymers are synthesized under solution state reaction condition and observed that in general when the metal to ligand (4,4'-BPNO) ratio is 1:0.5 one dimensional polymers are formed while a 1:1 ratio results in three dimensional coordination polymers. A schematic presentation for the synthesis of the coordination polymers of Tb(III) is depicted in scheme 4.1.1. The different complexes prepared and their IR stretching frequencies are tabulated in table 4.1.

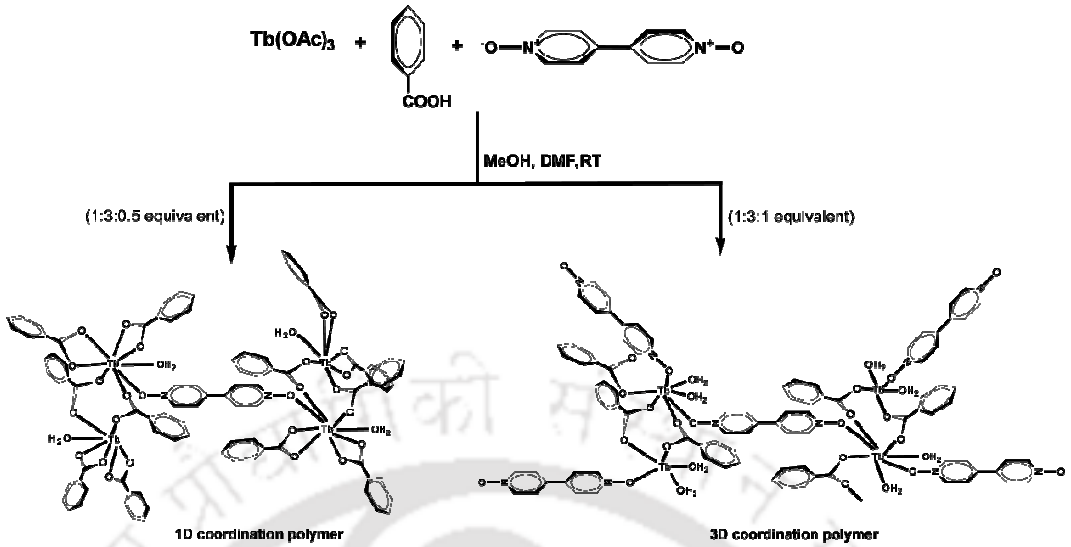

Scheme 4.1.1

Table 4.1: Different complexes prepared and their IR stretching frequencies

Complex	Composition	IR stretching (KBr, cm^{-1})
4.1	$[\{La(C_6H_5COO)_3(H_2O)_2\}.(4,4'\text{-}BPNO)_{0.5}C_6H_5COOH.DMF]_n$	3431 ($O\text{-}H_{str}$), 1542 ($\nu_{as}CO_2^-$), 1408 ($\nu_sCO_2^-$), 1276 ($N\text{-}O_{str}$)
4.2	$[\{Ce(C_6H_5COO)_3(4,4'\text{-}BPNO)(H_2O)_2\}.DMF]_n$	3430 ($O\text{-}H_{str}$), 1550 ($\nu_{as}CO_2^-$), 1402 ($\nu_sCO_2^-$), 1230 ($N\text{-}O_{str}$)
4.3	$[Tb(C_6H_5COO)_3(4,4'\text{-}BPNO)_{0.5}(H_2O)]_n$	3337 ($O\text{-}H_{str}$), 1560 ($\nu_{as}CO_2^-$), 1408 ($\nu_sCO_2^-$), 1245($N\text{-}O_{str}$),
4.4	$[\{La(C_6H_5COO)_3(4,4'\text{-}BPNO)(H_2O)_2\}.C_6H_5COOH]_n$	3437 ($O\text{-}H_{str}$), 1544 ($\nu_{as}CO_2^-$), 1408 ($\nu_sCO_2^-$), 1219 ($N\text{-}O_{str}$)
4.5	$[\{Eu(C_6H_5COO)_3(4,4'\text{-}BPNO)(H_2O)_2\}.C_6H_5COOH]_n$	3368 ($O\text{-}H_{str}$), 1548 ($\nu_{as}CO_2^-$), 1412 ($\nu_sCO_2^-$), 1218 ($N\text{-}O_{str}$)
4.6	$[\{Gd(C_6H_5COO)_3(4,4'\text{-}BPNO)(H_2O)_2\}.C_6H_5COOH]_n$	3233 ($O\text{-}H_{str}$), 1551 ($\nu_{as}CO_2^-$), 1414 ($\nu_sCO_2^-$), 1217($N\text{-}O_{str}$)
4.7	$[\{Tb(C_6H_5COO)_3(4,4'\text{-}BPNO)(H_2O)_2\}.C_6H_5COOH]_n$	3239 ($O\text{-}H_{str}$), 1552 ($\nu_{as}CO_2^-$), 1414 ($\nu_sCO_2^-$), 1216 ($N\text{-}O_{str}$)

The infrared spectra of complexes are very similar to each other ν_{as} (COO) stretching appearing around 1550 cm^{-1} and ν_s (COO) stretching around 1410 cm^{-1}. The N-O stretching appears at 1276 cm^{-1} for complex **4.1** where it is un-coordinated. In all the other complexes, the N-O stretching appears in the range 1215-1240 cm^{-1}

signifying electron donation from the aromatic *N*-oxide ligand. In addition, band at ca. 3400 cm^{-1} indicates the existence of coordinated water in the structure.

Reaction of La(III) acetate, benzoic acid and 4,4'-BPNO (1:3:0.5 equivalent) in methanol/DMF reaction mixture led to the formation of the one dimensional coordination polymer **4.1** with the composition $[\{La(C_6H_5COO)_3(H_2O)_2\}.(4,4'\text{-}BPNO)_{0.5}.\ C_6H_5COOH.DMF]_n$. It crystallizes in the triclinic space group *P-1* and the asymmetric unit contains the metal center coordinated by three benzoate ligands and two aquo ligands and the uncoordinated one each of 4,4'-BPNO, benzoic acid and DMF molecules. Thus **4.1** can also be described as a multi component molecular complex where a one dimensional coordination polymer co-crystallize with three other organic molecules. The coordination polymer **4.1** comprises of one-dimensional linear chains where the nearby La(III) centers are bridged by benzoate ligands with a La-La distance of 4.20 Å. As shown in figure 4.1.1b, each La(III) ion is nine-coordinated by seven carboxylate oxygen atoms from six benzoate ligands, and two oxygen atom from two coordinated water molecules. The La-O distances range from 2.470(1) to 2.861(1) Å and the longer La-O distances are associated with the benzoate oxygen atom O6 that acts as a μ^2-O bridge linking two La centers. The benzoate ligands connect the metal centers through two different binding modes: the $\eta^2{:}\mu^2$ mode and $\eta^2{:}\mu^3$ mode. This bridging extends the polymer along the *a* crystallographic axis. A closer look at the coordination polymer shows that it contains dinuclear La(III) cores that act as repeating units connected by O4-C8-O8 benzoate bridges. Although there are reports on nine coordinated lanthanide complexes,[143-148] complex **4.1** is important in terms of new avenue generated for encapsulating assemblies of guest molecules constructed through hydrogen bonding between benzoic acid and BPNO. The hydrogen bond interaction between the benzoic acid and BPNO makes assemblies HBen···BPNO···HBen in step like arrangement so as to have a 22.38 Å length of each unit and these units are placed in the interstices of this polymer. Identification of such assemblies is important as they may lead to isolation of intermediate species that would lead to chemical reactions in interstitial sites.[59]

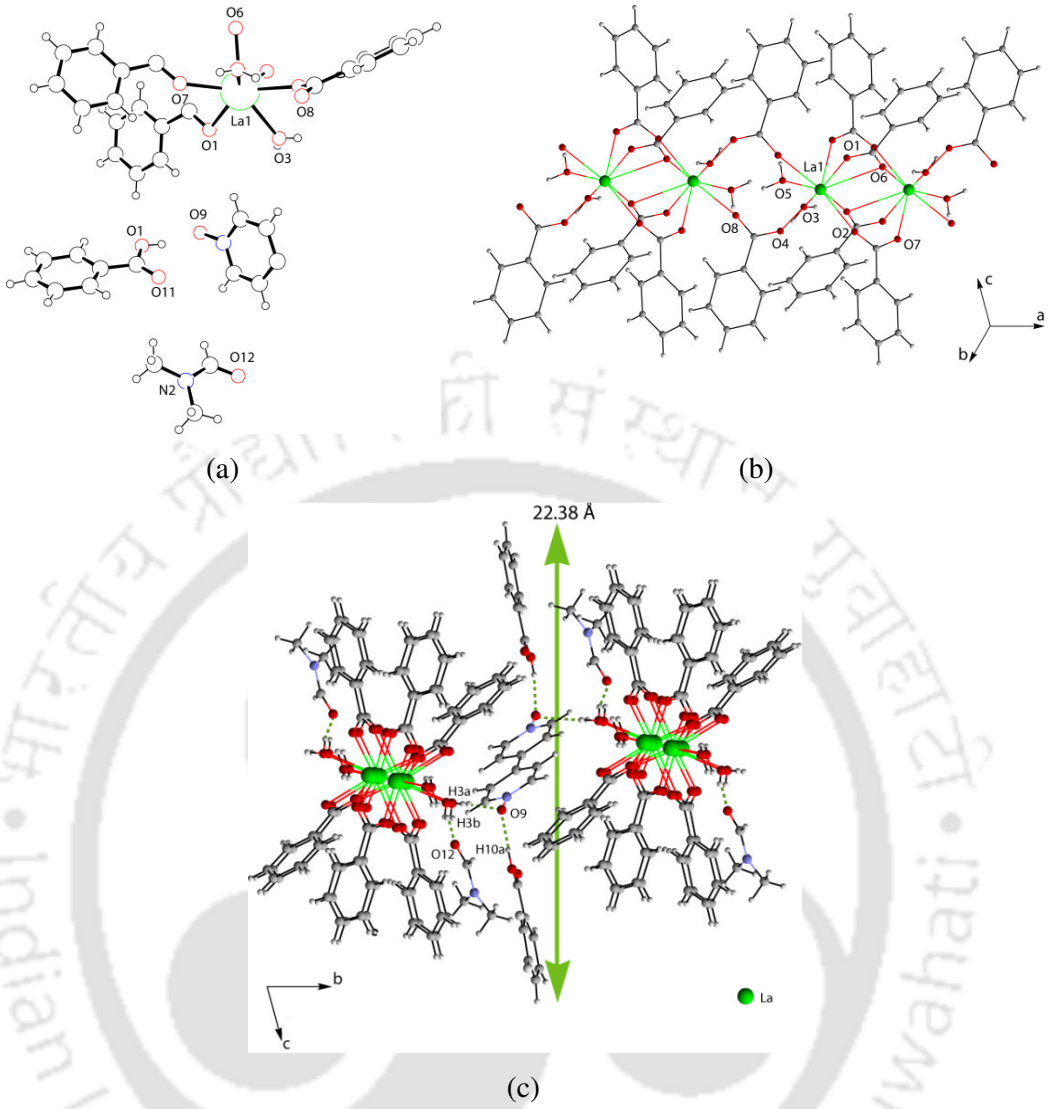

Figure 4.1.1: (a) Asymmetric unit of **4.1**, (b) one dimensional La(III)benzoate chain showing the coordination around the metal center, (c) encapsulation of HBen···BPNO···HBen units and DMF in between the 1D chains of **4.1** through weak interactions

The 4,4'-BPNO, benzoic acid and DMF molecules remains uncoordinated in the crystal lattice of **4.1** and are encapsulated between the 1D chains through weak interactions. The 4,4'-BPNO molecules are involved in O3-H3a···O9 interaction that bridges the two nearby one dimensional chains. Apart from this there exist another hydrogen bond O10-H10a···O9 between the 4,4'-BPNO molecule and the benzoic acid molecules. The DMF molecules are held in the lattice through the O3-H3b···O12 and

O5-H5a···O12 interactions with the coordinated aquo groups. These weak interactions impart the molecule two dimensional hydrogen bonded architecture (Figure 4.1.1c). The detailed hydrogen bond parameters are listed in table 4.2.

Table 4.2: Hydrogen bond parameters in the complexes **4.1** and **4.2**

D-H····A	d_{D-H}(Å)	$d_{H\cdots A}$(Å)	$d_{D\cdots A}$(Å)	< D-H····A(º)
Complex **4.1**				
O3-H3A····O9 [-x, 1-y, 1-z]	0.77	2.04	2.817(2)	175
O5-H5A···O12 [x, y-1, z]	0.80	1.96	2.75 (19)	164
O3-H3B···O12 [1-x, 1-y, 1-z]	0.79	2.18	2.935(2)	155
O5-H5B···O8	0.88	1.91	2.75(3)	156
O10-H10A···O9	0.82	1.76	2.563(2)	164
Complex **4.2**				
O4-H4A···O10 [x,1/2-y,1/2+z]	0.78	1.98	2.737(4)	163
O6-H6B····O11 [-x,1/2+y,1/2-z]	0.82	2.01	2.762(3)	152
C3-H3····O9 [-x,1-y,1-z]	0.93	2.44	3.253(4)	146

Similar reactions with of Ce(III) acetate led to the formation of a one dimensional coordination polymer **4.2** $[\{Ce(C_6H_5COO)_3(4,4'\text{-BPNO})(H_2O)_2\}.DMF]_n$ with monodentate coordination by 4,4'-BPNO ligands. The Ce1 center in **4.2** is coordinated to five carboxylate oxygen atoms of bridging benzoate groups, one oxygen atom of *N*-oxide and two water molecules (Figure 4.1.2a). The Ce centers in **4.2** are doubly bridged by the carboxylate groups of benzoate ligands to form an infinite 1-D chain (Figure 4.1.2a) with a closest Ce-Ce distance of 5.51 Å. The benzoate ligands connect the metal centers through the $\eta^2:\mu^2$ binding mode while there are a set of benzoate ligands that coordinate the metal center with *monodentate* binding mode. The bridging extends the polymer along the crystallographic *b* axis. The *N*-oxide ligand coordinates the metal centre with a monodentate binding mode which is a rare one to be observed for 4,4'-BPNO as it generally prefers a bidentate binding mode. This binding mode makes the *N*-oxo functionality susceptible towards hydrogen bond formation. Thus, the 4,4'-BPNO ligands are involved in both intra-chain and inter-chain hydrogen bond interactions with aquo groups (Table 4.2). The

inter-chain hydrogen bond interaction viz. O4-H4b···O10 interaction leads to formation of 2-D hydrogen bonded network. Apart from the hydrogen bond interactions, the aromatic rings of the *N*-oxide ligands are also involved in a very weak π-π interaction (inter centroid distance 3.8 Å). Moreover, the coordination polymer also contains hydrogen bonded DMF molecules that are held in the crystal lattice through O6-H6a···O11 interaction.

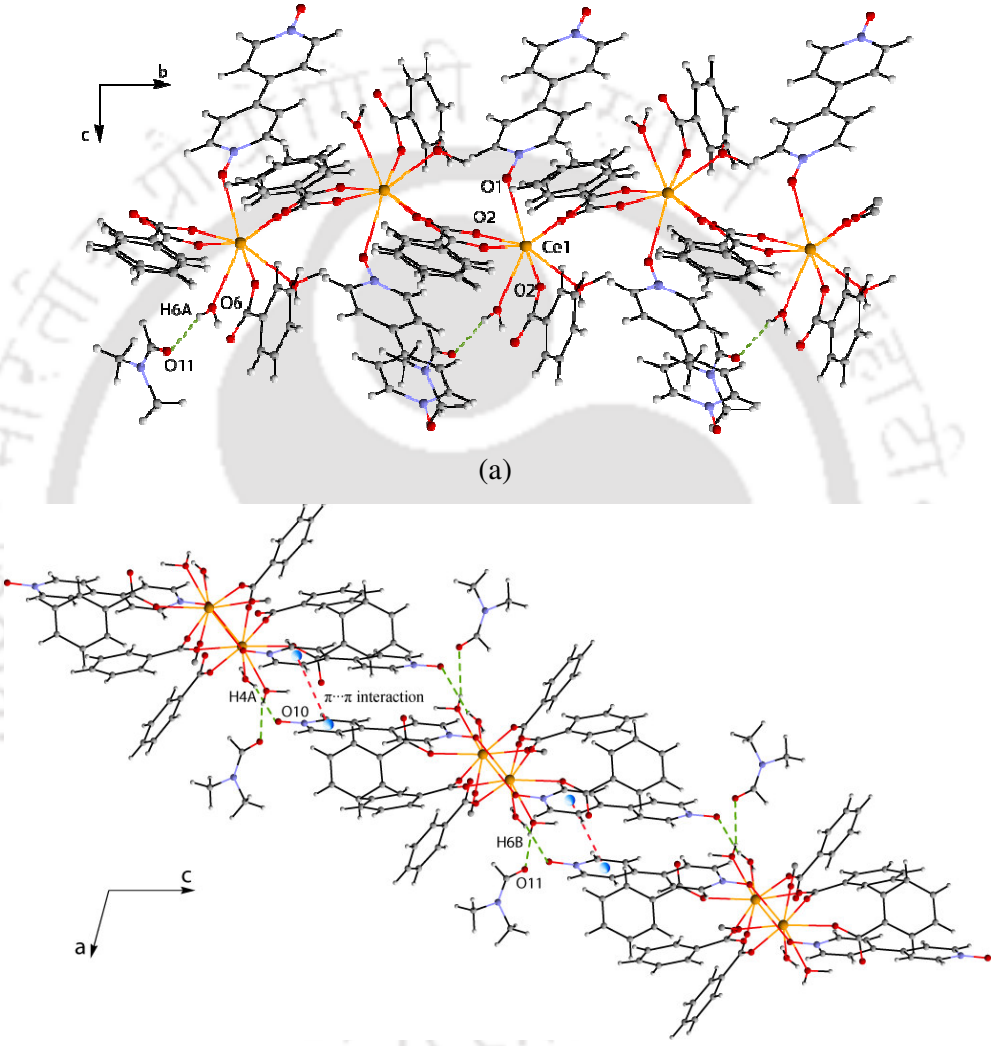

Figure 4.1.2: (a) One dimensional chain of **4.2** and (b) short range interactions in **4.2** leading to two dimensional hydrogen bonded network

Tb(III) acetate generated a zig-zag one dimensional coordination polymer $[Tb(C_6H_5COO)_3(4,4'\text{-BPNO})_{0.5}(H_2O)]_n$ (**4.3**) with 4,4'-BPNO ligands coordinating through the conventional *trans* $\eta^2{:}\mu^2$ bridging mode (Figure 4.1.3). The coordination polymer crystallizes in the monoclinic space group $P2_1/n$. Each of the Tb(III) centers

in **4.3** is coordinated by six benzoate oxygen atoms, one *N*-oxo oxygen atom and one aquo ligand. This structure is unique from the earlier two in that, here the terbium(III) benzoate forms a dinuclear core having two benzoate η^2:μ^2 bridges and four chelating benzoate coordinations between two metal centers. The metal centre adopts an eight coordinated geometry. The dinuclear core acts as repeating units and is connected to each other through the *N*-oxide spacer ligand with a distance of separation of 13.04 Å. This generates the zig-zag one dimensional coordination polymer extended along the *ab* diagonal of the unit cell. The coordination polymer is shown in figure 4.1.3. Solvent diffusion method yielded the similar one dimensional zig-zag chain coordination polymer of 4,4'-bipyridyl-*N,N'*-dioxide (4,4'-BPNO) with terbium(III) nitrate with the composition $[Tb(4,4'\text{-BPNO})(CH_3OH)(NO_3)_3]_n$.[50] The Tb-O bond lengths in **4.3** span the range 2.30-2.52 Å similar to those reported in the literature.[50, 59, 162]

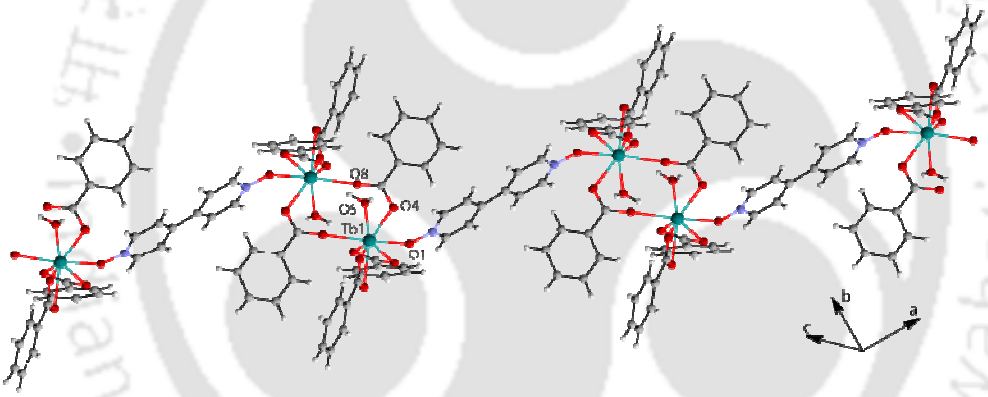

Figure 4.1.3: Zig-zag one-dimensional chain of the coordination polymer **4.3**

Reaction of La(III) acetate, benzoic acid and 4,4'-BPNO in 1:3:1equivalents in methanol/DMF reaction mixture yielded the three dimensional coordination polymer **4.4** bearing composition $[\{La(C_6H_5COO)_3(4,4'\text{-BPNO})(H_2O)_2\}.C_6H_5COOH]_n$. All the other three dimensional coordination polymers with Eu(III), **4.5**; Gd(III), **4.6** and Tb(III) **4.7** have a same general composition as **4.4** and possess similar three dimensional structure. All these coordination polymers have metal nodes with eight coordinated distorted square antiprismatic geometry (Figure 4.1.4a). As such structural details for only the complex **4.4** is outlined here as a representative example. All the La-O bonds in the complex **4** lie in the range 2.40-2.55 Å. The key feature of this structural type is the formation of a 3D honey-comb like structure that

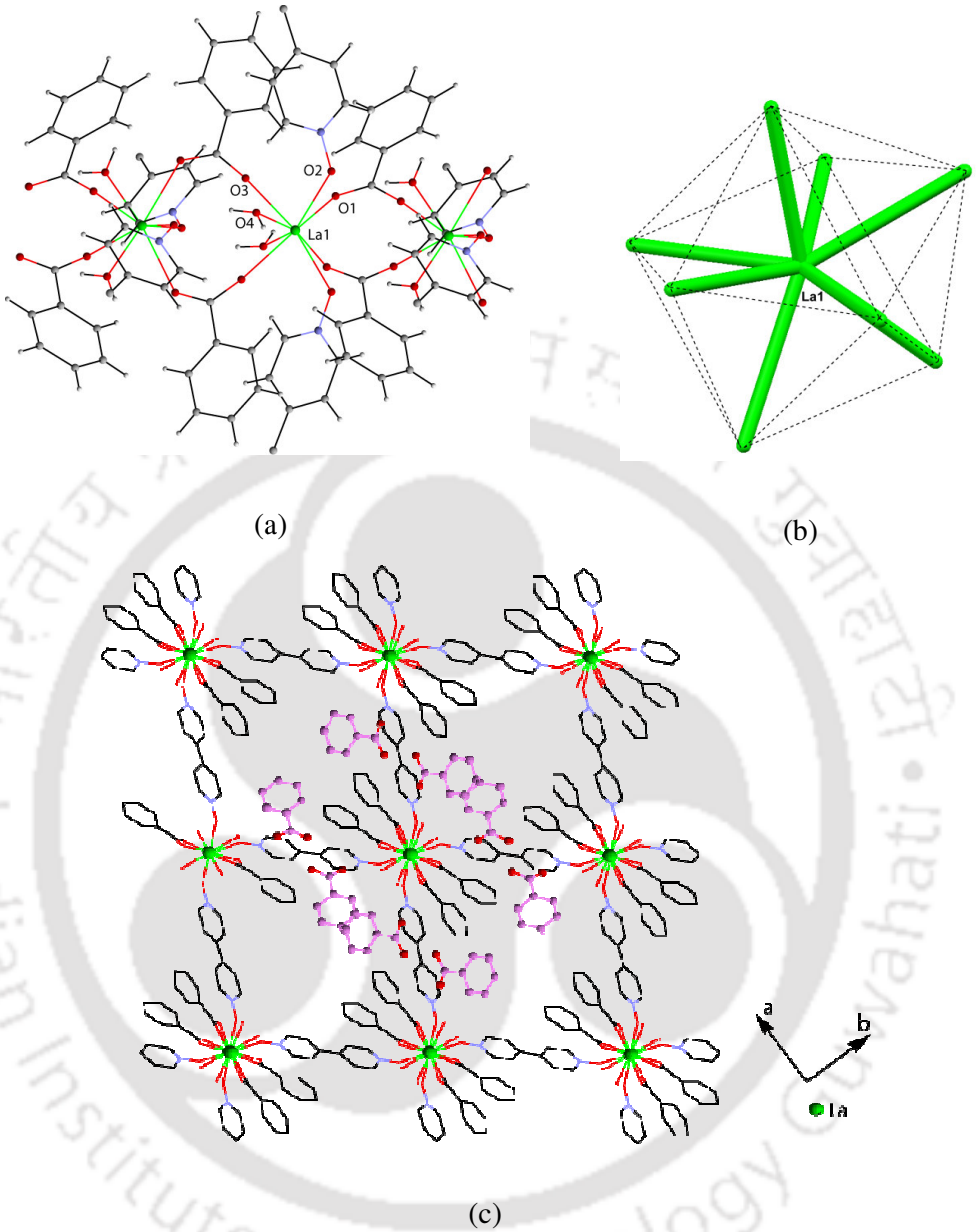

Figure 4.1.4: (a) One dimensional chain in **4.4** showing the coordination environment, (b) square antiprismatic geometry around La(III) in **4.4** and (c) 3D structure of **4.4** encapsulating benzoic acid molecules (hydrogen atoms are omitted for clarity)

encapsulates benzoic acid molecules in the interstices (Figure 4.1.4). The crystals of the coordination polymer **4.4** crystallize in the orthorhombic space group *Pnaa*. In the structure, each of the La(III) ions are coordinated by four benzoate oxygen atoms,

two *N*-oxo oxygen atoms and two aquo ligands. The benzoate ligands bridge the nearby metal centers through the $\eta^2:\mu^2$ binding mode extending the polymer along the crystallographic *a* axis. Such a bridging leads to one dimensional chains with the nearest La-La distance of 5.06 Å (Figure 4.1.4a). These one dimensional chains are then interconnected through the 4,4'-BPNO ligands that spreads the dimensionality of the complex to the three dimension. The 4,4'-BPNO ligands binds the La(III) centers through the *trans* $\eta^2:\mu^2$ bridging mode. This elongation of the structure around the dimension creates one-dimensional channels of dimension 14.1 Å x 14.1 Å that hold benzoic acid molecules in dimeric pairs. Recently such a three dimensional coordination polymer derived from 4,4'-BPNO ligands is reported that is shown to be used in separation purpose of C6-C8 aromatics.[57]PXRD analysis of the bulk samples of the coordination polymers **4.1**-**4.4** are carried out and found to match well with the simulated patterns. This depicts the pure phase of the synthesized compounds.

Thermogravimetric analysis and Luminescent Properties

Thermal stability of the complexes **4.1**-**4.3** and **4.6** is studied. Thermogram of the complexes **4.4**, **4.5** and **4.7** are expected to tally with that of **4.6** and are not recorded. Thermogravimetric analysis of the coordination polymer **4.1** shows weight loss of 4,4'-bipyridyl-*N,N*'-dioxide, DMF and benzoic acid molecules in different steps. In first step, weight loss occurs in the range 70-180 °C, which corresponds to 23.2 % of the total weight. This loss of weight is accounted for the loss of the uncoordinated DMF and benzoic acid molecules (theoretical weight loss 23.4 %). The second loss occurs in the range 225-360 °C corresponding to weight loss of 15.1% of the residue from the first step (calc. 14.8 %) due to loss of half a 4,4'-bipyridyl-*N,N*'-dioxide molecule per formula. In the third step, continuous degradation takes place due to the loss of the coordinated molecules. For the coordination polymer **4.2**, the first step within the range 45-95 °C corresponds to weight loss of 9.5 % (calc. 9.1 %) due to loss of the DMF molecule and the second step, 95-360 °C, is due to the loss of two water molecules and a 4,4'-bipyridyl-*N,N*'-dioxide molecule (experimental 31.9 % of the residue from the first step; calc. 30.8 %). Coordination polymer **4.3** also loses weight in two steps: the first step in the range 102-350 °C corresponds to weight loss of 16.8 % (calc. 7.7 %) due to loss of the two water molecules and half a 4,4'-bipyridyl-*N,N*'-dioxide per formula. Continuous degradation then takes place for the

removal of the anionic ligand. For the coordination polymer **4.6**, weight loss due to the uncoordinated benzoic acid molecule and the coordinated water molecules takes place in the range 95-185 °C corresponding to weight loss of 18.8 % (calc. 18.1 %).

The solid-state luminescence spectra of complexes **4.5** and **4.7** at room temperature are recorded. On excitation at 315 nm, complex **4.5** exhibits very strong red luminescence at 618 nm, which arises from $^5D_0 \rightarrow ^7F_2$ transition, a typical characteristic of Eu(III).[163] This is the main emission which is induced by electric dipole moment and is hypersensitive to the environment of the Eu(III). In addition, the $^5D_0 \rightarrow ^7F_1$ transition is also observed (Figure 4.1.5). The presence of the 4,4'-bipyridyl-*N,N'*-dioxide ligand exerts some more luminescent behaviour to this molecule. On irradiation at 315 nm the molecule emits at at two different wavelengths 373 nm and at 460 nm and is characteristic of the ligand. In the case of the complex **4.3** and **4.7** also, these two bands are observed. However, characteristic signals due to Tb(III) are not observed, may be due to overlap by the ligand bands.

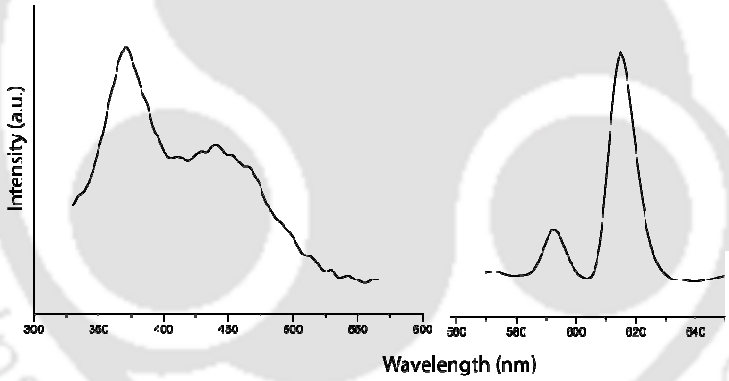

Figure 4.1.5: Solid state luminescence spectra of the complex **4.5**

Magnetic studies

Magnetic couplings between paramagnetic Ln(III) ions are notoriously hard to determine, due to orbital contributions ($L \neq 0$) which render the spin-Hamiltonian inapplicable and due to the low strength of those interactions, due to the effective shielding of the 4f electrons by the outer-shell electrons. Only in orbitally non-degenerate ($L = 0$) Gd(III) complexes, are magnetic interactions amenable to determination by magnetic susceptibility studies, since in all other cases the effect of magnetic exchange on thermal variation of the magnetic susceptibility is masked by

the effect of the thermal depopulation of the excited Stark levels upon cooling. For this reason, complex **4.6** $[\{Gd(C_6H_5COO)_3(4,4'\text{-BPNO})(H_2O)_2\}.C_6H_5COOH]_n$ was chosen for such studies, in order to obtain an estimate of the Ln(III)-Ln(III) magnetic interactions.

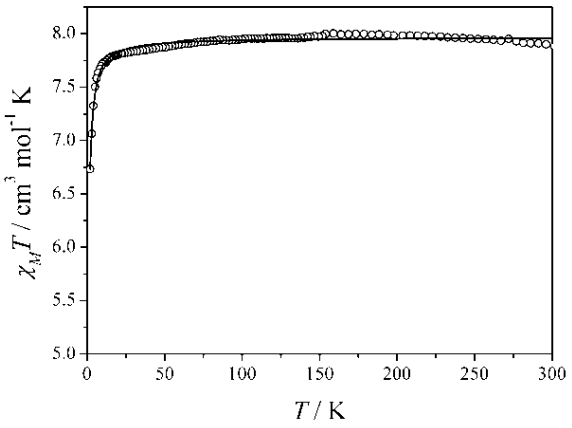

Figure 4.1.6: $\chi_M T$ vs T experimental data and calculated curve for **4.6**, according to the model described in the text.

The $\chi_M T$ value of **4.6** at 300 K is 7.88 cm^3 mol^{-1} K, typical of a $S = 7/2$ spin ($g = 2$). This remains relatively constant upon cooling, exhibiting a sharp decrease below 20 K. This was associated with the combined effects of Zeeman splitting inside the magnetic field and possible antiferromagnetic interactions. Initial attempts to account for this drop only through consideration of Zeeman splitting were unsuccessful. Consequently, magnetic exchange couplings were also included into our model, employing a mean-field correction. The corresponding Hamiltonian was $\hat{H} = g\mu_B \mathbf{H}\hat{\mathbf{S}} - 2zJ\langle S_z\rangle\hat{S}_z$, where z is the number of nearest neighbours and J is the magnetic exchange coupling constant.

Fits to this model yielded best-fit parameters zJ = -0.022 cm^{-1} and g = 2.01 with $R = 1.3\times10^{-5}$. Considering that from the crystal structure we derive $z = 2$, the exchange coupling is estimated to be -0.011 cm^{-1}. The very weak couplings between Gd(III) ions are typical of the strength of 4f-4f interactions.

AC susceptibility studies were carried out on the Tb(III) complex **4.7** to determine possible magnetic relaxation behaviour. However, no out-of-phase signals were detected over a large frequency range, thus such effects were ruled out.

4.2 Conclusion

One pot reactions of sodium benzoate and 4,4'-bipyridyl-*N,N*'-dioxide with various lanthanide(III) ions form coordination polymers whose composition is decided by the stoichiometry of the reactants. A series of lanthanide 1-D coordination polymers **4.1**-**4.3** are formed when metal to BPNO ratio used was 1:0.5 in the reaction mixture. The structures as well as the guest inclusion by these polymers prepared by deficiency of BPNO are random, rather depends on the metal ion under consideration. However, one such polymer is important in encapsulating selective one dimensional supramolecular unit in the interstices. The coordination polymer **4.1** is nine coordinated; holds hydrogen bonded units of HBen···BPNO···HBen with a length of 22.38Å. Isostructural $[\{Ln(C_6H_5COO)_3(4,4'\text{-BPNO})(H_2O)_2\}.C_6H_5COOH]_n$ where Ln = La, Eu, Gd, Tb coordination polymers prepared from similar reactions with metal to BPNO ratio 1:1 have eight coordinated distorted square antiprismatic geometry around the metal centers and able to form three dimensional channel structures having neutral benzoic acid molecules encapsulated. Complex **4.5** exhibits a strong red luminescence emission in the solid state, characteristic of Eu(III) complexes. Magnetic susceptibility of **4.6** revealed weak antiferromagnetic interactions between the Gd(III) ions.

4.3 Experimental section

Magnetic measurements

Variable-temperature dc magnetic susceptibility studies were carried out on a polycrystalline sample of **4.6** (2–300K) using a Quantum Design MPMS SQUID susceptometer under a magnetic field of 0.1 T. Ac studies were carried out on a Quantum Design PPMS system on a polycrystalline sample **4.7**. Diamagnetic corrections for the complexes were estimated from Pascal's constants. The magnetic susceptibility of **4.6** has been computed by exact calculation of the energy levels

associated with the spin Hamiltonian through diagonalization of the full matrix with a general program for axial symmetry. Least-squares fits were accomplished with an adapted version of the function-minimization program MINUIT. The error-factor *R* is defined as $R = \sum \frac{(\chi_{\exp} - \chi_{calc})^2}{N\chi_{\exp}^2}$, where *N* is the number of experimental points.

Detailed synthetic methodologies are given below. Analytical data as well as spectroscopic data are also listed along with each of the complex. The instrumental details are given in Appendix.

Complex 4.1: $[\{La(C_6H_5COO)_3(H_2O)_2\}.(4,4'\text{-BPNO})_{0.5}.C_6H_5COOH.DMF]_n$

To a solution of benzoic acid (1.5 mmol, 0.183 g) in methanol (15 mL) lanthanum(III) actetate hydrate (0.5 mmol, 0.158 g) was added and stirred for 10 minutes. To this reaction mixture 4,4'-bipyridyl-*N,N'*-dioxide hydrate (0.25 mmol, 0.047 g) was added with constant stirring at room temperature. The resulting precipitate was dissolved with addition of water (5 mL). 3mL DMF was added and the mixture was stirred for another 30 minutes. The solution was kept standing at room temperature. Block-shaped colorless crystals appeared after 7 days and dried in air. Yield of the pure crystalline complex was found to be ~70% (based on La).

IR (KBr, cm^{-1}): 3431 (bs), 1660 (s), 1625 (m), 1592 (m), 1542 (s), 1522 (m), 1477 (w), 1408 (s), 1276 (m), 1219 (m), 1184 (m), 843 (m), 722 (s), 712 (s).

Elemental analysis for $C_{36}H_{36}LaN_2O_{12}$: calculated (%) C, 52.88; H, 4.38; N, 3.38; found (%) C, 52.41; H, 4.47; N, 3.27.

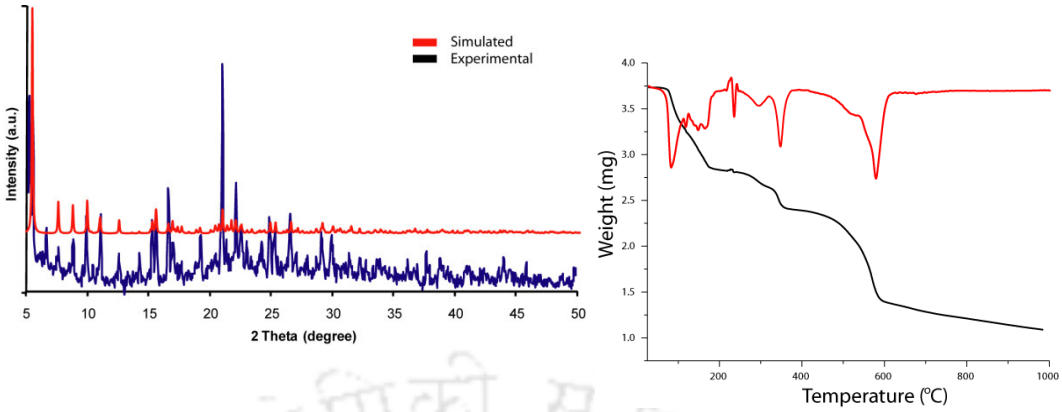

(a) (b)

Figure 4.3.1: (a) PXRD pattern of the complex **4.1** and (b) TGA plot of the complex **4.1**

Complex 4.2: $[\{Ce(C_6H_5COO)_3(4,4'\text{-BPNO})(H_2O)_2\}.DMF]_n$

To a solution of sodium benzoate (1.5 mmol, 0.216 g) in methanol (15 mL) cerium(III) nitrate hexahydrate (0.5 mmol, 0.217 g) was added and stirred for 10 minutes. The resulting precipitate was dissolved with addition of DMF (3 mL) and water (5 mL). Then, a solution of 4,4'-bipyridyl-*N,N'*-dioxide hydrate (0.5 mmol, 0.094 g) in methanol (5 mL) was added to the above mixture with continuous stirring for about 30 minutes. The resultant solution was filtered and left to stand at room temperature. Yellow needle shaped crystals suitable for X-ray analysis were produced by slow evaporation of the solvent for 5 days. Yield of the pure crystalline complex was found to be ~70% (based on Ce).

IR (KBr, cm^{-1}): 3430 (bs), 1661 (s), 1594 (s), 1550 (s), 1473 (m), 1402 (s), 1259 (w), 1230 (s), 1181 (m), 1100 (w), 1068 (w), 1025 (w), 838 (s), 718 (s), 670 (m).

Elemental analysis for $C_{34}H_{34}CeN_3O_{11}$: calculated (%) C, 50.99; H, 4.27; N, 5.25; found (%) C, 50.45; H, 4.21; N, 5.27.

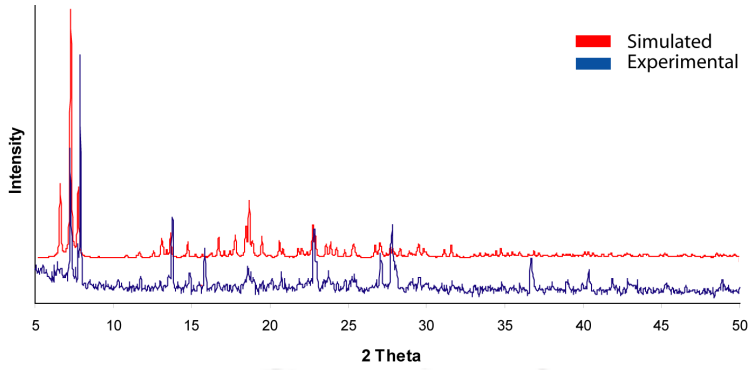

Figure 4.3.2: PXRD pattern of the complex **4.2**

Complex 4.3: $[Tb(C_6H_5COO)_3(4,4'\text{-}BPNO)_{0.5}(H_2O)]_n$

Complex **4.3** was synthesized in a similar procedure with Complex **4.1** except the use of terbium(III) acetate hydrate as the metal source. Pure block crystals suitable for X-ray analysis were collected after 6 days and dried in air. Yield of the pure crystalline complex was found to be ~75% (based on Tb).

IR (KBr, cm^{-1}): 3337 (bw), 1604 (s), 1560 (s), 1522 (s), 1492 (w), 1482 (m), 1427 (s), 1408 (s), 1245 (s), 1190 (w), 1069 (w), 1023 (w), 847 (s), 720 (s), 691 (m), 683 (m).

Elemental analysis for $C_{26}H_{21}NO_8Tb$: calculated (%) C, 49.22; H, 3.33; N, 2.20; found (%) C, 49.44; H, 3.62; N, 2.27.

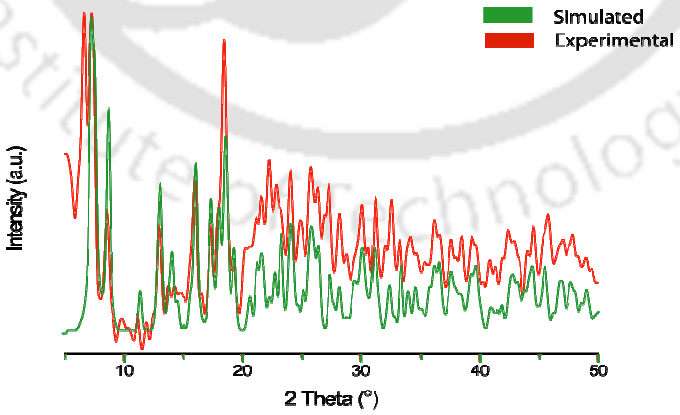

Figure 4.3.3: PXRD pattern of the complex **4.3**

Complex 4.4: $[\{La(C_6H_5COO)_3(4,4'\text{-BPNO})(H_2O)_2\}.C_6H_5COOH]_n$

The same synthetic procedure as that for complex **4.1** was used except that here the metal/BPNO ratio was 1:1. Diffraction quality crystals were collected after 4 days and dried in air. Yield of the pure crystalline complex was found to be ~65% (based on La).

IR (KBr, cm^{-1}): 3437 (bs), 1590 (m), 1544 (s), 1476 (s), 1408 (s), 1219 (s), 1185 (m), 1071 (w), 835 (s), 724 (s), 552 (m).

Elemental analysis for $C_{38}H_{33}LaN_2O_{12}$: calculated (%) C, 53.78; H, 3.92; N, 3.30; found (%) C, 53.81; H, 3.95; N, 3.27.

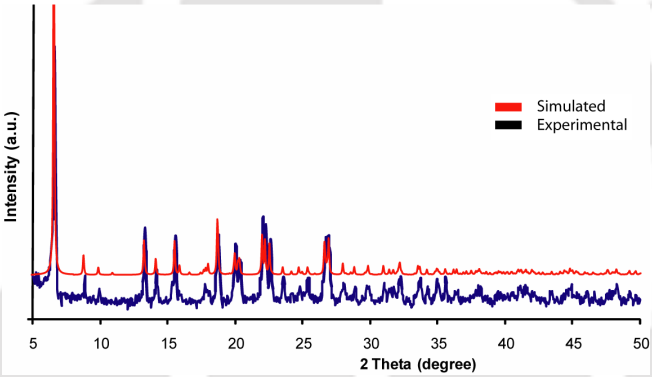

Figure 4.3.4: PXRD pattern of the complex **4.4**

Complex 4.5: $[\{Eu(C_6H_5COO)_3(4,4'\text{-BPNO})(H_2O)_2\}.C_6H_5COOH]_n$

Complex **4.5** was synthesized in a similar procedure with complex **4.4** but using europium (III) actetate hydrate as the metal source. Diffraction quality crystals were collected after 7 days and dried in air. Yield of the pure crystalline complex was found to be ~70% (based on Eu).

IR (KBr, cm^{-1}): 3368 (bm), 1591 (s), 1548 (s), 1475 (s), 1412 (s), 1321 (w), 1241 (s), 1218 (s), 1185 (m), 1071 (w), 1025 (w), 841 (s), 723 (s) 552 (w).

Complex 4.6: $[\{Gd(C_6H_5COO)_3(4,4'\text{-BPNO})(H_2O)_2\}.C_6H_5COOH]_n$

Complex **4.6** was synthesized with the same procedure that for complex **4.4** except that here gadolinium (III) actetate hydrate is used as the metal source. Diffraction quality crystals were collected after 5 days and dried in air. Yield of the pure crystalline complex was found to be ~85% (based on Gd).

IR (KBr, cm^{-1}): 3233 (bs), 1700 (bm), 1591 (s), 1551 (s), 1476 (m), 1414 (s), 1217 (s), 1184 (m), 1072 (w), 839 (m), 835 (m), 724 (s).

Complex 4.7: $[\{Tb(C_6H_5COO)_3(4,4'\text{-BPNO})(H_2O)_2\}.C_6H_5COOH]_n$

The same synthetic procedure as that for complex **4.3** was used except that here the metal/BPNO ratio was 1:1. Pure block crystals suitable for X-ray analysis were collected after 6 days and dried in air. Yield of the pure crystalline complex was found to be ~75% (based on Tb).

IR (KBr, cm^{-1}): 3239 (bs), 1699 (bm), 1591 (s), 1552 (s), 1476 (m), 1414 (s), 1216 (s), 1184 (m), 1072 (w), 835 (m), 724 (s), 658 (w).

Chapter 5

Supramolecular aspects of multi-component molecular complexes containing aromatic *N*-oxides: syntheses and characterizations

Formation of molecular complexes is governed by hydrogen bonds and other allied interactions.[164-168] Aromatic *N*-oxides are known to form molecular complexes and a few such co-crystals are reported to be of medicinal importance.[65, 169-173] The presence of the oxygen atom on aromatic *N*-oxides having partially negative charge makes them suitable hydrogen bond acceptor with a number of possible hydrogen bonding modes as shown in scheme 5.1.

Scheme 5.1

Information gathered from structural studies of such a particular class of compounds helps in establishing new interactions. Moreover, such multi-component molecular crystals are expected to throw light on the nucleation process during formation of metallo-organic hybrid complexes as well as on the role of intermolecular hydrogen bonding interactions in the synthesis of co-ordination polymers.[62, 63] With this objective we have studied formation of multi-component molecular complex between hexa aquo metal ions, aromatic *N*-oxides and aromatic carboxylate ions. This chapter describes the synthesis, characterization and supramolecular aspects of a number of such multi component molecular complexes.

5.1 Synthesis and characterisation of molecular complexes of pyridine *N*-oxide

In chapter 2 we have seen that the reaction between 4-nitrobenzoic acid, pyridine *N*-oxide and manganese(II) acetate tetrahydrate in methanol leads to the formation of one dimensional coordination polymer with μ^2 bridging pyridine *N*-oxide. The same reaction when carried out in aqueous methanol results in the formation of the molecular complex of pyridine *N*-oxide co-crystallizing with hexa aquo manganese(II) and 4-nitrobenzoate ions (Scheme 5.1.1). A similar reaction is observed with zinc(II) acetate dihydrate too. This reaction is highly substrate dependent and we could get such multi-component molecular complexes only from 4-nitrobenzoic acid out of several aromatic acids such as benzoic acid, methylbenzoic acids (all three isomers), 2-nitrobenzoic acid etc. The reaction procedure for preparation of molecular complexes is very simple and these complexes can be prepared by mixing the three reactants in aqueous methanol and stirring at room temperature for about 48 hours. The yield of the reaction is near quantitative.

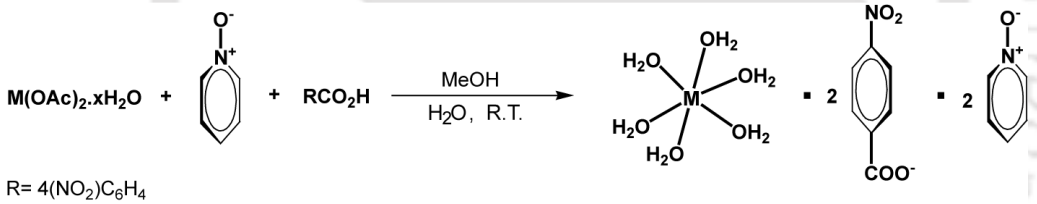

Scheme 5.1.1

The molecular complexes formed from the reaction between 4-nitrobenzoic acid, pyridine *N*-oxide and manganese(II) acetate tetrahydrate or zinc(II) acetate dihydrate have the composition $[\{Mn(H_2O)_6\}.(4\text{-}NO_2C_6H_4COO)_2.(PNO)_2]$ (**5.1**) and $[\{Zn(H_2O)_6\}.(4\text{-}NO_2C_6H_4COO)_2.(PNO)_2]$ (**5.2**) respectively. These complexes are isostructural and crystallizes in the monoclinic space group *P2(1)/c*. The structures of **5.1** and **5.2** are shown in figure 5.1.1a and 5.1.1b respectively.

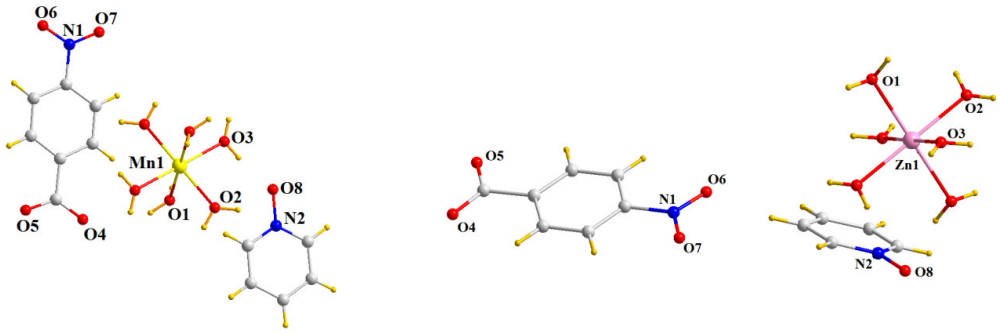

(a) (b)

Figure 5.1.1: Crystal structures of the molecular complexes (a) **5.1** and (b) **5.2**

As a representative example, let us consider the molecular complex **5.1**. The manganese(II) centres in **5.1** adopt a near octahedral geometry with all the Mn-O_{aquo} bond distances spanning the 2.15-2.19 Å range. The 4-nitrobenzoate as well as the pyridine *N*-oxide molecules remain hydrogen bonded to this hexa aquo manganese(II) core. The molecular complex is stabilized by extensive short range interactions existing between the aqua, *N*-oxo and the carboxylato groups. Pyridine *N*-oxide molecules are held in the lattice through the unconventional tri-furcated O-H···O interactions viz. O3-H3a···O8, O1-H1a···O8 and O1-H1···O8 interactions (Figure 5.1.2). The 4-nitrobenzoate groups are hydrogen bonded to the hexa aquo manganese(II) core through O2-H2a···O5 and O3-H3b···O4 interactions. These interactions impart the molecular complex an infinite two dimensional hydrogen bonded architecture. The details of the short range interactions in **5.1** are tabulated in table 5.1. Similar packing patterns are observed in the molecular complex **5.2**.

Table 5.1: H-bond parameters in the complex **5.1**

D-H····A	$d_{D\text{-}H}$(Å)	$d_{H\cdots A}$(Å)	$d_{D\cdots A}$(Å)	< D-H····A(°)
Complex **5.1**				
O(1)--H(1A)···O(8) [-x+1,y+1/2,-z+3/2]	0.820	1.926	2.720	162
O(2)--H(2A)···O(6) [-x+1, -y+2, -z+1]	0.820	1.815	2.624	168
O(3)--H(3A)···O(8)	0.820	2.073	2.856	159
O(2)--H(2B)···O(7) [-x+1, -y+1, -z+1]	0.804	2.000	2.798	172
O(3)--H(3B)···O(7) [x, y-1, z+1]	0.666	2.025	2.679	167
O(1)--H(1B)···O(8) [x, y+1, z]	0.831	1.895	2.714	168

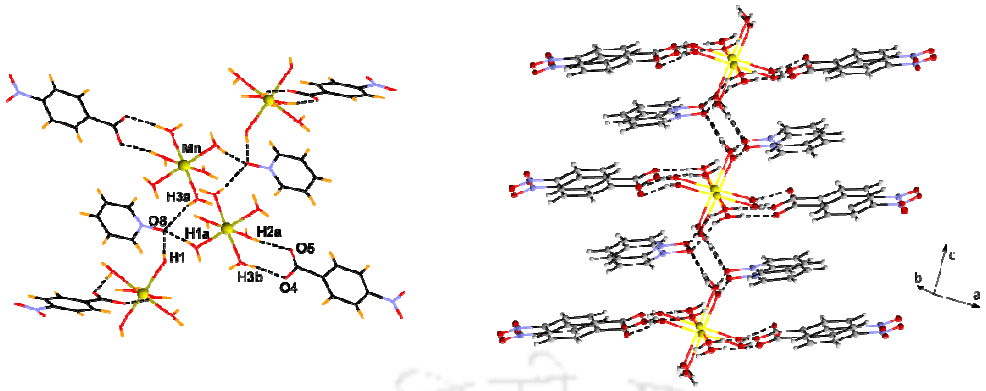

(a) (b)

Figure 5.1.2: (a) Hydrogen bond interactions in the molecular complex **5.1** and (b) Hydrogen bonded 2D architecture of **5.1**

Comparison of the solid state FT-IR spectra (Figure 5.1.3) of the molecular complex **5.1** and the corresponding coordination polymer **2.2** portrays significant differences in the stretching frequencies of the *N*-oxo groups in the two species. In the FT-IR spectrum of the **5.1** the broad band around 3350 cm^{-1} is well characteristic of the aquo groups present therein. Also it is spreading over the region 3350-2450 cm^{-1} signifying the involvement of aquo groups in strong hydrogen bonding interactions. As expected, no such band was observed in the coordination polymer **2.2**. The *N*-oxo stretching frequency of pyridine *N*-oxide appears at 1215 cm^{-1} in the molecular complex **5.1** whereas in the coordination polymer **2.2** it appears at 1207 cm^{-1}. The difference in the stretching frequencies arises as the pyridine *N*-oxide in the molecular complex **5.1** is not coordinating to the metal whereas it is coordinated to the metal with a μ^2 bridging mode in the coordination polymer **2.2**. The thermogravimetric study shows that the complexes **5.1** and **5.2** undergo dehydration in the temperature range of 50-110 ºC and lose weight corresponding to six water molecules.

However, the co-ordination polymers on dissolution in aqueous methanol and leaving for ~48 hours do not result in the corresponding molecular complexes. Thus, the compound **5.1** is not formed by ligand exchange in the co-ordination polymer **2.2**. However, it may be formed by ligand exchange in low nuclearity complex that are

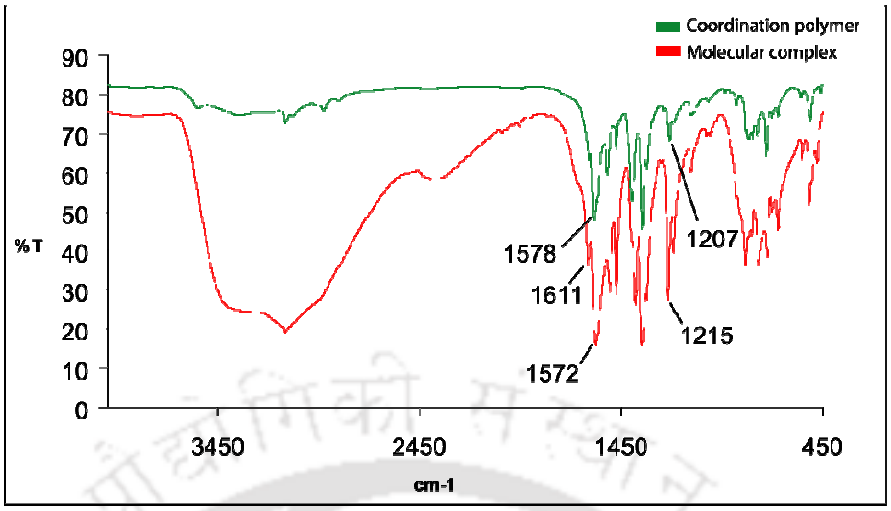

Figure 5.1.3: Solid state FT-IR spectra of the molecular complex **5.1** and the corresponding coordination polymer **2.2**

generally formed on reaction of manganese(II) or zinc(II) acetate with various aromatic acids. Further evidence to the ligand exchange reaction of low nuclearity complexes comes from the reaction of zinc(II) acetate dihydrate with 4-nitrobenzoic acid and pyridine *N*-oxide. This reaction when carried out initially for two hours and the solvent was evaporated, an intermediate mono-nuclear complex **5.3** could be isolated (Scheme 5.1.2). The mono-nuclear complex formed (**5.3**) is found to be di-aquo di-4-nitrobenzoato di-pyridine-*N*-oxide zinc(II) monohydrate. This complex has hexa coordinated geometry around the metal centre with two monodentate carboxylate groups, two *N*-oxide ligands and two aquo ligands. Each identical pair of ligands is in *trans* disposition to each other. The complex has a two dimensional infinite chain like structure growing through O-H··O interaction between aqua ligands and the water molecules of crystallization along the *b* and *c* crystallographic axes. The complex on re-dissolution in aqueous methanol and stirring for further two days gives molecular complex **5.2**. This suggests that there is a competition between water molecules to replace the *N*-oxide ligands and also the carboxylate ligands. In course of time these ligands come out of the coordination sphere facilitating formation of a neutral molecular complex **5.2**. Furthermore the short-range interactions between the *N*-oxide and 4-nitrobenzoate keep them apart as non-coordinating species.

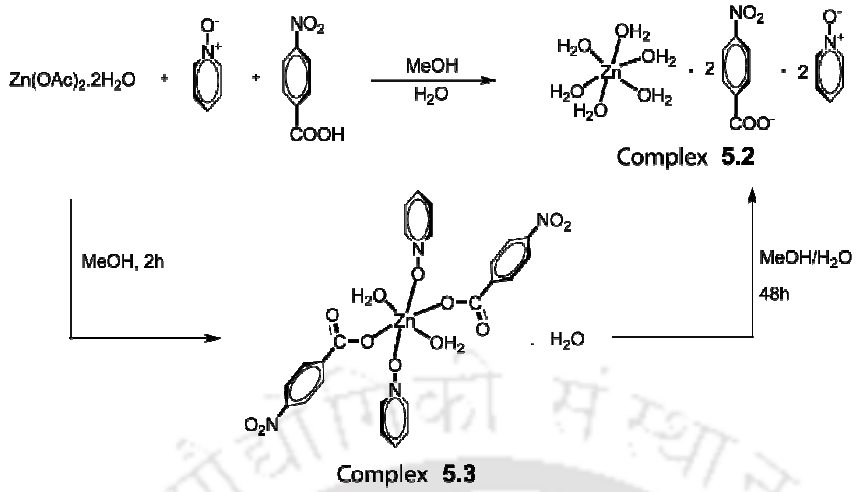

Scheme 5.1.2

5.2 Synthesis and characterisation of molecular complexes of quinoline *N*-oxide

The reaction between 4-nitrobenzoic acid, quinoline *N*-oxide and manganese(II) acetate tetrahydrate in aqueous methanol results in the formation of the molecular complex of quinoline *N*-oxide co-crystallizing with hexa aquo manganese(II) ion, 4-nitrobenzoate ion and water molecules of crystallization (Scheme 5.2.1).

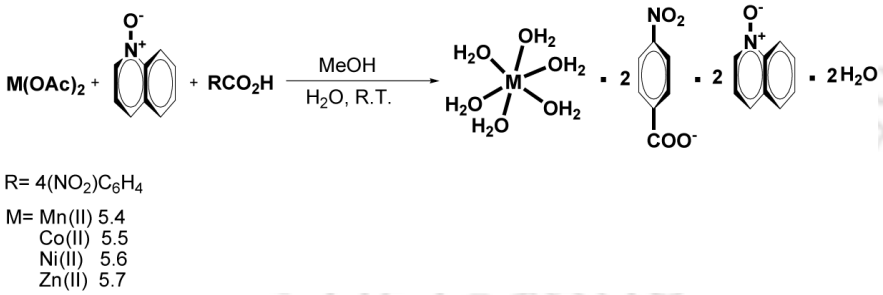

Scheme 5.2.1

As in the case with manganese(II), the reaction results in the formation of isostructural molecular complexes with each of cobalt(II), nickel(II) and zinc(II) and have a general composition of $[\{M(H_2O)_6\}.(4\text{-}NO_2C_6H_4COO)_2.(QNO)_2.2H_2O]$ (where, M=Mn(II), **5.4**; Co(II), **5.5**; Ni(II), **5.6**; Zn(II), **5.7** and QNO is quinoline *N*-

oxide). The molecular complexes crystallize in the triclinic space group *P-1* and have a similar packing pattern to each other. The hydrogen bonded assembly of the

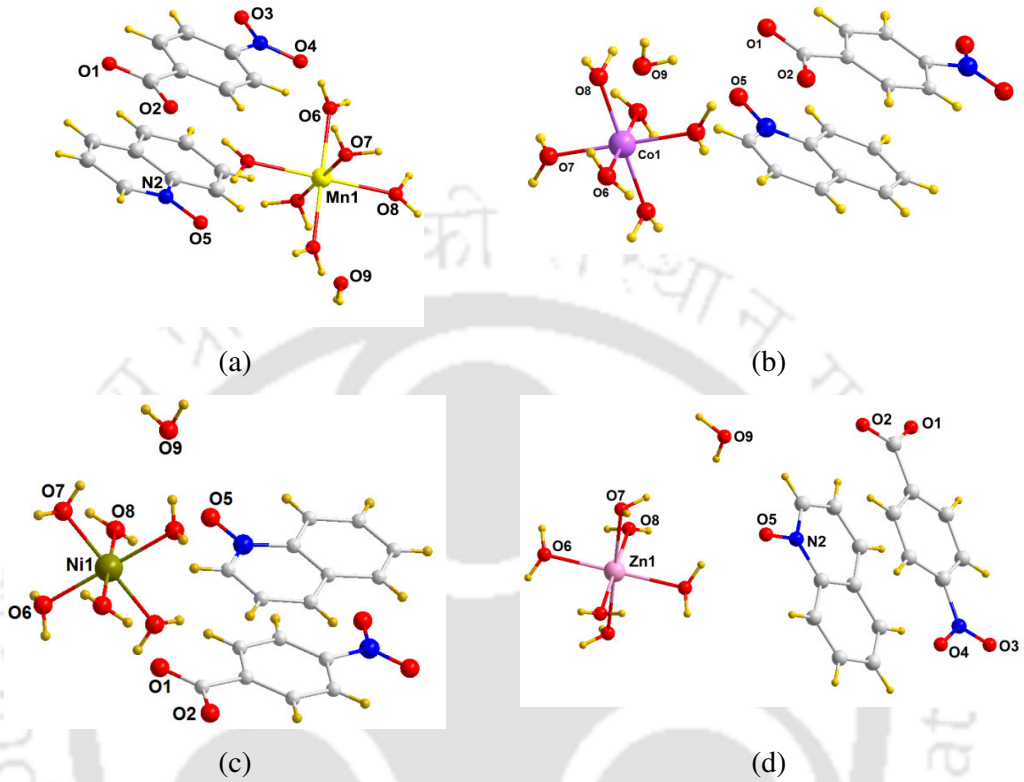

Figure 5.2.1: Crystal structures of the molecular complexes (a) **5.4**, (b) **5.5,** (c) **5.6** and (d) **5.7**

molecular complex **5.7** (as an illustrative example) is shown in figure 5.2.2. The zinc(II) centres in **5.7** adopt a near octahedral geometry with all the coordination sites occupied by aquo ligands. The Zn-O_{aquo} bond distances lie in the range 2.07-2.12 Å. The 4-nitrobenzoate and quinoline *N*-oxide molecule remain hydrogen bonded to the hexa aquo zinc(II) core through O8–H8A····O5, O8–H8B····O2, O7–H7A····O1, interactions. The water molecule of crystallization is hydrogen bonded to the hexa aquo zinc(II) core through the O6–H6B····O9 interaction and is connected to the quinoline *N*-oxide molecule through O9–H9B····O5 hydrogen bond. The details of these interactions are given in table 5.2. The aromatic rings of the carboxylic acid and the quinoline *N*-oxide are parallelly stacked and held together by strong π-stacking

interactions (interlayer separation ~3.4 Å). These short range interactions make the molecular complexes stable enough and prevent the formation of the coordination polymer through bridging *N*-oxide.

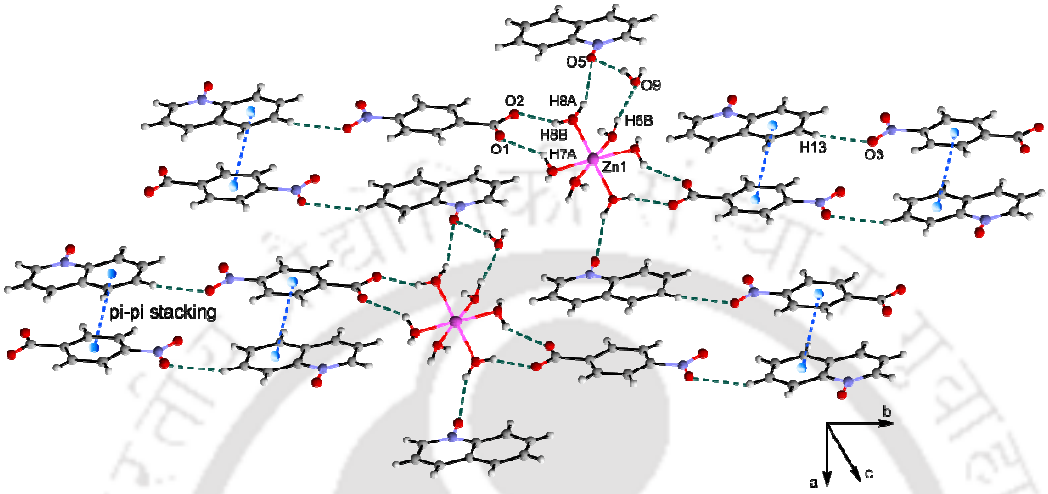

Figure 5.2.2: Short range interactions in the molecular complex **5.7** generating hydrogen bonded assembly

The thermogram of the complex **5.7** shows that it is thermally stable up to ~60 ^{o}C. The first weight loss occurs in the range 60-110 °C, which corresponds to 16.5% of the total weight. This loss of weight is accounted for the loss of the seven water molecules (theoretical weight loss 15.1%). The second loss occurs in the range 185-400 °C corresponding to weight loss of 53.9% of the residue (calc. 55.4%) due to loss of two quinoline *N*-oxide molecules.

5.3 Synthesis and characterisation of molecular complex of 4,4'-bipyridyl-*N,N*'-dioxide

Another interesting result is observed with 4,4'-bipyridyl-*N,N*'-dioxide. The reaction of benzoic acid, manganese(II) acetate and 4,4'-bipyridyl-*N,N*'-dioxide in methanol (MeOH) leads to the formation of the coordination polymer with the composition $[\{Mn_3(C_6H_5COO)_6(4,4'\text{-}BPNO)_2(MeOH)_2\}.(MeOH)_2]$ (**2.5**). However the same reaction when carried out in aqueous methanol leads to the formation of the

molecular complex **5.8** with the composition [{$Mn(H_2O)_6$}.$(C_6H_5COO)_2$.(4,4'-BPNO)$_4$] as shown in scheme 5.3.1.

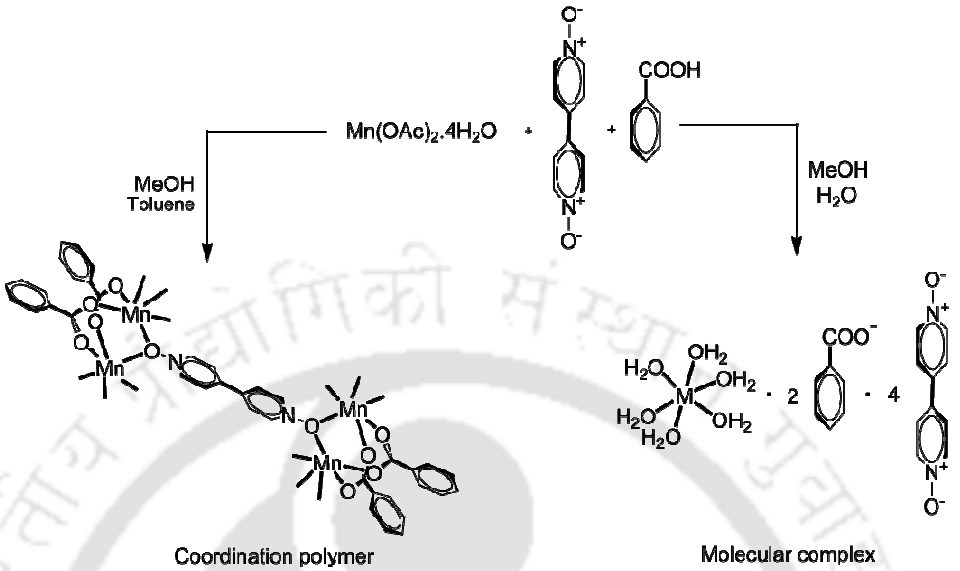

Scheme 5.3.1

As described in chapter 2 the N-O stretching of the *N*-oxide of the the coordination polymer **2.5** appears at 1219 cm^{-1}. The asymmetric and symmetric stretching of carboxylate groups appears at 1603 cm^{-1} and 1398 cm^{-1} respectively. The methanol O-H stretching appears at 3421 cm^{-1}. However, a significant difference in the stretching frequency in the IR spectrum of the molecular complex **5.8** is observed. The N-O stretching of the *N*-oxide in **5.8** appears at 1240 cm^{-1} while the asymmetric and symmetric stretching of carboxylate groups appears at 1670 cm^{-1} and 1381 cm^{-1} respectively. Moreover, a broad band around 3399 cm^{-1} signifies the presence of the aqua groups in the molecular complex. The differences in the position of the N-O stretching frequencies in the case of **2.5** and **5.8** clearly support the existence of coordinated and uncoordinated form of the ligands in **5.8**.

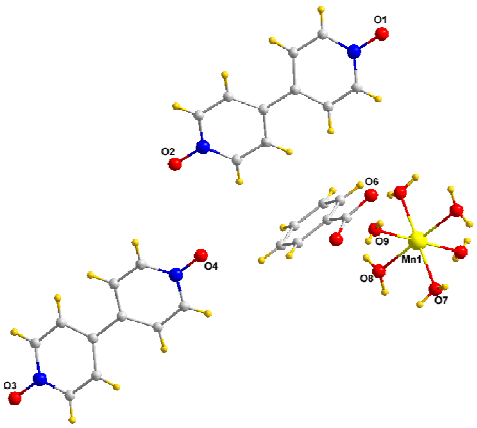

(a)

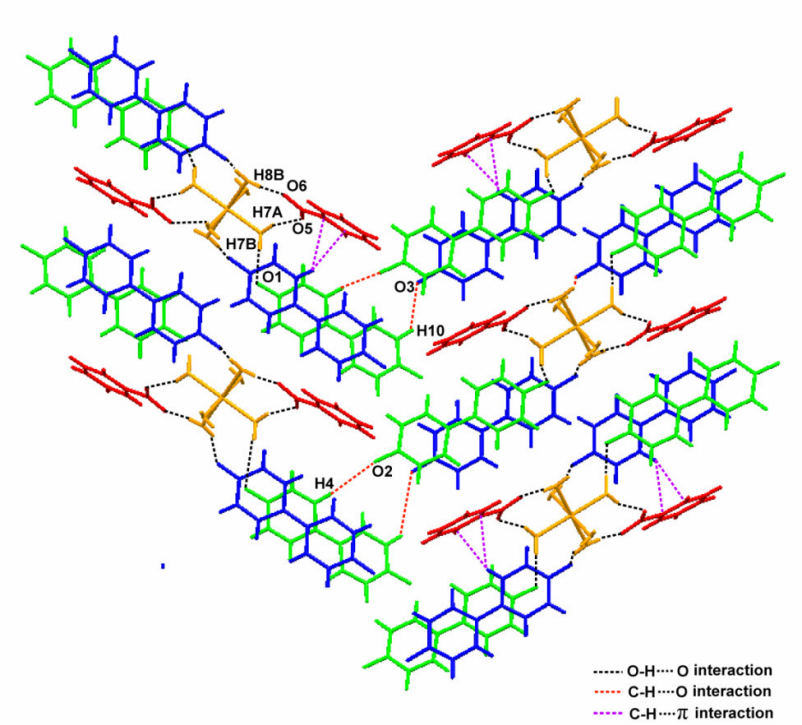

(b)

Figure 5.3.1: (a) Crystal structures of the molecular complex **5.8** (b) Hydrogen bond interactions in the molecular complex **5.8**

The molecular complex **5.8** is also characterized by X-ray crystallography and it is found to crystallize in monoclinic space group $P2_1/n$. The crystal structure reveals the co-crystallization of three components viz. benzoate ion, 4,4'-Bipyridyl-*N,N'*-dioxide and the hexaaquo manganese(II) ion. The three component molecular complex is found to be stabilized through weak interactions like O-H···O interaction,

Table 5.2: Hydrogen bond parameters of complexes **5.7** and **5.8**

D-H····A	$d_{D\text{-}H}$(Å)	$d_{H\cdots A}$(Å)	$d_{D\cdots A}$(Å)	< D-H····A(º)
Complex **5.7**				
O(9)--H(9B)···O(5) [-x+1, -y+1, -z]	0.898	1.897	2.783	168
O(9)--H(9A)···O(1) [x-1, y, z]	0.728	2.148	2.868	170
O(7)--H(7B)···O(1) [x-1, y, z]	0.757	1.992	2.740	169
O(6)--H(6B)···O(9) [-x+1, -y+1, -z]	0.812	1.873	2.683	174
O(8)--H(8A)···O(5)	0.805	1.973	2.774	173
O(8)--H(8B)···O(2) [x-1, y+1, z]	0.728	1.940	2.665	174
O(7)--H(7A)···O(1) [-x+1, -y+1, -z]	0.810	1.915	2.725	178
O(6)--H(6A)···O(5) [-x+1, -y+2, -z]	0.800	2.013	2.787	163
C(13)--H(13)···O(3) [1-x,1-y,-z]	0.93	2.59	3.486(11)	161
Complex **5.8**				
O(7)--H(7A)···O(5)	0.82	1.87	2.662(2)	164
O(7)--H(7B)···O(1) [1+x,y,1+z]	0.89(3)	1.77(3)	2.662(2)	180
O(8)--H(8A)···O(4) [1-x,-y,-z]	0.82	2.06	2.764(2)	144
O(8)--H(8B)···O(6)	0.90(3)	1.83(3)	2.724(2)	175
O(9)--H(9A)···O(4) [2-x,-y,-z]	0.95	1.93	2.854(2)	166
C(19)--H(19)···O(1) [1-x,-y,-z]	0.93	2.27	3.194(2)	175

C-H···O interaction as well as π···π interactions. All the *N*-oxide and the carboxylate ion are involved in hydrogen bonding interactions with the aquo groups present through O7-H7B···O1, O8-H8A···O4, O9-H9A···O4, O7-H7A···O5, O8-H8B···O6 interactions (table 5.2). Apart from this there exists C-H···O interactions viz. C10-H10···O3, C4-H4···O2 and π···π interactions viz. C1-C20 and C4-C12 interactions between the aromatic rings of the 4,4'-BPNO ligands. These interactions, force the two rings of the 4,4'-BPNO ligand to twist with respect to each other. The thermogram of the molecular complex **5.8** also matches well with the calculated weight loss of the aquo as well as the other groups.

Although the structures of the molecular complexes discussed above suggests that the complexes are co-crystals of hexa aqua metal(II) ion with carboxylate and aromatic *N*-oxide molecules, yet there is an alternative representation to explain their solid state structures. The structures can also be considered as molecular complexes of *N*-oxides, carboxylic acid and water co-crystallizing with $[M(OH)_2(H_2O)_4]$. This

inference was based on the facts that the structure solved as $[M(H_2O)_6]^{2+}$ with two carboxylate anions and neutral aromatic *N*-oxides and that of $[M(OH)_2(H_2O)_4]$ with two carboxylic acids and aromatic *N*-oxides are indistinguishable. Nevertheless the chemical reactivity of complexes are of prime concern and in solution the structure may be of $[M(H_2O)_6]^{2+}$; whereas in solid state it may either of the two structures. This anomaly is virtual and arises due to difficulty in location of exact position of hydrogen atoms in the lattice. Such a consideration may be attributed to packing effect in which the protons get displaced to make tight packed structure keeping the charge neutrality intact.

5.4 Conclusion

The formation of this kind of co-crystal suggests that there is a synergic effect in the aromatic *N*-oxide complexes of zinc and manganese carboxylate to dissociate and the stability of such complexes is dependent on the solvation *vs* stability of molecular complexes. These competitive effects lead to facile attack of water on any transient complex formed during the reaction of metal acetate with aromatic *N*-oxide and aromatic carboxylic acid to give molecular complexes. Competition of aquation vs. ligation in these complexes are found to be predominating factor to decide the composition of the complexes. The hydrogen bonding and packing effect also decides the co-ordination ability of *N*-oxide ligands. The strong π- π interactions in the quinoline *N*-oxide becomes important and this could be one of the reasons that carboxylate coordination polymer containing quinoline *N*-oxide ligands analogous to other aromatic *N*-oxides are not formed. The advantage of such competitive effect is taken to prepare molecular complexes with the 4,4'-bipyridyl-*N,N'*-dioxide ligand. The formation of these molecular complexes in aqueous medium opens a new avenue in the field of supramolecular chemistry.

5.5 Experimental section

Detailed synthetic methodologies are given below. Analytical data as well as spectroscopic data are also listed along with each of the complex. The instrumental details are given in Appendix.

Complex 5.1: $[Mn(H_2O)_6].(4\text{-}NO_2C_6H_4COO)_2.(PNO)_2$

To a solution of 4-Nitrobenzoic acid (2 mmol, 0.334 g) in methanol (20 mL) $Mn(OAc)_2.4H_2O$ (1 mmol, 0.245 g) was added and stirred for 30 minutes to obtain a homogeneous solution. To this reaction mixture pyridine *N*-oxide (2 mmol, 0.190 g) was added with constant stirring at room temperature. A little amount of water (2 mL) was added to dissolve the precipitate obtained. The reaction mixture was then allowed to stir for two days at room temperature. Good quality crystals were collected after 4/5 days. Yield of the complex was found to be > 70%.

IR (KBr, cm^{-1}): 3116 (bs), 1614 (s), 1574 (s), 1492 (m), 1345 (s), 1215 (m), 1174 (m), 839 (w), 724 (m), 693 (m), 678 (m).

Elemental analysis for $C_{24}H_{30}N_4O_{16}Mn$: calculated (%) C, 42.05; H, 4.40 ; found (%) C, 42.11; H, 4.41.

Magnetic moment: 5.64 BM at RT.

Complex 5.2: $[Zn(H_2O)_6].(4\text{-}NO_2C_6H_4COO)_2.(PNO)_2$

Complex **5.2** was synthesized in a similar procedure with Complex **5.1** except the use of zinc(II) acetate dihydrate as the metal source. Good quality crystals were collected after a week. Yield of the complex was found to be > 90%.

IR (KBr, cm^{-1}): 3110 (bs), 1622 (s), 1574 (s), 1340 (m), 1213 (w), 1048 (m), 844 (m), 726 (m), 688 (m), 674 (m).

Elemental analysis for $C_{24}H_{30}N_4O_{16}Zn$: calculated (%) C, 41.42; H, 4.34 ; found (%) C, 41.41; H, 4.34.

^{1}H NMR (DMSO-d^6): 8.86 (s, 1H), 8.11(s, 3H), 7.87(t, J=6.8Hz, 1H), 7.42(d, J=14.4Hz, 3H), 7.32(s, 3H).

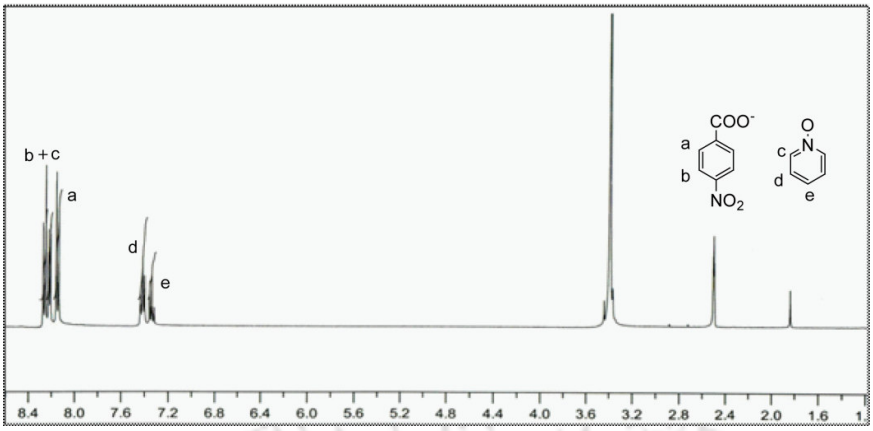

Figure 5.5.1: ^{1}H-NMR spectrum of the complex **5.2**

Complex 5.3: [Zn (4-$NO_2C_6H_4COO)_2$.$(PNO)_2$.$(H_2O)_2$].H_2O

To a solution of 4-Nitrobenzoic acid (2 mmol, 0.334 g) in methanol (15 mL) $Zn(OAc)_2.2H_2O$ (1 mmol, 0.219 g) was added and stirred for 30 minutes. To this reaction mixture pyridine *N*-oxide (2 mmol, 0.190 g) was added with constant stirring at room temperature. The reaction mixture was then allowed to stir for 2 h at room temperature. Solvent was evaporated to get the colorless complex **5.3**. Good quality crystals were obtained by recrystallization from methanol: toluene mixed solvent after a week. Yield of the complex was found to be ~ 80%.

IR (KBr, cm^{-1}): 3420 (bs), 3021 (w), 2929 (w), 1634 (s), 1609 (s), 1568 (s), 1335 (s), 1219 (m), 1157 (m), 1048 (m), 852 (m), 741 (m), 550 (m).

Complex 5.4: [$Mn(H_2O)_6$].(4-$NO_2C_6H_4COO)_2$.$(QNO)_2.2H_2O$

To a solution of 4-Nitrobenzoic acid (2 mmol, 0.334 g) in methanol (20 mL) $Mn(OAc)_2.4H_2O$ (1 mmol, 0.245 g) was added and stirred for 30 minutes to obtain a homogeneous solution. To this reaction mixture quinoline *N*-oxide (2 mmole, 0.290 g) was added with constant stirring at room temperature. 2 mL of water was added to dissolve the precipitate obtained. The reaction mixture was then allowed to stir for 2 days at room temperature. Good quality crystals were collected after a week. Yield of the crystalline complexes were found to be > 90%.

IR (KBr, cm^{-1}): 3308 (bs), 1617 (s), 1604 (s), 1576 (s), 1492 (m), 1338 (s), 1210 (m), 1174 (w), 724 (m), 693 (m), 678 (m).

Elemental analysis for $C_{32}H_{38}N_4O_{18}Mn$: calculated (%) C, 46.77; H, 4.66 ; found (%) C, 46.76.11; H, 4.67.

Complex 5.5: $[Co(H_2O)_6].(4\text{-}NO_2C_6H_4COO)_2.(QNO)_2.2H_2O$

Complex **5.5** was synthesized in a similar procedure with Complex **5.4** except the use of cobalt(II) acetate tetra hydrate as the metal source. Yield of the crystalline complex was found to be > 70%.

IR(KBr, cm^{-1}): 3308 (b), 1617 (s), 1578 (m), 1394 (m), 1382 (s), 1225 (m), 1096 (m), 883 (m), 797 (m).

Magnetic moment: 4.12 BM at RT.

Complex 5.6: $[Ni(H_2O)_6].(4\text{-}NO_2C_6H_4COO)_2.(QNO)_2.2H_2O$

Complex **5.6** was synthesized in a similar procedure with Complex **5.4** except the use of nickel(II) acetate tetra hydrate as the metal source. Yield of the crystalline complex was found to be > 70%.

IR(KBr, cm^{-1}): 3304 (b), 1619 (s), 1576 (m), 1395 (m), 1375 (s), 1230 (m), 1096 (m), 880 (m), 798 (m).

Magnetic moment: 2.83 BM at RT.

Complex 5.7: $[Zn(H_2O)_6].(4\text{-}NO_2C_6H_4COO)_2.(QNO)_2.2H_2O$

Complex **5.7** was synthesized in a similar procedure with Complex **5.4** except the use of $Zn(OAc)_2.2H_2O$ as the metal source. Good quality crystals were collected after a week. Yield of the crystalline complex was found to be > 90%.

IR (KBr, cm^{-1}): 3059 (bs), 1567 (s), 1449 (m), 1403 (s), 1214 (m), 1174 (m), 1048 (m), 693 (m), 678 (m).

Elemental analysis for $C_{32}H_{38}N_4O_{18}Zn$: calculated (%) C, 46.19; H, 4.60; found (%) C, 46.23; H, 4.54.

^{1}HNMR (DMSO-d^6): 8.86 (s, 1H), 8.11(s, 3H), 7.87(t, J=6.8Hz, 1H), 7.42(d, J=14.4Hz, 3H), 7.32(s, 3H).

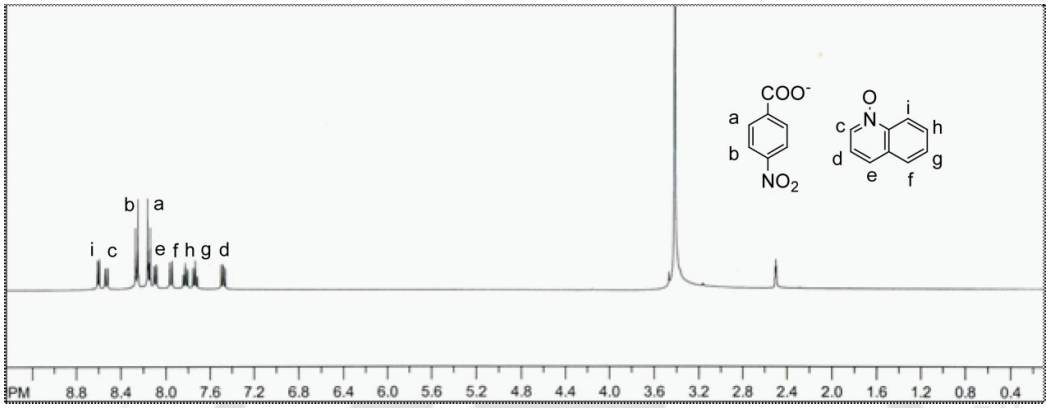

Figure 5.5.2: ^{1}H-NMR spectrum of complex **5.7**

Complex 5.8: $[Mn(H_2O)_6].(C_6H_5COO)_2.$(4,4'-BPNO)$_4$

To a solution of benzoic acid (2 mmol, 0.244 g) in methanol (20 mL) manganese(II) acetate tetrahydrate (1 mmol, 0.245 g) was added and stirred for 30 minutes to obtain a homogeneous solution. To this reaction mixture 4,4′-bipyridyl-*NN*′-dioxide (2 mmol, 0.376 g) was added with constant stirring at room temperature. The solution turns red. To the reaction mixture water (2 mL) was added. The solution becomes colourless which was allowed to stir overnight. Colourless crystals of **5.8** were obtained after about two weeks. Yield of the crystalline compound was 25%.

IR(KBr, cm^{-1}): 3399 (b), 3102 (m), 1670 (s), 1596 (m), 1547 (m), 1462 (m), 1381 (s), 1240 (s), 1167 (m),1022 (m), 835 (m), 745 (m).

Magnetic moment: 5.69 BM at RT.

Chapter 6

Supramolecular aspects of molecular complexes of aromatic *N*-oxides with phenyl boronic acid: syntheses, characterizations and DFT calculations

Weak interactions are of general interest in chemistry and biology.[164-168] Despite susceptibility of boronic acid towards organic reactions[174-177] a good number of host–guest chemistry of boronic acids are available.[178–182] Due to its structural similarity with carboxylic acids, boronic acids have been widely employed for generation of supramolecular assemblies.[183-186] Accordingly, numbers of literature are available on homo-molecular and hetero-molecular assemblies of boronic acids.[187-194] Among them, the 1,4-benzenediboronic acid (*p*-phenylenediboronic acid, BDBA) is of special interest. The presence of the two $B(OH)_2$ units makes it a better node for construction of supramolecular architectures. BDBA possesses a number of hydrogen bonding modes as illustrated in scheme 6.1 to form supramolecular assemblies.

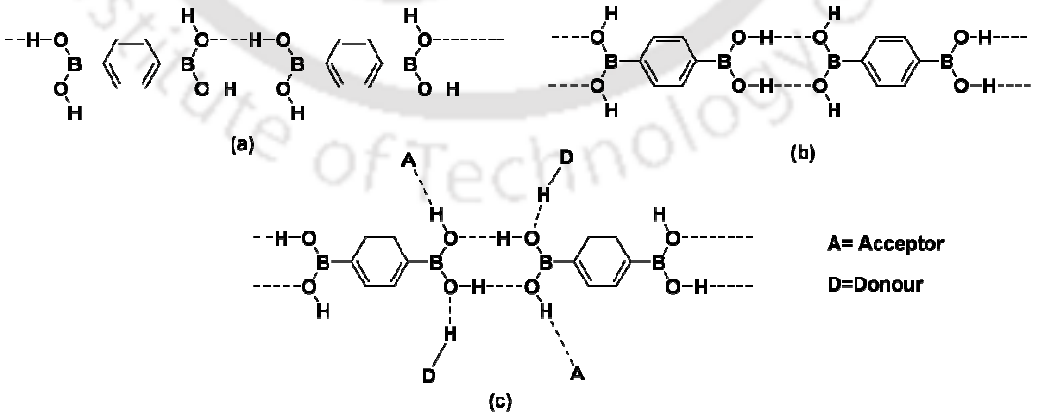

Scheme 6.1

Such assemblies can be reorganized by interactions with guest molecules that are capable of forming relatively stronger hydrogen bonds over the existing ones. For this purpose an aromatic *N*-oxide can be of choice, as they are capable of forming strong hydrogen bonds.[169-173, 195-197] We have designed a few supramolecular assemblies of 1,4-benzenediboronic acid with aromatic *N*-oxides viz. pyridine *N*-oxide (**6.1**), quinoline *N*-oxide (**6.2**), isoquinoline *N*-oxide (**6.3**), and 4,4'-Bipyridyl-*N,N'*-dioxide (**6.4**) and the study on the interactions in these molecular complexes is the content of this chapter. The experimentally observed weak interactions are correlated with theoretical ones by carrying out DFT calculations on different model assemblies of the molecular complexes.

6.1 Synthesis and characterisation of the molecular complexes

The molecular complexes of 1,4-benzenediboronic acid with different aromatic *N*-oxides namely pyridine *N*-oxide (PNO), quinoline *N*-oxide (QNO), isoquinoline *N*-oxide (IQNO), and 4,4'-bipyridyl-*N,N'*-dioxide (4,4'-BPNO) are easily prepared by mixing respective solution of the corresponding *N*-oxide with the 1,4-benzenediboronic acid. The molecular complexes exhibit characteristic IR absorptions in the range 1211–1253 cm^{-1} due to N-O stretching of the aromatic *N*-oxides. The structures of each of them are determined by means of crystallography and their packing patterns are analysed. Each of these adducts exhibit the O-H···O hydrogen bond interaction as the primary interaction to form a network structure along with other weak interactions. The common point in each of these structures is the strong hydrogen bonding interactions between the *N*-oxo groups of aromatic *N*-oxides with the B–OH groups of the *p*-phenylenediboronic acid molecules. These interactions over-power the original hydrogen bonding interactions between the B–OH groups of parent *p*-phenylenediboronic acid molecules responsible for homomeric assembly formation. Apart from the conventional O-H···O and C-H···O interactions relatively less conventional weak interaction such as the B···π (aromatic) interaction is found to exists.

The molecular complex, **6.1**, of pyridine *N*-oxide with BDBA reveals the presence of strong O-H···O interactions with $d_{D\text{-}H\cdots A}$ (Å), O2-H2a···O1, 1.92; O3-H3a···O1, 1.71 and ∠D-H···A (º), ∠O2-H2a···O1, 158; ∠O3-H3a···O1, 176. Apart

from these, there exist a number of C-H···O interactions viz. C1-H1····O3, C5-H5····O3, and C6-H6····O1. These interactions hold four PNO molecules attached to the two $B(OH)_2$ groups per molecule of BDBA. Moreover, each of the $B(OH)_2$ groups anchors two pyridine *N*-oxide molecules through B···π (aromatic) interactions between the boron atoms and the aromatic ring of the pyridine *N*-oxide molecules. In the co-crystals, two pyridine *N*-oxide rings sandwich a $B(OH)_2$ unit through η^2 and η^3 types of B-π (aromatic) interactions as shown in figure 6.1.1. The distance of separation between the *N*-oxide rings and $B(OH)_2$ units are 3.60 Å (η^3-type) and 3.75 Å (η^2-type). All these weak interactions are responsible for a two dimensional hydrogen bonded assembly of **6.1**. The hydrogen bond parameters are listed in table 6.1.

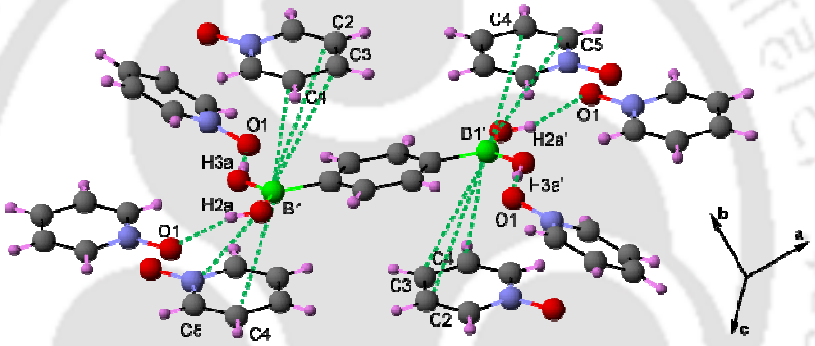

Figure 6.1.1: Weak interactions stabilizing the molecular complex **6.1**

Table 6.1: Hydrogen bond parameters in the molecular complex **6.1**

D-H····A	$d_{D\text{-}H}$(Å)	$d_{H\cdots A}$(Å)	$d_{D\cdots A}$(Å)	< D-H····A(º)
O2-H2A····O1[-x, -1/2+y, 1/2-z]	0.82	1.92	2.694(6)	158
O3-H3A····O1[-x, 1-y, -z]	0.99	1.71	2.702(6)	176
C1-H1····O3 [-x, 1-y, -z]	0.93	2.60	3.289(7)	131
C5-H5····O3 [-x, 1/2+y, 1/2-z]	0.93	2.35	3.258(7)	165
C6-H6····O1 [-x, 1-y, -z]	0.93	2.47	3.367(7)	161

The quinoline *N*-oxide forms a 2:1 co-crystal whereas isoquinoline *N*-oxide forms 4:1 co-crystal with *p*-phenylenediboronic acid. These co-crystals assemble through strong hydrogen bond interactions between the *N*-oxo and the O-H groups. In both of these cases extensive C-H···O and O-H···O hydrogen bond interactions are observed. The co-crystal (**6.2**) of quinoline *N*-oxide is devoid of any π-interaction but

in the case of the co-crystal (**6.3**) of isoquinoline *N*-oxide, π-stacking effect persists. In the lattice of the co-crystal (**6.2**) between quinoline *N*-oxide and *p*-phenylenediboronic acid, O2-H2····O1 and O3-H3····O1 are the only O-H···O interactions along with a number of C-H···O interactions. The *N*-oxo groups of quinoline *N*-oxide are involved in the formation of trifurcated hydrogen bond interactions, two O-H···O and one C-H···O interactions (Figure 6.1.2a).The O-H···O interactions in **6.2** connect both the components together and leads to a ladder like arrangement as shown in figure 6.1.2b.

In the case of the molecular complex **6.3,** C-H···π and π-π interactions are of importance for assembly formation along with the O-H···O and C-H···O interactions. Here the O-H···O interactions connect the IQNO molecules with the two $B(OH)_2$ units per BDBA molecule. However, the extension of the assembly takes place through the C-H···O interactions viz. C10-H10···O1 and C1-H1···O2 among the IQNO molecules and C-H···π interactions between the IQNO and BDBA molecules through C6-H6···C21 ($d_{D\text{-}H\cdots A}$ (Å), 2.86) and C15-H15···C19 ($d_{D\text{-}H\cdots A}$ (Å), 2.79). The π–π separation between the aromatic rings of IQNO is 3.34 Å which is within the generally referred limit of π-stacks.[198]

It may be mentioned here that in the molecular complex **6.2** the quinoline *N*-oxide molecules are placed in a head-to-tail arrangement, whereas in **6.3** the isoquinoline *N*-oxide molecules are positioned in a head-to-head arrangement. The

Table 6.2: Hydrogen bond parameters in the molecular complexes **6.2** and **6.3**

D-H····A	$d_{D\text{-}H}$(Å)	$d_{H\cdots A}$(Å)	$d_{D\cdots A}$(Å)	< D-H····A(º)
Complex **6.2**				
O2-H2····O1 [-x, 1-y, 1-z]	0.82	2.03	2.808(2)	157
O3-H3····O1 [1-x, 1-y,1 -z]	0.82	2.11	2.811 (19)	144
C1-H1····O3 [x, y, 1+z]	0.93	2.59	3.502(2)	168
C5-H5····O2	0.93	2.42	3.264(3)	150
C12-H12····O1 [-x, 1-y, 1-z]	0.93	2.49	3.339(2)	152
Complex **6.3**				
O3-H3····O1 [1-x, 1-y, -z]	0.82	1.98	2.713(4)	149
O4-H4····O2 [x, y, -1+z]	0.82	2.01	2.762(3)	152
C10-H10····O1 [-1+x, y, 1+z]	0.93	1.93	2.851(4)	171

head-to-head stacking arrangement is electro-statistically unfavourable, but due to the complementarities for hydrogen bond formation they prefer to have the dimeric arrangement as shown in figure 6.1.2c. These dimers are formed through C10-H10···O1 and C1-H1···O2 interactions. The hydrogen bond parameters of the weak interactions in both the complexes **6.2** and **6.3** are tabulated in table 6.2.

The molecular complex of the 4,4'-bipyridyl-*N,N'*-dioxide and 1,4-benzenediboronic acid (**6.4**) possesses conventional O-H···O and C-H···O as well as less conventional B···π (N-O) interactions. The strong O-H···O interactions between the *N*-oxide and B–OH groups namely O2-H2···O1 and O3-H3···O1 along with the C5-H5···O2 interactions make a sheet like assembly of **6.4** (Table 6.3).

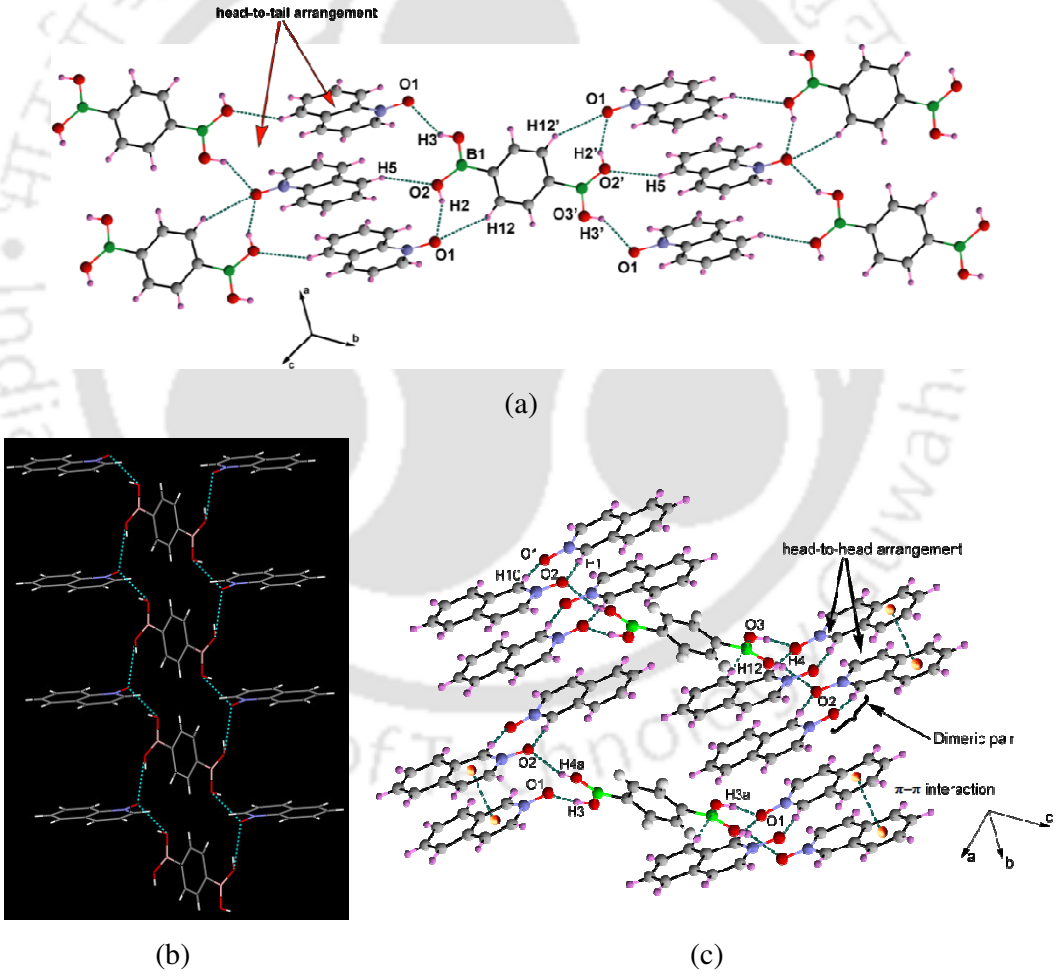

(a)

(b) (c)

Figure 6.1.2: (a) The short range interactions in the molecular complex **6.2**, (b) O-H···O interactions leading to the ladder like arrangement in **6.2** and (c) assembly formation in the molecular complex **6.3**

Table 6.3: H-bond parameters in the molecular complex **6.4**

D-H····A	$d_{D\text{-}H}$(Å)	$d_{H\cdots A}$(Å)	$d_{D\cdots A}$(Å)	< D-H····A(º)
O2-H2····O1	0.82	2.09	2.865(3)	157
O3-H3····O1 [1+x, y,z]	0.82	2.03	2.785(2)	152
C5-H5····O2 [-1+x, y, z]	0.93	2.56	3.452(3)	161

In general, a B-O interaction is expected between the lone pair of oxygen of the *N*-oxo group with a vacant π -orbital of boron atom. However, the 4,4'-bipyridyl-*N,N'*-dioxide molecules in the co-crystal **6.4** are oriented in such a way that the oxygen atom of *N*-oxide is involved in O-H···O, C-H···O interactions to form the layered structure (Figure 6.1.3). Flanked by the layers, the oxygen atom of *N*-oxide occupies a space just above the boron atom with a distance of separation 3.10 Å. Based on this distance of separation and projection of the lone pair of oxygen of *N*-oxide it may be proposed that there exists some B···π interactions between the boron atom and the *N*-oxo group. These type of B···π interactions are seldom found in the literature.[199-203]

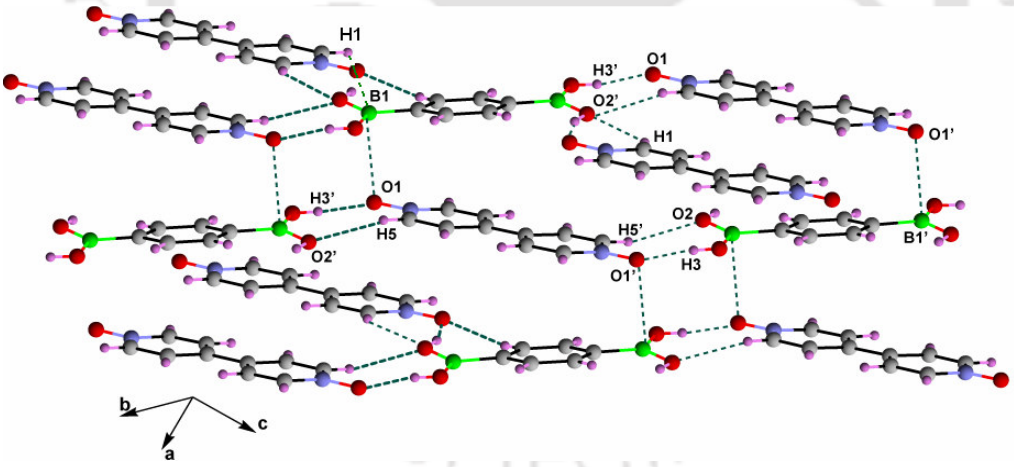

Figure 6.1.3: Assembly formation in the molecular complex **6.4** with the aid of the weak interactions

From the crystal structures of the molecular complexes we have observed that there exists two different types of hydrogen bonded orientations (with different bond length and bond angles) between the -$B(OH)_2$ and *N*-oxo synthons: type-1 and type-2. These orientations are observed for all the cases except BDBA-IQNO (**6.3**) system

where the hydroxyl groups of the BDBA molecule takes up a *cis* orientation rather than the *trans* orientation. The two orientations are shown in the scheme 6.1.1.

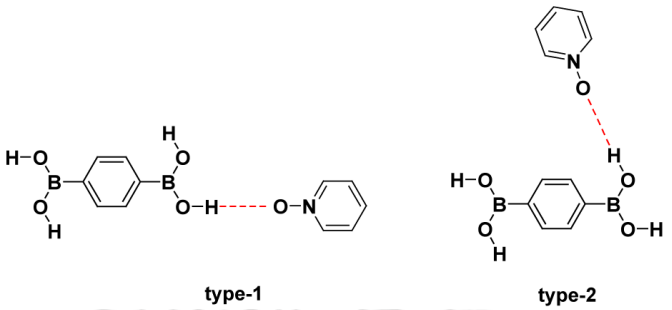

Scheme 6.1.1

6.2 Theoretical study on the weak interactions in the molecular complexes 6.1-6.4

In order to understand the weak interactions in the molecular complexes **6.1-6.4** the following theoretical aspects are studied.

1. Energy optimized structures of the hydrogen bonded systems and relevance to their crystal structure.
2. Energies of the type-1 and type-2 orientations.
3. Interactions between the HOMO of the aromatic *N*-oxides and LUMO of the acid to establish the feasibilities of B-π interactions.

6.2.1 Energy optimized structures of the molecular complexes 6.1-6.4

We have optimized the 1:1 structures of the molecular complexes **6.1-6.4** at B3LYP/6-31++G(d) level of theory and compared them with those obtained experimentally. The optimized structure of the molecular complex of BDBA and PNO (Figure 6.2.1a), reveals the presence of a strong O-H···O interaction with $d_{D\text{-}H\cdots A}$ (Å), O3-H4···O21, 1.77 and ∠D-H···A (º), ∠O3-H4···O21, 171 along with a secondary C-H···O interaction with $d_{D\text{-}H\cdots A}$ (Å), C31-H32···O1, 2.21 and ∠D-H···A (º), ∠C31-H32···O1, 170. The optimized structure is in good accord with the type-1 orientation in the crystal structure of **6.1** where the O-H···O interactions lie in the range 1.71-1.92 Å. We have performed similar calculations in the case of the molecular complex of BDBA with QNO (**6.2**). The optimized structure of the 1:1 molecular complex of BDBA and QNO is shown in figure 6.2.1b. Like in the earlier case the optimized

structure shows the presence of a strong O-H···O interaction with $d_{D\text{-}H\cdots A}$ (Å), O3-H4···O21, 1.75 and ∠D-H···A (º), ∠O3-H4···O21, 172 along with a secondary C-H···O interaction with $d_{D\text{-}H\cdots A}$ (Å), C25-H26···O1, 2.24 and ∠D-H···A (º), ∠C25-H26···O1, 168. However, in this case the experimentally obtained crystal structure doesn't tally the optimized structure. The crystal structure of the molecule reveals the existence of O-H···O hydrogen bonding between the -$B(OH)_2$ units and QNO molecules, but no C-H···O interaction. The experimental structures differs significantly from the optimized structure in that, in the later case both the molecules are almost coplanar (the aromatic rings of both the molecules involved in the molecular complex makes an angle of 157^o). However, experimentally the two rings are found to be almost orthogonal to each other thereby nullifying any possibility of existence of C-H···O interactions.

The optimized structure of the 1:1 molecular complexes of BDBA and IQNO is shown in figure 6.2.1c. BDBA can orient in two different conformations: *cis* and *trans*; we have considered the *cis*-conformation as observed experimentally in the molecular complex **6.3**. The optimized structure shows the existence of a bifurcated hydrogen bonding involving the -OH units of BDBA and *N*-oxo of IQNO with $d_{D\text{-}H\cdots A}$

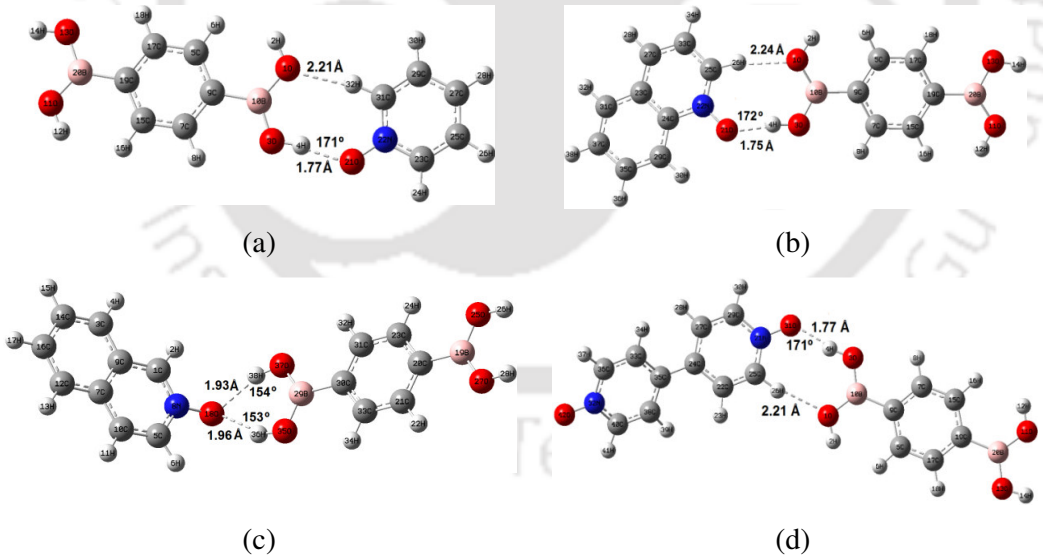

Figure 6.2.1: Optimized structure of 1:1 molecular complex of (a) BDBA and PNO (**6.1**), (b) BDBA and QNO (**6.2**), (c) BDBA and IQNO (**6.3**), and (d) BDBA and 4,4'-BPNO (**6.4**) .

(Å), O35-H36···O18, 1.96; O37- H38···O18, 1.93 and ∠D-H···A (º), ∠O35-H36···O18, 153; ∠O37-H38···O18, 154. The corresponding bond lengths in the

experimental structures are in the range 1.98-2.01 Å. However in the experimental structure the aromatic rings of the two components lie orthogonal to each other which is in contrary to the optimized structure.

Finally, figure 6.2.1d shows the optimized structures of the 1:1 molecular complexes of BDBA and 4,4'-BPNO (**6.4**). As in the case of **6.1** and **6.2** here also the two components are held together through an O-H···O interaction ($d_{D\text{-}H\cdots A}$ (Å), O3-H4···O31, 1.77 and ∠D-H···A (º), ∠O3-H4···O31, 171) and a secondary C-H···O interaction ($d_{D\text{-}H\cdots A}$ (Å), C25-H26···O1, 2.21 and ∠D-H···A (º), ∠C25-H26···O1, 170) which is in accordance with the experimental structure with type-1 orientation. An interesting difference observed between the optimized structure and the structure obtained experimentally is that in case of the optimized structure the two aromatic rings of the 4,4'-bipyridyl-*N,N'*-dioxide molecule is not exactly coplanar but remains twisted making an angle of 31º with each other, however, this twisting is absent in the experimental structure.

6.2.2 Strength of the type-1 and type-2 interactions

To compare the energies of the two types of orientations (type-1 and type-2) in each of the cases except BDBA-IQNO system, we have performed single point calculations at different levels of theory. We have performed the calculations using the BHandH functional, which is used for study hydrogen bond interactions.[204] Such calculations are used for narrating weak interactions such as π-π interactions in molecular complexes.[205, 206] The results obtained from BHandH/6-31++G(d) calculations are further supported by MP2/6-31++G(d) level calculations. The comparative energies of the 1:1 molecular complexes in their type-1 and type-2 orientations are shown in table 6.4. Comparison shows that in each of the cases, the type-2 orientation is energetically more favorable as compared to the type-1 orientation. This difference in the stability can be accounted for by the short-range interactions available in each of the different packing patterns. In 1:1 molecular complex between BDBA and PNO, the type-1 orientation provides space for one O-H···O and one C-H···O interactions. In contrast, the type-2 orientation ends up with one O-H···O and two C-H···O interactions. Moreover, the D-H···A distances for type-2 orientation are found to be shorter than the type-1 counterpart. The same is true for

BDBA–QNO and BDBA–BPNO molecular complexes. In both the type-1 and type-2 orientations, the molecular complex **6.1** exhibits exceptionally high values of interaction energies and this can be accounted for by comparatively smaller size of the PNO molecule and hence less steric congestion. The absence of steric congestion in BDBA–PNO molecular complex allow strong interactions with shorter O-H···O bond distances (1.91 in type-1 and 1.71 in type-2, compared to >2.0 in other complexes).

Table 6.4: BSSE corrected interaction energies (in kcal/mol) in type-1 and type-2 orientations at BHandH/6-31++G(d) and MP2/6-31++G(d) levels of theory

Molecular complex	type-1		type-2	
	BHandH/6-31++G(d)	MP2/6-31++G(d)	BHandH/6-31++G(d)	MP2/6-31++G(d)
6.1	-38.81	-36.86	-49.00	-43.59
6.2	-8.91	-6.20	-12.63	-11.40
6.4	-9.53	-7.63	-12.41	-10.55

6.2.3 Interactions between the HOMO of the aromatic *N*-oxides and LUMO of the acid to establish the feasibilities of B-π interactions

The HOMO of the electron donor (H-acceptor) and LUMO of the electron acceptor (H-donor) plays important role during the formation of hydrogen bonds.[207] During formation of molecular complex the HOMO of the aromatic *N*-oxide and LUMO of BDBA are involved. The HOMO of the four *N*-oxides are shown in figure 6.2.2(a-d) and the LUMO of 1,4-benzenediboronic acid are shown in figure 6.2.2e.

It can be easily seen from figure 6.2.2 that in all four examples the HOMO is associated with the O atoms and some portion spread over the aromatic N-C bond. This depicts that the O atom can act as an electron donor and consequently it readily participates in hydrogen bonding. The LUMO of 1,4-benzenediboronic acid is quite symmetric and it spreads over the B-C and C-C bond of the aromatic ring. A careful look on the HOMO of the PNO and BPNO shows that the HOMO is symmetrically distributed over the aromatic ring, whereas, in case of QNO and IQNO the HOMO is

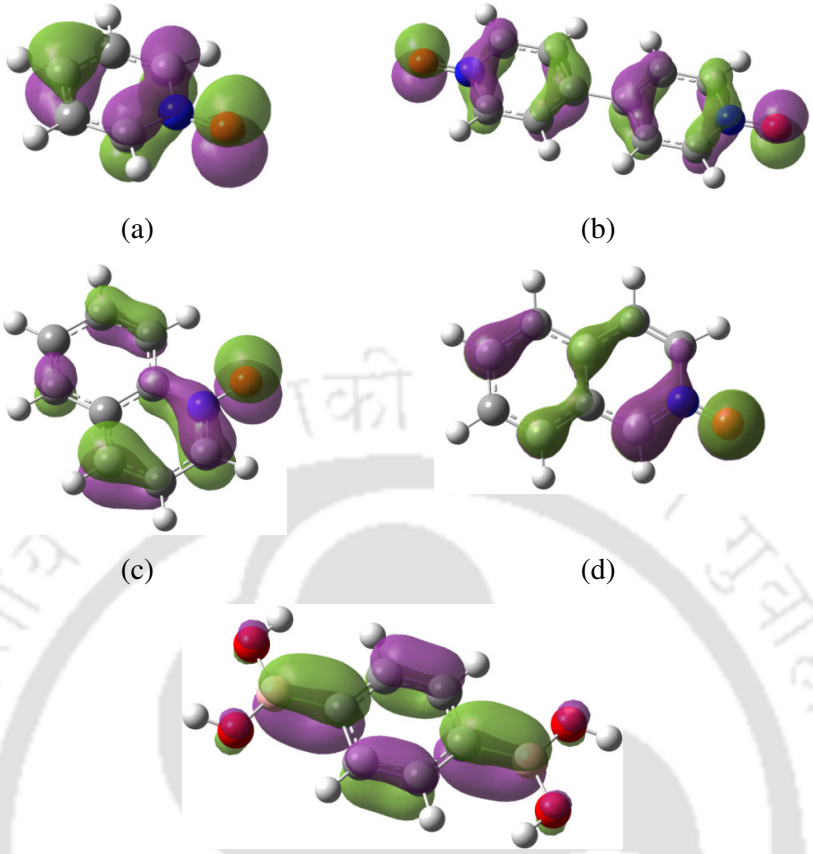

(a) (b)

(c) (d)

(e)

Figure 6.2.2: HOMO of (a) PNO molecule, (b) BPNO molecule, (c) QNO molecule, (d) IQNO molecule, and (e) LUMO of 1,4-benzenediboronic acid

less symmetric. This symmetric arrangement of the HOMO of PNO and BPNO explains the B-π interactions of PNO or BPNO with BDBA molecule.The perspective of HOMO-LUMO for the occurrence of B-π interaction in the case the BDBA-PNO molecular complex is shown in figure 6.2.3.

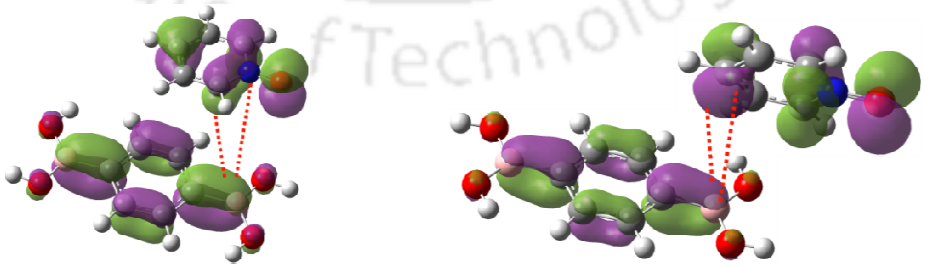

Figure 6.2.3: HOMO-LUMO perspective of the B-π interactions in the case the BDBA-PNO molecular complex

6.3 Conclusion

In conclusion, structural aspects of few co-crystals of 1,4-benzenediboronic acid with aromatic *N*-oxides are studied and observed that the interactions in each case are different and rare interaction such as B-π interaction is present in this class of molecules. During formation of the molecular complexes, two different types of hydrogen bonding orientation are found depending on the orientation of the hydrogen atoms of B-OH bonds. There exists significant difference in the interaction energies of the different 1:1 molecular complexes of BDBA and aromatic *N*-oxides in these different orientations. The orientations of the HOMOs of aromatic *N*-oxides and the LUMO of BDBA clearly depict the B-π interactions in the BDBA-PNO and BDBA-BPNO molecular complexes. A generalized approach to understand weak interaction in molecular complexes of boronic acid with aromatic *N*-oxides is brought forward. The study suggests about ample avenues for looking at the new interactions in the co-crystals of boronic acids.

6.4 Experimental section

Computational details

DFT and MP2 methods are used to observe the strength of hydrogen bonds. The initial coordinates are taken from the geometries obtained from the single crystal X-ray diffraction data. B3LYP and BHandH functionals are used in the DFT calculations.[208, 209] We have used 6-31++G(d) basis set as it is found to be sufficient to predict reliable properties for hydrogen-bonded systems in gas phase.[210-214] The 1:1 models considered of the molecular complexes are optimized using the B3LYP functional and compared with structures obtained experimentally. All calculations are performed using *Gaussian03* program.[215]

Detailed synthetic methodologies are given below. Analytical data as well as spectroscopic data are also listed along with each of the complex. The instrumental details are given in Appendix.

Molecular Complex 6.1: [($C_6H_8B_2O_4$) . 2(C_5H_5NO)]

By mixing 1,4-benzenediboronic acid (0.165 g, 1 mmol) and pyridine *N*-oxide (0.190 g, 2 mmol) in a mixed solvent methanol/toluene (4:1) gave the corresponding co-crystals of **6.1**. The crystals were obtained after seven days.

IR (KBr, cm^{-1}): 3209 (b), 1615 (m), 1510 (m), 1472 (m), 1423 (m), 1401 (m), 1369 (s), 1340 (s), 1235 (s), 1192 (s) 1165 (s), 1192 (m), 1139 (m), 1094 (m), 1058 (m), 836 (s), 759 (m).

^{1}H-NMR (DMSO-d^6, 400 MHz): 8.2 (4H, d, J = 8.0 Hz), 8.0 (2H, s), 7.7(2H, s), 7.4 (4H, t, J = 8.0 Hz), 7.3 (2H, t, J = 8.0 Hz).

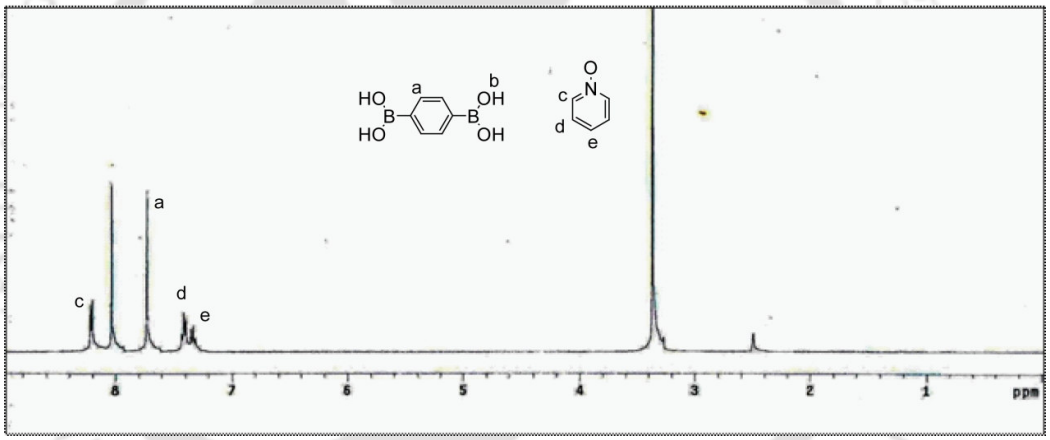

Figure 6.4.1: ^{1}H-NMR spectrum of complex **6.1**

Molecular Complex 6.2: [($C_6H_8B_2O_4$) . 2(C_9H_7NO)]

Layering an aqueous solution of 1,4-benzenediboronic acid (0.165 g, 1 mmol) over a quinoline *N*-oxide (0.290 g, 2 mmol) solution in toluene yielded pure crystalline cocrystals of **6.2** after about two weeks.

IR (KBr, cm^{-1}): 3303 (b), 1638 (m), 1577 (m), 1514 (m), 1430 (m), 1399 (s), 1380 (s), 1329 (s) 1311 (s), 1263 (s), 1229(m), 1211(m), 1162 (s), 1135 (s), 1084 (m), 1043 (s), 1008 (s), 880 (m), 848 (s), 804 (s), 776 (s).

^{1}H-NMR (DMSO-d^6, 400 MHz): 8.6 (1H, d, J = 8.0 Hz), 8.5 (1H, d, J = 8.0 Hz), 8.1 (1H, d, J = 8.0 Hz), 8.0 (4H, s), 7.9 (1H, d, J = 8.0 Hz), 7.8 (2H, m), 7.7 (4H, s), 7.4 (1H, q, J = 8.0 Hz).

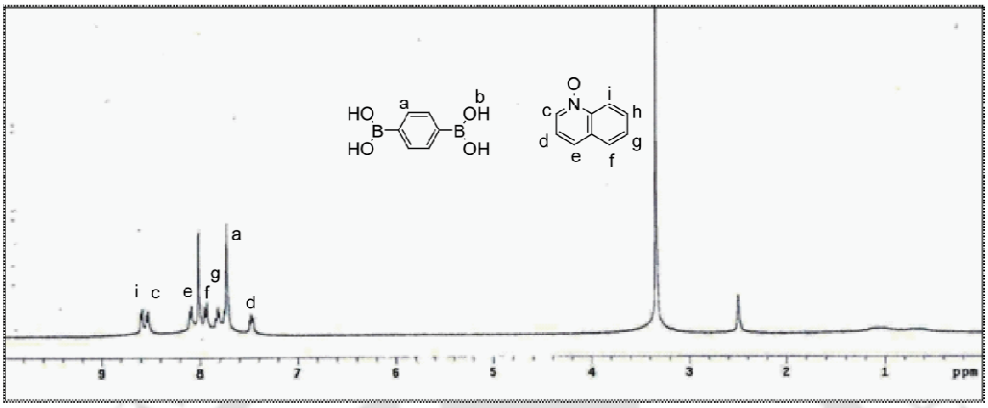

Figure 6.4.2: ^{1}H-NMR spectrum of complex **6.2**

Molecular Complex 6.3: [($C_6H_8B_2O_4$) . 4(C_9H_7NO)]

The co-crystals of isoquinoline *N*-oxide with 1,4-benzenediboronic acid were grown in a similar way as in the case of **6.2**.

IR (KBr, cm^{-1}): 3293 (b), 1634 (m), 1567 (m), 1424 (m), 1399 (s), 1380 (s), 1329 (s) 1311 (s), 1265 (s), 1238 (m), 1212 (m), 1168 (s), 1127 (s), 1064 (m), 1043 (s), 880 (m), 848 (s).

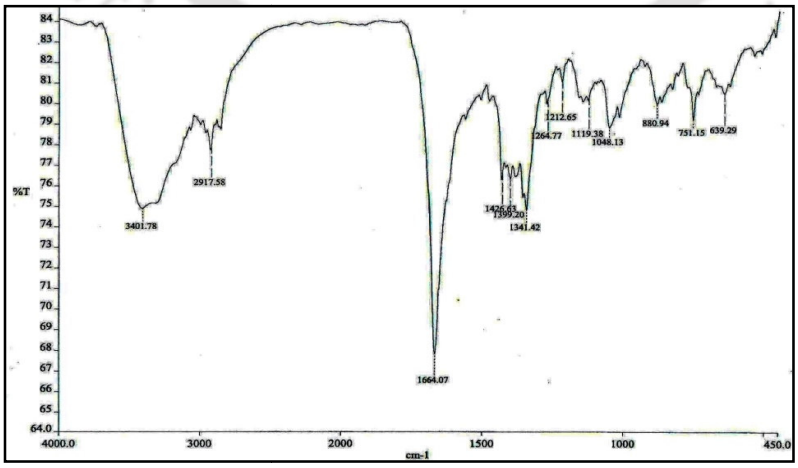

Figure 6.4.3: FT-IR spectrum of complex **6.3**

Molecular Complex 6.4: [($C_6H_8B_2O_4$) . ($C_{10}H_8N_2O_2$)]

A dimethyl sulfoxide solution of p-phenylenediboronic acid (0.165 g, 1 mmol) and 4,4'-bipyridyl-*N,N'*-dioxide (0.376 g, 2 mmol) led to the formation of co-crystals **6.4**.

IR (KBr, cm^{-1}): 3400 (b), 1633 (s), 1508 (m), 1480 (s), 1437 (m), 1398 (m), 1361 (m), 1328 (s), 1257 (m), 1237 (s), 1195 (m), 1155 (s), 1116 (m), 1097 (m), 1051 (m), 1026 (m), 820 (s), 730 (m).

^{1}H-NMR ($CDCl_3$, 400 MHz): 8.3 (4H, d, J = 8.0 Hz), 7.6 (4H, d, J = 8.0 Hz), 7.3 (8H, s).

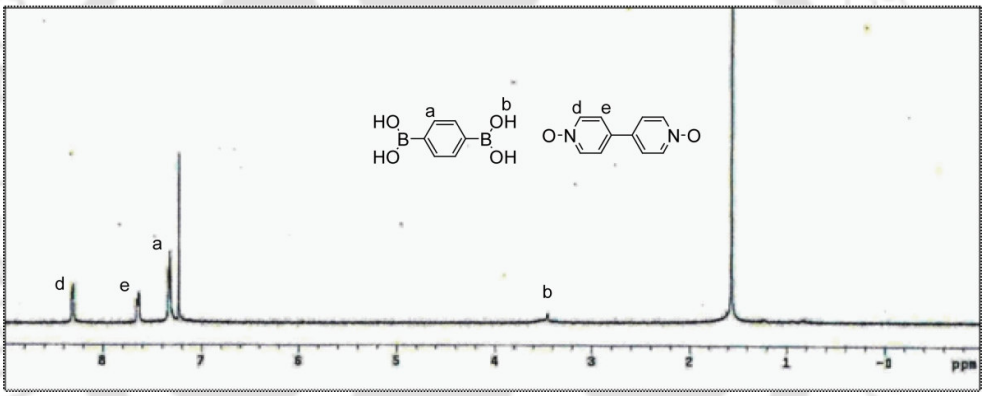

Figure 6.4.4: ^{1}H-NMR spectrum of complex **6.4**

Conclusion

Aromatic *N*-oxides exhibit enormous flexibility as supramolecular ligands. They can coordinate to metal cations to generate low nuclear as well polynuclear complexes/polymers. Furthermore, they can act as hydrogen-bond acceptors via its O-centres and form aromatic π–π stacking interactions via the aromatic rings thereby leading to supramolecular complexes. Looking at such diversity of the aromatic *N*-oxide ligands as linkers and spacers, a good number of metal complexes/ coordination polymers are synthesised and studied. Supramolecular aspects of a number of molecular complexes of aromatic *N*-oxides are also studied.

Pyridine *N*-oxide interconnects metal nodes by acting as μ^2 bridging ligand although in a few instances non-bridging monodentate coordination is observed. It appears that 4,4'-bipyridyl-*N,N'*-dioxide favors η^2-μ^2 coordination mode either *cis* or *trans*. Coordination modes such as η^2-μ^2:μ^0 or η^2-μ^2:μ^1 are scares though obtained in a couple of instances in this study. The η^2-μ^2:μ^2 coordination mode of 4,4'-bipyridyl-*N,N'*-dioxide is observed with metal ions with comparatively larger ionic radii such as lead(II) and lanthanides and is supported by literature reports. We have obtained preferential *trans* bidentate bridging binding mode of 2,2'-bipyridyl-*N,N'*-dioxide to form copper(II) coordination polymer rather than chelating mode, which is frequently come across. The η^2-μ^2:μ^2 coordination mode of 2,2'-bipyridyl-*N,N'*-dioxide is also observed in the case of coordination towards lead(II).

It has been found that reaction conditions such as solvent used or the metal to ligand ratio can have control over the dimensionality of the desired product. To encourage multidimensional architecture construction it is necessary to avoid competing solvents such as aqueous solutions and strongly coordinating anions as metal cationic centres readily bind water and anions to the exclusion of the *N*-oxide ligands resulting in molecular rather than polymeric species.

Coming to the future aspects of this work the aromatic *N*-oxide ligands discussed in this thesis are able to further generate an extremely rich solid-state chemistry. The utilization of the second and third transition series metal ions as nodes in designing extended structures remains largely unexploited. Attempts to obtain heterobimetallic assemblies using these ligands will be really interesting. Such systems could exhibit interesting magnetic, electric, optical or catalytic properties.

1. A. Albini, S. Pietra, *Heterocyclic N-Oxides,* CRC Press: Boca Raton, FL, **1991**.
2. S. Youssif, *ARKIVOC* **2001**, 242.
3. R. Sarma, J. B. Baruah, *J. Mole. Struct.* **2009**, *920*, 350.
4. B. Yan, Y. S. Song, *J. Fluoresc.* **2004**, *14*, 289.
5. A. Thellend, P. Battioni, W. Sanderson, D. Mansuy, *Synthesis* **1997**, 1387.
6. (a) R. W. Murray, K. Iyanar, J. Chen, J. T. Wearing, *Tetrahedron Lett*. **1995**, *36*, 6415. (b) *Tetrahedron Lett*. **1996**, *37*, 805.
7. I. Wolfle, J. Lodaya, B. Sauerwein, G. B. Schuster, *J. Am. Chem. Soc.* **1992**, *114*, 9304.
8. P. G. Simpson, A. Vinciguerra, J. V. Quagliano, *Inorg. Chem.* **1963**, *2*, 282.
9. F. E. Cislak, *Ind. Eng. Chem.* **1955**, *47*, 800.
10. L. -C. Campeau, S. Rousseaux, K. Fagnou, *J. Am. Chem. Soc.* **2005**, *127*, 18020.
11. K. S. Kanyiva, Y. Nakao, T. Hiyama *Angew. Chem. Int. Ed.* **2007**, *46*, 8872
12. J. A. Pool, B. L. Scott, J. L. Kiplinger *J. Am. Chem. Soc.* **2005**, *127*, 1338.
13. A. A. Ponaras, O. Zaim, *J. Heterocyclic Chem.* **2007**, *44*, 487.
14. M. Toganoh, K. Fujino, S. Ikeda, H. Furuta, *Tetrahedron Lett*. **2008**, *49*, 1488.
15. M. Mangle, K. R. Ganesh, *Tetrahedron* **2007**, *63*, 126.
16. D. D. Perrin. *J. Am. Chem Soc.* **1960**, *83*, 5642.
17. A. B. Burg, J. H. Bickerton, *J. Am. Chem Soc.* **1945**, *67*, 2261.
18. R. L. Carlin *J. Am. Chem Soc.* **1961**, *83*, 3773.
19. C. M. Harris, E. Kokot, S. L. Lenzer, T. N. Lockyer, *Chem. Ind. (London)* **1962**, 651.
20. J. V. Quagliano, J. Fujita, G. Franz, D. J. Phillips, J. A. Walmsley, S. Y. Tyree, *J. Am. Chem Soc.* **1961**, *83*, 3770.
21. W. E. Hatfield, J. S. Paschal, *J. Am. Chem Soc.* **1964**, *86*, 3888.
22. H. L. Schafer, J. C. Morrow, H. M. Smith, *J. Chem. Phys.* **1965**, *41*, 504.
23. R. S. Sager, R. J. Williams, W. H. Watson, *Inorg.Chem.* **1967**, *6*, 951.
24. R. S. Sager, R. J. Williams, W. H. Watson, *Inorg.Chem.* **1969**, *8*, 694.
25. J. E. Whinnery, W. H. Watson, *J. Coord. Chem.* **1971**, *1*, 207.
26. E. D. Estes, D. J. Hodgson *Inorg.Chem.* **1976**, *15*, 348.

27. W. D. Horrocks, D. H. Templeton, A. Zalkin, *Inorg.Chem.* **1968**, *7*, 1552.
28. N. M. Karayannis, C. M. Paleos, L. L. Pytlewski, M. M. Labes, *Inorg.Chem.* **1969**, *8*, 2559.
29. J. A. Bertrand, D. L. Plymale, *Inorg.Chem.* **1964**, *3*, 775.
30. L. C. Nathan, J. E. Armstrong, *Inorg. Chim. Acta.* **1979**, *35*, 293.
31. W.L Purcell, *Inorg. Chem.* **1989**, *28*, 2312.
32. W. E. Hatfield, D. B. Copley, R. Whyman, *Inorg. Nucl. Chem. Letters* **1966**, *2*, 373.
33. R. W. Kluiber, W. D . Horrocks, *J. Am. Chem Soc.* **1966**, *88*, 1899.
34. J. H. Nelson, L. C. Nathan, R. O. Ragsdale, *Inorg.Chem.* **1968**, *7*, 1840.
35. J. J. MacDougall, L. C. Nathan, J. H. Nelson, *Inorg. Chim. Acta.* **1976**, *17*, 243.
36. P. G. Simpson, A. Vinciguerra, J. V. Quagliano, *Inorg.Chem.* **1963**, *3*, 282.
37. (a) S. K. Madan, W. E. Bull, *J. Inorg. Nucl. Chem.* **1964**, *26*, 2211. (b) S. K. Madan, A. M. Donohue, *J. Inorg. Nucl. Chem.* **1966**, *28*, 1303.
38. U. Sartorally, F. Canziani, F. Zingales, *Inorg.Chem.* **1966**, *5*, 2233.
39. D. M. Mehs, S. K. Madan, *J. Inorg. Nucl. Chem.* **1968**, *30*, 3017.
40. W. V. Miller, S. K. Madan, *J. Inorg. Nucl. Chem.* **1969**, *31*, 1427.
41. A. R. Al. Karaghouli, R. Day, J. S. Wood, *Inorg.Chem.* **1978**, *17*, 3702.
42. J. W. Steed, J. L. Atwood, *Supramolecular Chemistry*, John, Willey& Sons Ltd. **2009**.
43. Y. P. Nizhnik, A. S. Hojniak, I. Deperasińska, L. B. Jerzykiewicz, M. Korabik, M. Hojniak, V. P. Andreev, *Inorg. Chem.* **2008**, *47*, 2103.
44. M. Brasse, J. Cámpora, P. Palma, E. Álvarez , V. Cruz, J. Ramos, M. L. Reyes, *Organometallics* **2008**, *27*, 4711.
45. D. Ghoshal, G. Mostafa, T. K. Maji, E. Zangrando, T.-H. Lu, J. Ribas, N. R. Chaudhuri, *New J. Chem*. **2004**, *28*, 1204.
46. L. -L. Wen, D. -B. Dang, C.-Y. Duan, Y.-Z. Li, Z. –F. Tian, Q. –J. Meng, *Inorg. Chem.* **2005**, *44*, 7161.
47. M. J. Plater, M. R. St. J. Foreman, A. M. Z. Slawin, *Inorg. Chim. Acta.* **2000**, *303*, 132.

48. B.-Q. Ma, S. Gao, H.-L. Sun, G. –X. Xu, *J. Chem. Soc*., *Dalton Trans*. **2001**, 130.
49. S. T. M. Andruh, A. Müller, M. Schmidtmann, C. Mathonière, G. Rombaut, *Chem. Commun.* **2001**, 1084.
50. D. –L. Long, A. J. Blake, N. R. Champness, C. Wilson, M. Schroder, *Chem. Eur. J.* **2002**, *8*, 2026.
51. Z. He, Z. –M. Wang, C. –H. Yan, *CrystEngComm* **2005**, *7*, 143.
52. S. C. Manna, E. Zangrando, M. G. B. Drew, J. Ribas, N. R. Chaudhuri *Eur. J. Inorg. Chem.* **2006**, 481.
53. S.A. Bourne, L.J. Moitsheki, *Polyhedron* **2007**, *26*, 2719.
54. D. -E Wang, F. Wang, X. –G. Meng, Y. Ding, L. –L. Wen, D. –F. Li, S. –M. Lan, *Z. Anorg. Allg. Chem.* **2008**, *634*, 2643.
55. Q. Gao, F. –L. Jiang, M. –Y. Wu, Y. –G. Huang, D. –Q. Yuan, W. Wei, M. –C. Hong, *CrystEngComm* **2009**, *11*, 918.
56. H. -Y. Wang, J. -Y. Cheng, J. -P. Ma, Y.-B. Dong, R. -Q. Huang *Inorg. Chem.* **2010,** *49,* 2416.
57. G. Xu, X. Zhang, P. Guo, C. Pan, H. Zhang, C. Wang, *J. Am. Chem Soc.* **2010**, *132*, 3656.
58. L.-P. Zhang, M. Du, W. -J. Lu, T. C. W. Maket, *Polyhedron* **2004,** *23*, 857.
59. J. W. Han, C. L. Hill, *J. Am. Chem. Soc.* **2007**, *129*, 15094.
60. D. Dang, Y. Bai, C. He, J. Wang, C. Duan, J. Niu, *Inorg. Chem.* **2010,** *49,* 1280.
61. T. Steiner, *Angew. Chem. Int. Ed.* **2002**, *41*, 748. (b) G. Desiraju, *Acc. Chem. Res.* **2002**, *35*, 5731.
62. S. A. Bourne, L. J. Moitsheki, *CrystEngComm* **2005**, *7*, 674.
63. O. Fabelo, J. Pasan, F. Lioret, M. Julve, C. R. Perez, *CrystEngComm* **2007**, *9*, 815.
64. V. V. Adrabinska, E Zaneczko, *Chem. Commun.* **1999**, 1527.
65. L. S. Reddy, N. J. Babu, A. Nangia, *Chem. Commun.* **2006**, 1369.
66. D. Bradshaw, J. B. Claridge, E. J. Cussen, T. J. Prior, M. J. Rosseinsky, *Acc. Chem. Res.* **2005**, *38*, 273.

67. B. Zhao, X. Y. Chen, P. Cheng, D. Z. Liao, S. P. Yan, Z. H. Jiang, *J. Am. Chem. Soc.* **2004**, *126*, 15394.
68. D. Venkataraman, G. F. Gardner, S. Lee, J. S. Moore, *J. Am. Chem. Soc.* **1995**, *117*, 11600.
69. W. Fujita, K. Awaga, *J. Am. Chem. Soc.* **2001**, *123*, 3601
70. M. Fujita, Y. J. Kwon, S. Washizu, K. Ogura, *J. Am. Chem. Soc.* **1994**, *116*, 1151
71. R.W. Gable, B.F. Hoskins, R. Robson, *J. Chem. Soc. Chem. Commun.* **1990**, 1677.
72. H. W. Roesky, M. Andruh, *Coord. Chem. Rev.* **2003**, *236*, 91.
73. Q.-H. Zhao, Y.-Q. Liu, M.-S. Zhang, R.-B. Fang *J. Struct. Chem.* **2007***, 48,* 523.
74. D. –L. Long, A. J. Blake, N. R. Champness, M. Schroder, *Chem. Commun.* **2000**, 2273.
75. R. L. Carlin, L. J. D. Jongh, *Chem. Rev.* **1986**, *86*, 659.
76. J. -G. Lin, Y. Su, Z. -F. Tian, L. Qiu, L. -L. Wen, Z. -D. Lu, Y. -Z. Li, Q. -J. Meng, *Cryst. Growth Des.* **2007**, *7*, 2526.
77. L. L. Wen, D. B. Dang, C. Y. Duan, Y. Z. Li, Z. F. Tian, Q. J. Meng, *Inorg. Chem.* **2005**, *44*, 7161.
78. J. –J. Zhang, Y. Zhao, S. A. Gamboa, A. Lachgar, *Cryst. Growth Des.* **2008**, *8*, 172.
79. L. –L. Wen, Z. –D. Lu, X. –M. Ren, C. –Y. Duan, Q. –J. Meng, S. Gao, *Cryst. Growth Des.* **2009**, *9*, 227.
80. V. V. Adrabińska, E. Janeczko, *Chem. Commun.* **1999**,1527.
81. R. L. Carlin, R. Block, *Proc. Indian Acad. Sci. (Chem. Sci.)* **1987**, *98*, 79.
82. A. R. Schake, J. B. Vincent, Q. Li, P. D. W. Boyd, K. Folting, J. C. Huffman, D. N. Hendrickson, G. Christou, *Inorg. Chem.* **1989**, *28*, 1915.
83. G. Christou, *Polyhedron* **2005**, *24*, 2065.
84. A. Ozarowski, I. B. Szymanska, T. Muzio, J. Jezierska, *J. Am. Chem. Soc.* **2009**, *131*, 10279.
85. K. Deka, N. Barooah, R. J. Sarma, J. B. Baruah, *J. Mole. Struct.* **2007**, *827*, 44.

86. (a) N. Barooah, A. Karmakar, R. J. Sarma, J. B. Baruah, *Inorg. Chem. Commun.* **2006**, *9*, 1251. (b) A. Karmakar, R. J. Sarma, J. B. Baruah, *Inorg. Chem. Commun.* **2006**, *9*, 1169. (c) K. Deka, R. J. Sarma, J. B. Baruah, *Inorg. Chem. Commun.* **2006**, *9*, 931.

87. M. Kato, Y. Muto, *Coord. Chem. Rev.* **1988**, *92*, 45.

88. Z. Jagličić, P. Šegedin, J. Zlatič, A. Zorko, J. Pirnat, Z. Trontelj, *J. Magn. Magn. Mater.* **2007**, *310*, 1444.

89. Y. -Q. Liu, X. -R. Zeng, L. -P. Lei, *Acta Cryst.* **2007**, *E63*, m2693.

90. P, Baran, M, Koman, D. Valigura, J. Mrozinski, *J. Chem. Soc. Dalton Trans.* **1991**, 1385.

91. S. Dalai, P. S. Mukherjee, E. Zangrando, F. Lloret, N. R. Chaudhuri, *J. Chem. Soc. Dalton Trans.* **2002,** 822 and references therein.

92. S. K. Ghosh, J. Ribas, P. K. Bharadwaj, *CrystEngComm* **2004**, *6*, 250.

93. R. L. Carlin, K. Kopinga, O. Kahn, M. Verdaguer, *Inorg. Chem.* **1986**, *25*, 1786.

94. (a) H. Muller, B. Bauer-Siebenlist, E. Csapo, S. Dechert, E. Farkas, F. Meyer, *Inorg. Chem.* **2008**, *47*, 5278. (b) Y. Zhang, J. Y. Liang, H. Huang, H. Ke, W. N. Lipscomb, *Biochemistry* **1993**, *32*, 1844. (c) R. Sarma, D. Kalita, J. B. Baruah, *Dalton Trans.* **2009**, 7428. (d) B. Dutta, P. Bag, U. Flörke, K. Nag, *Inorg. Chem.* **2005**, *44*, 147.

95. J. E. Huheey, E. A. Keiter, R. L. Keiter, *Inorganic Chemistry: Principles of Structure and Reactivity*, Pearson Education Asia, **2001**.

96. F. A. Mautner, C. Gspan, M. A. S. Goher, M. A. M. Abu-Youssef, *Monatshefte für Chemie* **2003**, *134,* 1311.

97. F. A. Mautner, M. A. M. Abu-Youssef, M. A. S. Goher, *Polyhedron* **1997,** *16*, 235.

98. M. A. S. Goher, F. A. Mautner, M. A. M. Abu-Youssef, A. K. Hafez, A. M. –A. Badr, *J. Chem. Soc. Dalton Trans.* **2002** 3309.

99. D. Sun, R. Cao, Y. Liang, Q. Shi, W. Su, M. Hong, *J. Chem. Soc. Dalton Trans.* **2001**, 2335.

100. H. J. Chen, X.-M. Chen, *Inorg. Chim. Acta.* **2002**, *329*, 13.

101. K. M. Kim, S. C. Song, S. B. Lee, H. C. Kang, Y. S. Sohn, *Inorg. Chem.* **1998**, *37*, 5764.
102. D. M. Poojary, H. Manohar, *Inorg. Chim. Acta.* **1984**, *93*, 153.
103. J. Parr, *Polyhedron* **1997**, *16*, 551.
104. A. Thirumurgan, R. A. Sanguramath, C. N. R. Rao, *Inorg. Chem.* **2008**, *47*, 823.
105. E. -C. Yang, J. Li, B. Ding, Q. -Q. Liang, X. –G. Wang, X. –J. Zhao, *CrystEngComm* **2008**, *10*, 158.
106. L. S. Linvny, J. P. Glusker, C.W. Bock, *Inorg. Chem.* **1998**, *37*, 1853.
107. J. Sanchiz, P. Esparza, D. Villagra, S. Domingues, A. Mederos, F. Brito, L. Araujo, A. Sanchez, J. M. Arrieta, *Inorg. Chem.* **2002**, *41*, 6048.
108. B. Adair, S. Natarajan, A. K. Cheetham, *J. Mater. Chem.* **1998**, *8*, 1477.
109. J. J. Vittal, *Coord. Chem. Rev.* **2007**, *251*, 1781 and the references therein.
110. M. Nagarathinam, J. J. Vittal, *Chem. Commun.* **2008**, 438.
111. C. Nather, G. Bhosekar, I. Jess, *Inorg. Chem.* **2007**, *46*, 8079.
112. H. Li, Hou, G. L. Li, X. Meng, Y. Fan, Y. Zhu, *Inorg. Chem.* **2003**, *42*, 4995.
113. C. –Y. Zhang, Q. Gao, Y. Cui, Y. –B. Xie, *Acta Cryst.* **2009**, *E65*, m785.
114. M. Nieuwenhuyzen, W. T. Robinson, C. J. Wilkins, *Polyhedron* **1991**, *10*, 2111.
115. Z. X. Yu, X. P. Wang, Y. Feng, *Acta Cryst.* **2004**, *C60*, m194.
116. Z. Soldin, D. Matkovic –Calovogic, G. Pavlovic, J. Popovic, M. Vinkovic, D. V. -Topic, Z. Popovic, *Polyhedron* **2009**, *28*, 2735.
117. D. Matkovic-Calogovic, J. Popovic, Z. Popovic, I. Picek, Z. Soldin, *Acta Cryst.* **2002**, *C58*, m39.
118. B. Kamenar, M. Penavic, *Inorg. Chim. Acta.* **1972**, *6*, 191.
119. R. W. H. Small, *Acta Cryst.* **1982**, *B38*, 2886.
120. K. M. Kim, S. C. Song, S. B. Lee, H. C. Kang, Y. S. Sohn, *Inorg. Chem.* **1998**, *37,* 5764.
121. A. W. Addison, T. N. Rao, J. Reedijk, J. van Rijn, G. C. Verschoor, *J. Chem. Soc., Dalton Trans.* **1984**, 1349.
122. J. Yang, G. -D. Li, J. -J. Cao, Q. Yue, G. –H. Li, J. –S. Chen, *Chem. Eur. J.* **2007**, *13*, 3248.

123. Y. Wei, H. Hou, L. Li, Y. Fan, Y. Zhu, *Cryst. Growth Des.* **2005***, 5,* 1405.

124. J. G. Mao, Z. Wang, A. Clearfield, *Inorg. Chem.* **2002**, *41*, 6106.

125. Y. Rodriguez-Martin, M. Hernadez-Molina, F. S. Delgado, J. Pasan, C. Ruiz-Perez, J. Sanchiz, F. Lioret, M. Julve, *CrystEngComm* **2002**, *4*, 522.

126. K. Bania, N. Barooah, J. B. Baruah, *Polyhedron* **2007**, *26*, 2612.

127. Z. He, E. Q. Gao, Z. M. Wang, C. H. Yan, M. Kurmoo, *Inorg. Chem.* **2005**, *44*, 862.

128. F. Renaud, C. Piguet, G. Bernardinelli, J. C. G. Bünzli, G. Hopfgartner, *J. Am. Chem. Soc.* **1999**, *121*, 9326.

129. C. Boucher, M. G. B. Drew, P. Giddings, L. M. Harwood, M. J. Hudson, P. B. Iveson, C. Madic, *Inorg. Chem. Commun.* **2002**, *5*, 596.

130. C. Tedeschi, J. Azéma, H. Gornitzka, P. Tisnès, C. Picard, *Dalton Trans.* **2003**, 1738.

131. D. -L. Long, A. J. Blake, N. R. Champness, C. Wilson, M. Schröder, *Angew. Chem. Int. Ed.* **2001**, *40*, 2444.

132. S. Faulkner, S. J. A. Pope, B. P. Burton-Pye, *Applied Spectro. Rev.* **2005**, *40*, 1.

133. Z-P. Deng, L-H. Huo, H.-Y. Wang, S. Gao, H. Zhao, *CrystEngComm* **2010**, *12*, 1526.

134. B. H. Koo, Y. Byun, E. Hong, Y. Kim, Y. Do, *Chem. Commun*. **1998**, 1227.

135. G. Bozoklu, C. Marchal, J. Pécaut, D. Imbert, M. Mazzanti, *Dalton Trans*. **2010**, 9112.

136. A. J. Dillner, C. P. Lilly, J. M. Knaust, *Acta Cryst.* **2010**, *E66*, m1156.

137. F. B. Tamboura, M. Diop, M. Gaye, A. S. Sall, A. H. Barry, T. Jouini, *Inorg. Chem. Commun.* **2003**, *6*, 1004.

138. D. Parker, H. Puschmann, A. S. Batsanov, K. Senanayake, *Inorg Chem.* **2003**, *29*, 864.

139. C. W. Haigh, *Polyhedron* **1996**, *15*, 605.

140. R. Hoffmann, B. F. Beier, E. L. Muetterties, A. O. Rossi, *Inorg. Chem.* **1977**, *16,* 511.

141. P. K. Baker, C. W. Haigh, *Polyhedron* **1994**, *13*, 417.

142. C. W. Haigh, *Polyhedron* **1994**, *13*, 2703.

143. T. M. Reineke, M. Eddaoudi, D. Moler, M. O'Keeffe, O. M. Yaghi, *J. Am. Chem. Soc*. **2000**, *122*, 4843.

144. E. Lee, J. Heo, K. Kim, *Angew. Chem. Int. Ed.* **2000**, *39*, 2699.

145. J. G. Mao, H. J. Zhang, J. Z. Ni, S. B. Wang, T. C. W. Mak, *Polyhedron* **1999**, *18*, 1519.

146. L. Pan, X. Huang, J. Li, Y. Wu, N. Zheng, *Angew. Chem. Int. Ed*. **2000**, *39*, 527.

147. T. M. Reineke, M. Eddaoudi, M. O'Keeffe, O. M. Yaghi, *Angew. Chem. Int. Ed*. **1999**, *38*, 2590.

148. T. M. Reineke, M. Eddaoudi, M. Fehr, D. Kelley, O. M. Yaghi, *J. Am. Chem. Soc.* **1999**, *121*, 1651.

149. D.-L. Long, A. J. Blake, N. R. Champness, M. Schröder, *Chem. Commun*. **2000**, 1369.

150. D.-L. Long, A. J. Blake, N. R. Champness, C. Wilson, M. Schröder, *J. Am. Chem. Soc.* **2001**, *123*, 3401.

151. Y. H. Wen, X. H. Wu, S. Bi, S. S. Zhang, *J. Coord. Chem.* **2009**, *8*, 1249.

152. X. S. Wu, Y. B. Zhang, X. Li, P. Z. Li, *J. Coord. Chem.* **2009**, *5*, 797.

153. Z. Ming, Y. Miao, S. Si, *J. Coord. Chem.* **2009**, *5*, 833.

154. P. I. Yan, J. Xing, G. Li, W. Sun, J. Zhang, G. Hou, *J. Coord. Chem.* **2009**, *13*, 2095.

155. L. Ma, O. R. Evans, B. M. Foxman, W. Lin, *Inorg. Chem.* **1999**, *38*, 5837.

156. Y. Bretonnire, M. Mazzanti, J. Pcaut, F. A. Dunand, A. E. Merbach, *Inorg. Chem.* **2001**, *40*, 6737.

157. R. Baggio, M. T. Garland, M. Perec, D. Vega, *Inorg. Chem.* **1996**, *35*, 2396.

158. G. Mathis, *Clinical Chem.* **1995**, *41*, 1391.

159. S. Aime, M. Botta, M. Fasano, E. Terreno, *Chem. Soc. Rev.* **1998**, *27*, 19.

160. C. Piguet, J. C. G. Bünzli, *Chem. Soc. Rev.* **1999**, *28*, 347.

161. C. Serre, J. Marrot, G. Frey, *Inorg. Chem.* **2005**, *44*, 654.

162. D.-L. Long, A. J. Blake, N. R. Champness, C. Wilson, M.Schröder, *Angew. Chem. Int. Ed. Eng.* **2001**, *40*, 2443.

163. G. Vicentini, L. B. Zinner, J. Zukerman-Schpector, K. Zinner, *Coord. Chem. Rev.* **2000**, *196*, 353.

164. G. R. Desiraju, *Angew Chem. Int. Ed.* **2007**, *46*, 8342**.**

165. T. Steiner, *Angew Chem. Int. Ed.* **2002**, *41*, 48.

166. H. -B. Bürgi, J. D. Dunitz, *Acc. Chem. Res*. **1983**, *16*, 153.

167. D. Braga, F. Grepioni, *Acc. Chem. Res*. **2000**, *33*, 601.

168. G. R. Desiraju, T. Steiner, *The Weak Hydrogen Bond in Structural Chemistry and Biology*; Oxford University Press: Oxford, **1999**.

169. E. Deiters, V. Bulach, M. W. Hosseini, *New J. Chem.* **2008**, *32*, 99.

170. I. Imaz, A. Thillet, J. P. Sutter, *Cryst. Growth Des.* **2007**, *7*, 1753.

171. E. Deiters, V. Bulach, M. W. Hosseini, *Dalton Trans.* **2007**, 4126.

172. D. G. Mantero, A. Neels, H. S. Evans, *Inorg. Chem.* **2006**, *45*, 3287.

173. J. Jia, A. J. Blake, N. R. Champness, P. Hubberstey, C. Wilson, M. Schröder, *Inorg. Chem.* **2008**, *47*, 8652.

174. N. Miyaura, A. Suzuki, *Chem. Commun.* **1979**, 866.

175. N. Miyaura, T. Yanagi, A. Suzuki, *Synth. Commun.* **1979**, 513.

176. S. V. Ley, A. W. Thomas, *Angew. Chem. Int. Ed*. **2003**, *42*, 5400.

177. S. Itsuno, T. Matsumoto, D. Sato, T. Inoue, *J. Org. Chem.* **2000**, *65*, 5879.

178. N. Christinat, R. Scopelliti, K. Severin, *Angew. Chem. Int. Ed.* **2008**, *47*, 848.

179. N. Iwasawa, H. Takahagi, *J. Am. Chem. Soc.* **2007**, *129*, 7754.

180. B. Victor, V. Raul, L. Rolando, G. A. Carolina, H. Herbert, B. I. Hiram, Z. R. Luis, S. Rosa, F. Norberto, *Inorg. Chem.* **2006**, *45*, 2553.

181. K. E. Maly, N. Malek, J. H. Fournier, P. Rodriguez-Cuamatzi, T. Maris, J. D. Wuest, *Pure Appl. Chem.* **2006**, *78*, 1305.

182. N. SeethaLekshmi, V. R. Pedireddi, *Cryst. Growth Des.* **2007**, *7*, 944.

183. J. H. Fournier, T. Maris, J. D. Wuest, W. Guo, E. Galoppini, *J. Am. Chem. Soc.* **2003**, *125*, 1002.

184. G. Rodriguez-Cuamatzi, P. Höpfl, *Angew Chem. In. Ed.* **2004**, *43*, 3041.

185. P. Rodriguez-Cuamatzi, O. I. Arillo-Flores, M. I. Bernal-Uruchurtu, H. Hoepfl, *Cryst. Growth Des.* **2005**, *5*, 167.

186. P. Rogowska, M. K. Cyranski, A. Sporzynski, A. Ciesielski, *Tetrahedron. Lett.* **2006**, *47*, 1389.

187. C. B. Aakeröy, J. Desper, B. Levin, D. J. Salmon, *ACA Transactions*, **2004**, *39*, 123.

188. P. Rodríguez-Cuamatzi, R. Luna-García, A. Torres-Huerta, M. I. Bernal-Uruchurtu, V. Barba, H. Höpfl, *Cryst. Growth Des.* **2009**, *9*, 1575.

189. J.-H. Fournier, T. Maris, J. D. Wuest, W. Guo, E. Galoppini, *J. Am. Chem. Soc.,* **2003**, *125*, 1002.

190. P. Rodríguez-Cuamatzi, G. Vargas-Díaz, H. Höpfl, *Angew. Chem. Int. Ed.* **2004**, *43*, 3041.

191. M. R. Shimpi, N. SeethaLekshmi, V. R. Pedireddi, *Cryst. Growth Des.* **2007**, *7*, 1958.

192. C. B. Aakeröy, J. Desper, B. Levin, *CrystEngComm* **2005**, *7*, 102.

193. P. Rodríguez-Cuamatzi, O. I. Arillo-Flores, M. I. Bernal-Uruchurtu, H. Höpfl, *Cryst. Growth Des.* **2005**, *5*, 167.

194. D. Braga, M. Polito, M. Bracaccini, D. D'Addario, E. Tagliavini, L. Sturba, *Organometallics* **2003**, *22,* 2142.

195. B. Hatano, A. Aikawa, H. Katagiri, H. Tagaya, H. Takahashi, *CrystEngComm* **2005**, *7*, 44.

196. V. Videnova-Adrabinska, E. Janeczko, *Chem. Commun.* **1999**, 1527.

197. N. J. Babu, S. L. Reddy, A. Nangia, *Mol. Pharm.* **2007**, *4*, 417.

198. C. Janiak, *J. Chem. Soc. Dalton Trans.* **2000**, 3885.

199. N. Kitamura, E. Sakuda, *J. Phys. Chem. A* **2005**, *109*, 7429.

200. P. Tarakeshwar, S.J. Lee, J.Y. Lee, K.S. Kim, *J. Phys. Chem. B* **1999**, *103*, 184.

201. S.X. Tian, H.-B. Li, Y. Bai, J. Yang, *J. Phys. Chem. A* **2008**, *112*, 8121.

202. M. Filthaus, I.M. Oppel, H.F. Bettinger, *Org. Biomol. Chem.* **2008**, *6*, 1201.

203. B. Zarychta, J. Zaleski, A. Sporzynski, M. Dabrowski, J. Serwatowski, *Acta Cryst.* **2004**, *C60*, o344.

204. K. Gkionis, J.G. Hill, P.S. Oldfield, A.J. Platts, *J. Mol. Model.* **2009**, *15*, 1051.

205. M.P. Waller, A. Robertazzi, J.A. Platts, D.E. Hibbs, P.A. Williams, *J. Comp. Chem.* **2006**, *27*, 491.

206. W.Z. Wang, M. Piton˘ak, P. Hobza, *Chem. Phys. Chem.* **2007**, *8*, 2107.

207. G.L. Miessler, A. Tarr, *Inorganic Chemistry,* Pearson Education, New Delhi, India, **2004**.

208. A. D. Becke, *J. Chem. Phys.* **1993**, *98*, 5648.

209. C. Lee, W. Yang, R.G. Parr, *Phys. Rev. B* **1988**, *37*, 785.

210. A. Dkhissi, L. Adamowicz, G. Maes, *J. Phys. Chem.* **2000**,*104*, 2112.

211. A. Dkhissi, L. Adamowicz, G. Maes, *Chem. Phys. Lett.* **2000,** *324*, 127.

212. A. Dkhissi, R. Ramaekers, L. Houben, G. Maes, *Chem. Phys. Lett.* **2000**, *331*, 553.

213. L. Qiu,W. Li, X. Fan, X. Ju, G. Cao, S. Luo, *Inorg. Chem. Comm.* **2008**, *11*, 727.

214. G. Chalasinski, M. Szczesniak, *Chem. Rev.* **1994**, *94,* 1723.

215. *GAUSSIAN03*, Revision B.05, Gaussian, Inc., Pittsburgh, PA, **2003**.

216. G. M. Sheldrick, *Acta Cryst.* **2008**, *A64*, 112.

217. J.-M. Clemente-Juan, C. Mackiewicz, M. Verelst, F. Dahan, A. Bousseksou, Y. Sanakis, J.-P. Tuchagues, *Inorg. Chem.* **2002**, *41*, 1478.

218. F. James, M. Roos, "*MINUIT Program*, a System for Function Minimization and Analysis of the Parameters Errors and Correlations" *Comput. Phys. Commun.* **1975**, *10*, 345.

Appendix

Details of the analytical instruments

X-Ray Crystallography

X-ray diffraction data were collected on Bruker 3-circle diffractometers with CCD area detectors ProteumM APEX or SMART 6000 or Bruker Nonius Apex 2, using graphite-monochromated Mo-$K\alpha$ radiation (λ = 0.71073 Å) from a 60W microfocus Bede Microsource® with glass polycapillary optics or a sealed tube.

X-ray diffraction data for all crystals were collected using Bruker SMART software. This software was also used for indexing and determination of the unit cell parameters. The structures were solved by direct methods and refined by full-matrix least squares against F^2 of all data, using SHELXTL software.[216] The CIF of all the compounds synthesized and characterized are included in the soft copy.

All non-H atom were refined by full-matrix least squares in anisotropic, all H atoms in isotropic approximation, against F^2 of all reflections. All non-H atoms were refined by full-matrix least squares in the anisotropic approximation and the hydrogen atoms attached to these atoms were treated as 'riding' in calculated positions and in some of the cases the hydrogen atoms have been located on the difference Fourier maps. In all cases the hydrogen atoms attached to polar atoms such as O and N were located on the difference Fourier maps and refined in the final structure in isotropic approximation. The crystallographic tables for all the compounds are given at the end of this section, which includes the crystal parameters and the refinement factors.

Magnetic measurements

Variable temperature magnetic susceptibility measurements were carried out on polycrystalline samples **2.7**-**2.9** (4–300K) using a Quantum Design MPMS SQUID susceptometer under magnetic fields of 0.5 T. Variable-temperature dc magnetic susceptibility studies for polycrystalline sample of **4.6** (2–300K) were carried out under a magnetic field of 0.1 T. Ac studies were carried out on a Quantum Design

PPMS system on the polycrystalline sample **4.7**. Diamagnetic corrections for the complexes were estimated from Pascal's constants. The magnetic susceptibility has been computed by exact calculation of the energy levels associated with the spin Hamiltonian through diagonalization of the full matrix with a general program for axial symmetry.[217] Least-squares fits were accomplished with an adapted version of the function-minimization program MINUIT.[218] The error-factor R is defined as $R = \sum \frac{(\chi_{\exp} - \chi_{calc})^2}{N\chi_{\exp}^2}$, where N is the number of experimental points.

UV-visible Spectroscopy, emission and IR Spectroscopy

UV-vis absorption spectra were recorded using Perkin-Elmer Lambda 750 spectrophotometer equipped with double cell compartments. All the chemicals and solvents used were as obtained from the satndard suppliers such as E.Merck Germany, Sigma Aldrich USA, Ranbaxy India. The solvents for spectroscopic were of HPLC grade (Aldrich or Merck) and used as obtained. The fluorescence spectra were recorded in Fluoromax-4, spectrofluorometer. The FT-IR spectra were recorded on Perkin-Elmer spectrum one spectrometer in the range 4000-400 cm^{-1}.

NMR Spectroscopy

The NMR spectra were recorded in a Bruker 400 MHz spectrometer. The chemical shifts in the NMR spectra are all given in ppm and tetramethylsilane as the internal standard.

Thermogravimetric Studies and Elemental analysis

The thermogravimetric studies were performed using a Mettler Toledo TGA/ STDA 851^e and Mettler Toledo DSC^e thermal analyser. Typically about 3-5 mg of the samples were mounted on platinum crucibles and the TG/DSC profiles recorded at the heating rate of 10 °C/min and under nitrogen atmosphere. Elemental analyses were done on a Perkin-Elmer PE 2400 II CHN analyzer 2400.

Crystallographic data and refinement parameters for the compounds

Compound No.	**2.1**	**2.2**	**2.3**
Formula	$C_{19}H_{15}MnNO_5$	$C_{19}H_{13}MnN_3O_9$	$C_{19}H_{15}MnNO_7$
Formula wt.	392.26	482.26	424.26
Crystal system	Orthorhombic	Monoclinic	Orthorhombic
Space group	*Pbcn*	*C2/c*	*Pbcn*
a /Å	16.5652(14)	25.6908(8	16.3506(6)
b /Å	13.3047(10)	9.7787(3)	13.7789(5)
c /Å	7.5755(6)	7.6613(3)	7.4632(3)
α/°	90.00	90.00	90.00
β/°	90.00	101.421(2)	90.00
γ/°	90.00	90.00	90.00
V/ Å^3	1669.6(2)	1886.58(11)	1681.41(11)
Z	4	4	4
Density/Mgm^{-3}	1.561	1.698	1.676
Abs. Coeff. /mm^{-1}	0.822	0.763	0.831
F(000)	804	980	868
Total no. of reflections	17272	11049	16982
Reflections, $I > 2\sigma(I)$	1640	2263	2079
Max. 2θ/°	28.37	28.29	28.29
Ranges (h, k, l)	$-20 \le h \le 20$ $-14 \le k \le 17$ $-10 \le l \le 10$	$-34 \le h \le 32$ $-12 \le k \le 13$ $-10 \le l \le 9$	$-21 \le h \le 21$ $-18 \le k \le 17$ $-9 \le l \le 9$
Complete to 2θ (%)	97.1	96.4	99.7
Data/ Restraints/Parameters	2033 / 0 / 121	2263/ 0/ 148	2079 / 0 / 131
Goof (F^2)	1.053	1.058	1.025
R indices [$I > 2\sigma(I)$]	0.0263	0.0276	0.0351
R indices (all data)	0.0358	0.0300	0.0517

Compound No.	**2.4**	**2.5**	**2.6**
Formula	$C_{19}H_{13}Cl_2MnNO_5$	$C_{66}H_{62}Mn_3N_4O_{20}$	$C_{68}H_{58}Cu_4N_2O_{20}$
Formula wt.	461.14	1396.02	1477.32
Crystal system	Orthorhombic	Monoclinic	Triclinic
Space group	*Cmcm*	$P2_1/c$	*P-1*
a /Å	27.0768(6)	12.6231(4)	10.6502(8)
b /Å	9.6242(2)	12.4371(5)	10.6939(8)
c /Å	7.47400(10)	22.8149(7)	15.4901(11)
α/°	90.00	90.00	101.970(4)
β/°	90.00	114.557(2)	105.362(4)
γ/°	90.00	90.00	96.011(4)
V/ $Å^3$	1947.67(6)	3257.84(19)	1640.2(2)
Z	4	2	1
Density/Mgm^{-3}	1.573	1.423	1.496
Abs. Coeff. /mm^{-1}	0.983	0.650	1.355
F(000)	932	1442	756
Total no. of reflections	10291	27448	17502
Reflections, $I > 2\sigma(I)$	1334	8066	5558
Max. 2θ/°	28.32	28.35	25.00
Ranges (h, k, l)	$-36 \le h \le 36$ $-12 \le k \le 12$ $-9 \le l \le 9$	$-7 \le h \le 16$ $-16 \le k \le 16$ $-30 \le l \le 25$	$-12 \le h \le 11$ $-12 \le k \le 12$ $-18 \le l \le 18$
Complete to 2θ (%)	99.9	98.9	96.2
Data/ Restraints/Parameters	1334 / 0 / 80	8066/ 0 / 424	5558/0/429
Goof (F^2)	1.135	1.047	1.049
R indices [$I > 2\sigma(I)$]	0.0290	0.0420	0.0299
R indices (all data)	0.0299	0.0620	0.0406

Compound No.	**2.7**	**2.8**	**2.9**	**2.10**
Formula	$C_{38}H_{26}Cu_2N_6O_{18}$	$C_{19}H_{14}CuNO_5$	$C_{38}H_{28}Cu_2N_2O_{10}$	$C_{24}H_{20}CuN_2O_9$
Formula wt.	981.73	399.85	799.70	543.96
Crystal system	Monoclinic	Monoclinic	Triclinic	Monoclinic
Space group	*$P2_1/c$*	*C2/c*	*P-1*	*C/c*
a /Å	11.3721(4)	20.6947(2)	10.693(3)	18.9930(7)
b /Å	10.1756(3)	10.10310(10)	10.808(4)	15.8109(7)
c /Å	19.7779(6)	19.1416(2)	17.446(7)	7.7635(3)
α/°	90.00	90.00	87.96(3)	90.00
β/°	117.384(2)	118.17(10)	83.08(3)	107.791(4)
γ/°	90.00	90.00	61.137(17)	90.00
V/ $Å^3$	2032.20(11)	755.32(13)	1752.2(10)	2219.86(15)
Z	2	8	2	4
Density/Mgm^{-3}	1.604	1.506	1.516	1.628
Abs. Coeff. /mm^{-1}	1.133	1.267	1.276	1.045
F(000)	996	1632	816	1116
Total no. of reflections	21419	18542	12713	12347
Reflections, $I > 2\sigma(I)$	3672	4373	5634	5104
Max. θ/°	25.50	25.00	24.98	28.93
Ranges (h, k, l)	$-13 \le h \le 13$ $-12 \le k \le 10$ $-24 \le l \le 24$	$-23 \le h \le 24$ $-11 \le k \le 12$ $-22 \le l \le 22$	$-12 \le h \le 12$ $-12 \le k \le 11$ $-20 \le l \le 18$	$-23 \le h \le 25$ $-21 \le k \le 21$ $-10 \le l \le 10$
Completeness to 2θ (%)	97.0	99.9	91.7	99.1
Data/ Restraints/Parameters	3672/ 0 / 289	3105/ 0 / 235	5634/ 0 / 469	5104/ 0 / 332
Goof (F^2)	1.081	1.052	1.128	1.082
R indices [$I > 2\sigma(I)$]	0.0349	0.0223	0.1501	0.0451
R indices (all data)	0.0459	0.0258	0.2527	0.0558

Compound No.	**2.11**	**2.12**	**2.13**
Formula	$C_{19}H_{15}NO_5Zn$	$C_{38}H_{28}N_2O_{10}Zn_2$	$C_{52}H_{44}N_4O_{26}Zn_4$
Formula wt.	402.69	803.36	1402.39
Crystal system	Orthorhombic	Triclinic	Monoclinic
Space group	*Pbcn*	*P-1*	*C2/c*
a /Å	16.6586(8)	10.7302(7)	7.1490(2)
b /Å	13.2244(6)	10.8063(8)	18.7059(6)
c /Å	7.3795(4)	17.2987(12)	39.2863(13)
α/°	90.00	88.083 (4)	90.00
β/°	90.00	83.829(4)	91.979(2)
γ/°	90.00	61.760(3)	90.00
V/ $Å^3$	1625.70 (14)	1756.5(2)	5250.6(3)
Z	4	2	4
Density/Mgm^{-3}	1.645	1.519	1.774
Abs. Coeff. /mm^{-1}	1.543	1.428	1.904
F(000)	824	820	2848
Total no. of reflections	19669	14225	35455
Reflections, $I > 2\sigma(I)$	2005	6206	6315
Max. θ/°	28.31	25.25	28.38
Completeness to 2θ (%)	99.1	97.7	98.8
Ranges (h, k, l)	$-22 \leq h \leq 22$ $-17 \leq k \leq 17$ $-9 \leq l \leq 9$	$-12 \leq h \leq 12$ $-12 \leq k \leq 12$ $-20 \leq l \leq 20$	$-9 \leq h \leq 9$ $-24 \leq k \leq 24$ $-52 \leq l \leq 52$
Data/ Restraints/Parameters	2005/ 0 / 121	6206/ 0 / 469	6315/ 0 / 415
Goof (F^2)	1.057	1.241	1.092
R indices [$I > 2\sigma(I)$]	0.0355	0.0789	0.0471
R indices (all data)	0.0477	0.0841	0.0615

Compound No.	**3.1**	**3.2**	**3.3**
Formula	$C_{19}H_{15}CdNO_5$	$C_{62}H_{50}Cd_3N_4O_{18}$	$C_{18}H_{14}CdN_2O_7$
Formula wt.	449.72	1476.26	482.71
Crystal system	Monoclinic	Monoclinic	Monoclinic
Space group	*C2/c*	$P2_1/c$	*C2/c*
a /Å	16.5227(8)	10.8299(15)	14.1125(6)
b /Å	13.4746(8)	22.931(3)	16.9373(6)
c /Å	7.7147(5)	12.2905(15)	8.9290(3)
α/°	90.00	90.00	90.00
β/°	90.024(3)	105.145(3)	127.151(2)
γ/°	90.00	90.00	90.00
V/ $Å^3$	1717.58(17)	2946.2(7)	1701.12(11)
Z	4	2	4
Density/Mgm^{-3}	1.739	1.664	1.885
Abs. Coeff. /mm^{-1}	1.302	1.150	1.331
F(000)	896	1476	960
Total no. of reflections	11717	24903	10188
Reflections, $I > 2\sigma(I)$	1767	4908	1668
Max. θ/°	26.49	25.00	26.00
Completeness to 2θ (%)	98.3	94.7	99.7
Ranges (h, k, l)	$-20 \leq h \leq 19$ $-16 \leq k \leq 16$ $-9 \leq l \leq 9$	$-12 \leq h \leq 12$ $-27 \leq k \leq 23$ $-13 \leq l \leq 14$	$-17 \leq h \leq 17$ $-20 \leq k \leq 20$ $-11 \leq l \leq 11$
Data/ Restraints/Parameters	1767/ 0 / 194	4908 / 0 / 402	1668 /0/128
Goof (F^2)	1.076	1.036	1.091
R indices [$I > 2\sigma(I)$]	0.0313	0.0220	0.0186
R indices (all data)	0.0357	0.0264	0.0192

Compound No.	**3.4**	**3.5**	**3.6**
Formula	$C_{24}H_{18}HgN_2O_6$	$C_{24}H_{18}HgN_2O_6$	$C_{33}H_{29}NO_{11}Pb_2$
Formula wt.	630.99	630.99	1029.95
Crystal system	Monoclinic	Monoclinic	Monoclinic
Space group	*C2/c*	*C2/c*	$P2_1/c$
a /Å	20.7776(10)	30.0366(10)	24.6141(3)
b /Å	9.6319(4)	10.5820(3)	6.97330(10)
c /Å	11.2188(5)	13.8463(4)	19.8426(3)
α/°	90.00	90.00	90.00
β/°	104.513(2)	101.925(2)	98.5510(10)
γ/°	90.00	90.00	90.00
V/ $Å^3$	2173.55(17)	4306.0(2)	3367.95(8)
Z	4	8	4
Density/Mgm^{-3}	1.928	1.947	2.031
Abs. Coeff. /mm^{-1}	7.126	7.194	10.045
F(000)	1216	2432	1944
Total no. of reflections	11779	16524	37639
Reflections, $I > 2\sigma(I)$	2257	3637	8322
Max. θ/°	26.49	25.00	28.27
Completeness to 2θ (%)	99.9	95.9	99.6
Ranges (h, k, l)	$-26 \leq h \leq 24$ $-12 \leq k \leq 10$ $-14 \leq l \leq 14$	$-29 \leq h \leq 34$ $-12 \leq k \leq 12$ $-16 \leq l \leq 15$	$-31 \leq h \leq 32$ $-9 \leq k \leq 9$ $-26 \leq l \leq 26$
Data/ Restraints/Parameters	2257/ 0/151	3637/ 0/298	8322 / 0 / 424
Goof (F^2)	1.063	1.037	1.084
R indices [$I > 2\sigma(I)$]	0.0721	0.0209	0.0252
R indices (all data)	0.0765	0.0315	0.0436

Compound No.	**3.7**	**3.8**	**3.9**	**3.10**
Formula	$C_{23}H_{19}NO_6Pb$	$C_{17}H_{13}N_3O_7Pb$	$C_{46}H_{35}N_5O_{11}Pb_2$	$C_{17}H_{14}N_4O_9Pb$
Formula wt.	612.58	578.49	1248.17	625.51
Crystal system	Monoclinic	Monoclinic	Triclinic	Monoclinic
Space group	$P2_1/c$	$P2_1/c$	$P\text{-}1$	$P2_1/n$
a /Å	12.4173(6)	14.006(5)	7.5260(3)	12.1032(5)
b /Å	6.9429(3)	7.436(2)	17.1547(7)	7.5460(3)
c /Å	25.6785(12)	22.741(6)	19.3844(8)	21.6511(8)
α/°	90.00	90.00	89.325(2)	90.00
β/°	103.888(3)	127.870(14)	84.013(2)	94.402(2)
γ/°	90.00	90.00	86.810(2)	90.00
V/ Å^3	2149.08(17)	1869.7(10)	2485.10(17)	1971.58(13)
Z	4	4	2	4
Density/Mgm^{-3}	1.893	2.055	1.668	2.107
Abs. Coeff. /mm^{-1}	7.890	9.069	6.825	8.617
F(000)	1176	1096	1196	1192
Total no. of reflections	27515	18138	33383	19740
Reflections, $I > 2\sigma(I)$	5373	4625	8670	4855
Max. θ/°	28.51	28.40	25.00	28.30
Completeness to 2θ (%)	98.3	98.7	99.2	99.2
Ranges (h, k, l)	$-16 \le h \le 16$ $-9 \le k \le 9$ $-34 \le l \le 33$	$-18 \le h \le 18$ $-9 \le k \le 9$ $-30 \le l \le 29$	$-8 \le h \le 8$ $-19 \le k \le 20$ $-22 \le l \le 23$	$-16 \le h \le 16$ $-9 \le k \le 10$ $-28 \le l \le 28$
Data/ Restraints/Parameters	5373 / 0 / 284	4625 / 0 / 272	8670 / 0 /560	4855 / 0 / 280
Goof (F^2)	0.998	1.007	1.072	1.039
R indices [$I > 2\sigma(I)$]	0.0422	0.0277	0.0727	0.0190
R indices (all data)	0.0530	0.0468	0.0440	0.0275

Compound No.	**3.11**	**3.12**	**3.13**	**3.14**
Formula	$C_{19}H_{15}N_3O_{10}Pb$	$C_{19}H_{13}N_3O_9Pb$	$C_{31}H_{20}N_6O_{17}Pb_2$	$C_{24}H_{16}N_4O_{10}Pb$
Formula wt.	652.53	634.51	1162.91	727.60
Crystal system	Triclinic	Monoclinic	Monoclinic	Monoclinic
Space group	*P-1*	$P2_1/c$	$P2_1/c$	$P2_1/c$
a /Å	6.8980(3)	10.62940(10)	17.6692(13)	13.061(2)
b /Å	11.7165(5)	7.71560(10)	8.1098(6)	7.4870(11)
c /Å	13.6190(7)	24.6416(3)	24.3357(17)	26.345(4)
α/°	72.189(3)	90.00	90.00	90.00
β/°	83.549(3)	98.6340(10)	100.471(4)	108.057(10)
γ/°	84.304(3)	90.00	90.00	90.00
V/ $Å^3$	1038.85(8)	1998.01(4)	3429.1(4)	2449.3(6)
Z	2	4	4	4
Density/Mgm^{-3}	2.080	2.109	2.253	1.973
Abs. Coeff. /mm^{-1}	8.184	8.504	9.896	6.955
F(000)	620	1208	2192	1400
Total no. of reflections	9628	26282	31952	25184
Reflections, $I > 2\sigma(I)$	3757	4903	8458	5996
Max. 2θ/°	25.50	28.37	28.33	28.45
Ranges (h, k, l)	$-5 \le h \le 8$ $-14 \le k \le 14$ $-16 \le l \le 16$	$-13 \le h \le 13$ $-10 \le k \le 10$ $-31 \le l \le 32$	$-21 \le h \le 23$ $-10 \le k \le 10$ $-31 \le l \le 32$	$-17 \le h \le 17$ $-9 \le k \le 9$ $-30 \le l \le 35$
Complete to 2θ (%)	96.9	97.9	99.0	97.0
Data/ Restraints/Parameters	3757/ 0 / 298	4903 / 0 / 289	8458 / 0 / 505	5996 / 0 / 352
Goof (F^2)	1.056	1.036	1.070	0.990
R indices [$I > 2\sigma(I)$]	0.0508	0.0197	0.0260	0.0463
R indices (all data)	0.0732	0.0275	0.0426	0.0826

Compound No.	**4.1**	**4.2**	**4.3**
Formula	$C_{36}H_{36}LaN_2O_{12}$	$C_{34}H_{34}CeN_3O_{11}$	$C_{26}H_{21}NO_8Tb$
Formula wt.	827.58	800.76	634.36
Crystal system	triclinic	Monoclinic	Monoclinic
Space group	*P-1*	$P2_1/c$	$P2_1/n$
a /Å	9.5174(3)	12.8612(12)	12.9343(7)
b /Å	12.5384(3)	10.2716(9)	8.2555(4)
c /Å	16.3714(4)	26.254(2)	24.1694(13)
α/°	80.0080(10)	90.00	90.00
β/°	81.4190(10)	112.500(4)	102.5180(10)
γ/°	69.0050(10)	90.00	90.00
V/ $Å^3$	1788.22(8)	3448.4(5)	2519.4(2)
Z	2	4	4
Density/Mgm^{-3}	1.537	1.542	1.672
Abs. Coeff. /mm^{-1}	1.260	1.384	2.856
F(000)	838	1620	1252
Total no. of reflections	23453	31305	12841
Reflections, $I > 2\sigma(I)$	6583	5886	4648
Max. θ/°	25.50	25.00	25.50
Ranges (h, k, l)	$-11 \le h \le 11$ $-15 \le k \le 13$ $-19 \le l \le 18$	$-14 \le h \le 15$ $-11 \le k \le 11$ $-31 \le l \le 33$	$-15 \le h \le 15$ $-3 \le k \le 10$ $-28 \le l \le 29$
Completeness to 2θ (%)	98.5	96.8	99.4
Data/ Restraints/Parameters	6583/0/478	5886 /0/444	4648/0/329
Goof (F^2)	1.084	1.076	0.964
R indices [$I > 2\sigma(I)$]	0.0206	0.0329	0.0366
R indices (all data)	0.0227	0.0433	0.0435

Compound No.	**4.4**	**4.5**	**4.6**	**4.7**
Formula	$C_{38}H_{33}LaN_2O_{12}$	$C_{38}H_{33}EuN_2O_{12}$	$C_{38}H_{33}GdN_2O_{12}$	$C_{38}H_{33}N_2O_{12}Tb$
Formula wt.	848.57	861.62	866.91	868.58
Crystal system	orthorhombic	Orthorhombic	Orthorhombic	Orthorhombic
Space group	*Pnaa*	*Pccn*	*Pnaa*	*Pccn*
a /Å	10.139	17.7412(8)	10.040	17.7423(5)
b /Å	17.804	19.8116(7)	17.788	19.7457(5)
c /Å	20.010	10.0546(3)	19.786	10.0389(3)
α/°	90.00	90.00	90.00	90.00
β/°	90.00	90.00	90.00	90.00
γ/°	90.00	90.00	90.00	90.00
V/ $Å^3$	3612.0	3534.0(2)	3533.6	3516.97(17)
Z	4	4	4	4
Density/Mgm^{-3}	1.560	1.619	1.630	1.640
Abs. Coeff. /mm^{-1}	1.250	1.843	1.946	2.080
F(000)	1712	1736	1740	1744
Total no. of reflections	10490	29134	30827	28661
Reflections, $I > 2\sigma(I)$	3334	3473	3458	3244
Max. θ/°	25.49	26.00	26.00	25.50
Ranges (h, k, l)	$-12 \le h \le 12$ $-20 \le k \le 18$ $-24 \le l \le 17$	$-18 \le h \le 12$ $-9 \le k \le 6$ $-25 \le l \le 26$	$-12 \le h \le 12$ $-21 \le k \le 21$ $-24 \le l \le 23$	$-21 \le h \le 21$ $-23 \le k \le 23$ $-7 \le l \le 11$
Completeness to 2θ (%)	99.0	99.7	99.3	99.0
Data/ Restraints/Parameters	3334/2/241	3473/0/248	3458/1/241	3244/2/248
Goof (F^2)	1.004	1.024	1.051	0.945
R indices [$I > 2\sigma(I)$]	0.0802	0.0266	0.0399	0.0194
R indices (all data)	0.1502	0.0493	0.0749	0.0290

Compound No.	**5.1**	**5.2**	**5.3**	**5.4**
Formula	$C_{24}H_{30}N_4O_{16}Mn$	$C_{24}H_{30}N_4O_{16}Zn$	$C_{24}H_{26}N_4O_{14}Zn$	$C_{32}H_{38}MnN_4O_{18}$
Formula wt.	685.46	695.89	659.86	821.60
Crystal system	Monoclinic	Monoclinic	Triclinic	Triclinic
Space group	*P2₁/c*	*P2₁/c*	*P-1*	*P-1*
a /Å	17.2531(6)	17.2349(3)	7.10720(10)	7.0862(2)
b /Å	6.3137(2)	6.27630(10)	7.19880(10)	7.7960(2)
c /Å	13.5707(4)	13.4417(2)	15.0684(3)	17.2461(4)
α/°	90.00	90.00	95.819(2)	82.1420(10)
β/°	94.9840(10)	95.4620(10)	91.2100(10)	78.2610(10)
γ/°	90.00	90.00	116.1620(10)	76.6880(10)
V/ Å^3	1472.68(8)	1447.41(4)	686.528(19)	903.71(4)
Z	2	2	1	1
Density/Mgm^{-3}	1.546	1.569	1.596	1.510
Abs. Coeff. /mm^{-1}	0.531	0.933	0.974	0.451
F(000)	710	720	340	427
Total no. of reflections	18436	18694	7706	11970
Reflections, $I > 2\sigma(I)$	3654	3511	3144	4331
Max. θ/°	28.30	28.28	28.29	28.28
Ranges (h, k, l)	$-22 \le h \le 23$ $-8 \le k \le 8$ $-17 \le l \le 17$	$-22 \le h \le 22$ $-8 \le k \le 8$ $-17 \le l \le 17$	$-9 \le h \le 8$ $-9 \le k \le 9$ $-18 \le l \le 18$	$-9 \le h \le 9$ $-10 \le k \le 10$ $-19 \le l \le 22$
Complete to 2θ (%)	99.8	97.7	92.0	96.0
Data/ Restraints/Parameters	3654 / 0 / 220	3511/ 0 / 220	3144/ 0 /204	4331/ 0 /254
Goof (F^2)	1.075	1.142	1.093	1.080
R indices [$I > 2\sigma(I)$]	0.0410	0.0262	0.0247	0.0310
R indices (all data)	0.0483	0.0334	0.0260	0.0370

Compound No.	**5.5**	**5.6**	**5.7**	**5.8**
Formula	$C_{32}H_{38}CoN_4O_{18}$	$C_{32}H_{38}N_4NiO_{18}$	$C_{32}H_{38}N_4O_{18}Zn$	$C_{54}H_{54}MnN_8O_{18}$
Formula wt.	825.59	825.37	832.05	1157.99
Crystal system	Triclinic	Triclinic	Triclinic	Monoclinic
Space group	*P-1*	*P-1*	*P-1*	$P2_1/n$
a /Å	7.0482(5)	7.0548(6)	7.06280(10)	7.07350(10)
b /Å	7.7158(5)	7.6837(7)	7.71580(10)	36.2009(4)
c /Å	17.2476(12)	17.2135(16)	17.2194(2)	10.41430(10)
α/°	82.100(4)	82.209(6)	82.2260(10)	90.00
β/°	78.455(5)	78.723(6)	78.7420(10)	103.9330(10)
γ/°	76.808(4)	76.749(4)	76.7740(10)	90.00
V/ $Å^3$	890.59(11)	886.68(14)	891.86(2)	2588.30(5)
Z	1	1	1	2
Density/Mgm^{-3}	1.569	1.546	1.553	1.486
Abs. Coeff. /mm^{-1}	0.572	0.634	0.775	0.341
F(000)	429	430	434	1206
Total no. of reflections	10401	8894	9539	25907
Reflections, $I > 2\sigma(I)$	3083	3246	4372	4701
Max. θ/°	25.00	25.50	28.35	28.26
Ranges (h, k, l)	$-8 \le h \le 8$ $-9 \le k \le 9$ $-20 \le l \le 20$	$-8 \le h \le 8$ $-9 \le k \le 9$ $-20 \le l \le 20$	$-9 \le h \le 9$ $-10 \le k \le 9$ $-22 \le l \le 21$	$-8 \le h \le 8$ $-43 \le k \le 43$ $-12 \le l \le 12$
Complete to 2θ (%)	98.2	98.3	97.9	97.2
Data/ Restraints/Parameters	3083/ 3 / 255	3246 / 4 / 269	4372/ 0 /262	4701/ 2 /377
Goof (F^2)	1.071	1.062	1.059	1.115
R indices [$I > 2\sigma(I)$]	0.1123	0.0665	0.0291	0.0326
R indices (all data)	0.1485	0.0758	0.0318	0.0396

Compound No.	**6.1**	**6.2**	**6.3**	**6.4**
Formula	$C_{16}H_{18}B_2N_2O_6$	$C_{24}H_{22}B_2N_2O_6$	$C_{42}H_{36}B_2N_4O_8$	$C_{16}H_{16}B_2N_2O_6$
Formula wt.	355.94	456.06	746.37	353.93
Crystal system	Monoclinic	Triclinic	Triclinic	Triclinic
Space group	*P2₁/c*	*P-1*	*P-1*	*P-1*
a /Å	10.685(13)	6.8070(16)	8.1044(5)	6.6688(8)
b /Å	7.111(9)	7.777(2)	10.0572(6)	7.5984(10)
c /Å	12.140(14)	11.578(4)	12.6265(7)	8.2851(11)
α/°	90.00	106.447(12)	84.152(4)	100.157(11)
β/°	115.05(3)	99.512(12)	78.466(4)	106.987(9)
γ/°	90.00	101.721(9)	67.189(4)	92.944(9)
V/ $Å^3$	835.6(18)	559.2(3)	929.17(9)	392.85(9)
Z	2	1	1	1
Density/Mgm^{-3}	1.415	1.354	1.334	1.496
Abs. Coeff. /mm^{-1}	0.106	0.096	0.092	0.112
F(000)	372	238	390	184
Total no. of reflections	6351	4359	5296	2963
Reflections, $I > 2\sigma(I)$	1632	2695	2431	1424
Max. 2θ/°	26.50	28.38	23.10	25.48
Ranges (h, k, l)	-13 ≤ h ≤ 13 -6 ≤ k ≤ 8 -15 ≤ l ≤ 14	-9 ≤ h ≤ 3 -8 ≤ k ≤ 10 -15 ≤ l ≤ 15	-8 ≤ h ≤ 8 -11 ≤ k ≤ 11 -13 ≤ l ≤ 13	-8≤ h ≤ 7 -9≤ k ≤ 9 -10 ≤ l ≤ 10
Complete to 2θ (%)	94.9	96.1	93.3	97.6
Data/ Restraints/Parameters	1632 / 0 / 118	2695 / 0 / 156	2431 / 0 / 256	1424/ 0/ 120
Goof (F^2)	1.529	1.074	1.069	1.067
R indices [$I > 2\sigma(I)$]	0.1093	0.0458	0.0710	0.0454
R indices (all data)	0.1304	0.0626	0.0821	0.0622

List of Publication

1. **R. Sarma**, H. Deka, A. K. Boudalis, J. B. Baruah. Coordination polymers of lanthanide(III): towards encapsulation of well defined assembly of guest molecules.
   Crystal Growth & Design, **2011***, 11*, 547–554

2. **R.Sarma**, P. Bhattacharyya, J. B. Baruah. Short range interactions in molecular complexes of 1,4-benzenediboronic acid with aromatic *N*-oxides.
   Computational and Theoretical Chemistry, **2011***, 963,* 141–147

3. **R.Sarma**, A. K. Boudalis, J. B. Baruah. Aromatic *N*-oxide bridged copper(II) coordination polymers: synthesis, characterization and magnetic properties.
   Inorganica Chimica Acta, **2010**, *10*, 2279-2286

4. **R. Sarma**, J. B. Baruah. Variation in coordination modes of aromatic *N*-oxide in lanthanum(III) coordination polymers.
   Journal of Coordination Chemistry, **2010**, *63*, 457–463

5. **R. Sarma**, J. B. Baruah. A mixed anionic lead(II) N-oxide coordination polymer containing nitrato and benzoate ligands.
   Polyhedron **2009**, *28*, 553-558

6. **R. Sarma**, J. B. Baruah. B···π-aromatic and C-H···B interactions in cocrystals of aromatic amine N-oxides with p-phenylenediboronic acid.
   J. Molecular Structure, **2009**, *920*, 350-354

7. **R. Sarma**, A. Perumal, J. B. Baruah. Some aspects of *N*-oxide bridged manganese (II) co-ordination polymers.
   Journal of Coordination Chemistry, **2009**, *62*, 1513-1525

8. **R. Sarma**, J. B. Baruah. Transformation of mixed anionic coordination polymers of lead.
   Inorganica Chimica Acta, **2009**, *362*, 1681-1686

9. **R.Sarma**, A. Karmakar, J. B. Baruah. *N*-oxides in metal containing multi components molecular complexes.
   Inorganic Chemistry, **2008**, *47*, 763-765

10. **R. Sarma**, A. Karmakar, J. B. Baruah. Synthesis and characterization of pyridine *N*-oxide complexes of manganese, copper and zinc.
    Inorganica Chimica Acta, **2008**, *361*, 2081-2086